The Role of Copper Transporters in *In Vitro* Cytotoxicity of Oxaliplatin and Their Expression in Colorectal Cancer

By

Candidate: Haigang Cui (MSc)

Submitted in partial fulfillment of the requirement for the degree of

Doctorate of Philosophy (Pharmacy)

University of Tasmania

June 2018

Declaration of Originality

This thesis contains no material which has been accepted for a degree or diploma by the University or any other institution, except by way of background information and duly acknowledged in the thesis, and to the best of my knowledge and belief, no material previously published or written by another person except where due acknowledgement is made in the text of the thesis, nor does the thesis contain any material that infringes copyright.

17th Aug 2017

Authority of Access

This thesis is not to be made available for loan or copying for two years following the date this statement was signed. Following that time, the thesis may be made available for loan and limited copying and communication in accordance with the Copyright Act 1968.

17th Aug 2017

Statement of Ethical Conduct

The research associated with this thesis abides by the international and Australian codes on human and animal experimentation, the guidelines by the Australian Government's Office of

the Gene Technology Regulator and the rulings of the Safety, Ethics and Institutional Biosafety Committees of the University. Patient recruitment, sample collection and storage were conducted under the approval of the Tasmania Health and Medical Human Research Ethics Committee (Reference No. H0014706).

Statement Regarding Published Work Contained in Thesis

The publishers of the papers comprising parts of Chapters 1-5 hold the copyright for that content, and access to the material should be sought from the respective journals. The remaining non-published content of the thesis may be made available for loan and limited copying and communication in accordance with the Copyright Act 1968.

List of Publications and Statement of Co-authorship

The following people and institutions contributed to the publication of work undertaken as part of this thesis:

Peer-reviewed publications:

1. Cui H, Zhang A. J, McKeage M. J, Nott L. M, Geraghty D, Guven N, Liu J.J. Copper transporter 1 in human colorectal cancer cell lines: Effects of endogenous and modified expression on oxaliplatin cytotoxicity. Journal of Inorganic Biochemistry. 2017 Apr 25. doi: 10.1016/j.jinorgbio.2017.04.022. [Epub ahead of print]. **(see Appendix 1 for full article).**

Relevance to thesis: This paper presents approximately 80% of the results from Chapter 3-5, which provide the supportive evidence for the primary hypothesis of this thesis project on the

positive role of Cu transporter 1 in the uptake of oxaliplatin, and systematically characterize the expression profiles of copper transporters in human colorectal cancer cells.

Contribution of candidate: The candidate is the primary author, designed and performed the experiments, analysed and presented results, contributed to manuscript writing.

2. Cui H, Zhang A. J, Chen M, Liu J.J. ABC transporter inhibitors in reversing multidrug resistance to chemotherapy. Current Drug Targets 2015;16(12):1356-1371. **(see Appendix 2 for cover page).**

Relevance to thesis: This review is partially related to introductory Chapter 1 in this theis. It covers the general areas of membrane transporters and their roles in drug resistance, with a focus on ABC transporters and related compounds.

Contribution of candidate: The candidate is the primary author, searched and reviewed the literature, designed the structure of the paper, and contributed to the writing.

Manuscript in preparation:

Cui H, Chen M, Gou D, Li L, Liu J.J. Investigational agents targeting solute carrier transporters in the treatment of diabetes mellitus.

Relevance to thesis: This review is partially relevant to the introductory Chapter 1 of this theis. It provides an update of the research on drug transporters and their applications in the development of new anti-cancer drugs. The review focuses on SLC transporters and related agents as an extension to the main topics of this project.

Contribution of candidate: The candidate was the primary author, searched and reviewed the literature, designed the structure of the paper, and wrote an aproximately 60% of the texts.

We the undersigned agree with the above stated, “proportion of work undertaken” for the

above-mentioned published papers contributing to this thesis:

Signed:	Signed:
Assoc Prof Nuri Guven	*Prof Ben Canny*
Supervisor	*Head*
School of Medicine	*School of Medicine*
University of Tasmania	*University of Tasmania*
Date: 8/8/2017	Date: 08-8-2017

Conference Abstracts

1. Cui H, Zhang A. J, Nott L. M, Geraghty D, Guven N, Liu J.J. Expression of copper transporters in colorectal cancer cells and its relation to oxaliplatin. (3-minute oral presentation and poster). The Annual Scientific Meeting of The Australasian Society of Clinical and Experimental Pharmacologists and Toxicologists (ASCEPT), 2014, Melbourne, Australia.

2. Cui H, Zhang A. J, Nott L. M, Geraghty D, Guven N, Liu J.J. Expression of copper transporters in colorectal cancer cells and its relation to oxaliplatin. (3-minute oral presentation and poster). The Tasmanian Health Research Student Conference, 2015, Hobart, Tasmania.

3. Cui H, Zhang A. J, Nott L. M, Geraghty D, Guven N, Liu J.J. Regulation of copper transporters by platinum-based anticancer drug oxaliplatin in colorectal cancer cells. (3-

minute oral presentation and poster). The Annual Scientific Meeting of ASCEPT, 2015, Hobart, Tasmania.

4. Cui H, Zhang A. J, Nott L. M, Geraghty D, Guven N, Liu J.J. Targeting hCTR1 to improve the cytotoxicity of oxaliplatin in colorectal cancer cells. (3-minute oral presentation and poster). The Annual Scientific Meeting of ASCEPT, 2016, Melbourne, Australia.

Acknowledgements

First of all, I would like to give my sincere thanks to my primary supervisor Dr Johnson Liu for his continual encouragement, input, consideration, thoughtfulness and advice in these four years. This thesis would not have been possible without his help and support in every aspect of my PhD life in Australia. I feel very lucky and honored to be his student. To me, he is not just a professional supervisor, but also a warm-hearted and frank friend. I could always rely upon him whenever I ended up in some trouble or awkward situations. Meanwhile, I also feel great gratitude for his family's hospitality, friendship, and never-ending love and care.

I would like to thank my co-supervisor A/Prof Nuri Guven for his technical assistance and advice on improving my experimental design. He has also put immense effort in correcting my writing. I admire his knowledge and skills in science. His perspective and insights into experimental design, sound judgment and dedication to teaching and research amazed me and set a good example for me in my future academic life. I am also thankful for his support in sorting out and packing up experimental stuffs during my short stay in Launceston, my transition to Sydney and even during my stay in Sydney. Most importantly, thanks to him for coordinating with Dr Raj Eri at Launceston for providing the valuable slides for my project.

I would like to thank our senior research assistant Anna Zhang for helping me with the experiments in the lab. I feel fortunate to have the opportunity to learn from her. I made a lot of mistakes at the early stage of my project, thanks for being patient and correcting me as well as giving me chances to improve my technical skills. My appreciation also goes to Anna for her care, support and timely advice on adjusting myself to cope with other challenges of my life in Australia. Lastly, I admire her for her great sense of family, altruism to others, and kindness.

In addition, I would like to express my sincere gratitude to Dr Peter Traill and Mrs Heather Galloway, Mr Jack Voutnis, my study coordinator Dr Nicole Bye for their support and assistance in ordering, scholarship application, my accommodation and flight booking. I felt great sense of belonging to this big family, the School of Pharmacy (now Division of Pharmacy), especially when we cooked barbecues together in Waterworks Reserves.

My special thanks go to Dr Raj Eri, his students and all the staff working at Launceston. Thanks for providing facilities, instruments, reagents and training to me for my tissue-based immunohistochemistry studies.

I should not forget to mention my appreciation for the lab managing staff in Menzies Research Institute, including Dr David Steele and Mr Steve Weston for their helpful technical advice and support. My thanks also go to other colleagues and staff based in Menzies for your technical support and friendships.

Thanks to the staff working in the Royal Hobart Hospital for your effort, sacrifice, support for organizing group meetings, planning experiments, patient recruitments and consenting, tissue collection and storage, including but not limited to Dr Louise Nott, Miss Rossa King, Mrs Sue Davoren and Monika Corban.

I would also like to thank the Head of School of the University of New South Wales for allowing me to study and work in your School, and providing me with the facilities, training and instruments and reagents. I should always feel indebted to new friends, lab managers, senior researchers and technicians in the Wallace Wurth Building, staff in the teaching labs on level 1 and security officers in UNSW for your generosity, support and friendships during my last-year stay there. My special thanks are given to Allison, Josephine, Tianjun, Thomas and other members at the Department of Pharmacology. I will treasure this friendship forever.

Last but not least, thanks to my family, my mum and sister, and all my friends for their never-ending love, support and patience.

Table of Contents

Declaration of Originality....3

Statement of Ethical Conduct....3

Statement Regarding Published Work Contained in Thesis....4

List of Publications and Statement of Co-authorship....4

Conference Abstracts....6

Acknowledgements....8

Table of Contents....11

List of Abbreviations....16

List of Tables....17

List of Figures....18

Abstract....20

Chapter 1 Literature Review....22

1.1 Colorectal cancer....22

1.2 Oxaliplatin....23

1.2.1 Biotransformation....23

1.2.2 Mechanism of action....25

1.2.3 Tumor resistance and platinum accumulation....26

1.2.4 Cellular transport of OXL and membrane transporters....27

1.3 Copper transporters....27

1.3.1 Contribution of Cu transporters to oxaliplatin transport in cancer cells: current evidence....28

1.3.2 Effect of Cu chelators on the expression of hCTR1....34

1.3.3 Effect of Cu chelators on copper efflux transporters....35

1.3.4 Cu induces degradation or internalization of hCTR1....35

1.3.5 Cu induces trafficking of ATP7A and ATP7B....38

1.3.6 Expression of hCTR1, ATP7A and ATP7B in colorectal cancer tissues....39

1.4 Possible roles of copper in chronic colitis and colorectal cancer....42

1.4.1 Pathological transformation from chronic colitis to colorectal cancer....42

1.4.2 Copper homeostasis and chronic colitis 43
1.4.3 Contribution of copper to the development of colorectal cancer 45
1.4.4 Animal models of chronic colitis and colorectal cancer.....47
1.5 Rationale of study.....48
1.6 Aims of thesis 49

Chapter 2 Materials and Methods.....51
2.1 Chemicals and reagents 51
2.2 Cell culture.....51
2.3 Establishment of overexpressing DLD-1/hCTR1 colorectal cancer cells 52
2.3.1 pCMV6 vector 52
2.3.2 Transfection 53
2.4 MTT assay and colony forming assay 54
2.4.1 MTT assay 54
2.4.2 Colony forming assay.....54
2.5 Western blotting assay.....55
2.6 Reverse transcription polymerase chain reaction (RT-PCR) 56
2.7 Fluorescent immunocytochemistry.....57
2.8 Processing of tumor samples 58
2.8.1 Collection of human tissues.....58
2.8.2 Tissue embedding.....58
2.8.3 Sectioning of human tissues 58
2.8.4 Haematoxylin and eosin staining (H&E staining).....59
2.9 DAB-based immunohistochemistry 59
2.10 Statistical analysis.....60

Chapter 3 Recombinant Overexpression of hCTR1 Enhances Oxaliplatin Cytotoxicity and Uptake in Human Colorectal Cancer Cells.....61
3.1 Introduction.....61
3.2 Experimental design 62
3.2.1 Establishment of overexpressing DLD-1/hCTR1 colorectal cancer cells 62
3.2.2 Sensitivity of transfected cells to oxaliplatin and $CuCl_2$ (MTT and colony forming assay) 63
3.2.3 Detection of platinum anticancer drugs using a fluorescent probe FDCPt1 64
3.3 Results 65

3.3.1 Establishment of hCTR1-overexpressing colorectal cancer cell line 65
3.3.2 Overexpression of hCTR1 enhances the cytotoxicity of copper chloride in colorectal cancer DLD-1 cells 69
3.3.3 Overexpression of hCTR1 enhances the cytotoxicity of oxaliplatin in colorectal cancer DLD-1 cells 71
3.3.4 Overexpression of hCTR1 enhances cellular uptake of oxaliplatin in colorectal cancer cells 74
3.4 Discussion 76
Chapter 4 Effects of Cu Chelators and Cu chloride on Oxaliplatin Cytotoxicity in Colorectal Cancer Cells 80
4.1 Introduction 80
4.2 Experimental design 81
4.2.1 Characterization of the expression of copper transporters in colorectal cancer cell lines 81
4.2.2 Measurement of the sensitivity of colorectal cancer cell lines to oxaliplatin 82
4.2.3 Studies on the effect of compounds on hCTR1 expression using Western blotting 82
4.2.4 Studies on the effect of copper chelators, copper chloride and oxaliplatin on the cellular localization of copper transporters using immunocytochemistry 83
4.2.5 Toxicity assays of DLD-1 and SW620 cells in the presence of copper chelators or copper chloride 84
4.3 Results 85
4.3.1 Endogenous expression of Cu transporters hCTR1, ATP7A and ATP7B in human colorectal cancer cells 85
4.3.2 Differential sensitivity of colorectal cancer cell lines to oxaliplatin 95
4.3.3 Cu chelators up regulate hCTR1 expression in DLD-1 cells and SW620 cells colorectal cancer 98
4.3.4 Cu chelators enhance oxaliplatin cytotoxicity in DLD-1 cancer cells, but not SW620 cancer cells 104
4.3.5 Cu chelators do not alter expression pattern of ATP7A and ATP7B in colorectal cancer cells 106

4.3.6 Cu chloride does not alter the expression of Cu transporters and oxaliplatin cytotoxicity in colorectal cancer cells 109
4.3.7. Effects of oxaliplatin on the expression of hCTR1, ATP7A and ATP7B in colorectal cancer cells.....114
4.4 Discussion.....118
Chapter 5 Expression of Copper Transporters in Human Tumor Tissues of Patients With Colorectal cancer 124
5.1 Introduction.....124
5.2 Experimental design 125
5.2.1 Patient recruitment.....125
5.2.2 Histological examination of colon samples.....125
5.2.3 Evaluation of immuno-histochemical staining and statistical analysis 126
5.3 Results 126
5.3.1 Clinical and histologic information of the matched CRC tissues.....126
5.3.2 Development of semi-quantitative analysis of DAB stained immunohistochemical images.....128
5.3.3 Immunochemical findings 132
5.4 Discussion.....140
Chapter 6 Expression of Copper Transporters in Colon Tissues of Winnie Mice With Chronic Colitis or Colonic Dysplasia.....143
6.1 Introduction.....143
6.2 Experimental design 144
6.3 Results 146
6.3.1 Histological confirmation of chronic colitis in *Winnie mice* and colonic dysplasia in DSS-treated *Winnie* mice 146
6.3.2 Example of semi-quantitative analysis of DAB-stained images of immunohistochemistry 148
6.3.3 Expression of copper transporters in mouse tissues 151
6.4 Discussion.....157
Chapter 7 General Discussion 160
7.1 Human Cu uptake transporter 1 contributes to the uptake and cytotoxicity of oxaliplatin 161
7.2 Cu chelators enhance the cytotoxicity of oxaliplatin.....164

7.3 The differential expression of Cu transporters in colorectal cancer cells and tissues 167
7.4 The expression of Cu transporters in colon tissues of *Winnie* mice with chronic colitis or colonic dysplasia 168
7.5 Future directions 169
7.6 Conclusion 170
References 171
Supplementary Figures 192
Figure S-1: 192
Figure S-2: 198
Figure S-3: 204
Appendices 210
Appendix 1: Full article of Publication 1 by Cui H *et al.* 210
Appendix 2: Cover page of Publication 2 by Cui H *et al.* 219
Appendix 3: Human ethics approval letter: 220

List of Abbreviations

ATTM	ammonium tetrathiomolybdate
ATCC	American Type Culture Collection
ABC	human ATP-binding cassette proteins
BCS	bathocuprione disulphonate
hCTR1	human copper uptake transporter 1
CRC	colorectal cancer
CD	Crohn’s disease
CWQ	Chang-Wei-Qing
COX	cytochrome c oxidase
CMV	cytomegalovirus promoter
CFA	colony forming assay
D-P	D-penicillamine
DSBs	DNA double-strand breaks
DSS	dextran sulphate sodium
DMEM	Dulbecco's Modified Eagle's medium
H&E	hematoxylin and eosin staining
IHC	immunohistochemistry
ICC	immunocytochemistry
IBD	inflammatory bowel diseases
LOX	lysyl oxidase
MATE	multidrug and toxin extrusion protein
MCS	multiple cloning site
SOD	superoxide dismutase
OXL	oxaliplatin
OCT	organic cation transporter
SSAO	semicarbazide-sensitive amine oxidase
TGN	Trans-Golgi network

List of Tables

Table 2-1. Sense and anti-sense primers for copper transporter or GAPDH genes 56

Table 5-1. Patient characteristics.....126

Table 5-2. Semi-quantitative analysis of DAB-stained immunohistochemistry images for hCTR1 positivity in tumor tissues of human colorectal cancer.....132

Table 5-3. The expression of copper transporters in human colon samples.....139

Table 6-1. The expression percentage of copper transporters in colonic tissues of mice 156

List of Figures

Figure 1-1. Chemical structure of oxaliplatin....24
Figure 1-2. Oxaliplatin-DNA adducts....25
Figure 1-3. Molecular structure of hCTR1....29
Figure 1-4. Putative structure of ATP7A in plasma membrane....32
Figure 3-1. hCTR1 protein level of selected clones of colorectal cancer DLD-1 cells stably transfected with SLC31A1 gene or the corresponding empty vector....67
Figure 3-2. hCTR1 protein level in overexpressing DLD-1/hCTR1 line and mock control line....68
Figure 3-3. Overexpression of hCTR1 enhances the cytotoxicity of $CuCl_2$ in colorectal cancer DLD-1 cells....69
Figure 3-4. Overexpression of hCTR1 enhances the inhibitory effect of $CuCl_2$ on the colony forming ability of colorectal cancer DLD-1 cells....71
Figure 3-5. Overexpression of hCTR1 enhances the cytotoxicity of oxaliplatin in colorectal cancer cells measured by the MTT assay....72
Figure 3-6. Overexpression of hCTR1 enhances the inhibitory effect of OXL on the clonogenic potential of colorectal cancer DLD-1 cells measured by the CFA....74
Figure 3-7. Overexpression of hCTR1 enhances cellular uptake of oxaliplatin in colorectal cancer DLD-1 cells....76
Figure 4-1. Endogenous expression of hCTR1 in human colorectal cancer cells....87
Figure 4-2. Cellular distribution of hCTR1 protein in colorectal cancer cells....88
Figure 4-3. Localization of hCTR1 at plasma membrane of colorectal cancer cells....88
Figure 4-4. Endogenous expression of ATP7B in colorectal cancer cells....90
Figure 4-5. Cellular distribution of ATP7B in colorectal cancer cells....92
Figure 4-6. Endogenous expression of ATP7A in colorectal cancer cells....93
Figure 4-7. Cellular distribution of ATP7A protein in colorectal cancer cells....95
Figure 4-8. Cytotoxicity of oxaliplatin (OXL) in colorectal cancer cells following a 72 h-drug exposure....96
Figure 4-9. Short-exposure cytotoxicity of oxaliplatin (OXL) in colorectal cancer cells....97
Figure 4-10. Temporal effects of Cu chelators on hCTR1 protein levels in colorectal cancer DLD-1 cells....101
Figure 4-11. Temporal effects of Cu chelators on hCTR1 protein levels in colorectal cancer SW620 cells....103

Figure 4-12. Cu chelators potentiate oxaliplatin (OXL) cytotoxicity in colorectal cancer DLD-1 cells, but not SW620 cells 105
Figure 4-13. Cu chelators do not alter the expression of ATP7A in colorectal cancer DLD-1 and SW620 cells 107
Figure 4-14. Cu chelators do not alter the expression of ATP7B in the colorectal cancer cells DLD-1 and SW620 109
Figure 4-15. Cu chloride does not change the expression level and patterns of hCTR1 in DLD-1 and SW620 colorectal cancer cells 111
Figure 4-16. Copper chloride does not alter the expression of ATP7A and ATP7B in DLD-1 and SW620 colorectal cancer cells 112
Figure 4-17. Cu chloride does not alter oxaliplatin (OXL) cytotoxicity in colorectal cancer cells 114
Figure 4-18. Oxaliplatin (OXL) increases hCTR1 protein level in colorectal cancer cells ..116
Figure 4-19. Oxaliplatin (OXL) does not alter the expression pattern and intensity of Cu efflux transporters ATP7A and ATP7B in colorectal cancer cells 117
Figure 5-1. Histological confirmation of normal and cancerous colon and rectum tissues from patients with colorectal cancer.....128
Figure 5-2. Semi-quantitative analysis of DAB stained immunohistochemical images of hCTR1 in tumor tissues of colorectal cancer patient.....132
Figure 5-3. Representative immunohistochemical images of hCTR1, ATP7A and ATP7B in tumor and the matched normal tissues 138
Figure 6-1. Representative colon microphotographs of histology of colitis of *Winnie* mice and colonic dysplasia in DSS-treated *Winnie* mice.....147
Figure 6-2. Semi-quantitative analysis of DAB stained immunohistochemical images of mCTR1 in colonic tissues of *Winnie* mice 151
Figure 6-3. Semi-quantitative analysis of representative DAB-stained images showing immunostaining of mCTR1, ATP7A and ATP7B in colonic tissues 156
Figure S-1. Semi-quantitative analysis of representative DAB stained immunohistochemical images of hCTR1 in tumor and the matched normal tissues of four colorectal cancer patients.....197
Figure S-2. Semi-quantitative analysis of representative DAB stained immunohistochemical images of ATP7A in tumor and the matched normal tissues of four colorectal cancer patients.....203

Figure S-3. Semi-quantitative analysis of representative DAB stained immunohistochemical images of ATP7B in tumor and the matched normal tissues of four colorectal cancer patients.....209

Abstract

Colorectal cancer (CRC) is a major health problem and cause of morbidity and mortality worldwide. The clinical efficacy of oxaliplatin (OXL), a commonly used chemotherapy agent, is limited by tumor resistance largely due to reduced drug accumulation. The role of copper (Cu) transporters in the transport and pharmacology of OXL is unclear, including Cu uptake transporter 1 (CTR1), and efflux transporter Cu^{+}-transporting P-type ATPase ATP7A and ATP7B. The project aimed to investigate the contribution of Cu transporters to the uptake and cytotoxicity of OXL, and their expression in CRC.

CRC cells were engineered to overexpress *hCTR1* gene (hCTR1/DLD-1 cells) or the empty vector as mock control cells to study the uptake and cytotoxicity of OXL. A fluorescent probe FDCPt1 was used to visualize the cellular uptake of OXL-derived monofunctional platinum bio-transformed products. The expression profile of Cu transporters was characterized in colorectal cancer cell lines before evaluating the synergism between Cu chelators and OXL in colorectal cancer cells based on their regulation on hCTR1 protein. The expression of copper transporters was also investigated in paired patient tumor biopsies. In addition, a colitis model of *Winnie* mouse carrying point mutation of *Muc2* gene and a dextran sodium sulphate (DSS)-induced colonic dysplasia model were used to determine the correlation of Cu transporters with these precancerous conditions.

Overexpression of hCTR1 contributes to OXL cytotoxicity and uptake in recombinant colorectal cancer DLD-1 cells, with increased sensitivity and stronger FDCPt1-derived fluorescent signals than mock cells.

The mRNA of Cu transporters was detected at constantly high levels in colorectal cancer cell lines with different origins. hCTR1 protein was expressed abundantly with the expression intensity higher than ATP7A or ATP7B across cell lines. Cu chelators, ammonium tetrathiomolybdate, and D-penicillamine, and bathocuprione disulphonate up regulated hCTR1 protein levels and enhanced the cell-killing capacity of OXL in some of CRC cells.

Human colonic tissues were stained positive for Cu transporters with varying percentage of staining between individual patients. Semi-quantitative analysis using de-convolution method shows hCTR1 staining seems to be similar between tumor and the matched normal tissues. ATP7B expression exhibits a trend towards up regulation in tumor tissues compared to that of normal tissues, suggesting this protein may be involved in the development of colonic malignancy.

Chronic intestinal colitis and dysplasia were confirmed histologically in colonic tissues of *Winnie mice*, and DSS-treated *Winnie* mice, respectively. Mouse Cu transporter 1 (mCTR1) was detected in colonic tissues of these animals, but with varying localization and intensity. The percentage of mCTR1 staining increased in colonic tissues of *Winnie* mice, but decreased in tissues of dysplasia model compared to that of the normal colon tissues. ATP7A and ATP7B expression did not change in colitis tissues but decreased significantly in dysplasia tissues.

In conclusion, our work demonstrated for the first time the positive involvement of hCTR1 in the uptake and cytotoxicity of OXL in some colorectal cancer cells genetically or pharmacologically modified to overexpress hCTR1 protein. The abundant expression of hCTR1 in human colorectal cancer cells and tumor tissues highlighted again the importance of copper in the development of colorectal adenocarcinoma. The altered expression of copper transporters in the precancerous colonic tissues of *Winnie* mice suggests copper homeostasis may be disturbed during the chronic progress of colorectal carcinogenesis.

Chapter 1 Literature Review

1.1 Colorectal cancer

Colorectal cancer (CRC), also known as bowel cancer, is the third most common cancer and the fourth most common cause of cancer death globally [1]. In Australia, CRC is the second most common cancer with ~14,900 new cases and ~4,000 deaths annually over the past few years. These numbers are predicted to continue to increase in the future due to the aging population [2]. CRC causes significant economic and social burden in this country, with an estimated total health care expenditure of $235 million on this disease in 2001 [3].

Colorectal cancer is generally classified into three types, namely, sporadic, familial and hereditary CRC, accounting for ~80%, 15% and 5% of all cases respectively. The hereditary CRC is caused by inherited mutations of certain genes, such as familial adenomatous polyposis and hereditary non-polyposis colorectal cancer [4,5]. The TNM system is used clinically for staging CRC based on its severity and the spread according to three variables: size and extension of the primary tumor (T), nearby lymph nodes that are involved (N), and information about distant metastasis (M) [6]. Common diagnostic methods are immunochemical fecal occult blood test, sigmoidoscopy, colonoscopy and faecal DNA test.

Treatment options for CRC mainly include mainly surgery, radiotherapy and chemotherapy. Although factors such as the age of the patients and their health status can influence treatment options, the final selection of therapy modality is mainly based on the staging of the cancer. Although approximately 70-80% newly diagnosed cases are curable by surgery, half of these patients still develop incurable relapses after R0 resection [7]. Therefore, chemotherapy is required to control the recurrence of CRC by killing the non-visible residual tumor cells after surgery. For patients whose tumors are un-resectable, the administration of chemotherapy

drugs has extended median overall survival by 5 months compared to patients who received only supportive care [8].

Chemotherapeutic drugs used for the treatment of CRC include oxaliplatin (OXL), 5-fluorouracil (5-FU), capecitabine and irinotican [8]. Due to the limited efficacy and the tendency of the tumor to acquire resistance for single use of drugs, most of these chemo agents are used in combination as various chemotherapy regimens [9]. Detailed description of each regimen is beyond the scope of this thesis. This chapter primarily concentrates on the description of OXL, as it is the only effective third-generation platinum drugs for advanced CRC and serves as the essential component of many combination chemotherapies regimens.

1.2 Oxaliplatin

The addition of oxaliplatin (OXL) has significantly improved the treatment outcome of 5-FU-based therapy for metastatic colorectal cancer (mCRC), which had been used for decades in clinic with limited efficacy [10]. The role of OXL as an essential component of first-line or second-line treatment regimens for mCRC patients has been established in several landmark clinical trials due to its unique properties in its chemistry, biotransformation and mechanisms of action against colorectal cancer [11].

1.2.1 Biotransformation

OXL consists of an oxalate ligand as leaving group and the diaminocyclohexane (DACH) ligand (Fig. 1-1). The DACH ligand is chemically inert and the bi-dentate oxalate group is subject to attack by two H_2O, Cl_2 ions and HCO_3, forming monochloro-, dichloro-, and Pt(dach)-$(H_2O)_2$ in biological fluids *in vitro* and *in vivo.* These reactions are non-enzymatic and considered as key steps to the activation of the pharmacological effect of OXL [12].

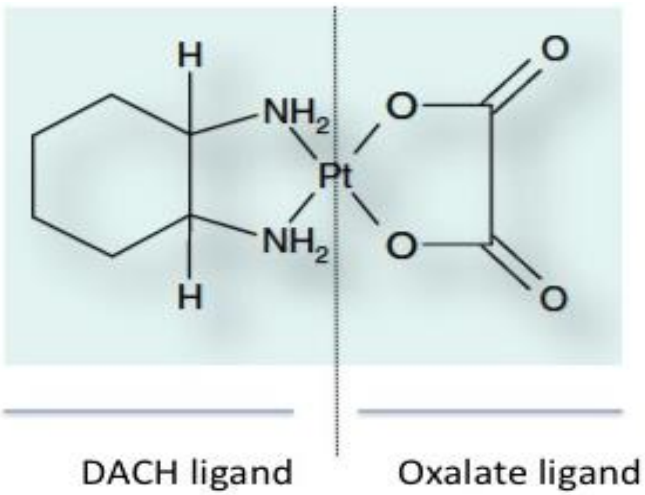

Figure 1-1. Chemical structure of oxaliplatin

Oxaliplatin is composed of DACH and oxalate ligands. Adapted from [13].

Two of the biotransformation products of OXL, namely, (dach)(H_2O)Cl and Pt(dach)-(H_2O)$_2$ have been shown to be 2.9- and 3.7-fold more cytotoxic than the parental drug against colon cancer HT-29 cells. These two derivatives display higher cellular uptake compared to parental OXL. When colon cancer HT-29 cells are incubated with these two drug metabolites, 71-74% of Pt(dach)(H_2O)Cl and Pt(dach)-(H_2O)$_2$ are detected in cytosol. In aqueous solution, OXL is about 40-fold less reactive than Pt (dach)Cl_2 and more than 900-fold less reactive towards DNA than Pt(dach)(H_2O)$_2$ [14].

Momofucntional species seem to be the predominant biotransformation products of OXL detected in *in vitro and in vivo* experiments. Using ^{3}H-labeled OXL, more than 17 platinum complexes in plasma ultrafiltrate have been identified after a 24-h incubation, including methionine-bound platinum products (6%), monochloro (37%), monochlorocreatinine (9%), dichloro (10%), monocreatinine (4%) and other species [15]. Similarly, monochloro-DACH platin accounts for 31-100% of the biotransformation products identified in the plasma ultrafiltrate of cancer patients after a 2-h infusion with 130 mg/m^2 OXL [16].

1.2.2 Mechanism of action

OXL exerts its pharmacological effect through the formation of Pt-DNA adducts [17]. Upon entering cancer cells, OXL binds to the N (7) site of the guanine residues, forming transient mono-adducts and stable di-adducts. The biotransformation products of OXL then form approximately 60–65% intra-strand GG, 25-30% intra-strand AG, 5-10% intra-strand GNG, and only 1-3% inter-strand GG adducts with DNA double strands [18]. Intra-strand adducts cause the most severe DNA lesions, which further inhibit DNA replication and transcription [19] (Fig. 1-2), leading to activation of apoptotic pathway involving caspase 3 activation, translocation of apoptosis regulator BAX in the mitochondria, and release of cytochrome C in the cytosol [17].

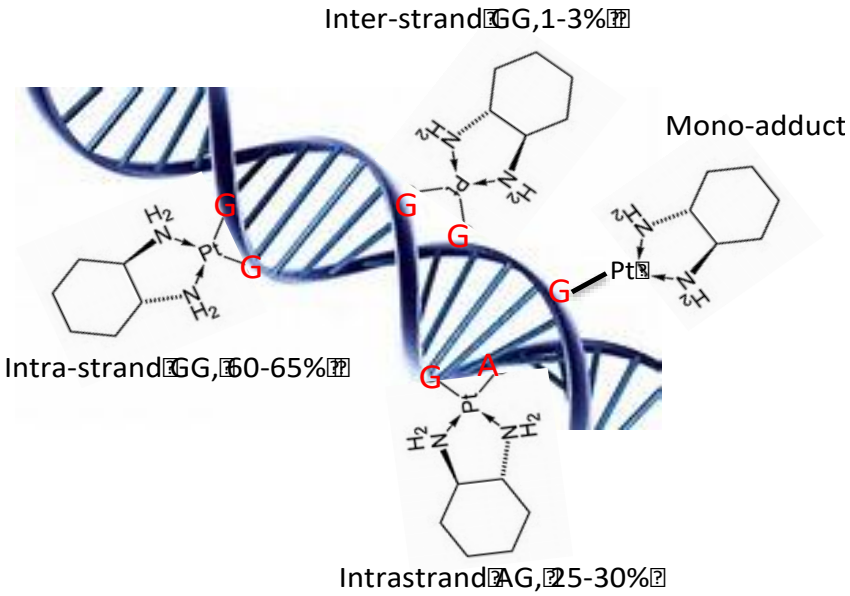

Figure 1-2. Oxaliplatin-DNA adducts

G, A represent guanine and adenine bases, respectively. OXL binds covalently with G and A, forming intra-strand GG, intra-strand AG and inter-strand GG. Figure was adapted from [20].

Although OXL and cisplatin form the same type of adducts at the same sites on DNA, the bulkier size of the DACH-Pt-DNA, and the constraint of the N–Pt–N bond angle can explain the superior cytotoxic effect over cisplatin. Moreover, these two features also prevent the mismatch repair proteins and some damage-recognition proteins from binding properly to OXL-GG adducts [21]. In addition, the cytotoxic effect of OXL on various malignancies is mediated through other less-defined pathways, including inhibition of DNA and messenger RNA synthesis as well as activation of immunologic death [22].

1.2.3 Tumor resistance and platinum accumulation

Despite improved efficacy and tolerability of OXL compared to other platinum drugs, the 5-year survival rate of CRC patients after OXL treatment is only 12.5% [23]. Intrinsic resistance and acquired resistance are considered as the significant limitation for its use [24]. Therefore, understanding the mechanisms behind drug resistance is essential to developing targeted therapies to overcome this problem.

The mechanisms of OXL resistance are not fully understood yet but it is generally thought to be a multiple factors including increased drug inactivation, improved drug-induced DNA damage repair, and evasion of apoptosis in tumor cells [25]. However, a reduced cellular accumulation of OXL has been frequently reported in unwanted drug-resistant human cancers including colorectal cancer, ovarian cancer, and squamous cancer. For instance, the cellular uptake of OXL and its DNA binding in OXL-resistant human colon cancer S1 cells is reported to be only 20% and 9% compared to the parental S1 cells, respectively. The uptake of OXL is inversely proportional to the IC_{50} for five S1 cell lines [26]. The accumulation of OXL in platinum resistant A2780-E (80) is only 3-38% of the parental A2780 cells over a broad drug concentration range [27]. The OXL-resistant human ovarian cancer 2008, A2780, IA-9 and

IGROV-1 cells and the squamous cancer UMSCC10b cell line exhibited an average of 27 ± 10 % reduction of cellular OXL uptake compared to that of the matched sensitive cells [28].

Cellular accumulation of drugs is dependent on the movement of drug in both directions, namely, an inward uptake process and an outward efflux process. Therefore, studying the determinants of these two transport processes is crucial to understanding drug accumulation and its relation to tumor resistance. This is particularly important to OXL, as high cellular OXL accumulation is correlated with increased platinum binding to its putative target, the nucleus DNA, and favorable antitumor activity [27].

1.2.4 Cellular transport of OXL and membrane transporters

For many years, it has been assumed that platinum drugs enter cells through passive diffusion, which is considered to be concentration-dependent and non-saturated [29,30]. However, it has become apparent that membrane transporters are likely to mediate the translocation of OXL across biological membrane. Membrane transporters that have been implicated in the cellular transport and tumor resistance to OXL, including organic cation transporters, multidrug and toxin extrusion protein and the human ATP-binding cassette proteins [31,32]. These transporters are thought to either control the influx of OXL as uptake transporters [33], or regulate the efflux of OXL as efflux transporters [34]. However, the association of copper transporters with cellular uptake of OXL is largely undefined yet compared to those above-mentioned membrane transporters.

1.3 Copper transporters

Cu transporters belong to a group of important proteins that are responsible for the maintenance of copper homeostasis in mammalian cells. The main members include Cu uptake transporter 1 (CTR1), efflux transporters Cu^{2+}-transporting P-type ATPase ATP7A and ATP7B [35]. Current evidence has shown copper transporters are implicated in the transport of OXL despite

the lacking of direct evidence. In addition, the cellular localization and expression of these transporters undergo changes in the presence of Cu chelators, copper salts or platinum anticancer drugs. The mechanisms of these interactions are not clear yet but may become the molecular basis to enhance the cellular accumulation and the cytotoxicity of OXL in colorectal cancer cells.

1.3.1 Contribution of Cu transporters to oxaliplatin transport in cancer cells: current evidence

1.3.1.1 Copper uptake transporter 1 (CTR1)

Human copper uptake transporter 1 (hCTR1) is a major Cu uptake transporter in cells. hCTR1 is a 190-amino acid protein of ~28 kDa, with an extracellular N-terminal domain, three transmembrane domains and a C-terminal tail region containing about 15 amino acids (Fig. 1-3A). hCTR1 is ubiquitously expressed in wide range of cell types, including hepatocytes, C cells of the thyroid and entero-endocrine cells [36]. The subcellular localizations of hCTR1 are reported to be either plasma membrane or peri-nucleus, depending on the cell types and the copper status in the culture of these cells [37]. hCTR1 delivers copper into cytoplasm for the synthesis of cuprous enzymes such as cytochrome c oxidase and copper/zinc superoxide dismutase. These enzymes are crucial to the biological processes such as respiratory oxidation, neurotransmitter synthesis and pigmentation [38]. Structurally, it is reported that three monomers of hCTR1 unit form a stable homotrimer that is embedded in the plasma membrane like a channel [39]. Copper is supposed to pass through this channel through a serial transchelation reactions with methionines, histidines and cystenines in the stacked rings inside this channel [40] (Fig. 1-3B).

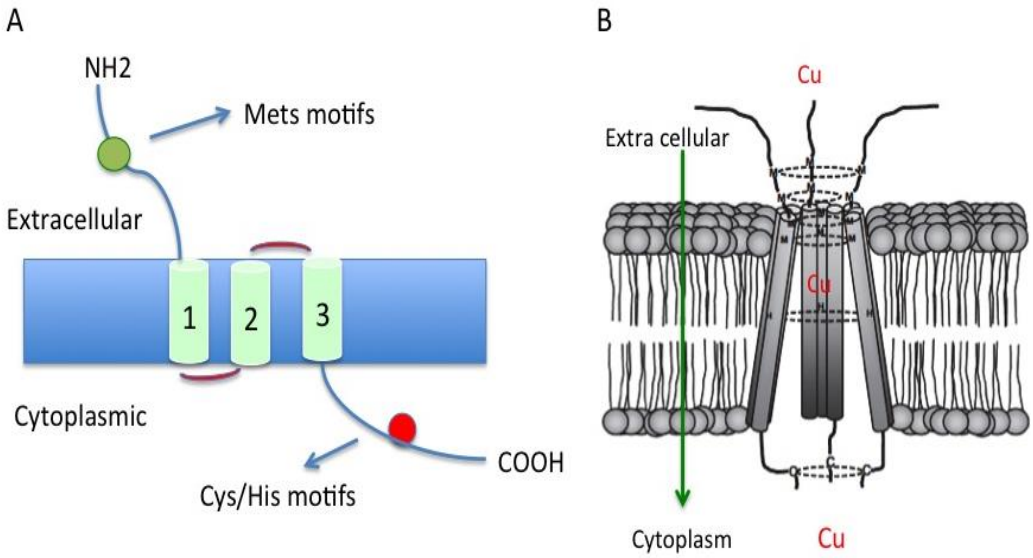

Figure 1-3. Molecular structure of hCTR1

A. hCTR1 monomer is composed of an extracellular N terminus and cytoplasmic C terminus, and three transmembrane domains. B. Three monomers form a channel-shaped trimer through which copper is trans-chelated into the cell [41].

Unexpectedly, early studies show CTR1 may regulate the OXL uptake in some non-cancerous cellular models such as yeast, mouse embryonic, and HEK293 cells. A significant decrease in OXL accumulation is observed in BY4741-YPR124W yeast cells genetically deleted of CTR1 gene compared to that of parental BY4741 strain when exposed to various concentrations of OXL for 1 h [42]. Loss of mouse CTR1 protein (mCTR1) in mouse embryonic fibroblast cells is associated with a substantial reduction of OXL accumulation by 63.7% compared to the $CTR1^{+/+}$ cells when exposed to 2 μM drug for 1 h. This is accompanied with a 1.7 ± 0.6-fold difference in sensitivity to OXL between these two cell lines [43]. When exposed to 300 μM OXL for 5 min, mouse embryonic fibroblasts $CTR1^{-/-}$ cells that do not express CTR1 only accumulate 32% of the drug compared to that of wild-type $CTR1^{+/+}$ cells [44]. Human embryonic kidney 293 cells (HEK293) that are transfected to stably express rat CTR1

(HEK/rCTR1) have shown about 4-fold higher OXL accumulation rate than in HEK293/mock cells (0.0004 vs 0.00012 nmol Pt/mg protein/min/mM). HEK/rCTR1 cells are 3-fold more sensitive than HEK293/mock cells to the cytotoxicity of OXL after 5 min drug exposure [45].

hCTR1 is implicated in the uptake of OXL in gastric adenocarcinoma or small cell lung cancer (SCLC). The role of hCTR1 in OXL transport is investigated in a study using wild type and recombinant gastric adenocarcinoma S3 cells. The RT-PCR analysis shows that hCTR1 mRNA level in resistant gastric adenocarcinoma S3 cells is about 20% lower than that in parental cells TSGH. When exposed to various concentrations of OXL for 4 h, the total platinum accumulation in S3 cells is only 12% of that in TSGH cells at the concentration of 100 μM. The amount of OXL–DNA adducts in S3 cells are about 85% less than that in TSGH cells at the concentration of 100 mM OXL. The amount of OXL–DNA adducts in S3 cells are also about 85% less than those in TSGH cells at the concentration of 100 mM OXL. More DNA double-strand breaks are identified in TSGH cells than that of S3 cells following a 24-h exposure to various concentrations of OXL [46]. Decreased uptake of OXL is found in resistant SCLC cells that exhibit a 50% reduction in hCTR1 mRNA expression compared to the parental SCLC cells. Transfection of hCTR1 gene in SCLC cells increases the uptake OXL compared to the empty vector transfected Mock cells. In addition, the hCTR1 transfected cells become more sensitive to the cytotoxic effect of OXL (IC_{50}: 24.5 ± 3.5 vs 15.5 ± 5.9 μM) [47].

Studies investigating the association of the expression copper transporters with OXL uptake and resistance in colorectal cancer (CRC) are limited. An early study demonstrated for the first time that reduced hCTR1 gene expression is related to OXL resistance in a colorectal cancer cell line. In this study, hCTR1 expression level is significantly reduced in OXL-resistant sub-lines HTOXAR1, HTOXAR2 and HTOXAR3 by 65%, 63% and 46%, respectively as compared to that in parental cell line HT-29 [48]. Similarly, hCTR1 mRNA expression levels is demonstrated to be positively correlated with the accumulation of OXL in a panel of CRC

cell lines including Caco-2 DLD-1, HCT-15, HCT116, LS180, SW620 and WiDr cells using a Pearson's correlation analysis [49]. The hCTR1 mRNA expression levels are highly related to the accumulation of OXL in CRC and ovarian cancer cells [50].

However, there are also some conflicting reports showing hCTR1 is unlikely to be the transporter of OXL. For instance, the uptake rate of OXL does not differ significantly between wild type mouse embryonic fibroblast cells and its subline without the expression hCTR1 [42]. The accumulation of OXL is found not hCTR1-dependent in CRC cells exposed to higher concentrations of OXL, suggesting the involvement of other mechanisms other than hCTR1 at this condition [51]. The hCTR1 expression levels in tumors of 39 CRC patients are not correlated with the treatment outcome for these patients following OXL-based chemotherapy in a recent small case control study [52].

1.3.1.2 Efflux transporters ATP7A and ATP7B

Human Cu transporting P-type ATPase ATP7A protein, also known as Menkes' protein, transports Cu outward across cell membrane using energy generated from ATP hydrolysis [53]. The protein structure consists of a cytosolic amino-terminus, eight transmembrane helices, an ATP-binding domain, an actuator domain and a cytosolic carboxyl-terminus (Fig. 1-4) [54]. The N-terminus of human ATP7A contains six metal binding sites that are capable of binding to Cu. The eight transmembrane helices form a channel for copper translocation.

In steady state, ATP7A is localized in the Golgi apparatus, where it is responsible for transporting Cu^{+} to copper-containing enzymes, such as lysyl oxidase, which is essential to maintaining the structure and function of connective tissue and the nervous system [55]. When extracellular copper levels are elevated, ATP7A traffics to the cellular membrane to excrete excessive Cu until a new copper equilibrium is reached [54]. ATP7A gene is expressed in all

tissues except the liver. The function of ATP7A is tissue specific. In the intestine, it regulates Cu^{+} absorption from food into blood circulation. In other tissues, it eliminates excess copper out of cells or delivers copper to Golgi apparatus for synthesis of important cuprous enzymes. [56]. Mutation of ATP7A gene severely blocks the transport of copper from lumen to portal circulation, causing severe copper deficient Menkes Disease.

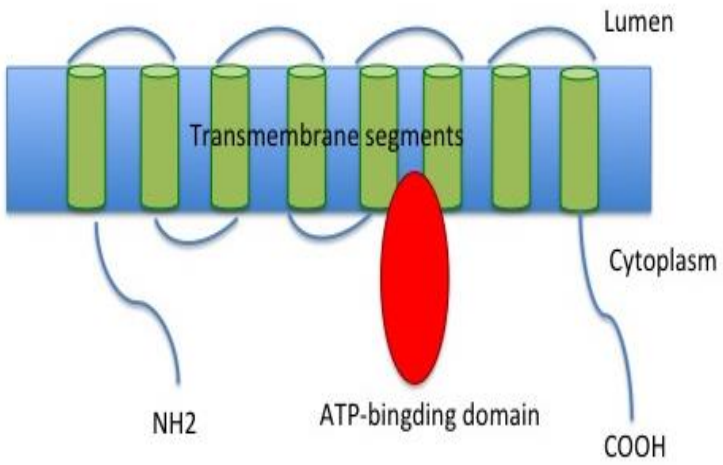

Figure 1-4. Putative structure of ATP7A in plasma membrane

ATP7A is composed of eight trans-membrane segments, one N terminus, one C terminus on the cytoplasmic and an ATP-binding domain providing the energy for transport of copper.

ATP7B is another Cu transporting P-type ATPase, also known as Wilson's disease protein (WND), which is approximately 57% homologous to the amino acid sequence of ATP7A. Like ATP7A, it is composed of a cytosolic amino-terminus, eight transmembrane helices, an ATP-binding domain, an actuator domain and a cytosolic carboxyl-terminus (Fig 1-4). ATP7B expression is more tissue specific than ATP7A with the highest expression in liver compared to ATP7A. ATP7B is predominantly localized in the trans-Golgi network of

hepatocytes, functioning to excrete excessive copper into the bile. In Wilson's disease, mutation of ATP7B gene leads to severe copper toxicity in liver and kidney [57].

Studies investigating the links between ATP7A or ATP7B and OXL resistance in colorectal cancer (CRC) are sparse, yet still suggest some correlation. An early clinical study shows patients with high mRNA levels of ATP7B in colorectal cancer have a poor treatment outcome after OXL-based therapy, suggesting that elevation of ATP7B expression is associated with OXL resistance [58]. The expression of ATP7A is positively correlated with the IC_{50} values of OXL in 7 CRC cell lines. [59]. The OXL-resistant CRC HTOXAR1, HTOXAR2 and HTOXAR 3 cells exhibit markedly lower ATP7A and ATP7B gene levels compared to that of parent HT-29 cells [60]. Recently, it has been reported that 5-FU could suppress the expression of the ATP7B in colon cancer LS180 cell line, which results in the re-sensitization of these cells to OXL. This is partly because of diminished capacity of ATP7B for sequestrating OXL into the endoplasmic reticulum [45]. The ATP7A expression levels are about 3-fold higher in S3 cells compared to that of parental TSGH cells, though the ATP7B protein levels are similar between these two cell lines [61-63]. Taken together, all these studies suggest that copper efflux transporters ATP7A and ATP7B are more or less associated with OXL resistance in different cancer types, although the mechanisms involved remain unclear.

However, there are some conflicting reports about the role of ATP7A and ATP7B in predicting treatment outcome of OXL, and their contribution to the OXL accumulation and cytotoxicity. While it has been reported that ATP7B expression level is inversely correlated with treatment of platinum drugs for various cancers [51], a recent small case control study does not show a correlation between the expression levels of ATP7B in tumor biopsies and the response to OXL in the CRC patients [64]. Contrary to expectation, the expression levels of ATP7A and ATP7B do not seem to be significantly altered in the resistant and sensitive small cell lung cancer cell lines [65]. The overexpression of ATP7A or ATP7B in MeMNK and MeWND

cells render these cells more sensitive to OXL, which is contradictory to other reports [66]. ATP7A-overexpressing ovarian cancer cells exhibit significantly higher accumulation of OXL compared to that of Me32a cells following exposure to 6 or 15 μM drug for 24 h [67]. Similarly, stable overexpression of ATP7A in human ovarian cancer A2780 cells reasonably causes a 0.6-fold more resistance of these cells to OXL compared to the empty vector-transfected control. This is correlated with a 1.7-fold more OXL accumulation in ATP7A-overexpressing cells other than the expected impairment of drug accumulation [68].

1.3.2 Effect of Cu chelators on the expression of hCTR1

The expression of hCTR1 is consistently reported to be elevated in cells cultured in copper-depleted conditions to meet the nutrition demand [69]. Therefore, Cu chelators can be utilized to enhance the cellular accumulation of platinum drugs in resistant cancer cells by increasing the expression of hCTR1, a possible uptake transporter of platinum drugs.

Earlier, it has been demonstrated that transfection of glutathione, an endogenous Cu scavenger up regulates hCTR1 protein level and enhances the uptake and cytotoxicity of cisplatin in small cell lung cancer cells [70]. Pre-incubation with non-toxic level of tetrathiomalybedate (ATTM), a clinically used Cu chelator, is shown to increase the sensitivity of human cervical cancer SiHa and ovarian cancer cells A2780, SKOV3 and OVCA4 to the cytotoxic effect of cisplatin, whereas this synergistic effect is not observed in CTR1-knockout mouse embryonic fibroblasts, suggesting a dependence on CTR1 [71]. ATTM, trientine and D-penicillamine (D-P) enhance the uptake and cytotoxicity of platinum anticancer drugs in ovarian cancer 2008, IGROV1, OVCAR3 and SKOV-3, glioblastoma A172 and small cell lung cancer cells, which is accompanied by an increase of hCTR1 expression [72].

Cu chelators have shown synergism with cisplatin in animal or human cancers in an *in vivo* context. D-P has been shown to potentiate the anti-tumour activity of cisplatin in a mouse

small cell cancer model which has higher hCTR1 expression in tumours [70]. ATTM enhances the antitumor activity of cisplatin in the HPV16/E2 mice, a cervical cancer model. This is accompanied with a 2.7-fold increase of cisplatin-induced Pt-DNA adducts in the cancerous cervix and a 23% reduction of blood plasma copper level [73]. Trientine has been shown to reduce plasma copper level and re-sensitize ovarian cancer patients to carboplatin with clinical responses in 4/5 patients who had advanced diseases that are resistant to previous chemotherapy [74].

1.3.3 Effect of Cu chelators on copper efflux transporters

Cu chelators are generally not considered to be able to change the localization of Cu efflux transporters, however they are found to reduce the expression of ATP7A [74]. Therefore, Cu chelators can be utilized to enhance the accumulation of platinum drugs by reducing the expression of Cu efflux transporter ATP7A, a possible efflux transporter of platinum drugs.

ATP7A is identified as a relevant factor for mediating the cisplatin resistance in human breast cancer cell lines in an RNAi library-screening assay. Cisplatin combined with ATTM down regulates the ATP7A expression *in vitro* and *in vivo* cancer models. The amount of cisplatin bound to nucleus DNA in cisplatin/ATTM treated cells is significantly increased compared to that of cisplatin resistant cells. Cisplatin/ATTM double treatment induces 20% decrease of total cell survival for human breast MB-MDA-231 cancer cell line compared to that of cells treated with cisplatin alone. The enhanced anti-cancer activity of this double therapy can be observed in MDA-MB-231 xenograft mice intraperitoneally injected with cisplatin at 6-mg/kg body weight [75].

1.3.4 Cu induces degradation or internalization of hCTR1

hCTR1 protein undergoes numerous biological events in wide range of cell lines that are exposed to excessive copper, including endocytosis, degradation and internalization [76].

These alterations are assumed to result in functional inhibition of hCTR1 to cope with the toxic effect of copper [76].

The hCTR1-copper interaction is firstly reported in both Chinese Hamster Ovary (CHO), and HEK293 cells [76]. hCTR1 localizes in plasma membrane of CHO cells cultured in basal medium. When exposed to elevated copper, it redistributes to the cytoplasm with an apparent punctate vesicular distribution throughout the cytoplasm. The endocytosis of hCTR1 is observed in HEK293 cells exposed to copper for 10 to 180 min. hCTR1 is degraded when the exposure is extended to 2 h. Interestingly, endocytosis even happens when cells are exposed to basal medium for 5 min. The endocytosis is tested to be clathrin-dependent after using specific markers for endocytosis [77].

The copper-induced endocytosis or degradation is a common occurrence in various cancer cells such as breast cancer PMC42-LA, ovarian cancer OVCAR3 and SCOV3 cells, human hepatic cancer HepG2 cells, and cervical cancer cells when exposed to both 2.5 μM and 20 μM copper for 30 min [77]. The phenomena are also repeatedly reported in other non-cancerous cell lines, including human epithelial kidney 293 cells, the Madin-Darby canine kidney epithelial cells, and CHO cell lines [78]. The conserved His-Cys-His residues are considered to be essential to the regulatory endocytosis of hCTR1 in response to elevated copper [79]. The model of endocytosis of CTR1 in mammalian cells has recently been proposed. According to this model, hCTR1 internalizes through clathrin or dynatin-mediated pathways. It translocates to the plasma membrane through Rab-11-dependent recycling pathway [80]. However, there are also conflicting reports regarding the response of hCTR1 to Cu. For example, it is found that CuO up regulates both the mRNA and protein levels of hCTR1 in Caco-2 cells [81].

Interestingly, such internalization and degradation of hCTR1 has also been reported following OXL addition to human cancers, probably through a proteasome-mediated pathway. Hence, compounds that can prevent the degradation of hCTR1 have the potential to enhance the cytotoxic effect of OXL, including bortezomib and some plant-derived anti-cancer compounds. The synergistic effect is firstly observed in combination study of OXL with bortezomib in the treatment of cisplatin-resistant ovarian cancer A2780, A2780cisR, A2780ZD0473R and SKOV-3 cells [82]. This is attributable to the role of bortezomib as proteosomal inhibitor to prevent the degradation of hCTR1 as documented in other studies.

Chang-Wei-Qing (CWQ), a Chinese herbal formula, used clinically to treat cancers shows synergistic effect with OXL for the treatment of colorectal cancer partly by restoring the down regulation of hCTR1 caused by OXL. OXL triggers the degradation of hCTR1 gene and protein in colon tumour tissue grafted in nude mice. The combination of CWQ/OXL restores the hCTR1 expression in the tumour and enhances the antitumor effect of OXL by 53.6%. The survival time of nude mice bearing the tumours is significantly prolonged in CWQ/OXL group compared to that of OXL group [83].

β-elemene, a compound extracted from the Chinese herb, Curcuma Wenyujin, has been approved by China's State Food and Drug Administration. The immunohistochemical study shows the hCTR1 in tumour tissue of a mouse model is decreased after treatment with OXL. The levels of hCTR1 in OXL/*β*-elemene group are restored to that of control group. Consistent with these results, OXL plus *β*-elemene significantly enhance the anti-tumour activity in the mouse model implanted with human hepatoma MHCC97H cells, compared to that of OXL alone [84].

1.3.5 Cu induces trafficking of ATP7A and ATP7B

ATP7A and ATP7B transporting proteins are closely related to each other in both structure and function. These two proteins have both biosynthetic and protective roles in cellular copper homeostasis. Under normal conditions, both proteins are located in the trans-Golgi network (TGN) of the cell. They resurface to the plasma membrane or vesicles around the membrane when cellular copper is excessive, thus pump out copper to restore copper homeostasis [85].

For instance, a 3-h incubation with 10 μM copper causes apparent trafficking of ATP7A from TGN to the cell periphery in B16F10 melanoma cells [86]. ATP7A shows predominant TGN localization in cervical cancer HeLa cells under steady-state conditions. When exposed to 200 μM $CuCl_2$ for 2 h, it moves to the cell surface [87]. Similar response modality is observed in human ovarian cancer 2008 cells, and human breast cancer PMC42 cells [80]. Similarly, copper also induces the redistribution of ATP7B from the TGN to a cytoplasmic vesicular compartment in hepatoma cells HepG2, human bladder carcinoma cells HBT9, and human cervical HeLa cells [88]. However, it is also possible that copper level can be rebalanced by changing the expression of ATP7A and ATP7B. For example, CuO and $CuSO_4$ increase the mRNA and protein levels of ATP7A in Caco-2 cells [89] in a concentration dependent way. Copper at 25 μM increases ATP7A mRNA level by 3.1 folds after 4 to 24-h exposure [90]. Copper at 200 μM for 16 h induces a significant 1.8-fold increase of its protein expression in rat intestinal epithelial (IEC-6) cells [91].

Similarly, platinum drugs such as cisplatin seems to have similar effects on the localization of Cu efflux transporters, as copper does, to detoxify the toxic effect of these chemicals. Thus, blocking the trafficking machinery is a possible strategy to overcome the platinum drug resistance. Cisplatin at 5 μM for 1 h is able to change the localization of both ATP7A and ATP7B in A2780 cells from the perinucleus region to more peripherally located sites in the

cytosol. This is reversible 1 h after drug is removed from the culture medium. No effect is observed in resistant cell lines [92]. The effect of cisplatin on localization of ATP7B is evaluated in human ovarian carcinoma cells expressing a cyan fluorescent protein-tagged ATP7B (2008/ECFP-ATP7B). ECFP-ATP7B is localized in the perinucleus region in absence of drug exposure and that 2 μM cisplatin for 1 h causes the redistribution of this complex to more peripheral vesicles [93].

Proton pump inhibitors are clinically used drugs for the treatment of gastro-oesophageal reflux disease as they reduce gastric acid production from gastric parietal cells. They act by irreversibly blocking the hydrogen/potassium adenosine triphosphatase enzyme in these cells [85]. A recent study shows PPIs have the potential to block ATP7A relocalization from the trans-Golgi network to the plasma membrane in response to elevated copper concentrations in melanocytes [94], therefore, this type of drugs have the potential to enhance the sensitivity of cisplatin in cancers as part of a patent registration [95,96].

1.3.6 Expression of hCTR1, ATP7A and ATP7B in colorectal cancer tissues

While previous sections discuss the roles of copper transporters in the transport of platinum drugs, information about their expression in CRC is equally important, as knowing this is a guide for targeting copper transporters to increase the sensitivity of cancer cells to platinum drugs. Moreover, their expression status in tumour tissues is also likely to become a molecular marker to predict some treatment outcomes for OXL-based chemotherapies. Therefore, this section summarizes current literature about the expression of hCTR1, ATP7A and ATP7B in CRC tissues.

1.3.6.1 hCTR1

Copper is an essential micronutrient for normal cellular physiology. Since cancer cells have a significantly higher proliferative rate compared to normal cells, it is thought that they require

more copper than normal cells. Copper also affects additional aspects of cancer growth, such as angiogenesis and metastasis [70]. Considering the roles of copper in the development of cancer, it can be expected that hCTR1 expression be up regulated in cancers to meet the metabolic and nutritional requirement for copper. Early studies seem to support this hypothesis. For example, significant elevation of mouse CTR1 protein (mCTR1) level is detected in the cervical tumor of the HPV16/E2 mice compared to the wild-type cervix [97]. The mRNA levels of mCTR1 in the pancreatic islets undergoing tumorigenesis are found to be elevated compared to that in the wild-type mice, and this phenomena is linked to copper-independent growth of tumors through oxidative phosphorylation [98].

Although hCTR1 expression in human CRC has been investigated by several recent studies recently, the results are not consistent. hCTR1 mRNA levels are reported to be significantly up regulated in human CRC Caco-2, HT-29, and HCT-116 cell lines compared to that of the normal colon mucosa [99]. Its gene expression is also increased in 27 CRC tumour samples compared to that of 19 matched normal colonic tissue controls [100]. However, hCTR1 protein expression seems to be only related to the staging of cancer, since positive rates for hCTR1 staining are measured as 0/45, 5/21, 0/21, 14/21 for colonic adenomas, adenocarcinoma T1 or T2, adenocarcinoma T3 or T4 and carcinoma metastatic to lymph nodes respectively. In contrast, hCTR1 are not detected in rectal carcinoma (0 out of 6 cases). Therefore, hCTR1 seems to be reduced in CRC cancers (19 out of 108 cases) compared to positive rate of normal colon tissue (16 out of 42 cases) [101].

hCTR1 protein expression is detected in 75 colorectal cancer patients with cytoplasmic staining pattern [51], which is replicated by a second study where hCTR1 exhibits moderate cytoplasmic staining in 31 colorectal cancer patients [102]. However, comparative information in relation to staining intensity of normal colon tissue samples is not provided in these studies, which makes the interpretation of those results questionable.

1.3.6.2 ATP7A and ATP7B

Literature about the expression of the human copper efflux transporters ATP7A or ATP7B in CRC is limited, however the information about their expression in other cancers suggests they might be elevated in the development of CRC.

ATP7A is expressed in 8 of 34 cases (23.5%) clinical colon cancer specimens but not in the adjacent normal epithelium [103]. ATP7A is more frequently detected in cancers including the prostate, breast, stomach, colon, lung, ovary, thyroid and pancreas than in normal tissues [104]. In addition, ATP7A expression is present exclusively in 41.6% of non-small cell lung cancer patients but not in the normal tissues [105]. Overall, the current data show that ATP7A is more abundantly and differentially expressed in cancer tissues than their normal counterparts, suggesting its involvement in cancer development.

Similarly, information about the expression of ATP7B in human CRC tissues is scarce and not conclusive. Recent study shows ATP7B is expressed in most colon cancer tissues (47 of 50 cases) with various levels of expression intensity for both protein and mRNA [101]. In addition, ATP7B is detected in all 75 colon cancer specimens with nucleus-associated localization in comparison with the widely reported trans-Golgi network-related localization in other cells [106].

However, ATP7B seems to be differentially expressed in many human cancers including ovarian cancer, oral cancer, gastric cancer, breast cancer and hepatic cancer. ATP7B gene is detected in 43.9% of ovarian carcinoma patients [63]. While ATP7B staining is negative in normal squamous epithelial cells, it is detected in 54.9% in human oral squamous carcinoma with cytoplasmic staining pattern [107]. Variable degrees of cytoplasmic staining of ATP7B are observed in 51.0% of gastric cardiac carcinomas tumor compared to 22.4% for the adjacent non-neoplastic epithelium [108]. Its expression is reported in 22% breast cancer samples,

while no staining is detected in the normal duct tissue [109]. Similar staining pattern is found in hepatic carcinoma with 21% positive staining rate compared to the negative staining in normal tissues [110].

In summary, this section shows that copper transporters seem to be changed in the chronic process from normal tissues to cancer. To study the mechanisms for these alterations in carcinogenesis, it is necessary to look at the possible changes of copper, copper-containing enzymes in the pre-cancerous conditions such as chronic colitis or colonic dysplasia.

1.4 Possible roles of copper in chronic colitis and colorectal cancer

1.4.1 Pathological transformation from chronic colitis to colorectal cancer

The development of CRC starts from an abnormal growth of tissue such as polyps and adenoma in the colon and rectum, which have the ability to transform into adenocarcinomas over a period of more than 10 years [111]. This malignant transformation can be accelerated by multiple factors including chronic inflammation, diet, environmental factors and family history [112]. Chronic inflammation of colon normally takes the form of ulcerative colitis (UC) and occasionally Crohn's disease (CD). UC is a chronic, relapsing inflammation of colon and is consistently considered to be a well-established biological risk factor for the development and progression of colorectal cancer. Although inflammation-related CRC is estimated to be responsible for less than 2% of all CRC cases diagnosed annually, the mortality from colorectal cancer in the setting of UC is higher than that of sporadic colorectal cancer [113].

Long-standing inflammation in colon causes colonic dysplasia, which is a transitional stage between UC and CRC, and therefore it is routinely examined as a surveillance marker for neoplasm in colon of patients with intestinal colitis [114]. Interestingly, the molecular alterations that are responsible for the development of CRC also have been detected in dysplastic tissues including the mutations of cyclooxygenase-2, p53, and adenomatous

polyposis coli [115]. Therefore, the development of CRC in the setting of inflammation seems to follow a stepwise colitis-dysplasia-carcinoma process, which has also been reported in lung cancer [116] and liver cancer [117].

1.4.2 Copper homeostasis and chronic colitis

Copper has been described to possess pro-inflammatory property [118]. Copper generates reactive oxygen species in the process of biochemical reactions, which triggers the release of pro-inflammatory cytokines such as interleukin 1 beta, tumor necrosis factor and cyclooxygenase 2 (COX-2) [119]. Moreover, components of copper homeostasis seem to be deregulated in inflammatory conditions of colon [120]. For a complete understanding of the biochemical role of copper in chronic inflammation of colon, it is essential to interrogate the role of copper transporters and copper-containing enzymes in inflammation.

1.4.2.1 Copper levels

Copper levels are found to be higher in inflamed tissues of colon from patients with UC and CD, although the exact role of copper in these diseases is still not clear yet. In a multicenter clinical study to monitor the serum copper levels in 47 patients with CD, 117 patients with UC, and 123 healthy controls, significantly high levels of serum copper are found in patients with these two disorders after adjusting for age, sex, and county of residence. This is the first large-scale study to measure the relative copper levels in patients with intestinal inflammation compared to the healthy patients. The study links the excess of copper to be a factor for worsening the inflammatory process in UC and CD, as copper has the ability to catalyze free radical formation and increases the oxidative stress of the mucosa [121]. Similar finding is reported in a case-control study with 50 patients with UC, and 49 healthy volunteers. Mean serum copper level in patients with UC is 138.3 ± 42.6 μg/dl compared to 110.0 ± 38.5 μg/dl in the healthy individuals [122]. In children with CD, serum copper is also elevated compared

to healthy controls (22.7 ± 5.49 vs 20.76 ± 4.06 mmol/L). However, in children with UC, copper levels are not changed [123].

1.4.2.2 Copper containing enzymes

Copper appears to have fundamental roles in inflammatory processes as described above. While the theory of free radicals can partially explain the elevated copper levels in inflammation [124], other factors such as copper-containing enzymes should not be ignored as they may be implicated in the development of inflammatory conditions of the colon, including lysyl oxidase, semicarbazide-sensitive amine oxidase (SSAO) and superoxide dismutase (SOD). A preclinical model shows that lysyl oxidase can suppress the secretion of monocyte chemoattractant protein-1 in cultured vascular smooth muscle cells, which inhibits the progression of inflammation [125]. In a recent study, gene profiling is conducted to identify any differentially expressed genes in the colon of rats with colitis induced by 2, 4, 6-trinitrbenzene sulfonic acid administration. The gene of lysyl oxidase is found significantly increased in colonic tissues of the colitis model compared to the normal tissues, suggesting of a direct role in the pathology of UC [126].

Increased levels of SSAO have been associated with the development of UC. The pro-inflammatory role of SSAO observed in these studies may be related to its ability to facilitate leukocyte tissue infiltration [127]. A subsequent animal study demonstrates that small molecule SSAO inhibitor LJP1207 could have a therapeutic effect against both acute and chronic inflammatory diseases. In the mouse model of UC, LJP 1207 significantly reduces mortality, and colonic cytokine levels as well as inflammation, injury and ulceration scores in mice [128].

However, there are some cases where copper enzyme levels are decreased in UC. It is a known fact UC is induced in part from oxidative stress and SOD prevents the injury in the

gastrointestinal mucosa due to its free-radical scavenging role. In intestinal tissues from UC patients, the levels of Cu-SOD have been reported to be decreased which implies an adaptive response to inflammation [128].

1.4.3 Contribution of copper to the development of colorectal cancer

Cellular copper homeostasis is tightly regulated through the coordination between copper transporting proteins and copper chaperones. While the disruption of these components causes severe genetic diseases such as Wilson's or Menkes's diseases [129], they might be also altered in the development of malignancy in normal tissues. The observation that copper or copper-containing enzymes rise in many cancers provides more evidence to support this speculation.

1.4.3.1 Elevated copper levels in colorectal cancer tissues

Early studies consistently show copper level appears to be increased in colorectal cancer (CRC) and other cancer tissues in comparison with the normal counterparts. Atomic absorption spectrometry demonstrates that the average copper level is increased by 46% in tumor tissues compared to normal tissues (2.08 ± 0.76 vs 1.42 ± 0.44 μg/g) [130]. Copper level is also higher in CRC than in normal tissues (1.9 vs 1.53 μg/g) [131]. In another study, mean copper level in CRC tissues is reported to be 170% to 180% of that in benign tissues derived from 25 patients [132]. Higher concentration of copper is also detected in CRC tissues from 30 patients compared to non-cancerous tissues (2.78 vs 1.79 μg/g) [95,96]. Similar findings are reported in breast cancer (21.0 ± 10.7 vs 9.3 ± 2.3 μg/g, dry weight) [133], and lung cancer (1.53 ± 0.35 vs 1.17 ± 0.26 mg/g) [134].

The exact reason for the elevation of copper in CRC has not been fully understood yet. Copper is an essential micronutrient for sustaining the physiology of normal cells. CRC cells have higher proliferation rate therefore they require more copper than normal cells. Copper also has effect on multiple aspects of cancer growth, including angiogenesis and metastasis [135].

Copper depletion has demonstrated efficacy against various types of cancers such as colon cancer, breast cancer, bladder cancer and ovarian cancer [136]. Copper may also act as a pro-cancer factor in the development of cancer. Early studies show copper generates hydroxyl-containing radicals that can bind to DNA and further break DNA strands leading to carcinogenesis [136]. Due to unknown defects, cancer tissue has stronger binding affinity for copper thus traps more copper as DNA-damaging element.

1.4.3.2 Alteration of copper-containing enzymes in colorectal cancer tissues

Copper ion is never free in cytoplasm of cells due to its high chemical reactivity. It exits as various copper-containing enzymes to fulfil the biochemical and metabolic functions required by cells [137]. In many cancers, especially CRC, the elevated copper level is also paralleled with enhanced expression of copper enzymes including lysyl oxidase (LOX), manganese superoxide dismutase (Mn-SOD), and cytochrome c oxidase (COX). These phenomena seem to be an interpretation for the elevation of copper in many cancers.

LOX is a secreted copper-dependent amine oxidase whose primary function is to catalyse the covalent cross-linking of collagens and elastin in the extracellular matrix [138]. A recent study shows it is elevated in CRC tissue compared to the adjacent normal tissue and this up regulation is associated with the progression of CRC [139].

Mn-SOD is a metalloenzyme that catalyses the dismutation of the superoxide anion to H_2O_2. Higher level of Mn-SOD level is frequently reported in colon cancer [140], human renal cell carcinomas [141], gastric adenocarcinoma and squamous cell oesophageal carcinoma [142] compared to the normal counterparts. Recent study shows the up regulation of Mn-SOD observed in these cancers facilitates the glycolysis of cancer cells [143].

COX is a large transmembrane protein complex present in the mitochondrion of mammalian cells. It is an important enzyme in the respiratory electron transport chain of mitochondria

[144]. One of its subunit COX IV protein and gene levels are reported to be significantly overexpressed in CRC tissue samples compared to the paired precancerous tissues [145]. While COX intensity progressively decreases in dysplastic epithelium, it is significantly increased in cancerous colon tissue [146]. However, cytochrome c oxidase subunit I shows decreased expression in crypts of CRC compared to that of the normal tissue (1.7 vs 22.8) [147].

1.4.4 Animal models of chronic colitis and colorectal cancer

Animal models have demonstrated to be important tools for testing potential therapeutic agents and for investigating the mechanisms of pathogenesis. It has been reported that there are currently more than 60 colitis models, which can be broadly classified into 5 categories, namely, the gene knockout, transgenic, chemical, adoptive transfer, and spontaneous colitis models [148]. Although these models are widely used to study many important aspects of the pathophysiological mechanisms and the effects of emerging therapeutic strategies, most of these experimental animals represent acute form of intestinal colitis, which is very rare in human.

Winnie mouse has been developed as an animal model with *Muc2* mutation to recapitulate the pathogenesis and clinical symptoms of chronic intestinal colitis. The *Winnie* mouse was originally established from the offspring of C57BL/6 mice carrying a single missense mutation in the *Muc2* gene encoding the mucin protein produced by intestinal goblet cells, where the genetic mutation is induced by a mutagenic compound N-ethyl-N-nitrosourea. *Muc2* mutation-induced aberrant biosynthesis of mucin protein causes abnormal phenotypes similar to chronic colitis, such as impaired function of mucus barrier and increased susceptibility to luminal toxins in the intestine [148]. Phenotypically, *Winnie* mice display mild spontaneous distal intestinal inflammation at the age of six weeks with a 100% incidence, and 20% of the mice

develop severe clinical signs of chronic colitis by the age of one year. It has been assumed that the *Muc2* mutation induces misfolding of the mucin protein, which triggers endoplasmic reticulum stress and activates of unfolded protein response in *Winnie* mice [149].

Winnie mice are prone to colonic neoplasia due to the defective mucus barrier, chronic inflammation of colitis and continuous exposure to toxins in intestine. However, the rate of carcinogenesis is reported to be low in *Winnie* mice even at one year of age. Dextran sulphate sodium (DSS) is a commonly used chemical to cause colonic inflammation, dysplasia and carcinoma in mice.

DSS is reported to cause mutations of several genes that promote tumorigenesis in mice, such as *Cav1, Ccl5, Myc, Trp53* [150]. After administration three cycles of 1% DSS for 21 days (7 days/cycle) to *Winnie* mice, most of these animals display exacerbated colitis and sporadic dysplasia in the distal colon, which are considered to be relevant modeling of colorectal cancer arising from the context of chronic inflammation of colon [151].

1.5 Rationale of study

Oxaliplatin (OXL) is the backbone of many chemotherapy regimens for the treatment of advanced colorectal cancer. However, acquired resistance is a great barrier for its widespread long-term use. Efforts to prevent the resistance of OXL have thus far from been proven successful, and no effective strategy is available now to contain drug resistance. Reduced OXL accumulation is a predominant characteristic of many platinum-resistant cancers. Recently, membrane transporters mediating the trafficking of OXL have become a more acceptable theory. Therefore, targeting membrane transporters that control cellular OXL accumulation is a promising approach to circumvent drug resistance. Although several *in vitro* studies have shown that members of Cu transporters such as hCTR1, ATP7A or ATP7B may be also associated with cellular uptake and resistance of OXL, direct evidence is still lacking. The

information about the expression of copper transporters in colorectal cancer cell lines and determining their sensitivity to OXL are two necessary steps for selecting the appropriate models for following cell-based experiments. Understanding the expression of Cu transporters in colorectal cancer tissues relative to normal tissues is of great diagnostic and prognostic value. Moreover, elucidating their expression in the human colon specimens is helpful to translate the main findings from this project into a clinical context. Chronic colitis is a high-risk factor for the development of colorectal cancer. Copper and copper-containing enzymes are involved in the malignant transformation of colonic cells from a pro-inflammatory state to malignancy. Since copper transporters are key players in copper homeostasis, we hypothesized that the expression of Cu transporters may be changed in the sequential process that leads to cancer.

1.6 Aims of thesis

This project was undertaken with the hypothesis that hCTR1 determines the uptake and cytotoxicity of OXL in human colorectal cancer cells and it can be targeted with pharmacological compounds for the prevention of drug resistance.

The specific aims of this thesis are:

1) To determine the role of human copper transporter hCTR1 as an uptake transporter of OXL in colorectal cancer cells that stably overexpress the hCTR1 gene via recombinant plasmid-based transfection (Chapter 3).
2) To investigate the therapeutic value of Cu chelators in enhancing OXL cytotoxicity in colorectal cancer cells by modulating hCTR1 expression (Chapter 4).
3) To systematically investigate endogenous expression of the Cu uptake transporter hCTR1 and the efflux transporters ATP7A and ATP7B in tumor biopsy tissues of colorectal cancer patients (Chapter 5).
4) To determine the role of copper transporters in the development of colorectal cancer

by studying their expression in colonic tissues of *Winnie* mice with colitis, DSS-treated *Winnie* mice with dysplasia and wild-type C57B/6 mice as normal control (Chapter 6).

Chapter 2 Materials and Methods

2.1 Chemicals and reagents

Oxaliplatin, cisplatin, copper chloride, D-penicillamine, ammonium tetrathiomolybdate and bathocuproinedisulfonic acid disodium salt were obtained from Sigma-Aldrich (St Louis, MO, USA). SuperScrip III First-strand synthesis system (50) and the selective antibiotic geneticin (G418) were purchased from Life Tech (Carlsbad, CA, USA). The Lipofectamine LTX with Plus reagent was from Thermo Fisher Scientific (Walttham, MA, USA). The C-terminal Myc- and DDK-tagged pCMV6-Entry vector was purchased from Origene (Rockville, MD, US). The Amersham ECL Western blotting detection reagent was obtained from Lumigen (Lumigen, MI, US). DAB enhanced liquid substrate system was bought from Sigma-Aldrich. FDCPt1 was kindly provided by Dr Elizabeth New at the School of Medical Sciences, University of Sydney. All other reagents were from reputable suppliers, otherwise indicated.

2.2 Cell culture

Human colorectal cancer cell lines, DLD-1, SW620, HCT-15 and COLO205 were purchased from American Type Culture Collection (Manassas, VA, USA). All cells were maintained in Dulbecco's modified eagle medium (DMEM) (Sigma-Aldrich), supplemented with 10% fetal bovine serum and 1% penicillin-streptomycin (Invitrogen, Carlsbad, CA), at 37 °C in a humid atmosphere of 5% CO_2-95% air. The human copper uptake transporter 1 gene- DLD-1/ hCTR1 cells and the empty vector-transfected cells were maintained in fully supplemented DMEM medium containing 150 mg/mL G418. Cells were only used for experiments up to 20 passages and regularly tested for mycoplasma contamination.

2.3 Establishment of overexpressing DLD-1/hCTR1 colorectal cancer cells

2.3.1 pCMV6 vector

A pCMV6 expression vector containing the open reading frame (ORF) of human copper uptake transporter hCTR1 gene was constructed commercially by Origene (Fig 2-1). This vector is composed of bacteriophage f1 origin of replication (f1 ori), simian virus 40 origin of replication (SV40 ori), ColE1 origin of replication, a cytomegalovirus promoter (CMV), bacteriophage T7 promoter, and a multiple cloning site (MCS). The CMV and T7 promoters drive constitutive expression of hCTR1 protein in mammalian cells and bacteria, respectively. SV40 ori allows replication in mammalian cells. The MCS provides restriction sites for subcloning of the gene of interest. The hCTR1 gene is tagged with the Myc and DDK genes for identification and isolation of the protein complexes. In addition, the Kan/Neo resistance genes in this construct allow positive selection in bacterial and mammalian cells, respectively.

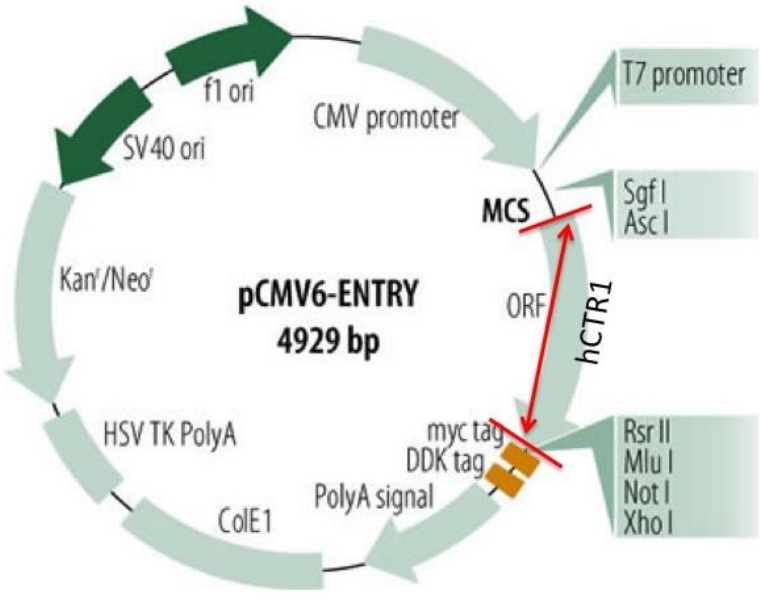

Figure 2-1. The structure of pCMV6-Entry vector containing the ORF of human hCTR1 gene

The location of hCTR1 gene in this construct is indicated with red arrows. In this vector, a TrueORF sequence is fused with a Myc/DDK tag at its carboxy terminus. The image was modified from the manufacturer's product information [152].

2.3.2 Transfection

Human colorectal cancer DLD-1 cells were stably transfected with pCMV6-Entry vector as indicated in section 2.3.1 or the corresponding empty vector to establish a mock control line according to the method previously developed in Dr Johnson Liu's lab [44]. Briefly, DLD-1 cells were seeded at a density of 400,000 cells/well of 6-well plates in fully supplemented DMEM growth medium and cultured overnight. On the next day, the transfection mixtures containing 10 μg purified DNA and Lipofectamine reagent were prepared and added into the cells in the 6-well plate according to the manufacturer's instructions. After culture for 48 h, cells were split at a 1:5 ratio into a 100 mm-petri dish containing DMEM added with 1200 μg/ml G418. The transfected cells were further cultured for extended period to allow the formation of colonies. After approximately two weeks, single colonies were isolated under a light microscope and screened for protein expression of hCTR1 using a Western blotting assay. The colony with the highest or lowest levels of hCTR1 was selected and further amplified through several passages to produce cell aliquots for long-term storage in liquid nitrogen. For maintenance, transfected cells were cultured in fully supplemented DMEM containing 150 μg/ml G418 for subsequent experiments. The Gene Technology Research Committee at the University of New South Wales approved the use of transfected cell lines as Genetically Modified Committee (See Appendix C).

Cells were seeded into a 6-well plate in triplicate and left overnight to adhere. Cells were exposed to 200, 400 and 800 μM $CuCl_2$ for 24 h or 1, 3 and 5 μM OXL for 2 h, and then cultured in drug-free media for about two weeks to allow colony formation. Cells were treated in parallel with drug vehicle as control.

2.4 MTT assay and colony forming assay

2.4.1 MTT assay

The cytotoxicity of oxaliplatin (OXL) and $CuCl_2$ was evaluated using an MTT-based assay. Colorectal cancer DLD-1, SW620, HCT-15 and SW620 cells were seeded at a density of 6000-8000 cells/well into 96-well plates in fully supplemented DMEM growth medium and left to attach to the plates overnight. On the next day, cells were incubated with serial dilutions of 0.01-500 μM OXL or $CuCl_2$ solutions in serum-reduced Opti-MEM medium (Thermo Fisher Scientific) and cultured for either 2 h or 72 h under different incubation conditions as described above. Subsequently, 20 μl of 5 mg/L MTT solution in PBS was added to each well for 1 h before the medium was discarded and replaced with 200 μl DMSO (Sigma-Aldrich). The plates were shaken gently for 15 min at room temperature before absorbance (A_{570}) was determined using a microplate reader (Spectra max, Bio-Strategy). The 50% growth inhibitory drug concentrations and the relative viability of cells were calculated using GraphPad Prism programs (GraphPad Software, Santiago, USA).

2.4.2 Colony forming assay

The colony forming assay (CFA) was performed to measure the inhibitory effect of OXL and $CuCl_2$ on the colony forming capacity of hCTR1-overexpressing DLD-1/hCTR1 cells and mock control cells. Cells were seeded at a seeding density of 600 cells/well in 6-well plates and cultured in fully supplemented DMEM medium overnight. On the next day, cells were exposed to either $CuCl_2$ or OXL under the experimental incubations described in section 3.4.2.

Cells were then maintained in drug-free culture for about two weeks while the media was only changed once during this period. At the end of the culture, cells were washed with 2 ml PBS for 1 min before 2 ml of 0.5% crystal violet solution (0.5% w/v crystal violet, 25% v/v methanol in PBS) was added to each well of the plate. Colonies were stained for 10 min at room temperature, followed by 2 washes with PBS to remove the excess dye. The blue-stained colonies containing more than 50 cells each were counted manually under a stereomicroscope and documented photographically. Images were processed using the Image J program (National Institute of Health, USA).

2.5 Western blotting assay

Human colorectal cancer cell lines, DLD-1, SW620, HCT-15 and COLO205 or DLD-1/hCTR1 or the mock transfected cells were cultured with in fully supplemented DMEM medium for 2 to 3 days until confluence reached at least 80%. Cells were incubated with different concentrations of copper chelators, $CuCl_2$, OXL or drug vehicle as control as described in Section 4.2. Following the treatments, cells were dissolved in ice-cold CelLytic lysis solution (Sigma) and centrifuged at 8000 ×g at 4°C for 15 min. The protein concentration of the resulting supernatant was measured using a NanoDrop 2000 spectrophotometer (Thermo Fisher Scientific, Waltham, MA). Protein samples (30 μg/lane) were heated at 90°C for 5 min, electrophoresed in 8% or 12% SDS-PAGE and then transferred to a PVDF membrane (Amersham, Buckinghamshire, UK) using a Transblot SD device (Bio-Rad, Hercules, CA). Following the blocking with 3% skimmed milk/bovine serum albumin in 0.2% Tween 20 (TBST) solution, the blot was incubated with the primary antibody anti-hCTR1 (1:1000 Novus Biologicals, Littleton, CO; Cat. No: NB100-402), anti-ATP7A (1:1000 Abcam, Cambridge, UK; Cat. No: ab131400), anti-ATP7B (1:2000 Abcam; Cat. No: ab135571) or anti-β-actin (1:5000 Abcam; Cat. No: ab8226), horseradish peroxidase (HRP)-conjugated anti-rabbit (1:500 Abcam; Cat. No: ab97051) or anti-mouse secondary antibody (1:500 Abcam; Cat. No:

ab97023), and the ECL Advance Detection reagent (Lumigen). The density of resolved electrophoretic bands was quantified using Image J program and expressed as a ratio to that of β-actin.

2.6 Reverse transcription polymerase chain reaction (RT-PCR)

Total RNA was extracted from colorectal cancer DLD-1, SW620, HCT-15 and COLO205 cells using an EZ-10 DNAway RNA kit following manufacturer's instruction (Bio Basic, Ontario, Canada). 0.25-0.5 μg RNA of each sample was reverse-transcribed into cDNA using a SuperScript III first-strand synthesis system and a thermal cycler (Bio-Rad). The cDNA synthesis reaction was conducted in 20 μl of reaction buffer at 42 °C for 50 min and was terminated by heating the mixture at 70 °C for 15 min. 5 μg cDNA of each sample was used to PCR amplify copper transporters and glyceraldehyde 3-phosphate dehydrogenase (GAPDH) using platinum PCR SuperMix. cDNA was amplified by PCR in a reaction mixture containing dNTP, $MgCl_2$, platinum Taq DNA polymerase and custom primers indicated in Tab 2-1 (Geneworks, Thebarton, SA, Australia), using a C1000 thermal cycler (Bio-Rad). PCR was carried out with 35 cycles of 15 s at 94 °C, 30 s at 55 °C and 30 s at 72 °C. PCR products were electrophoresed on 1.5% agarose gel, stained with SYBR Safe DNA Gel Stain (Thermo Fisher Scientific, Waltham, MA), and photographed using Molecular Imager Gel Doc XR System (Bio-Rad). Gel images were further analyzed using Image J software.

Table 2-1. Sense and anti-sense primers for copper transporter or GAPDH genes

Gene	Primer sequence	Size (bp)
hCTR1	F 5'-AAGATAGCCCGAGAGAGCCT-3' R 5'-AATCGATAAGGCCACGCCAT-3'	346
ATP7A	F 5'-TGGTGAAGTCGTGCTGAAGAT-3' R 5'-TCATTGGTATGATGGACTCCTTTG-3'	322
ATP7B	F 5'-GAGGGCTATCGAGGCACTTC-3' R 5'-GAGCCACTTCCTGCACAGAT-3'	446

GAPDH	F 5'-TTCTTTTGCGTCGCCAGCC-3' R 5'-CATGGTTCACACCCATGACGA-3'	455

2.7 Fluorescent immunocytochemistry

Human colorectal cancer cell lines, DLD-1, SW620, HCT-15 and COLO205 or DLD-1/hCTR1 or the mock transfected cells were cultured in fully supplemented DMEM medium in 24-well plates for 2 to 3 days until the confluence reached 60-80%. Cells were incubated with different concentrations of copper chelators, copper chloride, oxaliplatin or drug vehicle as control as described in Section 4.2. After the incubation, cells were rinsed with cold PBS, followed by fixation with 4% formaldehyde in PBS for 15 min at room temperature, before being permeabilized with or without 0.2/% Triton X-100/PBS for 15 min. After permeabilization, Image-iT FX signal enhancer (Life Tech) was added to the cells according to the manufacturer's instructions and incubated for 30 min at room temperature under humid conditions. Cells were then incubated with blocking buffer (PBS containing 0.2% Triton X-100, 3% goat serum and 2% bovine serum albumin) for 1 h at room temperature before being exposed to the primary antibodies, polyclonal rabbit anti-hCTR1 (1:500 Novus), mouse anti-ATP7A (1:500 Abcam), rabbit anti-ATP7B (1:50 Abcam) or mouse anti-Na^+/K^+ ATPase (1:1000 Abcam; Cat.No: ab58475) diluted in immuno-buffer (3% goat serum in PBS) overnight at 4ºC, followed by incubation with secondary antibodies, Alexa Fluor 488-labelled anti-rabbit IgG (1:1000; Life Tech: A11034) or Alexa Fluor 594- labelled anti-mouse IgG (1:1000) (Life Technologies, Carlsbad, CA; Life Tech: A11032) diluted in immunobuffer for 3 h at 4 °C, protected from light. At the end of incubation, cells were rinsed and cover-slipped with Vectashield mounting medium containing 4,6-diamidino-2-phenylindole (DAPI) (Vector Laboratories, Burlingame, CA). Images were captured using a Leica fluorescence microscope (Leica Biosystems, VIC, AU) or confocal microscope (Nikon Instruments, Melville, USA) and

analyzed using NIS-ELEMENTS D 3.2 (Nikon, Tokyo, Japan) and Image J software (National Institute of Health, Bethesda, MD).

2.8 Processing of tumor samples

2.8.1 Collection of human tissues

Tumor and the adjacent normal tissues collected from the bowel of colorectal cancer patients were identified by pathologists at the Royal Hobart Hospital. In total, 3 tumor samples and 3 normal tissue samples from each patient were taken and rinsed with cold PBS before they were placed in cryovials and snap-frozen in liquid nitrogen. Tissues were then stored at -80ºC until use.

2.8.2 Tissue embedding

Frozen colon samples were fixed in pre-chilled PBS containing 4% paraformaldehyde overnight at room temperature, followed by dehydration in serial ethanol solutions (70-100%), clearing with xylene, and perfusion with paraffin before being embedded into tissue blocks by pathologists at the UNSW. Some non-fixed snap-frozen samples were also immersed in 30% sucrose in PBS solution at 4ºC overnight until the tissue sank, followed by embedding in Tissue-Tek optimal cutting temperature embedding compound (Sakura Finetek, Torrance, CA, USA), snap frozen in liquid nitrogen, and stored at -80ºC until used for cryosection.

2.8.3 Sectioning of human tissues

Paraffin or OCT-embedded tissues were sectioned following instructions. Briefly, paraffin blocks were placed on ice for at least 5 min before being cut into 4 μm-thick sections with a microtome (Leica Biosystems) at room temperature. Paraffin ribbons were placed in a water bath at about 40-45 ºC and mounted onto tissue slides coated with poly-lysine. Next, sections

were subject to air-drying for 30 min before being baked at 45-50 ºC overnight. OCT-embedded frozen tissues were sectioned using a cryostat (Leica Biosystems) at −20 °C at a thickness of 4 μm before being mounted on poly-lysine coated slides, and stored at −80°C.

2.8.4 Haematoxylin and eosin staining (H&E staining)

H&E staining was performed according to established in-house protocols. Briefly, paraffin-embedded mouse tissue slides were de-waxed by immersion in xylene (2×5 min), absolute ethanol (2×2 min), 70% ethanol (1×1 min) and 1 min under running tap water. Frozen sections were excluded from this step and directly warmed up for 1 min at room temperature. Slides were then dipped into haematoxylin solution for 4 min, followed by a 1-min wash under running water. Slides were differentiated in 1% acetic acid in ethanol for 30 secs before being washed under running tap water for 1 min. Slides were developed in 0.2 % ammonia water for 30 secs to 1 min and counterstained using eosin solution for 3 min. Subsequently, slides were dehydrated in absolute alcohol (2×2 min), xylene (2×3 min) before excess xylene was drained off and the sections were mounted using a DPX mounting medium and analyzed by light microscopy.

2.9 DAB-based immunohistochemistry

DAB-based immunohistochemistry (IHC) was performed on paraffin-embedded or cryo-sectioned tissues as previously reported [153]. Antigen retrieval of the tissue sections was conducted by microwaving the tissue slides at 105 ºC for 15 min in pH 6.0 citrate buffer containing 10 mM sodium citrate and 0.05 % Tween 20 in distilled water. Tissue sections were then immersed in 0.3 % hydrogen peroxide (Sigma-Aldrich) in blocking buffer to inhibit endogenous peroxidases and block the nonspecific protein. Slides were then incubated with the primary antibodies, polyclonal rabbit anti-hCTR1 (Novus 1:250), mouse anti-ATP7A (Abcam 1:2000), or rabbit anti-ATP7B (Abcam 1:300) in immuno-buffer overnight at 4 ºC in

a humid condition. Negative controls were just incubated with immuno-buffer. On the next day, slides were then washed 3x 5 min with TBST and incubated with biotinylated secondary rabbit or mouse antibodies (Sigma-Aldrich) in immuno-buffer (1:500) for 2 h, followed by three washes with TBST. Slides were then incubated with a 1:500 dilution of HRP-conjugated extrAvidin (Sigma-Aldrich) for 1 h, and 30-50 µl DAB-substrate per tissue section for 30 secs, counterstained for 10 secs with haematoxylin and rinsed using running tap water for 1 min. Lastly, coverslips were mounted onto sections using DPX mounting medium (Sigma-Aldrich) and were air dried at room temperature before microscopic analysis.

2.10 Statistical analysis

All data are presented as mean ± standard deviation or as percent change compared to the untreated control. Statistical analyses were performed using GraphPad Prism (GraphPad Software Inc, CA, USA). Statistical significance of the data was evaluated using Student's t-test or paired t-test, and one-way analysis of variance (ANOVA), where appropriate, followed by Dunnett's multiple comparison tests to evaluate the difference between different groups and control. A *P*-value of < 0.05 was considered statistically significant. IC_{50} values were calculated using a nonlinear regression curve fit with 4 parameters.

Chapter 3 Recombinant Overexpression of hCTR1 Enhances Oxaliplatin Cytotoxicity and Uptake in Human Colorectal Cancer Cells

3.1 Introduction

The goal of this chapter was to determine the role of human copper transporter 1 (hCTR1) in the transport of oxaliplatin (OXL) in colorectal cancer cells that were engineered to overexpress the transporter gene. The DLD-1 cell line is derived from the epithelial tissue of Duke's type C human colon adenocarcinoma from an adult Caucasian patient [156]. The DLD-1 cell line carries genetic mutations of *TP53, KRAS, PIK3CA, BRAF and PTEN,* which are caused by chromosomal instability, microsatellite instability, and CpG island methylator phenotype pathways [157]. These genetic mutations and phenotypes are common in colorectal cancer, therefore, the use of DLD-1 line in this project aims to provide clinical relevance to the results. Herein, DLD-1 cells were transfected to stably overexpress hCTR1 as a valid cell model system (DLD-1/hCTR1) to study Cu transporter. In addition, DLD-1 cells were transfected with the corresponding empty vector to establish a mock control line. Western blotting assay was performed to detect elevated protein levels of hCTR1 in DLD-1/hCTR1 cells in comparison to mock control cells. The function of hCTR1 in DLD-1/hCTR1 cells was verified based on enhanced sensitivity to copper chloride, the prototype substrate of hCTR1. OXL cytotoxicity and uptake were further measured in DLD-1/hCTR1 cells in comparison with that of mock control cells.

Enhanced OXL accumulation in DLD-1/hCTR1 would be evident if hCTR1 contributes to its cellular uptake. Several biotransformation products of OXL are known to be responsible for

its pharmacological activity through the formation of Pt-DNA adducts, interfering with DNA replication and transcription, and leading to cancer cell death [158]. The hydrolysis products, including monofunctional monoaquatic Pt species, are more potent than the parent platinum drugs [159]. FDCPt1 is a fluorescein-based compound bearing a dithiocarbamic acid moiety. FDCPt1 exhibits a major absorption peak at 516 nm and an emission maximum at 540 nm. FDCPt1 could bind specifically with monofunctional metabolites of Pt drugs through Pi-Pi non-covalent interactions, which cause an increase of fluorescence emission by ~70 folds. This property has been used to detect the monofunctional metabolites of OXL, cisplatin and carboplatin in colorectal cancer cells [160]. Herein, we have utilized FDCPt1 as a specific fluorescent probe to monitor cellular accumulation of OXL-derived monofunctional biotransformation products in hCTR1-overexpressing DLD-1/hCTR1 cells and mock control cells for comparison.

3.2 Experimental design

3.2.1 Establishment of overexpressing DLD-1/hCTR1 colorectal cancer cells

Human colorectal cancer DLD-1 cells were stably transfected with pCMV6-Entry vector as indicated in section 2.3.1 or the corresponding empty vector to establish a mock control line. Briefly, DLD-1 cells were seeded at a density of 400,000 cells/well of 6-well plates in fully supplemented DMEM growth medium and cultured overnight. On the next day, the transfection mixtures containing 10 μg purified DNA and Lipofectamine reagent were prepared and added into the cells in the 6-well plate according to the manufacturer's instructions. After culture for 48 h, cells were split at a 1:5 ratio into a 100 mm-petri dish containing DMEM containing 1200 μg/ml G418 for selection. The transfected cells were further cultured for extended period to allow the formation of colonies. After approximately two weeks, single colonies were isolated under a light microscope and screened for protein

expression of hCTR1 using Western blotting. The colonies with the highest and lowest levels of hCTR1 were selected and further amplified through several passages to produce cell aliquots for long-term storage in liquid nitrogen. For maintenance, transfected cells were cultured in fully supplemented DMEM containing 150 μg/ml G418 for all subsequent experiments. The Gene Technology Research Committee at the University of New South Wales approved the use of transfected cell lines (See Appendix C).

3.2.2 Sensitivity of transfected cells to oxaliplatin and $CuCl_2$ (MTT and colony forming assay)

Following the stable transfection and overexpression of hCTR1, the sensitivity of DLD-1/hCTR1 cells to Cu chloride, a prototypic substrate of hCTR1, was further tested in comparison to the mock cells using the MTT and colony forming assays (CFA). These cell viability assays are designed to measure the metabolic activity and colony-forming ability of cancer cells. The MTT assay is a colorimetric assay for measuring the capacity of NAD (P) H-dependent cellular oxidoreductase enzymes to reduce yellow 3-(4,5-dimethythiazol-2-yl)-2,5-diphenyl tetrazolium bromide (MTT) to purple colored formazan. The MTT assay is commonly used method to measure the cytotoxicity of anticancer drugs, since only viable cells are metabolically active and are able to convert the dye [157]. In addition, the CFA measures the clonogenic potential of cells and is commonly used as a surrogate method to evaluate long-term cytotoxicity of anticancer drugs on cultured cells [161]. Therefore, the short and long-term cytotoxicity of Cu chloride and OXL were fully evaluated in DLD-1 cells and mock cells using both the MTT and CFA assays.

Briefly, DLD-1/hCTR1 or mock control cells were seeded into 96-well plate at a density of 6000 cells/well in quadruplicate and cultured overnight. Cells were incubated with 5, 10, 30, 50, 100, 300, 500 and 1000 μM $CuCl_2$ for 72 h or 0.3-300 μM OXL for 2 h, and then cultured

in drug-free media for 72 h, followed by the conduction of the MTT assay. For CFA, DLD-1/hCTR1 cells or mock cells were seeded at 600 cells/well into a 6-well plate in triplicate and left overnight to adhere. Cells were exposed to 200, 400 and 800 μM $CuCl_2$ for 24 h or 1, 3, 5, 10, 30 μM OXL for 2 h, and then cultured in drug-free media for about two weeks to allow colony formation. Cells were treated in parallel with drug vehicle as control. The selection of concentration range for each type of assay was based mostly on our preliminary results (unpublished data). The drug concentration ranges to be used in the MTT assays were intended to achieve a minimum and maximal killing effect for each particular chemical under the corresponding experimental conditions. In a preliminary copper MTT assay, a range of 0.3-500 μM for both DLD-1/hCTR1 or mock control cells achieved an approximate reduction of cell viability between 5% and 90% (data not presented). Therefore, to achieve a maximal killing effect, the dose range was adjusted to 0.3-1000 μM in the formal test. Likewise, using 0-300 μM of OXL in the MTT assay was also intended to achieve a minimum and maximal killing effect. In addition, the OXL concentration range for MTT assay (0-300 μM) or CFA assay (1-30 μM) was selected to simulate typical blood plasma concentrations of OXL in cancer patients (14.6 ± 3.1 μM) [64]. However, since no viable cells were found following exposure to 100 and 300 μM of in the MTT assay, only the results for the 0-50 μM dose range were reported. Likewise, since OXL at 10 and 30 μM almost yielded a complete loss of colonies in CFA assay, only the data for the 1-5 μM dose range was presented in the figure.

3.2.3 Detection of platinum anticancer drugs using a fluorescent probe FDCPt1

The fluorescence probe FDCPt1 has been recently reported to detect platinum drugs in colorectal cancer cells, including oxaliplatin (OXL), cisplatin and carboplatin [161]. This probe provided an opportunity for us to examine the role of hCTR1 in the uptake transport of OXL in colorectal cancer cells since hCTR1 overexpression would be expected to enhance cellular uptake of OXL, if it plays a positive role in this regard. Briefly, hCTR1-overexpressing

DLD-1/hCTR1 cells and empty vector-transfected mock control cells were seeded at a density of $8x10^4$ cells/well onto a sterile coverslip mounted on a 24-well plate. Cells were cultured under standard conditions for 2 days until the cellular confluence reached at least 50%. Cells were then exposed to 30 µM OXL for 2 h, respectively. Subsequently, cells were washed once with 2 ml pre-warmed PBS followed by the addition of 100 µM FDCPt1 prepared in warm PBS. After light protected incubation under standard culture conditions for 30 min, cells were washed once with 2 ml PBS and fixed with cold methanol for 15 min. After fixation, cells were washed three times with 2 ml PBS. The coverslip with fixated cells was removed from the well and mounted onto a microscopic slide, using Vector mounting media (Vector Laboratories, Burlinggame, CA, USA). Fluorescence images were captured using an upright fluorescence microscope (Olympus, Melville, NY, USA) at a wavelength of 488 nm for FDCPt1 signal, and 358 nm for nucleus, respectively. The concentrations and incubation times for FDCPt1 were selected based on the recommended experimental conditions used in a recent study [160]. In addition, 30 µM OXL was the optimal concentration based on the results of my previous pilot study(unpublished data).

3.3 Results

3.3.1 Establishment of hCTR1-overexpressing colorectal cancer cell line

In total, four G418-resistant colonies comprising of approximately 50-100 cells each were selected and subcultured in medium containing 150 µg/ml G418 as hCTR1-overexpressing clones. In parallel, two empty vector transfected clones were established in the same way of culture as mock control clones.

The hCTR1 protein level of these hCTR1-overexpressing clones and empty vector-transfected mock control clones was measured using Western blotting analysis. In general, the level of hCTR1 protein was higher in hCTR1-overexpressing clones than those mock control clones.

Based on the densitometry analysis, the hCTR1 protein level appeared to be the highest in the clone 2 among all hCTR1-transfected clones, whereas the lowest hCTR1 level was detected in the clone 2 of mock control clones (Fig. 3-1). Therefore, the hCTR1-transfected clone 2 was selected to represent the overexpressing subline, named as DLD-1/hCTR1, and the empty vector-transfected clone 2 was selected as the corresponding mock control subline for further quality tests.

A

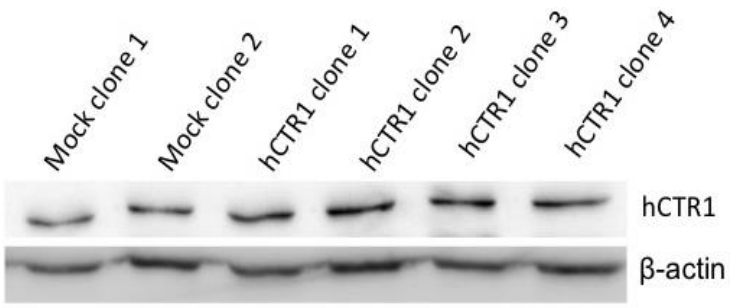

B

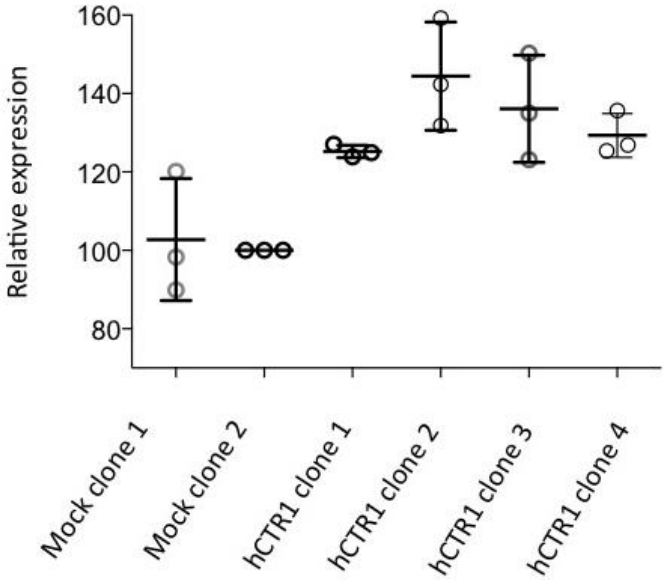

Figure 3-1. hCTR1 protein level of selected clones of colorectal cancer DLD-1 cells stably transfected with SLC31A1 gene or the corresponding empty vector

A. Representative immunoblots of hCTR1-transfected clones (hCTR1 clone 1-4) and mock clones (mock clone 1 and 2) measured by Western blotting in three independent experiments. B. Densitometry analysis of hCTR1 protein levels in four hCTR1-transfected clones and two mock clones. The hCTR1 protein level was normalized to the loading control β-actin. Data represent mean ± SD (n=3).

To monitor the stability of hCTR1 expression in the DLD-1/CTR1 and the mock control lines, hCTR1 protein levels were measured using Western blotting following four additional passages of these sublines maintained in fully supplemented culture media containing 250 μg/ml G418. As shown in Fig. 3-2, the densitometry analysis indicated that the hCTR1 protein level of DLD-1/hCTR1 cells was significantly higher than that of mock control cells by ~ 42 ± 10% ($P < 0.05$), which was consistent with the results of the initial clone selection as described above (Fig. 3-1).

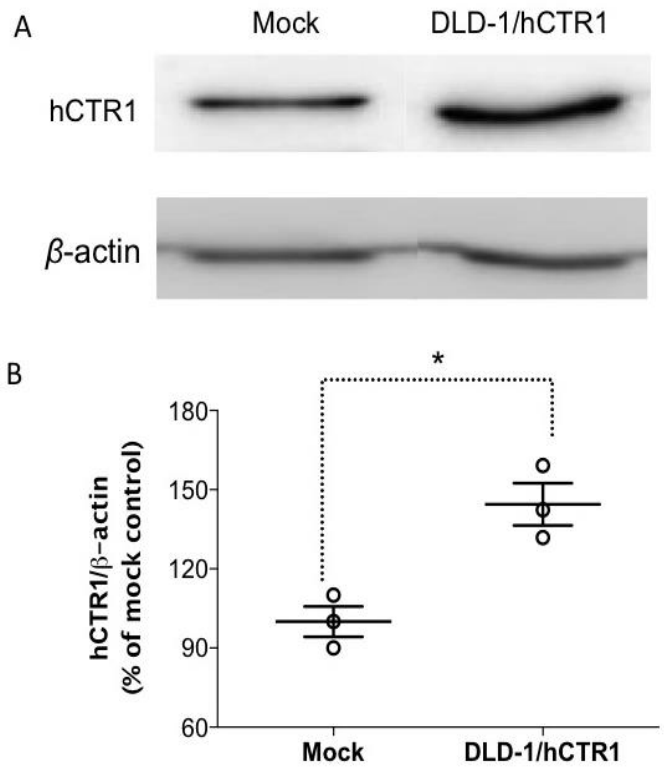

Figure 3-2. hCTR1 protein level in overexpressing DLD-1/hCTR1 line and mock control line

A. Representative Western blotting results of DLD-1/hCTR1 and mock control cells. B. Densitometry analysis of hCTR1 western blot results normalized to β-actin. The transferred membrane was incubated with an anti-hCTR1 primary antibody (1:2000) and an HRP-conjugated secondary antibody (1:2000). Data are expressed as mean ± SD (n=3). *$P < 0.05$ compared to mock control.

Based on the validation of stable hCTR1 expression, the DLD-1/hCTR1 subline and mock control subline were selected for all subsequent studies.

3.3.2 Overexpression of hCTR1 enhances the cytotoxicity of copper chloride in colorectal cancer DLD-1 cells

For the MTT assay, cells were first incubated with $CuCl_2$ at 5, 10, 30, 50, 100, 300, 500 and 1000 μM for 72 h before performing the assay. The loss of viability of DLD-1/hCTR1 cells was significantly higher compared to the mock cells following exposure to increasing concentrations of $CuCl_2$ (Fig. 3-3A). The IC_{50} of $CuCl_2$ was significantly lower in DLD-1/hCTR1 cells than that in mock cells by approximately 2.7 folds (28.3 ± 2.5 μM vs 76 ± 7.1 μM, $P < 0.05$, *t*-test) (Fig. 3-3B). The selection of $CuCl_2$ concentration ranges was based on its cytotoxicity in wild-type DLD-1 cells measured in our pilot experiments.

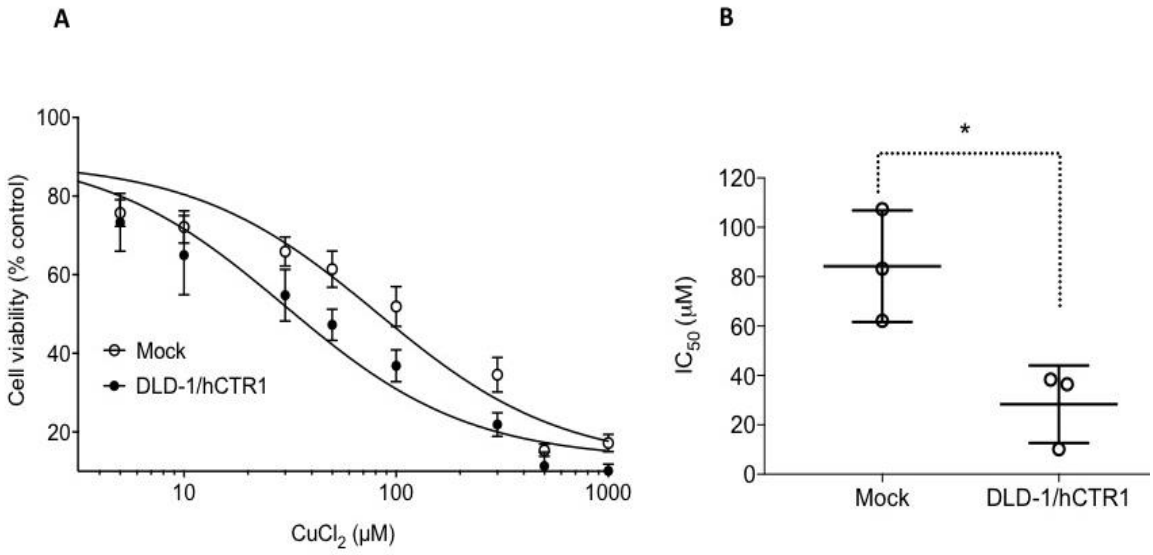

Figure 3-3. Overexpression of hCTR1 enhances the cytotoxicity of $CuCl_2$ in colorectal cancer DLD-1 cells

A. Growth curves of DLD-1/hCTR1 and mock cells exposed to indicated concentrations of $CuCl_2$ for 72 h, followed by the MTT cytotoxicity assay. Curve fitting was carried out using non-linear regression function of log (inhibitor) vs. response (three parameters). B. IC_{50} values of $CuCl_2$ in DLD-1/hCTR1 and mock cells. Data points represent mean ± S.D. of three independent experiments. $^{*}P < 0.05$ compared to mock control cells.

Next, the CFA was used to measure the sensitivity of DLD-1/hCTR1 cells and mock cells to $CuCl_2$. Briefly, cells were exposed to 200, 400 and 800 μM $CuCl_2$ or drug vehicle for 24 h, and then cultured in drug-free media for about two weeks to allow colony formation. Similar numbers of colonies were formed in vehicle-treated DLD-1/hCTR1 cells and mock control cells (263 ± 19 vs 257 ± 13, $P > 0.05$) (Fig. 3-4). However, a significantly reduced number of colonies were detected in DLD-1/CTR1 cells following exposure to 200 and 400 μM $CuCl_2$ by 54 ± 7 % ($P < 0.05$) and 92 ± 10 % ($P < 0.05$), respectively, when compared to the mock cells, while no colonies formed in both cell lines following exposure to 800 μM $CuCl_2$.

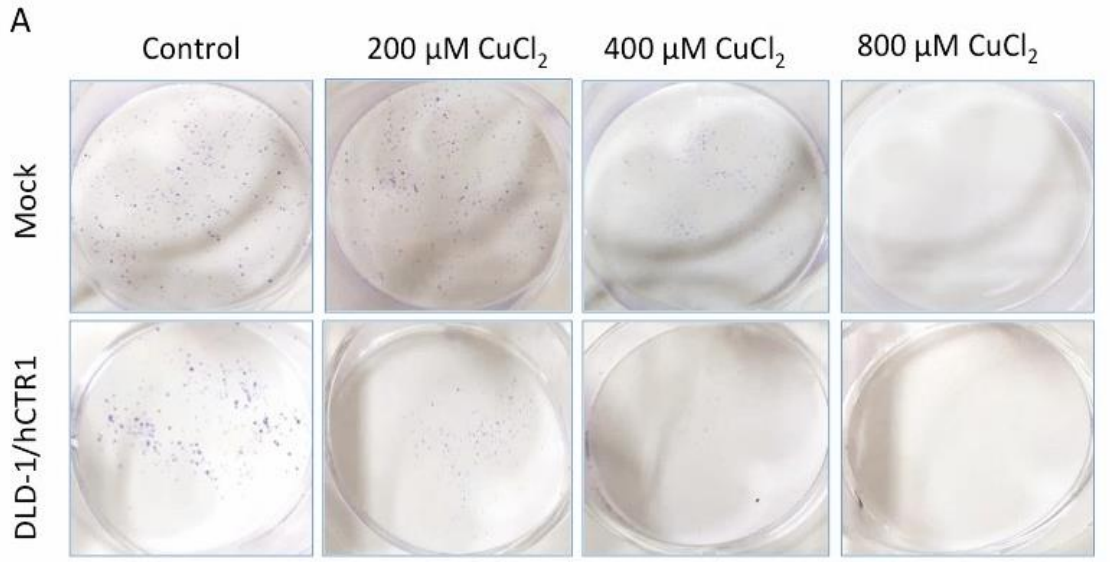

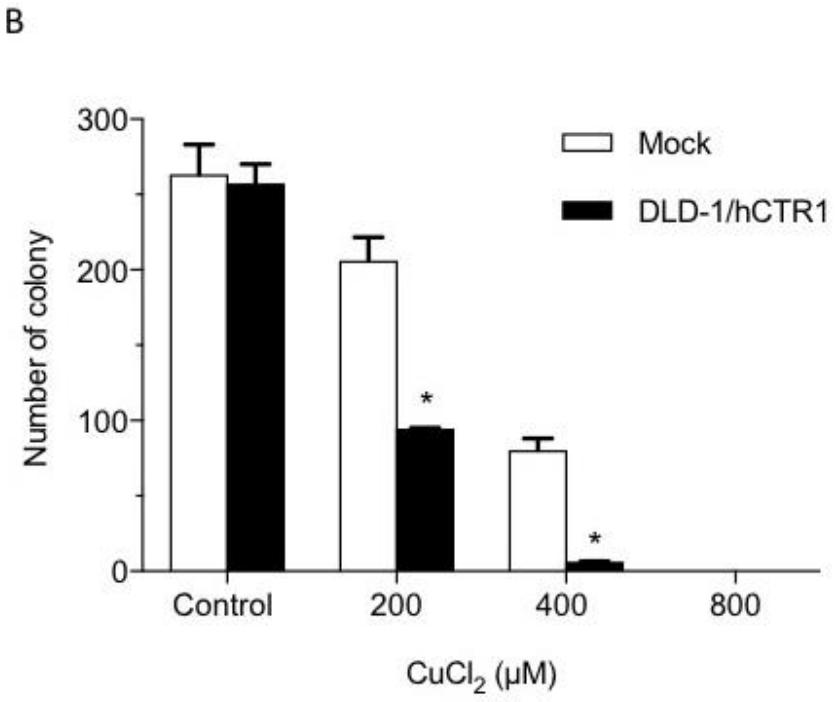

Figure 3-4. Overexpression of hCTR1 enhances the inhibitory effect of $CuCl_2$ on the colony forming ability of colorectal cancer DLD-1 cells

A. Representative image of a 6-well plate showing colonies formed in DLD-1/hCTR1 and mock control cells following exposure to 200, 400 and 800 μM $CuCl_2$. B. Number of colonies formed in DLD-1/hCTR1 and mock cells following exposure to indicated concentrations of $CuCl_2$. Data represent mean ± S.D. (n = 3). * $P < 0.05$ compared to mock control.

3.3.3 Overexpression of hCTR1 enhances the cytotoxicity of oxaliplatin in colorectal cancer DLD-1 cells

Following the confirmation of functional expression of hCTR1 as described above, DLD-1/hCTR1 cells were further examined for their sensitivity to oxaliplatin (OXL) in comparison with the mock control cells. The MTT assay and CFA were used to evaluate the short and long-term cytotoxicity of OXL.

For the MTT assay, cells were exposed to increase the concentration of OXL from 0.3-300 μM for 2 h, and then cultured in drug-free media for 72 h before performing the MTT cytotoxicity assay. The cellular viability of DLD-1/hCTR1 cells was significantly reduced by 8.5 ± 2.3% to 16 ± 3.6% compared to mock control cells at the concentrations tested ($P < 0.05$) (Fig. 3-5). However, we did not see significant difference between two cell lines at 100 and 300 μM (results not presented here).

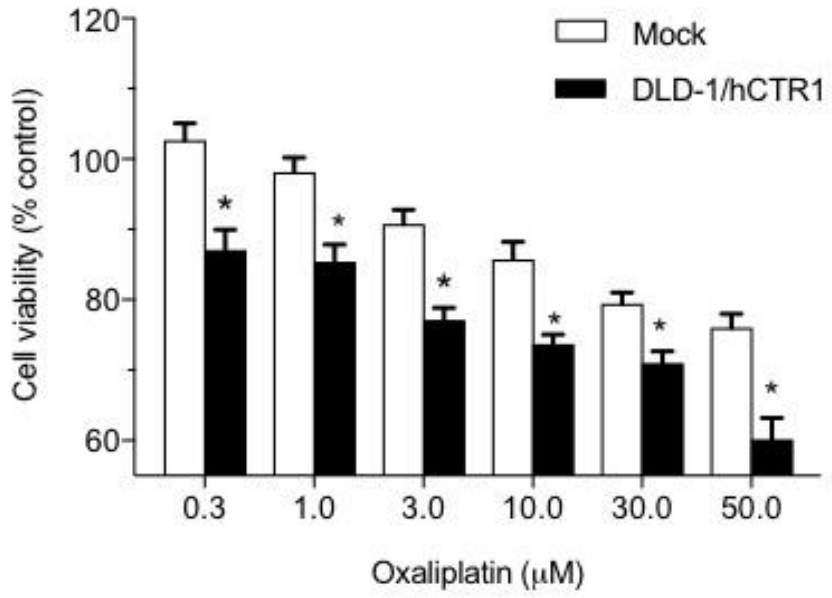

Figure 3-5. Overexpression of hCTR1 enhances the cytotoxicity of oxaliplatin in colorectal cancer cells measured by the MTT assay

The DLD-1/CTR1 and mock cells were seeded at 5000 cells per well in triplicate or quadruplicate in a 96-well plate and exposed to OXL at indicated concentrations before performing the MTT assay. Data values represent mean ± SD. (n=3 or 4). *$P < 0.05$ compared to mock control.

The results of the CFA of OXL cytotoxicity are shown in Fig. 3-6. Colonies appeared visibly fewer in DLD-1/hCTR1 cells than the mock cells when exposed to 3 or 5 μM OXL (Fig. 3-6A). Upon quantification of colonies, 364 ± 6 and 317 ± 8 colonies formed in drug vehicle-treated control wells of DLD-1/hCTR1 cells and mock cells respectively. Colony numbers for both cell lines reduced upon exposure to increasing concentrations of OXL. The number of colony did not change much in DLD-1/hCTR1 cells and mock cells following the treatment of cells with 1 μM OXL (348 ± 9 vs 315 ± 7, $P > 0.05$). However, colony numbers in DLD-1/hCTR1 cells were significantly reduced by 1.4 folds (221 ± 21 vs 310 ± 2, $P < 0.05$) following exposure to 3 μM OXL as compared to the mock cells. Following exposure to 5 μM OXL, the number of colonies in DLD-1/hCTR1 cells were significantly lower compared to the mock cells by 1.7 folds (173 ± 9 vs 291 ± 7, $P < 0.05$) (Fig. 3-6B). However, we did not see significant difference in cells treated with 10 and 30 μM OXL as both of these concentrations killed all the colonies (results not presented in the figure).

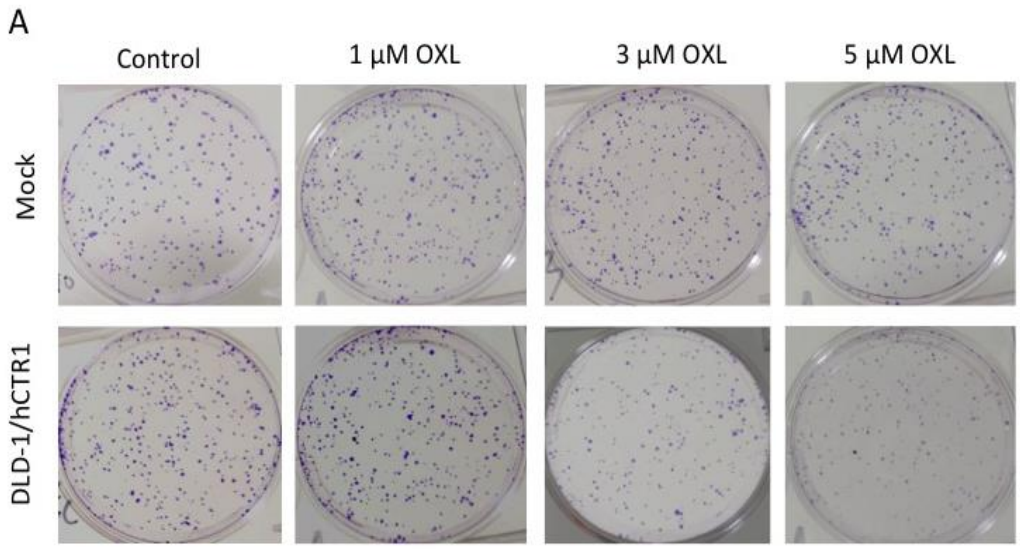

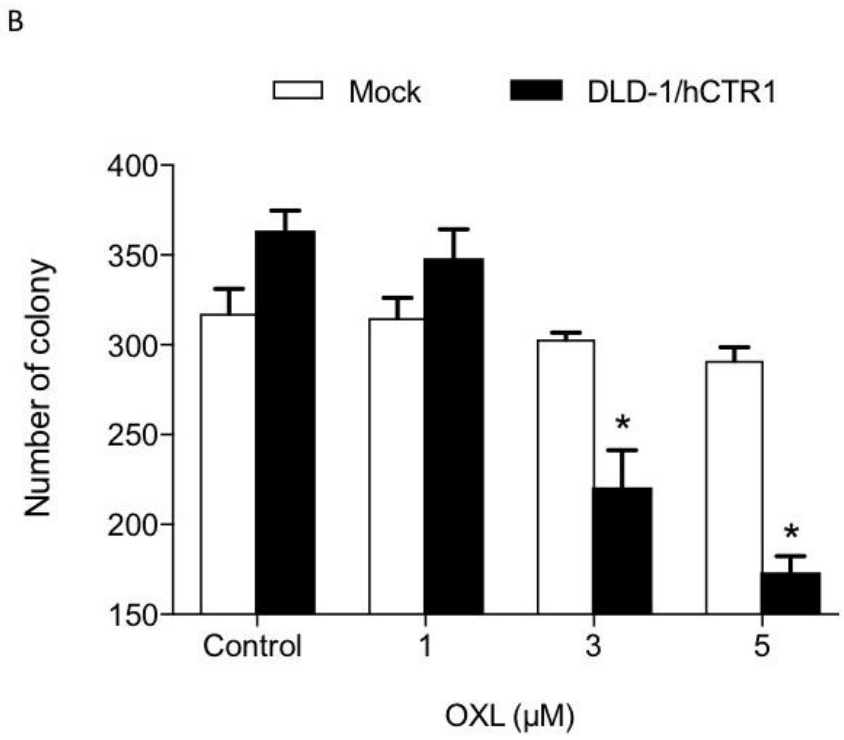

Figure 3-6. Overexpression of hCTR1 enhances the inhibitory effect of OXL on the clonogenic potential of colorectal cancer DLD-1 cells measured by the CFA

A. Representative image of a 6 well plate showing colonies formed in DLD-1/hCTR1 and mock control cells following exposure to vehicle or 1, 3, 5, 10 and 30 μM OXL. B. Number of colonies formed in DLD-1/hCTR1 and mock cells following exposure to vehicle or OXL at indicated concentrations. Data are expressed as mean ± SD. (n = 3). * $P < 0.05$ compared to mock cells.

3.3.4 Overexpression of hCTR1 enhances cellular uptake of oxaliplatin in colorectal cancer cells

No fluorescent signal was detected in DLD-1/hCTR1 cells and mock control cells following incubation with FDCPt1 alone (Fig. 3-7A). In contrast, a weak but visible fluorescence signal was detected in DLD-1/hCTR1 and mock cells following exposure to 30 μM OXL for 2 h. Fluorescence intensity increased in both cell lines following exposure to 30 μM OXL for 6 h,

with signal intensity markedly stronger in DLD-1/hCTR1 cells compared to mock cells. Digital quantification of fluorescence intensity showed that the signal in DLD-1/hCTR1 cells was ~1.48-fold higher than that of mock control cells after 6 h (Fig. 3-7B). In addition, FDCPt1-derived fluorescence signal was mainly localized to the plasma membrane in mock control cells, whereas it was predominantly localized to the cytoplasm in DLD-1/hCTR1 cells (Fig. 3-7A, inserts).

A

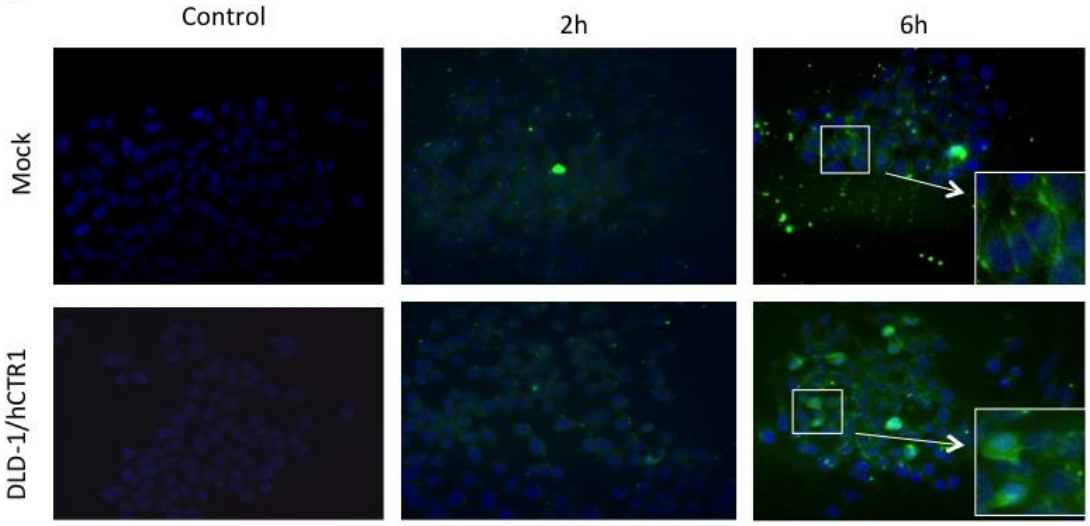

B

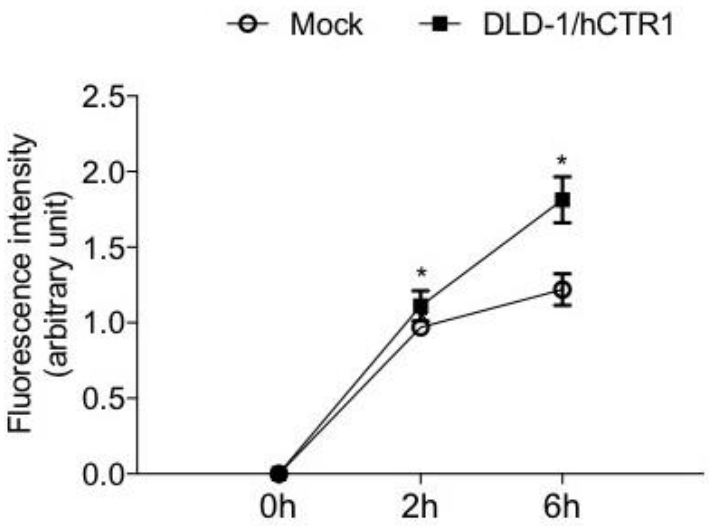

Figure 3-7. Overexpression of hCTR1 enhances cellular uptake of oxaliplatin in colorectal cancer DLD-1 cells

A. Fluorescent images of DLD-1/hCTR1 and mock cells treated with 100 μM FDCPt1 alone or after incubation with 30 μM OXL. OXL-activated FDCPt1 (green). Nucleus marker (blue). Mag. 40x. Insert is an enlargement of white-framed area. B. Quantitative analysis of FDCPt fluorescence intensity of DLD-1/hCTR1 and mock cells after incubation with 30 μM OXL. Data represents mean ± SD. (n = 3). * $P < 0.05$ compared to mock control cells. Cells were treated with 30 μM OXL for 2 and 6 h, and then incubated with 100 μM FDCPt1 for 30 min. Images were captured with a fluorescence microscope and analyzed using Image J software.

3.4 Discussion

In this study, we demonstrated the positive contribution of human copper transporter hCTR1 as an uptake transporter of OXL in colorectal cancer cells that stably express recombinant hCTR1 via plasmid-based transfection.

Firstly, we have successfully established a subline of colorectal cancer DLD-1 cells that stably express *hCtr1* gene (DLD-1/hCTR1) and a corresponding subline as the mock control cells that were transfected with the empty vector. The conditions for transfection and selection were optimized to obtain resistant clones of DLD-1 cancer cells under the cytotoxic pressure of G418. Recombinant hCTR1 protein levels in DLD-1/hCTR1 cells were about 40 % higher compared to the levels in mock control cells. This phenotype was consistently maintained over several population doublings following additional subculture, based on the verification of elevated hCTR1 protein expression in DLD-1/hCTR1 cells. Previously, varying levels of hCTR1 have been reported in different types of cancer cells that are transfected transiently or stably with constructs containing the hCtr1 gene, such as an ovarian carcinoma cell line [162]

and an non-small cell lung cancer cell line [163]. These cell-specific expression differences of target gene could be attributable to transfection efficiency, the specific plasmid backbones used, as well as endogenous hCTR1 levels. In our study, wild-type DLD-1 colorectal cancer cells displayed a discernable level of basal hCTR1 expression, which might limit the expression of recombinant hCTR1 in these cells.

The functional activity of hCTR1 in overexpressing DLD-1/hCTR1 cells was verified by measuring their sensitivity to $CuCl_2$, which is a prototype substrate of hCTR1. The cytotoxicity of $CuCl_2$ is known to be associated with its cellular accumulation [164,165]. In this study, the short-term toxicity of $CuCl_2$ to DLD-1/hCTR1 cells increased approximately by 2.7 folds when compared to the mock control cells based on their IC_{50} values derived from the MTT assay. In addition, long-term cytotoxicity of $CuCl_2$ was also increased in DLD-1/hCTR1 cells, based on their markedly reduced clonogenic capacity following drug exposure, which was measured by the colony forming assay. These data suggest that the elevated cytotoxicity of $CuCl_2$ in DLD-1/hCTR1 cells was likely induced by hCTR1-mediated increase of cellular Cu uptake.

The availability of an overexpressing DLD-1/hCTR1 colorectal cancer line was the basis to examine the role of hCTR1 in the cellular transport of OXL. Indeed, our results have demonstrated that overexpression of hCTR1 significantly increases the cytotoxicity and uptake of OXL in DLD-1/hCTR1 cancer cells. Compared to the mock control cells, the short-term cytotoxicity of OXL at pharmacologically relevant concentrations increased in DLD-1/hCTR1 cells by approximately 8.5~16% ($P < 0.05$), while the long-term toxicity of OXL increased in these cells by 1.4~1.7 folds ($P < 0.05$). This increased sensitivity was likely a direct consequence of hCTR1-dependent increased cellular uptake of OXL in DLD-1/ cells by approximately 1.5 folds. Compared to the mock control cells, DLD-1/hCTR1 cells displayed stronger cellular uptake of OXL in cytoplasm, which suggests a direct contribution of hCTR1 to the cellular uptake of OXL in these cells.

Our results support a positive role of hCTR1 in the cellular transport of OXL in colorectal cancer cells, which is consistent with other studies that used hCTR1-overexpressing small cell lung cancer cells [166], hCTR1-transfetced HEK293 cells [167], mouse Ctr1-knockout embryonic fibroblasts [163] and rCtr1-transfected HEK293 cells [163]. Nevertheless, the capacity of hCTR1 overexpression to increase cellular uptake and cytotoxicity of OXL appear to differ among different cell types. We observed a 1.4-fold increase in the sensitivity of DLD-1/hCTR1 cells to OXL compared to the mock cells, whereas others report a 3.3-fold increase in HEK293/hCTR1 cells transfected with a similar construct [166,168,169].

Notably, the capacity of hCTR1 to transport Cu and OXL, and to enhance their cytotoxicity appeared to differ in colorectal cancer DLD-1 cells. For example, the sensitivity of DLD-1/hCTR1 cells to $CuCl_2$ was increased by 2.7 folds, but their sensitivity to OXL was only increased by maximally 16% based on the results of the MTT cytotoxicity assay. This observation is consistent with a recent study that reports a ~70-fold increased toxicity of $CuCl_2$ compared to OXL-toxicity in hCTR1-transfected HEK/hCTR1 cells [155]. This may be attributable to differences in the uptake between Cu and platinum anticancer drugs. hCTR1-transfected HEK/hCTR1 cells are reported to accumulate Cu at a ~80-fold higher rate than that for taking up OXL (0.33 vs 0.004 nmol/mg protein/min/μM drug) [157]. It may also be attributable in part to differences in substrate specificity and affinity to hCTR1, cellular capacity of handling and tolerance to excess levels of Cu and Pt [170].

The fluorescence probe FDCPt1 was designed to specifically detect monofunctional Pt(II) species. OXL can be bio-transformed into numerous pharmacologically active Pt-containing species once entering the cell, including the monofunctional monochloro- and monoauqated Pt biotransformation products [68,70,73]. In our study, FDCPt1 was successfully used to trace the uptake and distribution of OXL-derived monofunctional Pt species in colorectal cancer DLD-1/hCTR1 cells and mock control cells. The sensitivity and reproducibility of FDCPt1

results were compatible with a previous report where FDCPt1 effectively detects monofunctional biotransformation products of OXL, cisplatin and carboplatin in HT-29 and Caco-2 colorectal cancer cells [72,171]. We also observed that DLD-1/hCTR1 cells displayed strong FDCPt1-associated fluorescence especially with a significant nucleus localization. This is supportive of enhanced OXL cytotoxicity, because its main pharmacological activity depends on the formation of nucleus DNA-Pt adducts [68,70,73].

Taken together, this data show for the first-time the capability of hCTR1 to mediate the uptake and cytotoxicity of OXL in colorectal cancer cells. Stable expression of recombinant hCTR1 increased both short-term and long-term cytotoxicity of OXL of DLD-1 colorectal cancer cells. Our data demonstrate that overexpression of recombinant hCTR1 enhances the cellular uptake of OXL. In particular, the hCTR1-mediated increased uptake of OXL with its cytoplasmic and nucleus accumulation of active Pt-containing biotransformation species appeared to contribute to the observed increased cytotoxicity in colorectal cancer cells.

Chapter 4 Effects of Cu Chelators and Cu chloride on Oxaliplatin Cytotoxicity in Colorectal Cancer Cells

4.1 Introduction

The results of the Chapter 3 demonstrated a positive role of hCTR1 in the uptake of oxaliplatin in colorectal cancer cells that overexpress recombinant hCTR1. Previously, pharmacological approaches to achieve this goal involve up regulation of hCTR1 expression in cancer cells, for example by Cu chelators [68,70,73]. Cu chelators have been reported to be able to increase endogenous hCTR1 protein expression and enhance the anticancer activity of cisplatin, another commonly used platinum anticancer drug used *in vitro* and *in vivo* preclinical models [172]. Cu chelators that are clinically used for the treatment of Wilson's disease have been reported to sensitize cells towards the anticancer activity of cisplatin via hCTR1- or mCtr1-mediated transport mechanism. Although, the Cu chelators ammonium tetrathiomolybdate (ATTM) and D-penicillamine (D-P) show this effect in human cervical and ovarian cancer cells [68,70,73], studies of this type have not been undertaken with OXL or in colorectal cancer cells.

All these results have set a basis for targeting hCTR1 to enhance the anticancer activity of OXL via improving its uptake into cancer cells. However, understanding the endogenous expression of copper transporters in appropriate cellular model is a prerequisite towards this goal. Therefore, we firstly systematically investigate the endogenous expression of the Cu uptake transporter hCTR1 and the copper efflux transporters ATP7A and ATP7B in native colorectal cancer cell lines. We selected four colorectal cancer cell lines HCT-15, DLD-1, COLO205 and SW620, which have also been included in National Cancer Institute's NCI-60 panel for drug screening [154]. In addition, these cell lines represent the primary or metastatic subtypes of the disease. DLD-1 and HCT-15 were derived from a primary Dukes'C colorectal

carcinoma specimen of the same patient but showing different karyotypes [154]. The SW620 line was derived from a lymph node metastasis in a patient with Dukes' C colorectal adenocarcinoma [76]. COLO205 was derived from ascetic fluid of a patient with colon carcinoma with multiple metastases [79]. COLO205 harbors the BRAF (V600E) mutation, whereas KRAS mutations are detected in DLD-1, HCT-15 and SW620 cells [174].

Therefore, the aim of this chapter was to investigate the therapeutic value of Cu chelators to enhance OXL cytotoxicity in colorectal cancer cells by modulating hCTR1 expression. The expression and the localization of copper transporters in the selected cell lines were investigated using RT-PCR, Western blotting and immunohistochemistry techniques. The cytotoxicity of drugs was measured using the MTT assay as described above. Cellular hCTR1 protein levels were measured using a reliable Western blotting assay in cancer cells undergoing treatment with different drugs and conditions. The effects of Cu chelators on the major Cu efflux transporters ATP7A and ATP7B were also measured in contrast with that on hCTR1. In addition, the effect of Cu chloride and OXL on hCTR1 expression was measured in colorectal cancer cells, since Cu chloride and cisplatin reportedly cause degradation of hCTR1 in other cancer cell types [173].

4.2 Experimental design

4.2.1 Characterization of the expression of copper transporters in colorectal cancer cell lines

Combinations of methods were used to characterize the expression of hCTR1, ATP7A and ATP7B in colorectal cancer cell lines including reverse transcription polymerase chain reaction (RT-PCR), Western blotting, and immunocytochemistry. All experiments were conducted in parallel in order to compare the expression of copper transporters across cell lines.

4.2.2 Measurement of the sensitivity of colorectal cancer cell lines to oxaliplatin

In theory, each of these four cells lines can be utilized as a cellular model for following modulation studies involving different chemicals. However, to show the contribution of hCTR1, the best model should be the most resistant one, therefore, MTT assay was performed to select a relatively OXL resistant cellular model among these cell lines. Technical details about the experimental procedures were described in section 2.4.1. In either 72-h or 2-h exposure experiments, the OXL dose range was selected to achieve minimal and maximal cytotoxicity of the colorectal cancer cell lines and was based on previous cytotoxicity studies performed in our lab [165].

4.2.3 Studies on the effect of compounds on hCTR1 expression using Western blotting

Prior to incubation with Cu chelators, $CuCl_2$ and oxaliplatin, DLD-1 cells or SW620 were seeded at a seeding density of 10^5 cells/well in a 12-well plate and cultured for 3 days until a ~50% of confluence was reached.

In incubation experiments of copper chelators, DLD-1 cells were then exposed to 30 μM ammonium tetrathiomolybdate (ATTM) for 1, 6, 9 and 24 h, 10 μM D-penicillamine (D-P) for 1, 6 and 16 h, or 50 μM bathocuproinedisulfonic acid disodium salt (BCS) for 1, 16, 24 and 72 h, respectively. SW620 cells were exposed to 30 μM ATTM or 50 μM BCS for 1, 6, 9 and 24 h, respectively, or drug vehicle as controls. The selection of time points for chelator incubation was based on the results of our pilot studies. For example, rapid changes of hCTR1 protein expression were noticed in SW620 cells at earlier timepoints (6 h and 9 h). In contrast, DLD-1 cells required longer incubation times (16 h) to induce apparent protein changes. In addition, the timepoint selection was also based on the previous studies performed in other cancer cell lines to capture the most possible drug effect on hCTR1 protein levels [73,225,226].

In incubation experiments of $CuCl_2$, time points for incubation of DLD-1 cells with 100 μM $CuCl_2$ were originally arranged as 1, 6, 9, 16 h. However, they were changed to 2, 4, 8 and 16 h due to technical error (addition of drug at 1 h missed). Since study shows the effect of CuCl2 on the expression of CTR1 tends to be very quick (shorter than 1 h) [76], this 1-h error may not cause significant deviation of data measured at two sets of time points. SW620 cells were exposed to 100 μM $CuCl_2$ for 1, 6, 9 and 16 h, respectively, or drug vehicle as controls. The maximal duration of incubation and concentration of $CuCl_2$ were selected to avoid the potential stress to cells.

In incubation experiments of oxaliplatin (OXL), DLD-1 cells were exposed to 10 μM OXL for 0.25, 1, 4 and 8 h. SW620 cells were exposed to 10 μM OXL for 1, 6, 9 and 16 h, respectively, or drug vehicle as controls. The selection of short exposure time of 0.25 h for DLD-1 cells was based on the results of our pilot study, where we observed a rapid change at this time point in DLD-1 cells but not in SW620 cells. This result is also consistent with the current literature suggesting that platinum drugs induce an instant change in the level of the hCTR1 protein within 15 min in ovarian cancer cells [86]. The selection of 10 μM for OXL was based on its pharmacological relevance to the plasma concentrations of OXL in cancer patients (14.6 ± 3.1 μM) [64].

At the end of experimental incubation, cell lysates were prepared for the measurement of hCTR1 protein level using the Western blotting analysis as described below.

4.2.4 Studies on the effect of copper chelators, copper chloride and oxaliplatin on the cellular localization of copper transporters using immunocytochemistry

Prior to incubation with the compounds, DLD-1 or SW620 cells were seeded at a density of $8x10^4$ cells/well onto a sterile coverslip mounted at the bottom of a 24-well plate. Cells were cultured for 2 days to reach ~ 50% confluence, following various experimental incubations as

shown below, immunocytochemistry were utilized to capture the possible changes that were accompanied with incubation:

In experiments to determine the effect of copper chelators on ATP7A or ATP7B expression, DLD-1 or SW620 cells were then exposed to 50 μM BCS, 30 μM ATTM and 10 μM D-P, for up to 24 h.

In experiments to determine the effect of $CuCl_2$ on the cellular localization of hCTR1, DLD-1 or SW620 cells were exposed to 20 or 100 μM $CuCl_2$ for 2 h. The short exposure of 2 h was chosen based on the literature that suggest this time period is still longer enough to induce the alteration of hCTR1 [77]. To study the effect of copper on ATP7A or ATP7B expression, DLD-1 cells or SW620 cells were exposed to 100 μM $CuCl_2$ for 1, 4 and 16 h, and 6, 24 and 48 h, respectively. The maximal duration of incubation was also cell line-specific to avoid the potential stress caused by $CuCl_2$.

In experiments to determine the effect of OXL on ATP7A or ATP7B expression, DLD-1 or SW620 cells were exposed to 10 μM OXL for 0.25, 4 and 8 h, and 1, 6 and 24 h, respectively. The time points of incubation were selected to be close to the experimental conditions used to study the effect of OXL on the expression of hCTR1 as mentioned in Section 4.2.3.

Cells were treated in parallel with drug vehicle as control. At the end of incubation, the cellular localization of ATP7A or ATP7B was explored using immunocytochemistry staining.

4.2.5 Toxicity assays of DLD-1 and SW620 cells in the presence of copper chelators or copper chloride

To determine the effect of copper chelators or $CuCl_2$ on the cytotoxicity of colorectal cancer cells, DLD-1 or SW620 cells were seeded at a seeding density of 6000 cells/well in a 96-well plate in a triplicate, left overnight for attachment and incubated with 50 μM BCS or 30 μM

ATTM or 100 μM $CuCl_2$ for 16, 6 and 2 h respectively, followed by exposure to 100 μM OXL alone for 2 h and a 72-h drug free culture before performing MTT assay. Cells were treated in parallel with drug vehicle as control.

Shorter exposure (2 h) is used for observing the drug uptake and toxicity for oxaliplatin, as the initial stage of the drug uptake process is more likely mediated by drug transporters. Whereas, the drug uptake process becomes more dominated by passive diffusion mechanisms with extensive incubation [28]. Higher concentration was selected for oxaliplatin (100 μM), because it is the minimal drug level to achieve measurable toxicity with such a short incubation time, which has been shown in our pilot experiments and by others [70].

4.3 Results

4.3.1 Endogenous expression of Cu transporters hCTR1, ATP7A and ATP7B in human colorectal cancer cells

4.3.1.1 Cu uptake transporter hCTR1

hCTR1 mRNA levels were detected in DLD-1, SW620, HCT-15, and COLO205 cells by RT-PCR (Fig. 4-1A). The results of two independent experiments are reproducible and consistent with the hCTR1 mRNA levels reported for these cell lines in the NCI60 cancer cell expression dataset (U133A) [190], which is accessible via the BioGPC gene portal [191]. The density of electrophoretic bands of PCR products for hCTR1 on agarose gel appeared to be similar across the cancer cell lines, despite the semi-quantitative nature of the RT-PCR assay.

We next measured hCTR1 protein levels by Western blotting using an anti-hCTR1 antibody. In all four cancer cell lines hCTR1 could be clearly detected as a protein band of ~35 kDa. In three independent experiments, the density of hCTR1 bands, normalized to β-actin, was similar for the four cell lines (Fig. 4-1B).

A

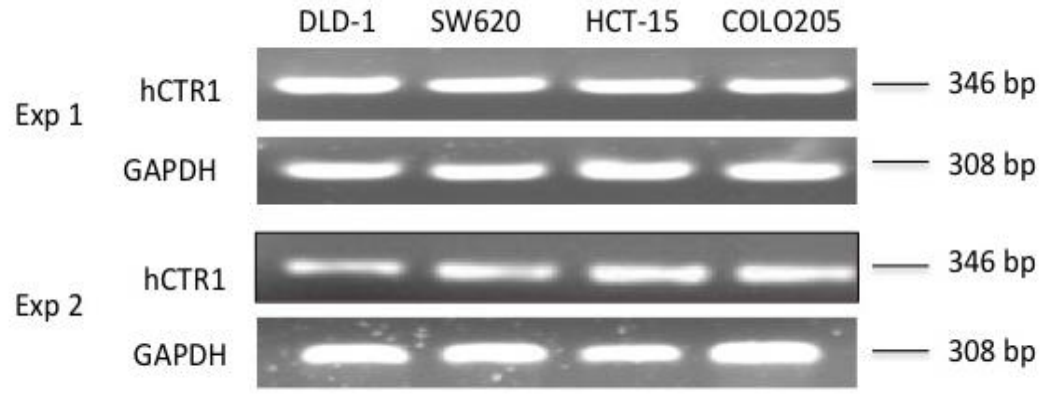
DLD-1
SW620
HCT-15
COLO205
Exp 1
hCTR1
GAPDH
346 bp
308 bp
Exp 2
hCTR1
GAPDH
346 bp
308 bp

B

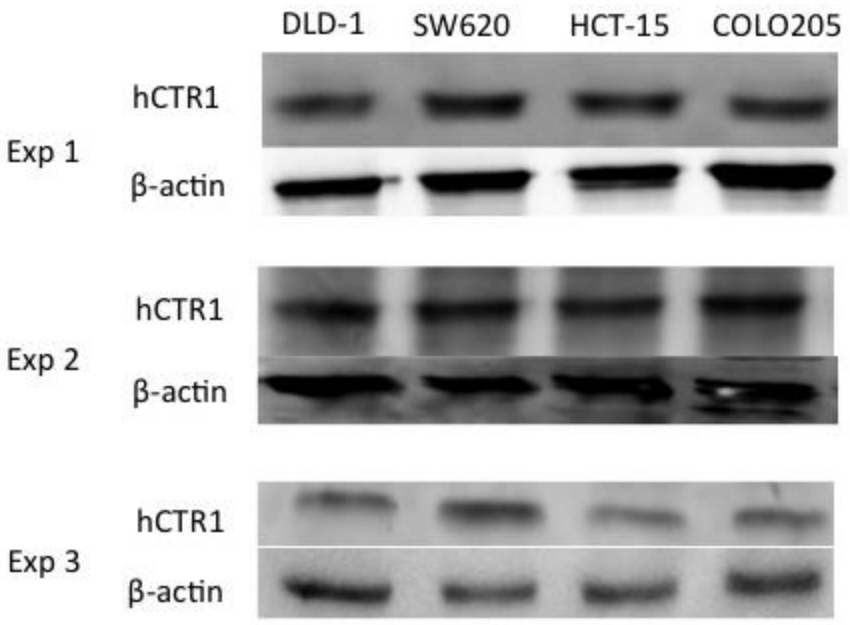
DLD-1
SW620
HCT-15
COLO205
Exp 1
hCTR1
β-actin
Exp 2
hCTR1
β-actin
Exp 3
hCTR1
β-actin

Figure 4-1. Endogenous expression of hCTR1 in human colorectal cancer cells

A. Detection of hCTR1 mRNA levels by RT-PCR in two independent experiments. B. Detection of hCTR1 protein levels measured by Western blotting in three independent experiments. GAPDH gene and *β*-actin protein were probed, respectively as loading controls.

We then performed immunofluorescence using the same primary hCTR1 antibody to visualize the cellular distribution of hCTR1. Immunoreactivity to hCTR1 was detected in all cell lines, albeit with slightly different distribution patterns and intensities (Fig. 4-2). Overall, a stronger hCTR1 immunoreactivity was associated with the plasma membrane of DLD-1 and SW620, HCT-15 cells compared to COLO205, whereas diffuse, weak but stable immunostaining was observed in the cytoplasm of all cell lines, without distinct compartment-specific localization. When excluding Triton X-100, a cell membrane permeabilizing reagent, from the immunostaining protocol, hCTR1 immunoreactivity exclusively localized to the cell surface of DLD-1, SW620, HCT-15 and COLO205 cells (Fig. 4-2).

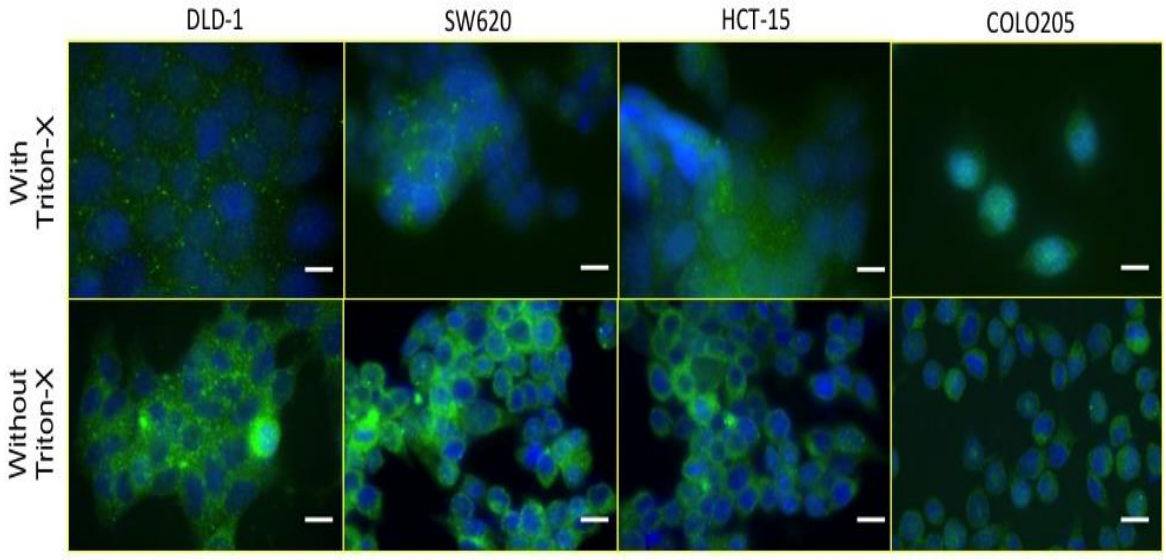

Figure 4-2. Cellular distribution of hCTR1 protein in colorectal cancer cells

DLD-1, SW620, HCT-15 and COLO205 cells were treated with or without permeabilizing agent Triton X-100 before stained with the primary anti-hCTR1 antibody and Alexa Fluor® 488-conjugated secondary antibody (green). DAPI (blue) was used as nucleus marker. Scale bars represent 10 μm.

The hCTR1 immunoreactivity was found to co-localize with that of Na^+/K^+-ATPase protein, a specific plasma membrane marker (Fig. 4-3).

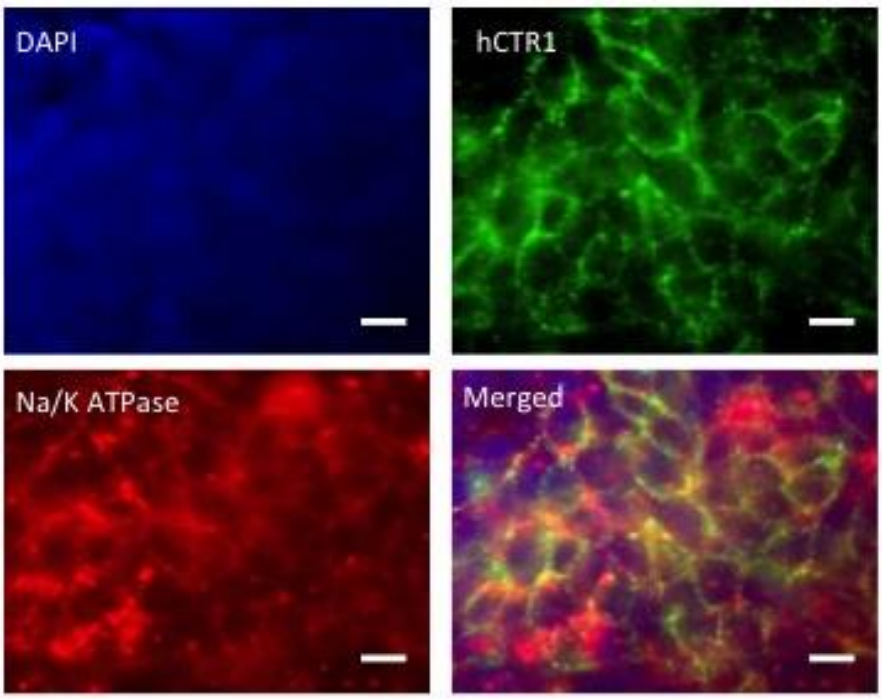

Figure 4-3. Localization of hCTR1 at plasma membrane of colorectal cancer cells

Immunofluorescent co-staining was performed in SW620 cancer cells using an anti-hCTR1 primary antibody, an anti-Na^+/K^+ ATPase primary antibody, and the corresponding Alexa 488- and Alexa 594-conjugated secondary antibodies. Partial co-localization (yellow) was observed

between hCTR1 immunoreactivity (green) and Na^+/K^+ ATPase immunoreactivity (red). DAPI (blue) was used as nucleus marker. Scale bars represent 10 μm.

4.3.1.2 Cu efflux transporter ATP7B

Next, we characterized the expression of Cu efflux transporter ATP7B in colorectal cancer cells. The mRNA of ATP7B was detected abundantly across all the four cell lines by RT-PCR analysis without apparent differences between cell lines (Fig. 4-4A). A PCR amplicon of 446bp corresponding to ATP7B mRNA was shown consistently in two independent experiments. Moreover, Western blotting identified a clear but a relatively weak protein band with the expected molecular weight of ~165 kDa in DLD-1, SW620, HCT-15 and COLO205 cancer cells using a specific anti-ATP7B antibody (Fig. 4-4B). The intensity of ATP7B protein band appeared to be much lower than that of hCTR1.

A

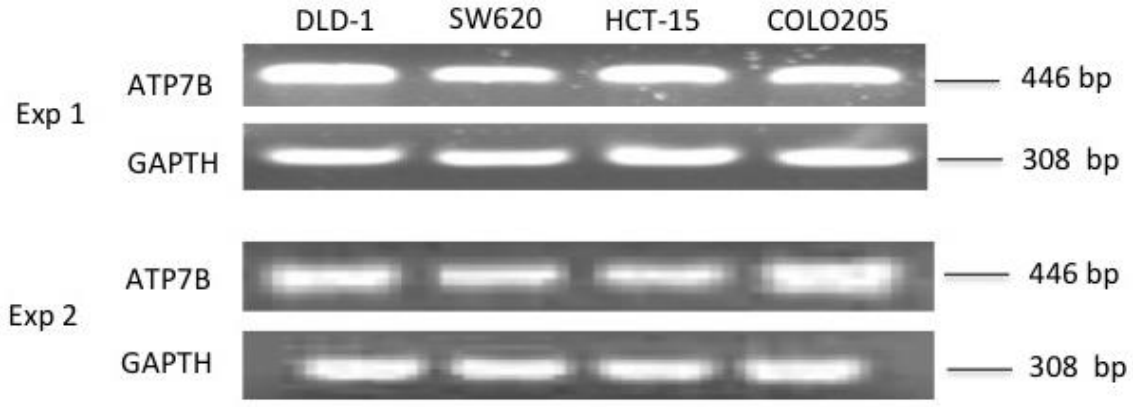

B

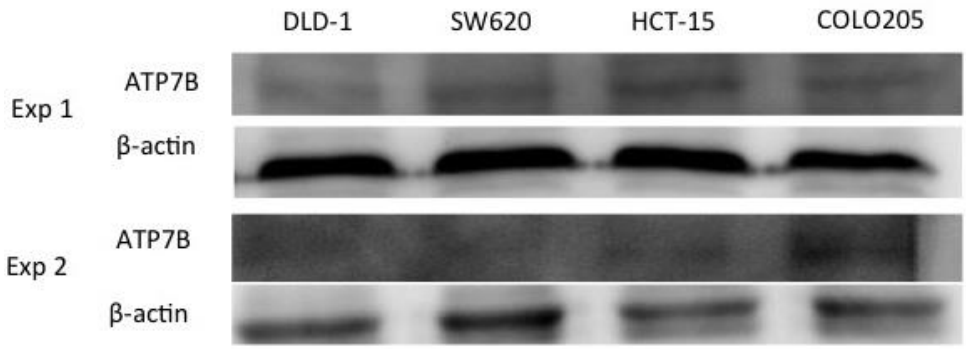

Figure 4-4. Endogenous expression of ATP7B in colorectal cancer cells

A. Detection of ATP7B mRNA expression by RT-PCR. B. Detection of ATP7B protein levels by the Western blotting of DLD-1, SW620, HCT-15 and COLO205 cancer cell extracts. GAPDH gene and *β*-actin protein were probed, respectively as loading controls.

The immunoreactivity of ATP7B was detected in all colorectal cancer cell lines, namely, DLD-1, SW620, HCT-15 and COLO205 cells (Fig. 4-5). Relatively strong plasma membrane immunoreactivity for ATP7B was detected in all four cell lines (Fig. 4-5A), which was further confirmed by co-localization of ATP7B with the plasma membrane marker Na^+/K^+ ATPase in SW620 cancer cells (Fig. 4-5B).

A

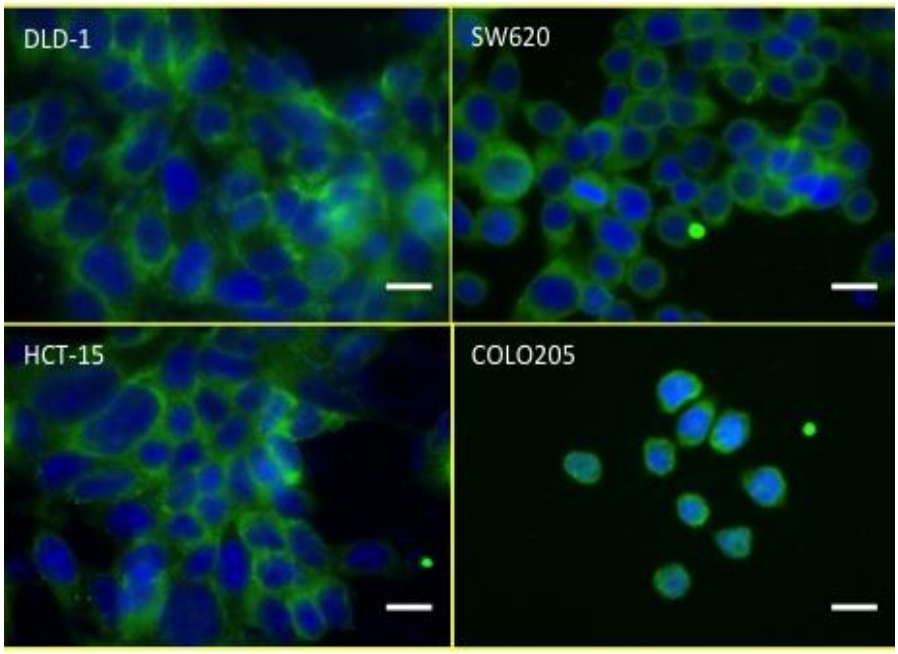
DLD-1
SW620
HCT-15
COLO205

B

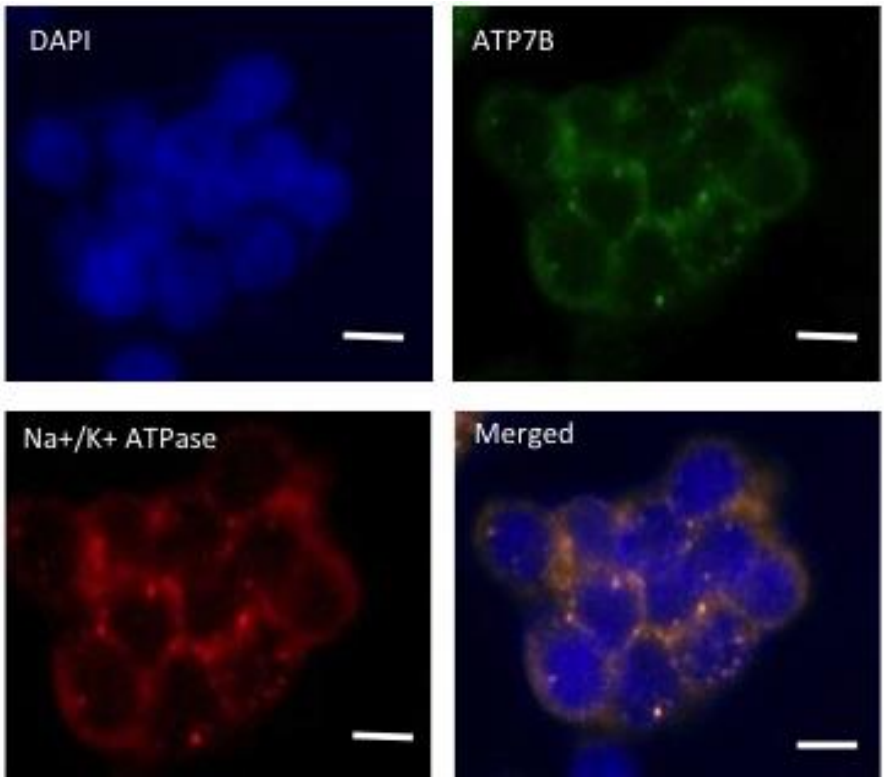

Figure 4-5. Cellular distribution of ATP7B in colorectal cancer cells

A. Immunofluorescence detection of ATP7B (green) in DLD-1, SW620, HCT-15 and COLO205 cancer cells. B. Immunofluorescence co-staining of ATP7B (green) and Na^+/K^+ ATPase (red) indicates co-localization (yellow). Species-specific Alexa 488- or Alexa 594-conjugated secondary antibodies were used with DAPI (blue) as a nucleus marker. Scale bars represent 10 μm.

4.3.1.3 Cu efflux transporter ATP7A

ATP7A mRNA was detected across the four colorectal cancer cell lines DLD-1, SW620, HCT-15 and COLO205, with no apparent differences between cell lines (Fig. 4-6A). A PCR product with an amplicon size of 322 bp was consistently detected in two independent experiments.

The intensity of the amplified ATP7A cDNA bands appeared to be lower than that of hCTR1 and ATP7B, after normalizing to the internal loading control GAPDH.

A

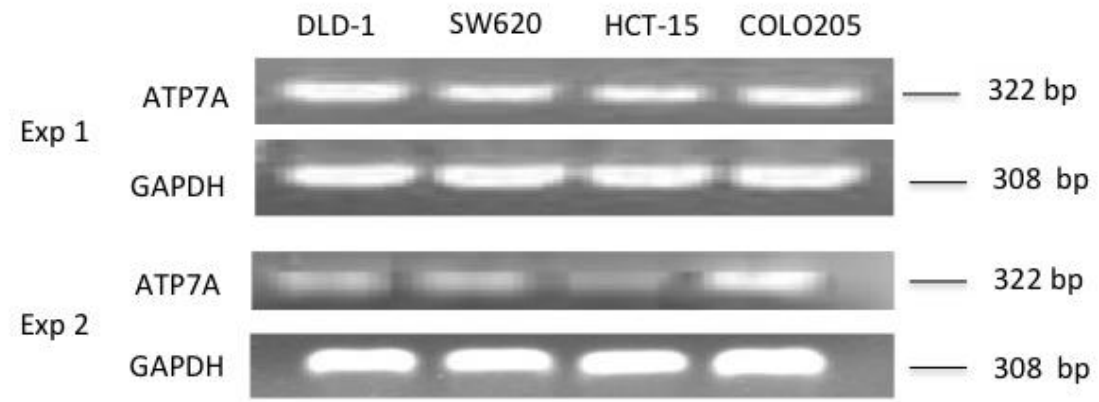

B

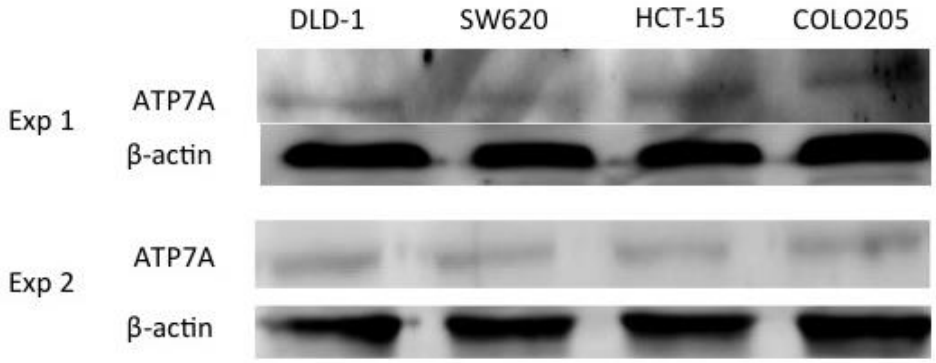

Figure 4-6. Endogenous expression of ATP7A in colorectal cancer cells

A. ATP7B mRNA detected by RT-PCR. B. ATP7A protein levels detected by Western blotting in DLD-1, SW620, HCT-15 and COLO205 cancer cells. GAPDH gene and *β*-actin protein were probed, respectively as loading controls.

Next, we measured ATP7A protein levels using Western blotting. As shown in Fig 4-6B, a protein band with the expected molecular weight of ~165 kDa was identified in DLD-1,

SW620, HCT-15 and COLO205 cancer cells using a previously validated antibody [192]. The intensity of this band appeared to be similar across all cell lines, but lower than that of hCTR1.

As shown in Fig. 5-7A, ATP7A was detected in all cell lines with different distribution patterns using immunofluorescence detection. Plasma membrane-associated immunoreactivity appeared to be stronger in DLD-1, HCT-15 and COLO 205 than SW620 cells, while all lines showed diffuse, granular and cytoplasmic staining (Fig. 4-7A). This staining pattern was confirmed by confocal microscopy, where in addition to xy-images also the z-section views were acquired (Fig. 4-7B).

A

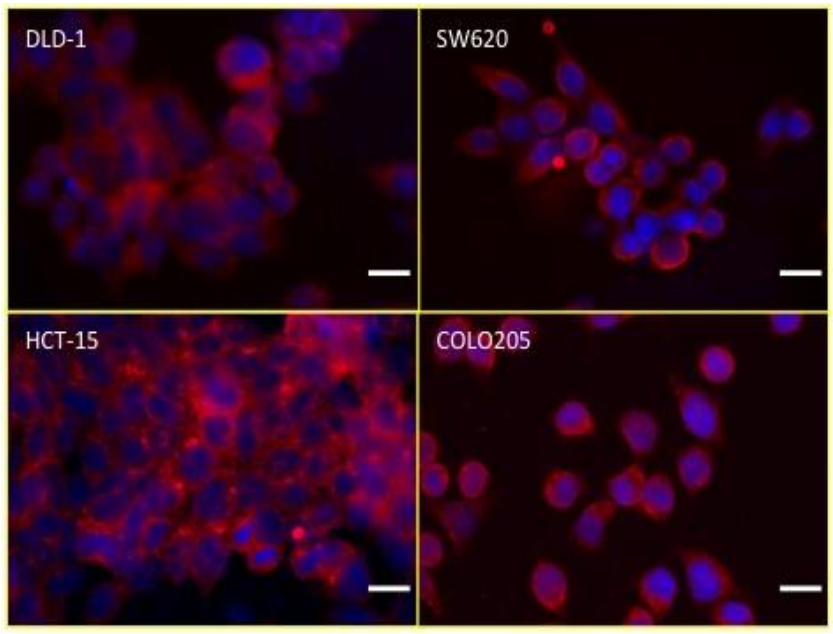

B

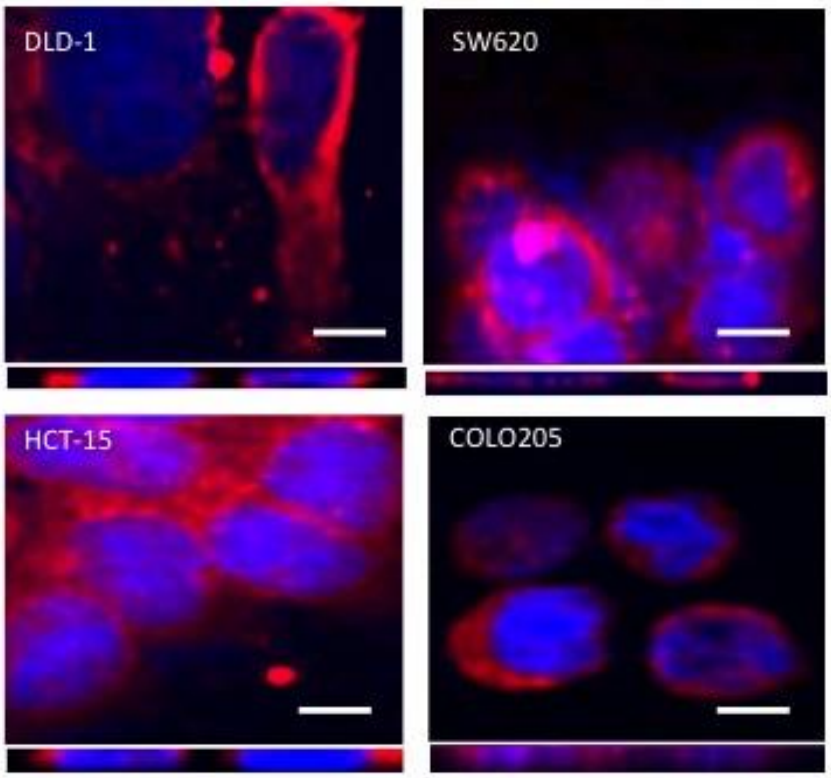

Figure 4-7. Cellular distribution of ATP7A protein in colorectal cancer cells

A. Fluorescence immunocytochemistry showing ATP7A immunoreactivity (red) in DLD-1, SW620, HCT-15 and COLO205 cancer cells. B. Confocal microscopic images of ATP7A (red) and DAPI (blue) in cancer cells, xy-plane (top) and z-sections (bottom stripes) are shown. Scale bar represents 5 μm.

4.3.2 Differential sensitivity of colorectal cancer cell lines to oxaliplatin

These cell lines display significant differences in their sensitivity to OXL following a 72-h drug exposure, with IC_{50} values of 0.8 ± 0.2, 3.2 ± 0.2, 15.4 ± 2.3 and 15 ± 3.1 μM for SW620, COLO205, DLD-1 and HCT-15, respectively (Fig. 4-8). DLD-1, HCT-15 and COLO205 cells were significantly more resistant to OXL by about 19, 18, and 4 folds, respectively, when compared to the most sensitive cell line tested, SW620.

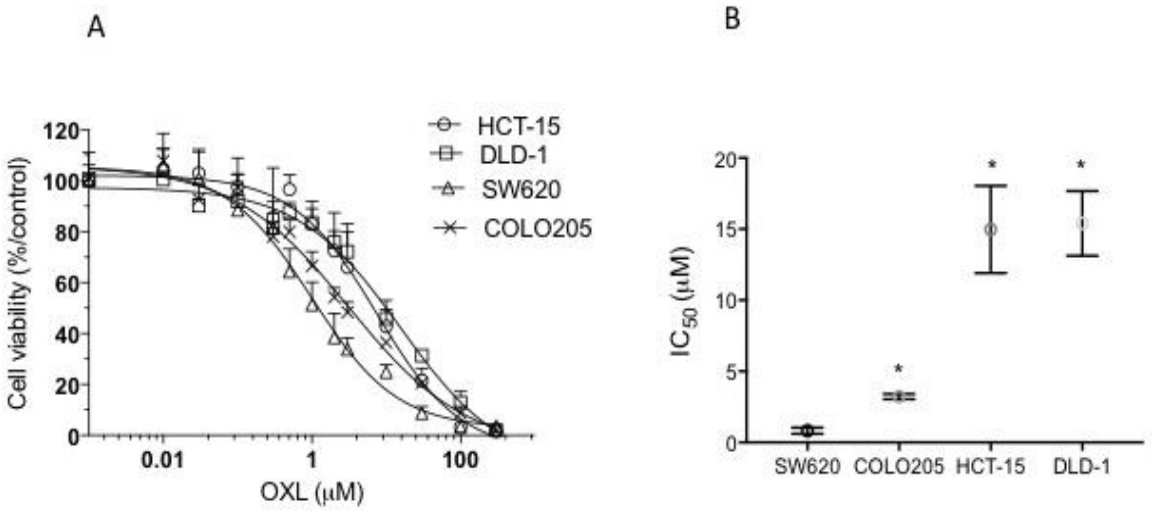

Figure 4-8. Cytotoxicity of oxaliplatin (OXL) in colorectal cancer cells following a 72 h-drug exposure

A. Viability curves of cancer cells following exposure to a range of OXL concentrations. B. Comparison of IC_{50} values of OXL in different cell lines. * $P < 0.05$ compared to SW620. Cells were treated with OXL at varying concentrations for 72 h before viability was measured by the MTT assay. Data represent mean ± SD (n = 3 or 4).

Moreover, we measured OXL cytotoxicity under conditions of short-term drug exposure (2 h-exposure), to select appropriate, non-toxic concentrations of OXL for the following incubation studies. These cell lines display significant differences in their sensitivity to OXL following a 2-h drug exposure, with IC_{50} values of 12.4 ± 5.6, 87.4 ± 11.8, 350.7 ± 35.5 and 241.8 ± 27.8 μM for SW620, COLO205, DLD-1 and HCT-15, respectively (Fig. 4-9B). DLD-1, HCT-15 and COLO205 cells were significantly more resistant to OXL by about 28, 20, and 7 folds, respectively, when compared to the most sensitive cell line tested, SW620.

In addition, the ranking of sensitivity of these cell lines to OXL after a 2 h-exposure was the same as the ranking following a 2 h-exposure. DLD-1 was the least sensitive cell line, followed by HCT-15 and COLO205, whereas SW620 was the most sensitive line to OXL (Fig. 4-9).

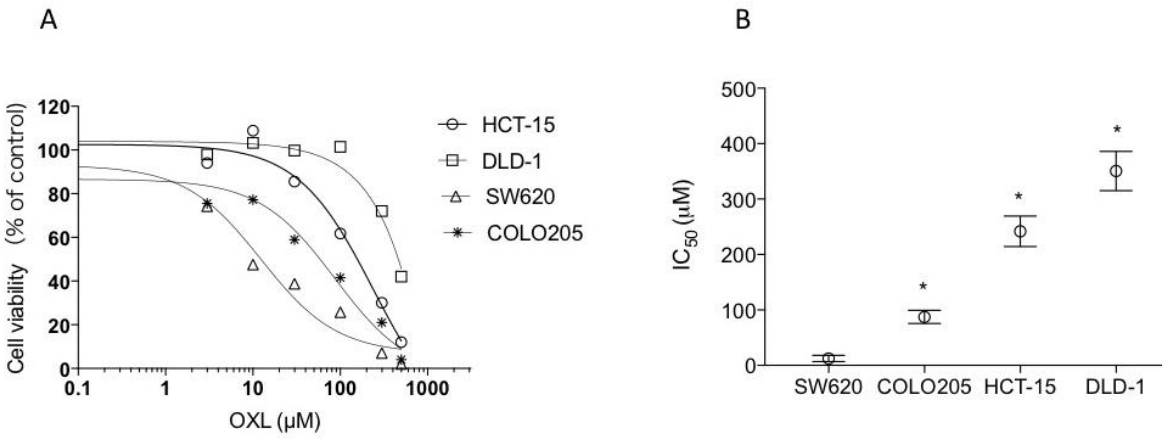

Figure 4-9. Short-exposure cytotoxicity of oxaliplatin (OXL) in colorectal cancer cells

Cells were exposed to 3, 10, 30 or 100, 300 or 500 μM OXL for 2 h, followed by a 72-h drug-free culture before preforming the MTT assay. Data represent mean ± SD. (n≥3). * $P < 0.05$ compared to drug vehicle-treated control cells (One-way ANOVA).

The reason for the different sensitivity of these colorectal cell lines to OXL is unclear but it is likely attributable to their intrinsic genetic and phenotypic characteristics. The selection of the two colorectal cancer cell lines DLD-1 and SW620 for this study was based on their abundant endogenous expression of hCTR1 and distinctive sensitivity to oxaliplatin. The colorectal cancer DLD-1 cells and SW620 cells were selected to represent a relatively resistant cell line and a sensitive cell line, respectively, to allow the subsequent comparative studies of the contribution of hCTR1 transporter. In addition, the selection of these two colorectal cancer cell lines was considered based on their origins. The DLD-1 cell line was derived from a primary

colorectal cancer tissue, whereas the SW620 line from tumor tissues of a metastatic site in the lymph node [76, 154].

4.3.3 Cu chelators up regulate hCTR1 expression in DLD-1 cells and SW620 cells colorectal cancer

The results of Chapter 3 demonstrated the presence of Cu transporters in human colorectal cancer cells and a positive role for the overexpression of recombinant hCTR1 in the cellular uptake of OXL. This prompted us to test whether Cu chelators could up regulate hCTR1 expression and thereby enhance OXL sensitivity in colorectal cancer cells. For this purpose, we tested the clinically used ammonium tetrathiomolybdate (ATTM), D-penicillamine (D-P), and an experimental Cu-chelating compound called bathocuprione disulfonate (BCS). The kinetic effects of Cu chelators on hCTR1 protein expression were measured by Western blotting using the colorectal cancer cells DLD-1 and SW620. The concentrations and incubation periods of these Cu chelators were nontoxic based on the prior cytotoxicity studies.

DLD-1 cells were exposed to 30 μM ATTM for 1, 6, 9 and 24 h, 10 μM D-P for 1, 6 and 16 h, or 50 μM BCS for 1, 16, 24 and 72 h, followed by the preparation of cell lysates for Western blotting analysis. The results of three independent experiments were relatively reproducible for the Cu chelators (Fig. 4-10 A, B & C). hCTR1 protein increased over time in DLD-1 cancer cells and the increase became statistically significant after a 6-h exposure to 30 μM ATTM (132 ± 12.5% of control, $P < 0.01$, ANOVA, Fig. 5-2A), 10 μM D-P (121 ± 13.3% of control, $p < 0.01$, ANOVA, Fig. 4-10B) or after 16 h of 50 μM BCS (124 ± 4.4% of control, $P < 0.01$, ANOVA, Fig. 4-10C). Expression of hCTR1 returned to control levels following extended periods of exposure to D-P and BCS in contrast to ATTM that induced increased expression up to 24 h.

A

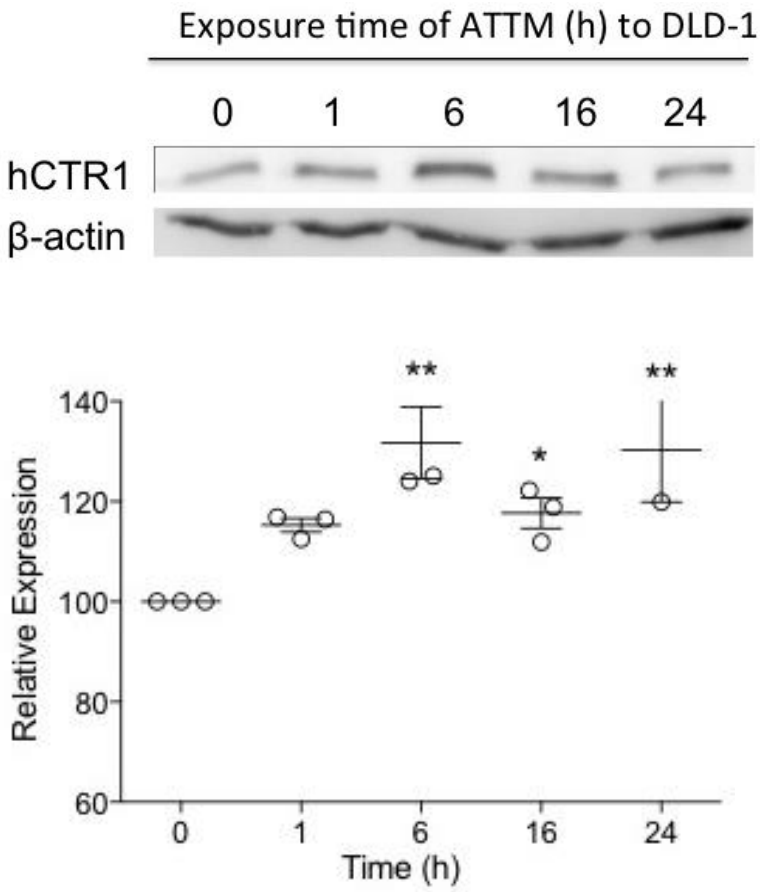
Exposure time of ATTM (h) to DLD-1
0
1
6
16
24
hCTR1
β-actin
Relative Expression
140
120
100
80
60
**
*
**
0
1
6
16
24
Time (h)

B

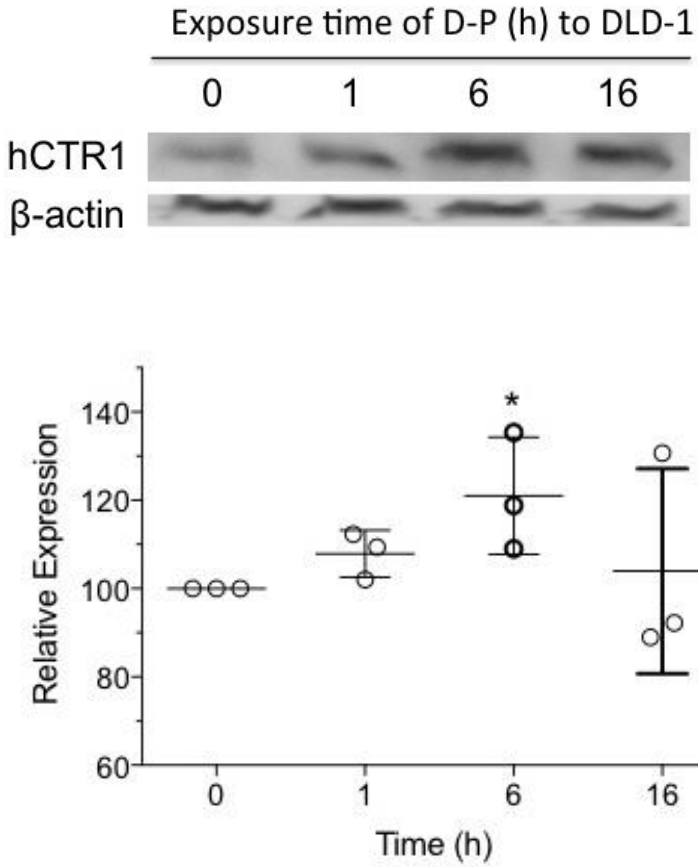
Exposure time of D-P (h) to DLD-1
0
1
6
16
hCTR1
β-actin
Relative Expression
140
120
100
80
60
*
0
1
6
16
Time (h)

C

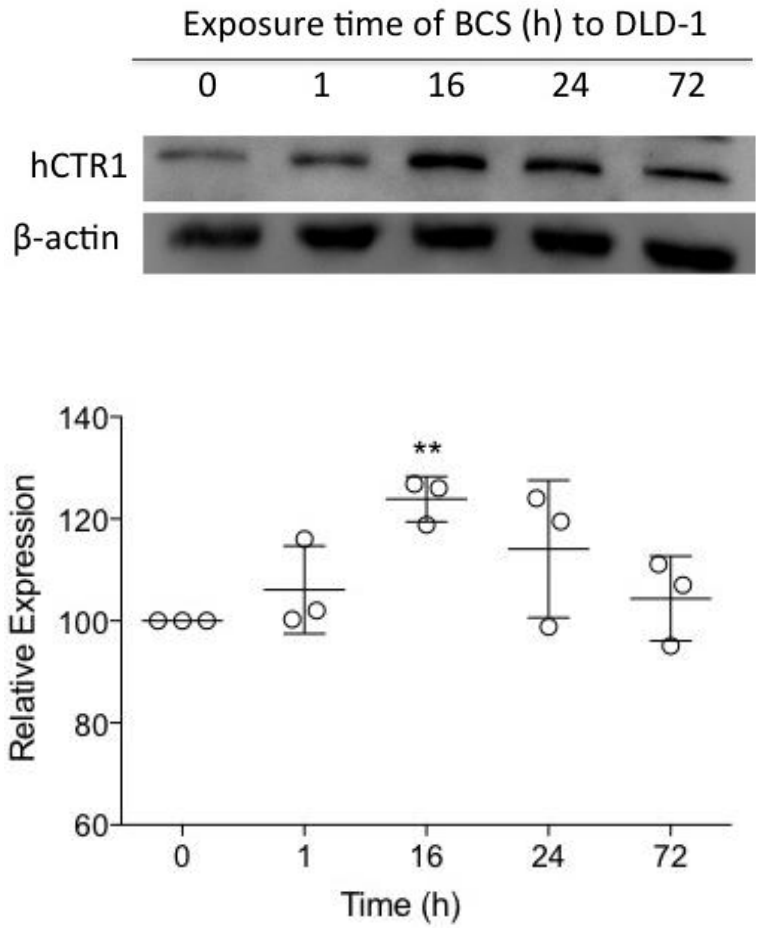

Figure 4-10. Temporal effects of Cu chelators on hCTR1 protein levels in colorectal cancer DLD-1 cells

A. Western blotting analysis of hCTR1 protein levels in DLD-1 cells following exposure to ATTM. B. Western blotting analysis of hCTR1 protein levels in DLD-1 cells following exposure to D-P. C. Western blotting analysis of hCTR1 protein levels in DLD-1 cells following exposure to BCS. Cells were exposed to 30 μM ammonium tetrathiomolybdate (ATTM) (A), 10 μM D-penicillamine (D-P) (B) or 50 μM BCS (C) for the indicated time periods, followed by the Western blotting analysis indicated with the representative blotting bands from one of three independent experiments. Bar graphs indicate densitometric

measurement of hCTR1 protein level normalized to β-actin. Data represent means ± SD (n=3). * $P < 0.05$, ** $P < 0.01$ compared to control (ANOVA).

In addition, SW620 cells were exposed to 30 μM ATTM for 1, 6, 9 and 24 h or 50 μM BCS for 1, 6, 9 and 24 h, followed by the preparation of cell lysates for Western blotting analysis. As shown in Fig. 4-11, hCTR1 protein levels increased significantly after exposure to 30 μM ATTM for 6 h ($P < 0.05$ compared to control, ANOVA, Fig. 4-11A) or 50 μM BCS for 9 h ($P < 0.05$ compared to control, ANOVA, Fig 4-11C). hCTR1 protein levels then returned to the control levels following drug exposure over 6 h. The results were relatively consistent among the three independent experiments.

A

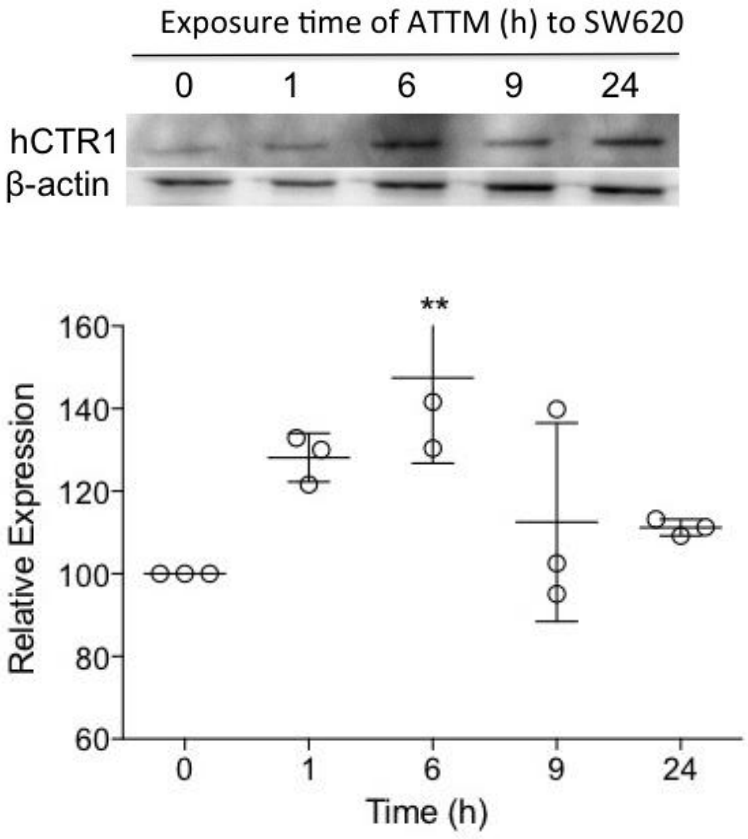

B

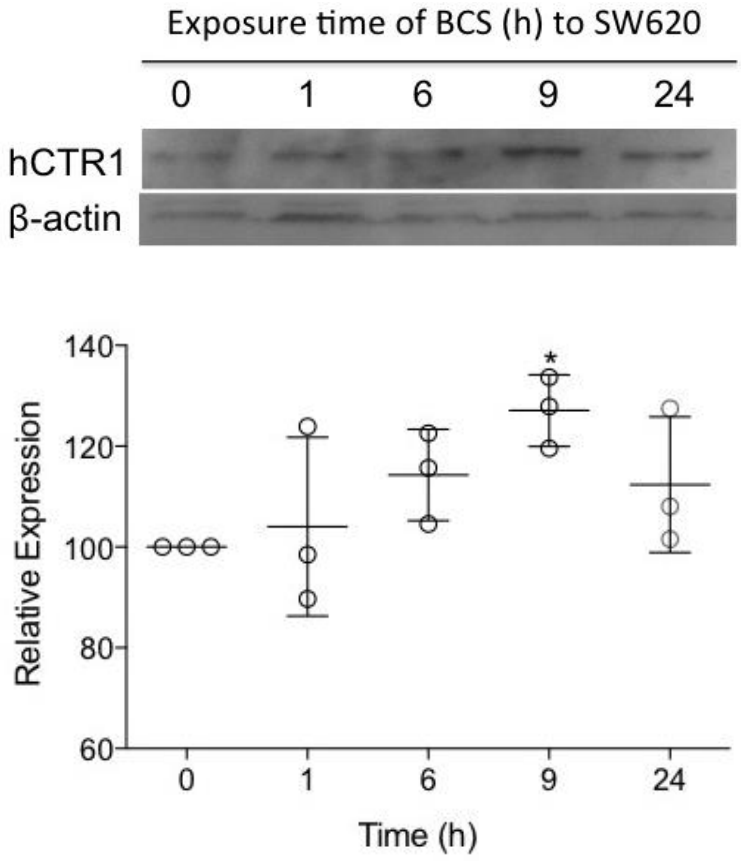

Figure 4-11. Temporal effects of Cu chelators on hCTR1 protein levels in colorectal cancer SW620 cells

A. Western blotting analysis of hCTR1 protein levels in SW620 cells following exposure to ATTM. B. Western blotting analysis of hCTR1 protein levels in SW620 cells following exposure to BCS. Cells were exposed to 30 μM ammonium tetrathiomolybdate (ATTM) (A) or 50 μM BCS (B) for indicated time period, followed by the Western blotting analysis indicated with the representative blotting bands from one of three independent experiments. Bar graphs indicate densitometric measurement of hCTR1 protein level relative to β-actin. Data represent as means ± SD (n=3). * $P < 0.05$, ** $P < 0.01$ compared to control (ANOVA).

4.3.4 Cu chelators enhance oxaliplatin cytotoxicity in DLD-1 cancer cells, but not SW620 cancer cells

To examine whether the up regulation of hCTR1 by Cu chelators could be translated into enhanced OXL cytotoxicity, we further compared the cell killing capacity of OXL with or without pre-incubation with Cu chelators at indicated concentrations and time periods in the colorectal cancer cells DLD-1 and SW620.

As shown in Fig. 4-12A-B for DLD-1 cells, there was no significant loss of cell viability observed after cells were exposed to 50 μM BCS alone for 16 h (96 ± 0.6% of control, $P > 0.05$, ANOVA, Fig. 4-12A) or 30 μM ATTM alone for 6 h (93 ± 6% of control, $P > 0.05$ compared to control, ANOVA, Fig. 4-12B). Incubation of DLD-1 cells with 100 μM OXL alone for 2 h displayed significant loss of viability in both experiments (67 ± 8% of control, Fig. 4-12A; 87 ± 1.2% of control, Fig. 4-12B) ($P < 0.05$ compared to control, ANOVA). Interestingly, OXL-induced loss of viability was further increased by pre-incubation of DLD-1 cells with 50 μM BCS for 16 h (80 ± 2.7% of control, $P < 0.05$ compared to OXL alone, ANOVA, Fig. 4-12A) or 30 μM ATTM for 6 h (67 ± 1.2% of control, $P < 0.05$ compared to OXL alone, ANOVA, Fig. 4-12B).

In SW620 cells, there was no significant loss of cell viability after cells were exposed to 50 μM BCS alone for 16 h (92.7 ± 3.5% of control, $P > 0.05$, ANOVA, Fig. 4-12C) or 30 μM ATTM alone for 6 h (93.3 ± 1.7% of control, $P > 0.05$, ANOVA, Fig. 4-12D). Incubation of SW620 cells with 100 μM OXL alone for 2 h displayed significant loss of viability in both experiments (56.9 ± 1.3% of control, Fig. 5-5C; 53.2 ± 0.8% of control, Fig. 4-12D) ($P < 0.05$ compared to control, ANOVA). OXL-induced cytotoxicity was not altered after pre-incubation of SW620 cells with 50 μM BCS for 16 h (58.7 ± 1.2% of control, $P > 0.05$ compared to OXL

alone, AVOVA, Fig. 4-12C) or 30 μM ATTM for 6 h (57.4 ± 0.6% of control, $P > 0.05$ compared to OXL alone, Fig. 4-12D).

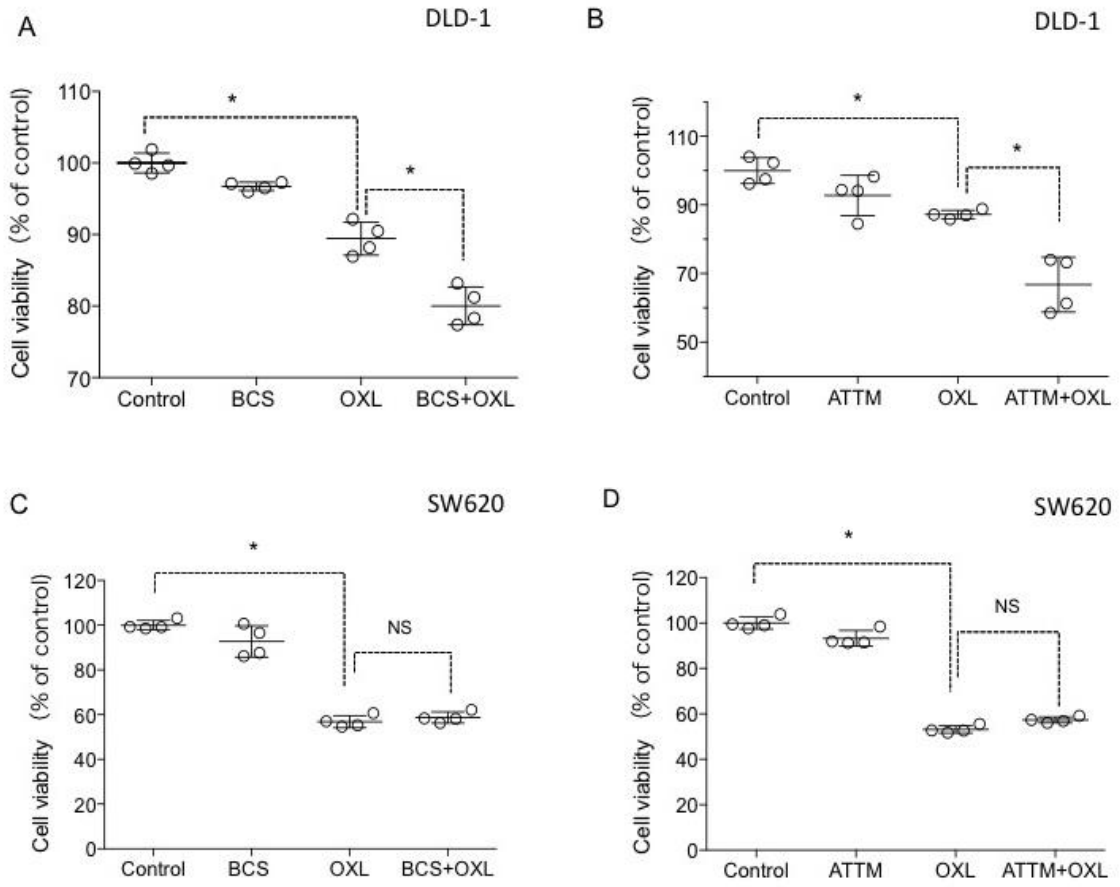

Figure 4-12. Cu chelators potentiate oxaliplatin (OXL) cytotoxicity in colorectal cancer DLD-1 cells, but not SW620 cells

A. Cellular viability of DLD-1 cells following exposure to BCS and OXL alone or in combination. B. Cellular viability of DLD-1 cells following exposure to ATTM and OXL alone or in combination. C. Cellular viability of SW620 cells following exposure to BCS and OXL alone or in combination. D. Cellular viability of SW620 cells following exposure to ATTM and OXL alone or in combination. Cells were pre-incubated with 50 μM BCS for 16 h or 10 μM ATTM for 6 h, followed by a 2-h incubation with 100 μM OXL and a 72-h drug-

free culture before performing a MTT cytotoxicity assay. Data represent as mean ± SD (n≥4). * $P < 0.05$, NS, not significant, ANOVA.

4.3.5 Cu chelators do not alter expression pattern of ATP7A and ATP7B in colorectal cancer cells

Maintenance of cellular Cu homeostasis relies on concerted functionality of Cu uptake transporter hCTR1 and Cu efflux transporters ATP7A or ATP7B [76]. We therefore determined whether Cu chelators also influence the expression of ATP7A and ATP7B in the colorectal cancer cells DLD-1 and SW620.

Immunoreactivity against ATP7A in DLD-1 and SW620 cells was mainly localized to the cytoplasm and plasma membrane. The expression density and pattern of ATP7A staining appeared to be unaltered in both cell lines following exposure to 50 µM BCS, 30 µM ATTM and 10 µM D-P over the indicated time periods (Fig. 4-13).

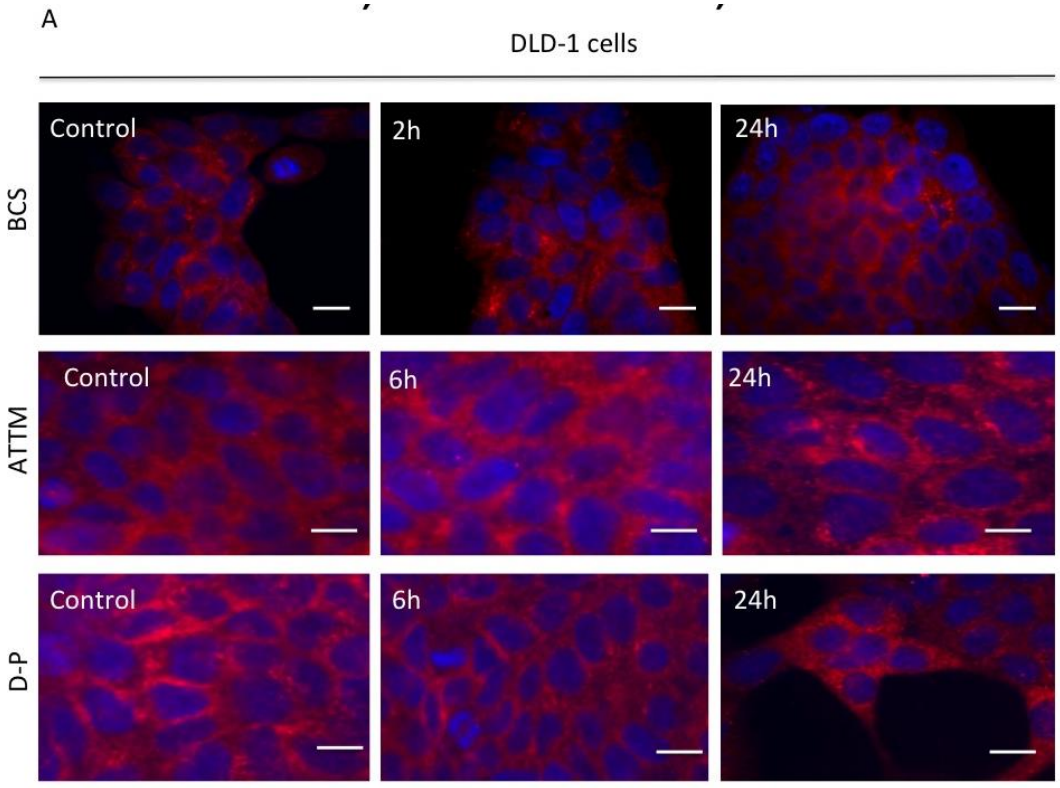

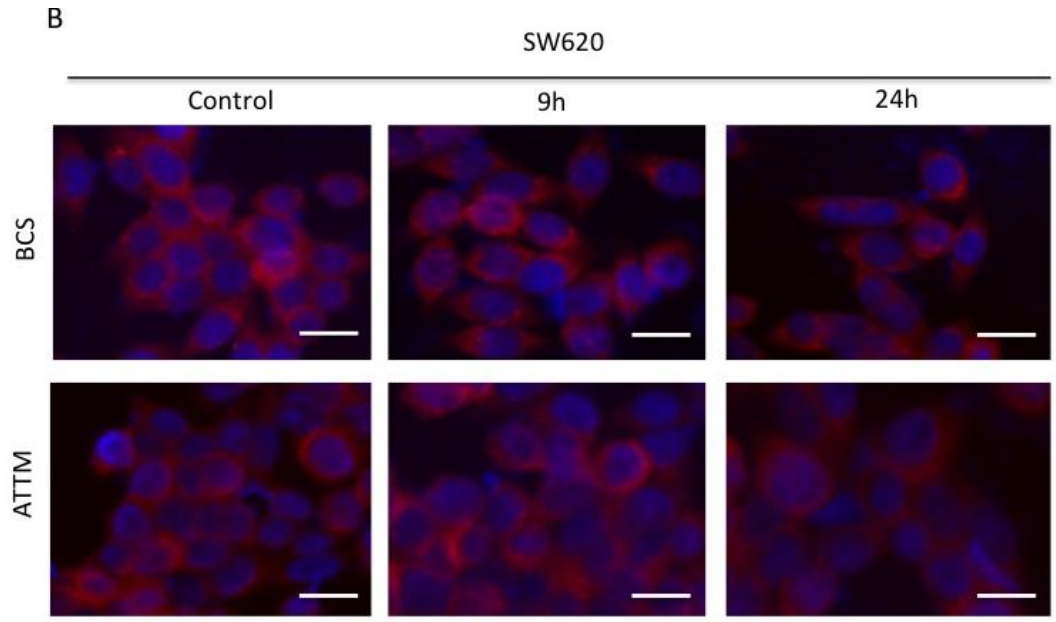

Figure 4-13. Cu chelators do not alter the expression of ATP7A in colorectal cancer DLD-1 and SW620 cells

A. Representative immunocytochemistry images of DLD-1 cancer cells incubated with 50 μM BCS, 30 μM ATTM or 10 μM D-P for indicated time period**.** B. Representative immunocytochemistry images of SW620 cancer cells incubated with 50 μM BCS, 30 μM ATTM or 10 μM D-P for indicated time period. Immunofluorescence staining was performed to visualize cellular ATP7A immunoreactivity (red) using an anti-human ATP7A primary antibody and an Alexa 594-conjugated secondary antibody. Nuclei were stained with DAPI (blue). Scale bars represent 10 μm.

Under drug vehicle-treated control conditions, ATP7B immunoreactivity was mainly localized to the cytoplasm and the plasma membrane in DLD-1 cells (Fig. 4-14A) and SW620 cells (Fig. 4-14B). The staining intensity and distribution patterns of ATP7B appeared not to be altered by the incubation of DLD-1 cells (Fig. 4-14A) and SW620 cells (Fig. 4-14B) with 50 μM BCS for 1, 2 and 24 h, 30 μM ATTM for 6 and 24 h, and 10 μM D-P for 6 and 24 h, respectively.

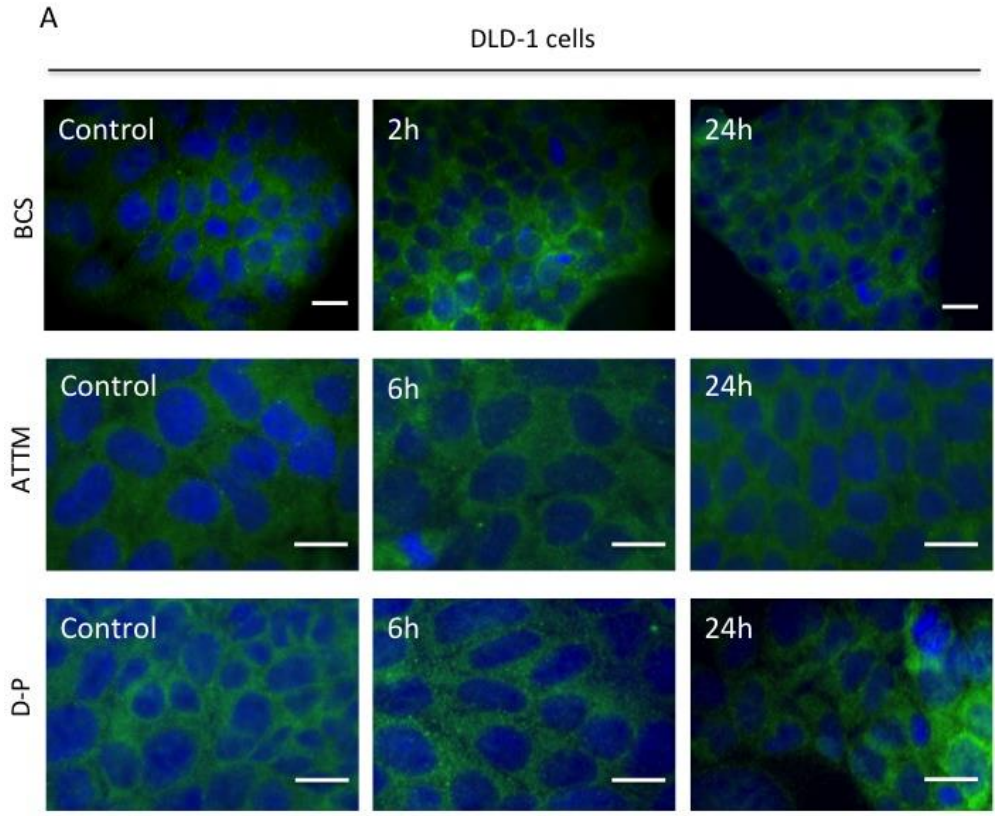
A
DLD-1 cells
Control
2h
24h
BCS
Control
6h
24h
ATTM
Control
6h
24h
D-P

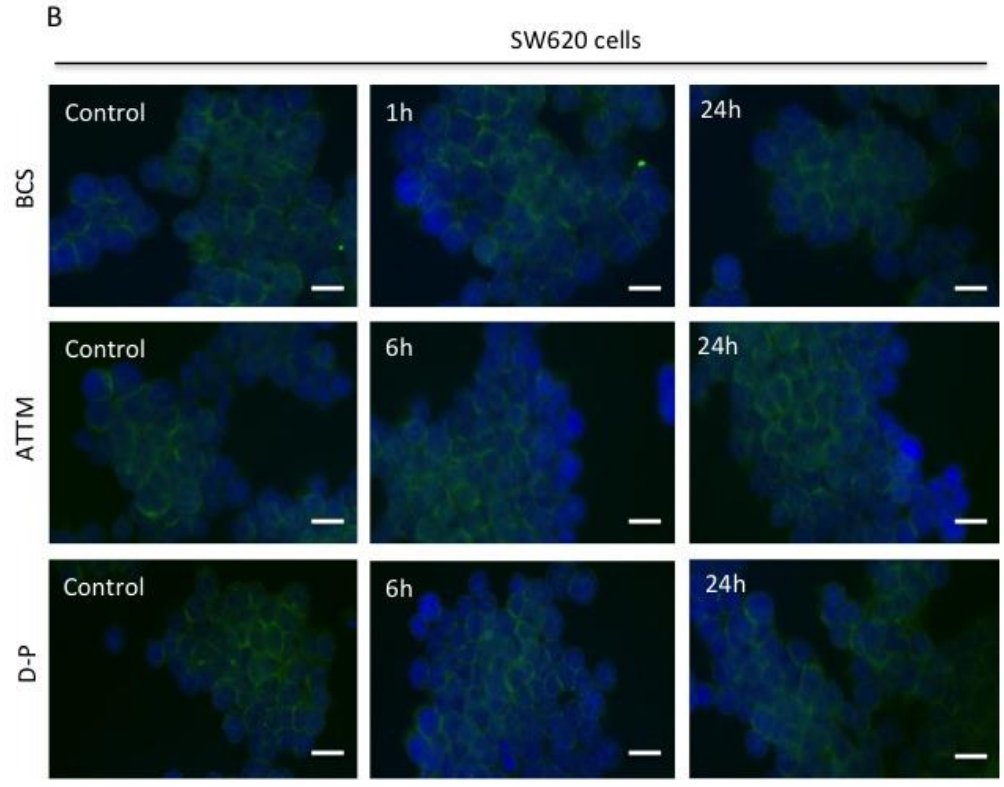
B
SW620 cells
Control
1h
24h
BCS
Control
6h
24h
ATTM
Control
6h
24h
D-P

Figure 4-14. Cu chelators do not alter the expression of ATP7B in the colorectal cancer cells DLD-1 and SW620

A. Representative images of ATP7B immunofluorescence of DLD-1 cancer cells exposed to 50 μM BCS, 30 μM ATTM or 10 μM D-P for indicated time periods**.** B. Representative images of immunocytochemistry of SW620 cancer cells exposed to 50 μM BCS, 30 μM ATTM or 10 μM D-P for indicated time periods**.** Immunofluorescence detection of ATP7B (green) employed a primary anti-human ATP7B antibody and an Alexa 488-conjugated secondary antibody. DAPI was used as nucleus marker (blue). Scale bars represent 10 μm.

4.3.6 Cu chloride does not alter the expression of Cu transporters and oxaliplatin cytotoxicity in colorectal cancer cells

Altered levels and distribution patterns of the Cu transporters hCTR1, ATP7A and ATP7B have been reported in response to Cu overloading for some cell types. Extracellular Cu overload induces internalization and degradation of hCTR1 in some cell types, such as in the breast cancer cell line PMC42-LA [79], hCTR1-overexpresing human embryonic kidney cells (HEK293/hCTR1) [174], but not in human cervical cancer cell line HeLa, Caco-2 colon carcinoma cells or T47D breast cancer cells [36]. Some cell lines show trafficking of ATP7A and ATP7B towards the plasma membrane after exposure to elevated extracellular Cu levels, such as HeLa cells [175] and 2008 ovarian cancer cells [66], whereas other cell lines do not show this response, such as the A2780 ovarian cancer cells, and HepG2 human liver cancer cells [176]. In this study, we have examined whether addition of $CuCl_2$ could change the expression levels or distribution patterns of Cu transporters in the colorectal cancer cell lines DLD-1 and SW620.

As shown in Fig. 4-15, hCTR1 protein level did not change over time in DLD-1 h (Fig. 4-15A) and SW620 cells (Fig. 4-15B) exposed to 100 μM $CuCl_2$ at any time point. There was only a marginal reduction of hCTR1 in DLD-1 cells following exposure to $CuCl_2$ for 16 h (85.9 ± 1.9%), but this trend did not reach statistical significance ($P > 0.05$ compared to control, ANOVA). Meanwhile, the immunostaining density and patterns of hCTR1 were not affected by exposure of DLD-1 and SW620 cells respectively to 20 and 100 μM $CuCl_2$ for 2 h (Fig. 4-15C).

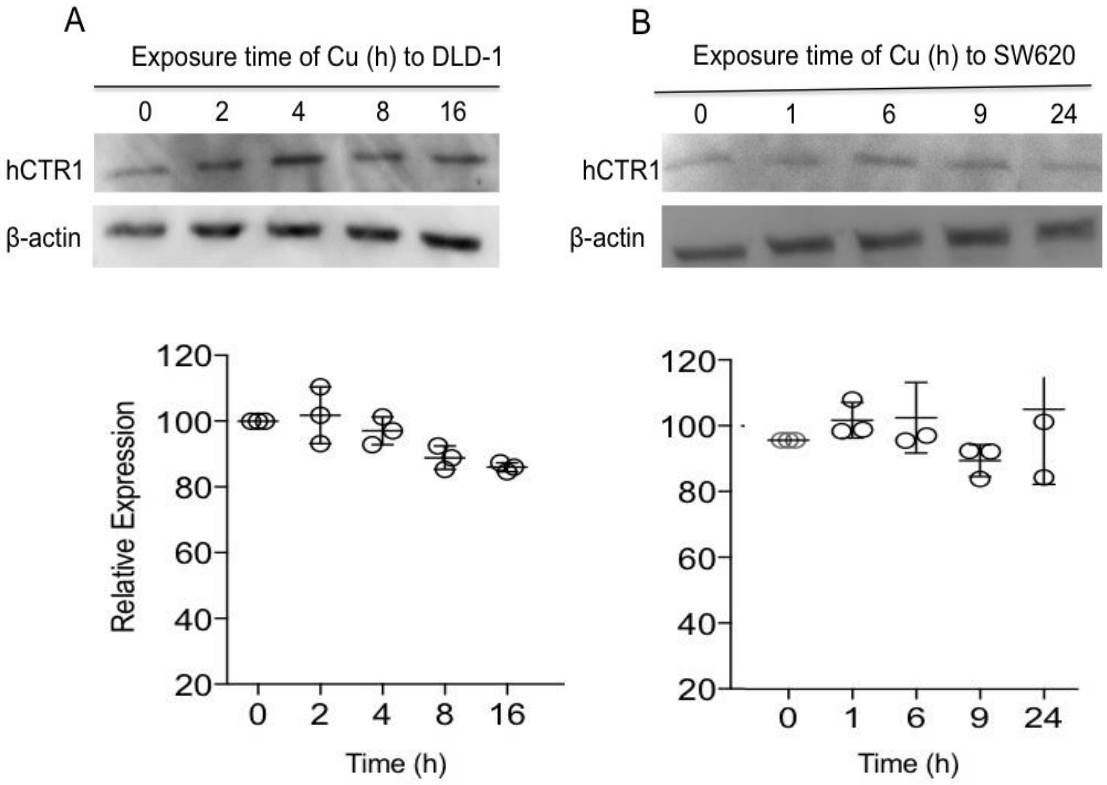

C

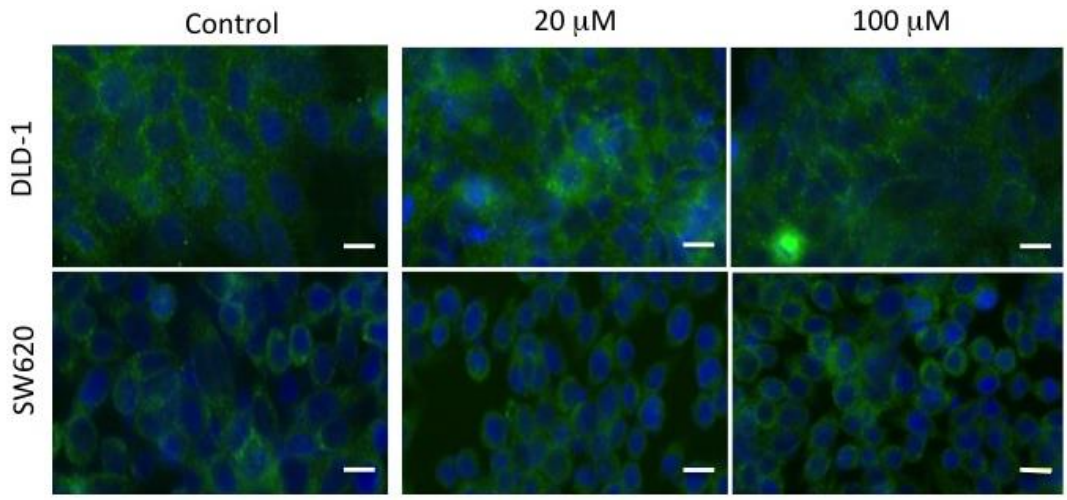

Figure 4-15. Cu chloride does not change the expression level and patterns of hCTR1 in DLD-1 and SW620 colorectal cancer cells

A. Western blotting analysis of hCTR1 protein levels in DLD-1 cells following exposure to 100 μM $CuCl_2$ for up to 16 h. B. Western blotting analysis of hCTR1 protein levels in SW620 cells following exposure of the cells to 100 μM $CuCl_2$ for up to 16 h**.** Bar graphs indicate the relative expression level of hCTR1 normalized to *β*-actin by densitometric analysis. Data represent mean ± SD (n=3 independent experiments). C. Cellular distribution of hCTR1 immunofluorescence (green) in DLD-1 and SW620 cells following exposure to 20 μM or 100 μM $CuCl_2$ for 2 h, using a primary anti-hCTR1 antibody and an Alexa 488-conjugated secondary antibody. DAPI was used as nucleus marker (blue). Scale bars represent 10 μm.

We further tested the effect of $CuCl_2$ on the expression of the Cu efflux transporters ATP7A or ATP7B in colorectal cancer cells. As shown in Fig. 4-16, the immunoreactivity against ATP7A or ATP7B was detectable and localized predominantly to the cytoplasm and the plasma membrane in both cell lines. The expression pattern and staining intensities of ATP7A and ATP7B appeared not to be altered after exposure of DLD-1 cells to 100 μM $CuCl_2$ for 1,

4 and 16 h respectively (Fig. 4-16A). The same lack of response was observed for ATP7A after exposure of SW620 cells to 100 μM $CuCl_2$ for 6, 24 and 48 h respectively (Fig. 4-16B).

A

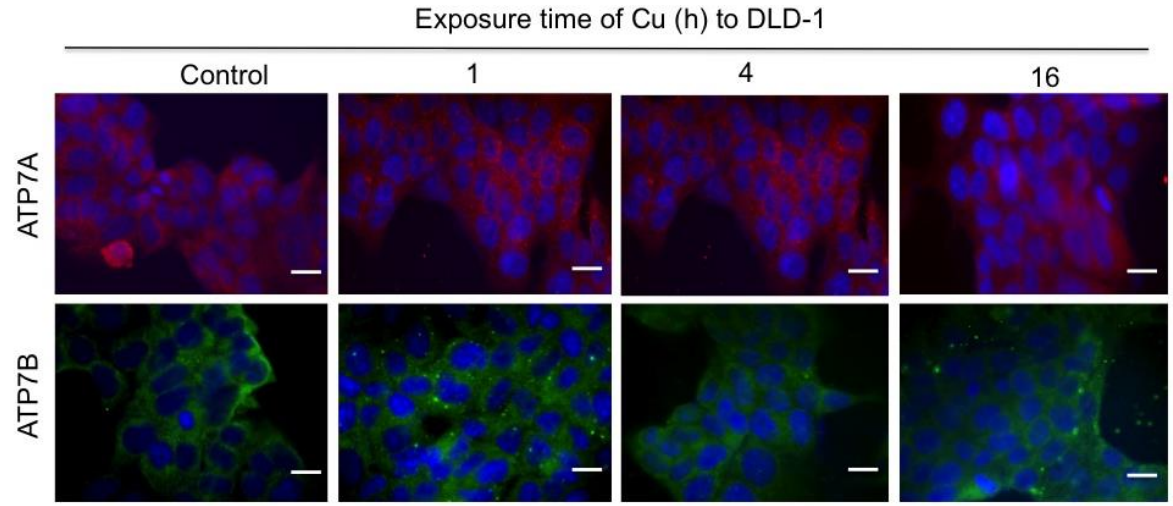

B

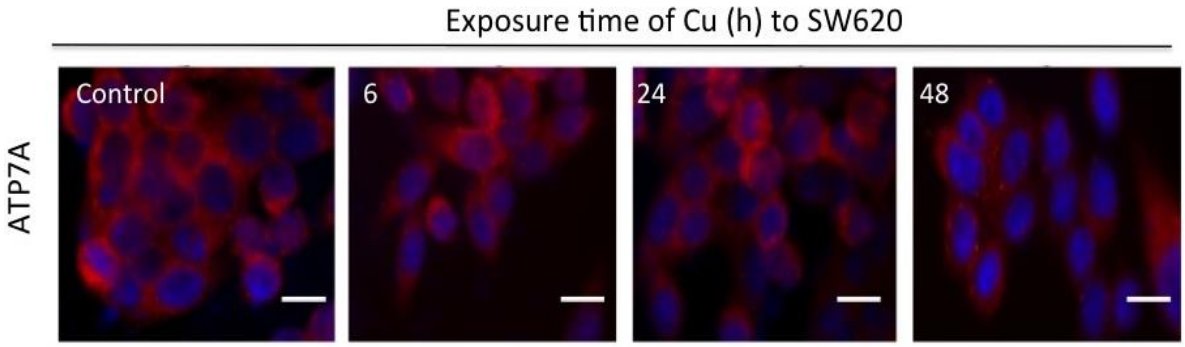

Figure 4-16. Copper chloride does not alter the expression of ATP7A and ATP7B in DLD-1 and SW620 colorectal cancer cells

A. Representative immunofluorescence images of cellular ATP7A (red) and ATP7B (red) distribution in DLD-1 cells after exposure to 100 μM $CuCl_2$ for 1, 4 and 16 h. B. Representative images of cellular distribution of ATP7A immunofluorescence (red) in SW620 cells after exposure to 100 μM $CuCl_2$ for 6, 24 and 48 h. Immunofluorescence was performed using

primary anti-ATP7A or anti-ATP7B antibodies, and an Alexa 594 or Alexa 488-conjugated secondary antibody. DAPI was used as nucleus marker (blue). Scale bars represent 10 μm.

We next examined whether $CuCl_2$ could influence OXL cytotoxicity in colorectal cancer cells. As shown in Fig. 4-17A, DLD-1 cancer cells displayed no reduced viability after incubation with 100 μM $CuCl_2$ for 2 h, but a significant loss of viability after exposure to 100 μM OXL alone (65.9 ± 1.4%, $P < 0.05$ compared to control, ANOVA). Pre-incubation with $CuCl_2$ did not alter OXL-induced cytotoxicity (64.4 ± 0.9%. $P > 0.05$ compared to OXL alone). As shown in Fig. 4-17B, SW620 cancer cells also displayed no loss of viability after incubation with 100 μM $CuCl_2$ for 2 h, but a significant loss of viability after exposure to 100 μM OXL alone (37.4 ± 1.9%, $P < 0.05$ compared to control, ANOVA). Similar to the DLD-1 cells, pre-incubation with $CuCl_2$ did not alter OXL-induced cytotoxicity (37.7 ± 2.2%. $P > 0.05$, compared to OXL alone, ANOVA).

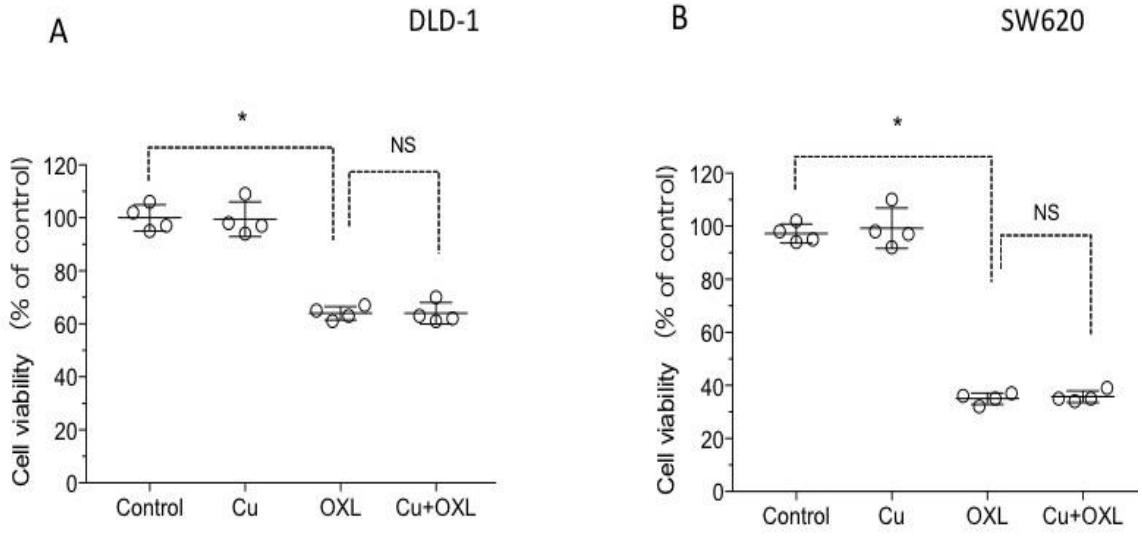

Figure 4-8. Cu chloride does not alter oxaliplatin (OXL) cytotoxicity in colorectal cancer cells

A. Cell viability of DLD-1 cancer cells following exposure to $CuCl_2$, OXL alone or in combination. B. Cell viability of SW620 cancer cells following exposure to $CuCl_2$, OXL alone or in combination. Cells were pre-incubated with 100 μM $CuCl_2$ for 2 h followed by a 2 h-incubation with 100 μM OXL and a 72-h drug free culture before performing MTT viability assay. Cells were exposed to drug vehicle as control. Data represent mean ± SD (n = 3 or 4). * $P < 0.05$. NS: not significant (ANOVA).

4.3.7. Effects of oxaliplatin on the expression of hCTR1, ATP7A and ATP7B in colorectal cancer cells

Cisplatin, another common platinum anticancer drug, has been reported to interact with the expression of the Cu uptake transporter hCTR1 [177] and Cu efflux transporters ATP7A and ATP7B [91,92] in ovarian cancer cells. In this study, we therefore examined whether oxaliplatin (OXL) could also influence the expression of hCTR1, ATP7A and ATP7B in colorectal cancer DLD-1 and SW620 cells by two different methods.

In DLD-1 colorectal cancer cells, hCTR1 protein increased in a time dependent manner, which became statistically significant following an exposure to 10 μM OXL for 4 h (118.7 ± 4.3%, $P < 0.05$ compared to control, ANOVA). Subsequently, hCTR1 protein levels appeared to return to control levels after 8-h OXL exposure (Fig. 4-18A). The results were reproducible among three independent experiments.

In SW620 colorectal cancer cells, there was a trend towards increased hCTR1 protein level following exposure of cells to 10 μM OXL for 1 h (116.1 ± 0.5%, $P > 0.05$ compared to control, ANOVA) and 6 h (116.6 ± 2.8%, $P > 0.05$ compared to control, ANOVA), which however did

not reach statistical significance. hCTR1 protein level then appeared to return to control levels following exposure to OXL for exposure periods over 9 h (Fig. 4-18B). The results were reproducible among three independent experiments.

A

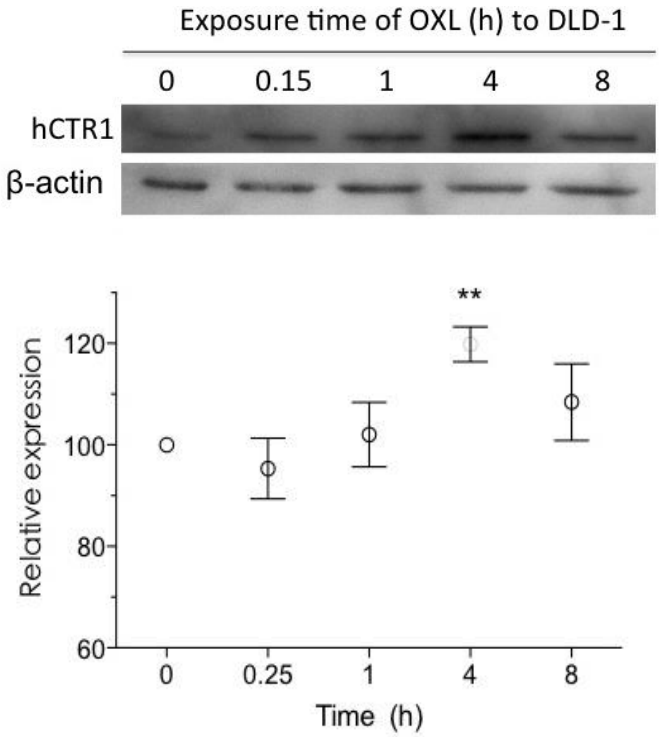

B

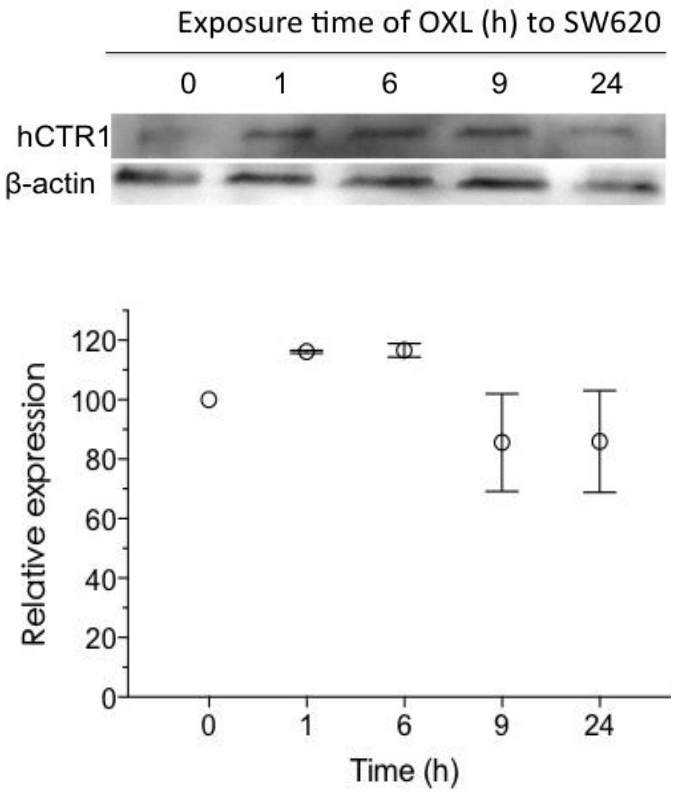

Figure 4-9. Oxaliplatin (OXL) increases hCTR1 protein level in colorectal cancer cells

A. Western blotting analysis of hCTR1 protein level in DLD-1 cancer cells exposed to OXL for indicated time period. B. Western blotting analysis of hCTR1 protein level in SW620 cancer cells exposed to OXL for indicated time period. Cells were incubated with 10 μ M OXL for indicated time periods, followed by Western blotting analysis indicated with the representative blotting bands from one of three independent experiments. Relative hCTR1 levels were normalized to β-actin. Data represent means $\pm$ SD of three independent experiments. * $P < 0.05$ compared to control (ANOVA).

In addition, the influence of OXL on ATP7A and ATP7B expression was examined using immunofluorescence staining. Intensity and patterns of ATP7A and ATP7B staining did not show apparent changes in DLD-1 cells following incubation of the cells with 10 μM OXL for

0.25, 4 and 8 h (Fig. 4-19A). In these cells, the immunoreactivity of ATP7A and ATP7B was localized to the cytoplasm and the plasma membrane. Likewise, the staining intensity and patterns of ATP7A also appeared to be unaltered by exposure of SW620 cells to 10 μM OXL for 1, 6 and 24 h (Fig. 4-19B). In SW620 cancer cells ATP7A immunoreactivity was predominantly cytoplasmic (Fig. 4-19B).

A

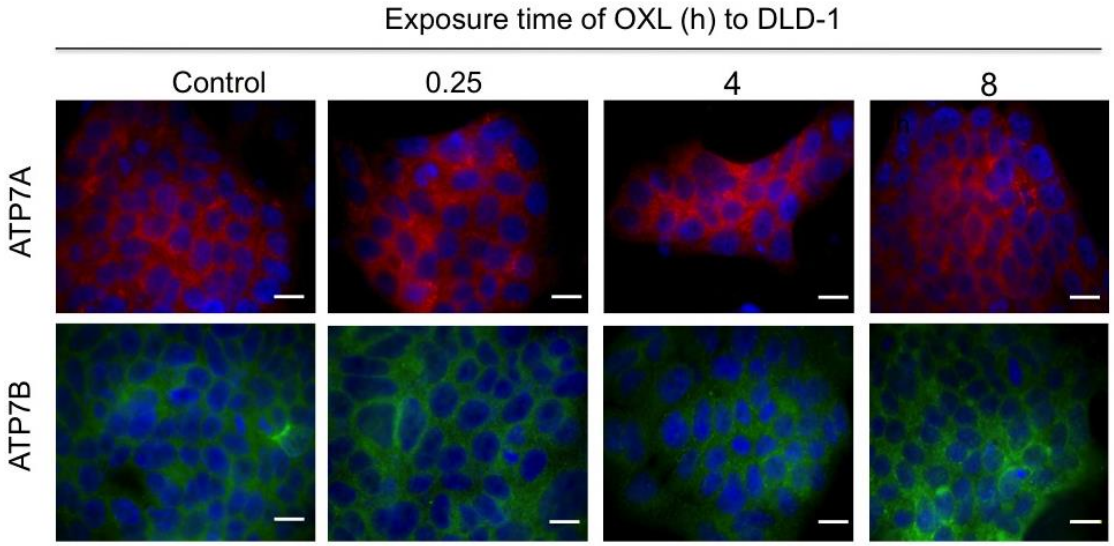

B

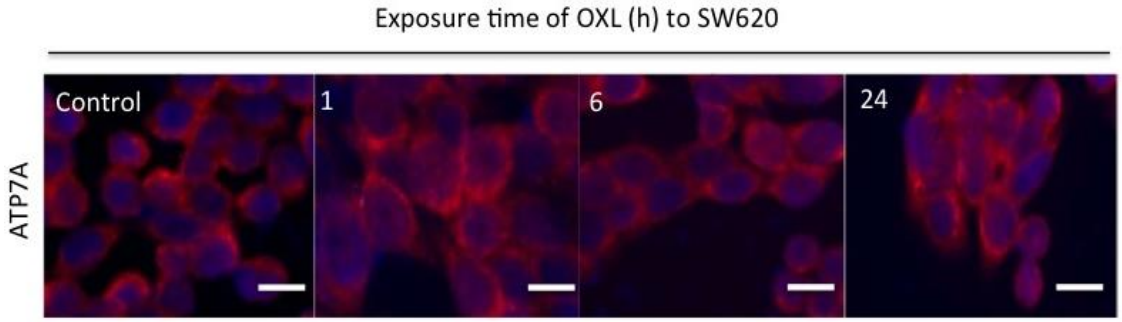

Figure 4-10. Oxaliplatin (OXL) does not alter the expression pattern and intensity of Cu efflux transporters ATP7A and ATP7B in colorectal cancer cells

A. Representative images of ATP7A (red) and ATP7B (green) immunofluorescence in DLD-1 cancer cells exposed to OXL for 0.25, 4 and 8 h. B. Representative images of ATP7A (red)

immunofluorescence in SW620 cancer cells exposed to OXL for 1, 6 and 24 h. Cells were incubated with 10 μM OXL for indicated time periods, followed by performing fluorescent detection using primary anti-ATP7A and anti-ATP7B antibodies and Alexa 488- or Alexa 594-conjugated secondary antibodies. Nuclei were stained with DAPI (blue). Scale bars represent 10 μm.

4.4 Discussion

We have systematically studied the expression of Cu transporters hCTR1, ATP7A and ATP7B in colorectal cancer cells. Overall, hCTR1 was expressed more abundantly than ATP7A and ATP7B in colorectal cancer cells. The results of this chapter have also indicated that all tested Cu chelators up regulated hCTR1 protein in a time-dependent manner in colorectal cancer DLD-1 and SW620 cells, co-treatment with these Cu chelators enhanced the cytotoxicity of OXL in DLD-1 colorectal cancer cells, which is likely a consequence of increased hCTR1-mediated cellular uptake of platinum.

Firstly, hCTR1 mRNA and protein were detected abundantly in colorectal cancer DLD-1, SW620, HCT-15 and COLO205 cells by RT-PCR, Western blotting analysis and fluorescence immunocytochemistry. An hCTR1 band of high density with the expected molecular weight was detected across all cell lines without apparent differences in abundance. The distribution pattern of hCTR1 appeared similar among the cell lines. Predominant plasma membrane localization was demonstrated in DLD-1, SW620 and HCT-15 cells with more diffuse cytoplasmic staining, whereas COLO205 cells displayed mainly cytoplasmic staining with weaker plasma membrane staining. It is unclear whether the difference in hCTR1 distribution is related to the different origins from which these colorectal cancer cell lines were derived, such as the primary or metastatic sites. Cell type-specific subcellular localization of hCTR1

has been reported previously, such as the plasma membrane of HT29 colon cancer cells and A2780 ovarian cancer cells [193], cytoplasmic vesicular compartments and perinucleus region in Caco2 cells, HeLa cervical carcinoma cells, A549 and H441 lung carcinoma cells, and HepG2 hepatocellular carcinoma cells [194]. The biological significance of high basal levels of hCTR1 expression in colorectal cancer cells is unclear, but it may be related to their high demand of Cu to maintain elevated Cu levels [195] that are necessary for the function of superoxidase dismutase [196] and several pro-angiogenic proteins, such as vascular endothelial growth factor [197], basic fibroblast growth factor [198] and interleukin-8 [199].

Maintenance of cellular Cu homeostasis relies on the concerted function of hCTR1 and the efflux transporters ATP7A and ATP7B [200]. We detected abundant mRNA for ATP7A and ATP7B in DLD-1, SW620, HCT-15 and COLO205 colorectal cancer cells. However, measured by Western blot, ATP7A and ATP7B protein levels were much lower compared to hCTR1 levels in these cell lines. Furthermore, ATP7A protein appeared to be expressed more profoundly when compared to the minimal expression of ATP7B protein. This suggests that ATP7A is the dominant Cu efflux transporter in colorectal cancer cells, but further studies are required to substantiate this. Previously, varying levels of ATP7A mRNA and protein are reported for colorectal cancer cells [201] and tumor tissues [202-204]. We observed different distribution patterns for ATP7A among these colorectal cancer cell lines, with localization to plasma membrane and cytoplasm in DLD-1, SW620 and HCT-15 cells, while a diffuse, granular and perinucleus staining was detected in COLO205 cells. These findings are consistent with previous reports that report ATP7A localization to the trans-Golgi network in ovarian, endometrial, cervical and breast cancer cells [205,206]. It is hypothesized that this localization indicated a recycling of ATP7A between the trans-Golgi network and the plasma membrane under normal culture conditions in Chinese hamster ovary cells [207]. Our immunostaining results showed mainly plasma membrane localized staining of ATP7B in

these colorectal cancer cells, which is consistent with previous reports [201,203]. Nevertheless, the functionality and contribution of ATP7A and ATP7B to Cu homeostasis in colorectal cancer cells remains to be determined.

However, we did not observe the same synergism of these compounds with OXL in SW620 cancer cells, which suggests a cell-specific effect. Previously, these Cu chelators have been reported to enhance cytotoxicity of cisplatin in various cancer cells [70], increase antitumor activity of cisplatin in animal models [178] and improve the clinical response of ovarian cancer patients to carboplatin [179]. It is assumed that these effects are a consequence of increased hCTR1- or mCtr1-mediated drug uptake. Nevertheless, further studies are required to investigate whether hCTR1 is the major uptake transporter *in vivo* that determines the antitumor activity of OXL against colorectal cancer.

Conversely, in this study, Cu chelators appeared not to alter the expression and distribution of the Cu efflux transporters ATP7A or ATP7B in colorectal cancer cells in our study. The staining intensity and distribution patterns of ATP7A and ATP7B did not display apparent changes between the cytoplasm and the plasma membrane following exposure to 30 μM ATTM for 6 h or 50 μM BSC for 16 h, respectively. This is consistent with previous reports of a stable plasma membrane staining of ATP7A at the apical and brush-border of duodenal enterocytes [180] and stable expression of ATP7B at the apical membrane of rat hepatocytes [181], which were unaltered by BCS-induced Cu depletion. Our results however, are in contrast to studies that report that BCS enhanced the perinucleus presence of ATP7A in HeLa cervical cancer cells [182] and mouse enterocytes [183] as well as ATP7B in HepG2 hepatocellular carcinoma cells [184] and A2780 ovarian cancer cells [185]. Consequently, cellular trafficking of ATP7A and ATP7B needs to be investigated further in colorectal cancer cells under different culture and Cu-level conditions. Nevertheless, the enhancement of OXL cytotoxicity by Cu chelators, at least in the colorectal cancer cells used in this study, appears

to be mediated by their ability to up regulate hCTR1 expression, but not that of the efflux transporters ATP7A and ATP7B.

In addition, we also did not observe any apparent reduction of hCTR1 in the colorectal cancer cell lines DLD-1 and SW620 in the presence of excessive extracellular level of Cu for up to 24 h, which indicates a relatively stable expression of hCTR1 in the presence of varying concentrations of Cu. This finding is consistent with a previous report that excessive Cu concentrations showed little effect on the cellular localization of endogenous hCTR1 protein in Caco-2 colon cancer cells and HeLa cervical cancer cells [36]. In contrast to our data, Cu overload is reported to trigger endocytosis, internalization or degradation of hCTR1 from the plasma membrane in ovarian cancer cells [186]. The reduction of hCTR1 localized to the plasma membrane is thought to be a self-protective response that prevents Cu toxicity by excessive hCTR1-mediated Cu uptake [71]. This degradation of hCTR1 has also been associated with the resistance to cisplatin in ovarian cancer cells, because proteasome inhibitor-mediated prevention of hCTR1 degradation is reported to re-sensitize these resistant cancer cells to platinum drugs [187]. The reason for the discrepancy is unclear, but it seems likely the consequence of cell type-specific responses that depend on the intrinsic cell type differences with regards to capacity of uptake, adaptability and tolerance to extracellular Cu-overload conditions.

In this study, Cu overload did not seem to alter the cellular expression and distribution patterns of ATP7A or ATP7B. The DLD-1 and SW620 cancer cells did not display apparent changes of plasma membrane or cytoplasmic immunoreactivity of ATP7A and ATP7B, which indicates a lack of intracellular trafficking of these transporters. However, ATP7B is known to reside normally in the trans-Golgi network of hepatocytes. Therefore, it is likely that ATP7B could move rapidly to the apical domain of these cells to increase Cu excretion under conditions of high extracellular Cu concentrations and return back to physiological membrane under normal

extracellular Cu levels [188]. However, it has to be noted that at least in renal cells ATP7B has not shown this type of Cu concentration-dependent trafficking [88], while a concentration-dependent trafficking mechanism is proposed for ATP7A in intestinal enterocytes and certain cancer cells, such as HeLa cervical cancer cells [175]. Therefore, these trafficking mechanisms of ATP7A or ATP7B could at least in theory be applicable to colorectal cancer cells. One possible explanation for that we did not observe any apparent intracellular movement of these transporters could be due to the limitation of the sensitivity of the immunofluorescence detection used in our study, which has to be regarded as a largely semi-quantitative method. For future studies, the use of confocal microscopy or single-protein detection could be a more adequate tool to provide sufficient resolution to trace the intracellular trafficking of these Cu transporters in detail.

Finally, we demonstrated that OXL is able to up regulate hCTR1 protein levels in colorectal cancer cells. Expression of hCTR1 protein increased significantly in DLD-1 cells following exposure to 10 μM OXL for 4 h. This finding suggests a possible interaction between OXL and hCTR1. OXL might behave similar to Cu chelators by competitively inhibiting Cu binding to hCTR1, which would directly reduce cellular Cu uptake. Subsequently, this effect is likely to trigger a feedback loop to increase hCTR1 expression to compensate for reduced intracellular Cu levels. Interestingly, our results are consistent with another study that reported a cisplatin-dependent up regulation of hCTR1 expression in ovarian cancer cells, both at the mRNA and protein levels. This observation leads the authors to suggest a similar feedback loop-based regulatory mechanism [75]. However, cisplatin has also been reported to trigger degradation or endocytosis of hCTR1 in other cancer cell types, which is thought to induce inactivation of and cellular resistance to cisplatin [189], [187]. Apparently, the exact mechanisms of interaction between OXL and hCTR1, and its influence on Cu uptake, needs to be investigated in colorectal cancer cells in more detail with appropriate methods.

In summary, the results of this chapter have demonstrated that treatment with the clinically used Cu chelators, ammonium tetrathiomolybdate and D-penicillamine, can up regulate hCTR1 expression and enhance the cytotoxic capacity of OXL in some but not all colorectal cancer cell lines. Addition of high level of Cu neither altered hCTR1 protein levels, the expression intensities and patterns of the efflux transporters ATP7A and ATP7B nor OXL cytotoxicity in colorectal cancer cells. Interestingly, OXL, like Cu chelators, up regulated hCTR1 protein expression with no apparent influence on the cellular distribution of ATP7A and ATP7B. The anticancer synergism between Cu chelators and OXL will have to be evaluated further in additional colorectal cancer cell lines *in vitro* and *in vivo*.

Chapter 5 Expression of Copper Transporters in Human Tumor Tissues of Patients with Colorectal cancer

5.1 Introduction

Copper transporters seem to be differentially expressed in numerous malignancies compared to the matched normal tissues, including the hCTR1 in the cervical tumor of the HPV16/E2 mice compared to the wild-type cervix [97], ATP7A in the non-small cell lung cancer patients [105] and ATP7B in human oral squamous carcinoma [107].

There is even report that hCTR1 mRNA levels are up regulated in human CRC cell lines compared to that of the normal colon mucosa [99]. However, information about their expression status in human CRC tissues is scare. Previous results from Chapter 3 have demonstrated the positive role of hCTR1 an uptake transporter in the cytotoxicity of OXL. Chapter 4 has also proven the feasibility of using copper chelators to enhance the cytotoxicity of OXL in CRC cell lines. However, understanding their expression in CRC is equally important to add more translational value to this project. Moreover, their expression status in tumour tissues is also likely to become a molecular marker to predict some treatment outcomes for OXL-based chemotherapies.

Therefore, this chapter was undertaken to characterize the expression of Cu transporters in colorectal tumor biopsy tissues. Tumor tissue samples and matched normal colon tissues were collected from chemotherapy naïve colorectal cancer patients, followed by histological examination of the tissues collected using H&E staining, immunohistochemical staining, and semi-quantitative analysis of DAB stained images.

5.2 Experimental design

5.2.1 Patient recruitment

Patients with colorectal cancer were recruited for this study from the Oncology Department of the Royal Hobart Hospital in Hobart, Tasmania. The eligibility criteria that were applied for patient recruitment included: patients were clinically diagnosed with adenocarcinoma of colon or rectum with the confirmation of radiological and histological examinations; patients had no history of chemotherapy and were prescribed by a clinical oncologist for surgical tumor resection; patients were ≥ 18 years old with adequate renal (serum creatinine ≤1.5 mg/dl) and liver function (serum transaminases ≤3 times the upper limit of normal). These criteria were used to minimize the number of variables that could influence the expression of Cu transporters such as age, gender or history of chemotherapy. The study was conducted with the approval of the Tasmanian Health and Medical Human Research Ethics Committee (Reference No: H0014706). Written informed consent was obtained from all patients included in this study.

5.2.2 Histological examination of colon samples

H&E staining was performed to histologically confirm the presence of tumors in the tissues collected according to established protocols described in detail in Section 2.8.4. Briefly, paraffin-embedded mouse tissue slides were de-waxed by immersion in xylene, absolute ethanol, 70% ethanol and 1 min under running tap water, followed by haematoxylin staining, differentiation in 1% acetic acid in ethanol, counterstaining using eosin solution and dehydration. Dry sections were mounted using a DPX mounting medium and analyzed by light microscopy. Particular interests were given to the structure of crypts, the nucleus to cytoplasm of the glandular cells and the differentiation degree of the tumors.

5.2.3 Evaluation of immuno-histochemical staining and statistical analysis

DAB-based immunohistochemistry (IHC) was performed on paraffin-embedded or cryo-sectioned tissues as described in detail in Section 2.9. Following immuno-histochemical detection of the expression of copper transporters in human colorectal cancer and normal tissue samples, we developed a semi-quantitative analysis method from human colon tissues to quantify the DAB-based IHC images in, which is based on a previous report [155]. The method is compatible with the open resource digital image analysis software Image J and creates a pixel-by-pixel analysis profile of a deconvoluted IHC image and further assigns a score in a four-tier system. Detailed procedures and examples were given in Section 5.3.2. Expression of the 3 copper transporters in tumor and normal tissues was compared using a paired t-test and paired analysis of variance (ANOVA). A *p* value of 0.05 or less was considered statistically significant.

5.3 Results

5.3.1 Clinical and histologic information of the matched CRC tissues

A total of eight patients with colorectal cancer were recruited for this study at the Oncology Department of the Royal Hobart Hospital at Hobart, Australia. Patient characteristics are summarized in Tab 5-1.

Table 5-1. Patient characteristics

Parameter	**No of patient (%)**
Gender	
Male	7 (87.5)
Female	1 (12.5)

Mean age (range)	74 (65-86)
Location of primary tumor	
Sigmold	3 (37.5)
Caecal	2 (25)
Right colon	3 (37.5)

Tumor tissue samples and matched adjacent normal colon or rectum were collected from each patient. We verified the tissue specimens for all patients histologically using Haematoxylin and Eosin (H & E) staining before using them for immunohistochemistry analysis. Representative H & E stained images are shown for the normal and tumor colonic tissues that were collected from the same patient (Fig. 5-1). Normal colon tissue displayed clearly defined mucosa, submucosa, muscularis propria and crypts. In contrast, tumor tissues displayed loss of crypt architecture, distorted and complex glandular structures and increased nucleus to cytoplasm ratio, with varying degree of differentiation (Fig. 5-1). However, we only selected 6 tumor specimens that were paired up with the matched normal tissues for the subsequent immunohistochemistry studies.

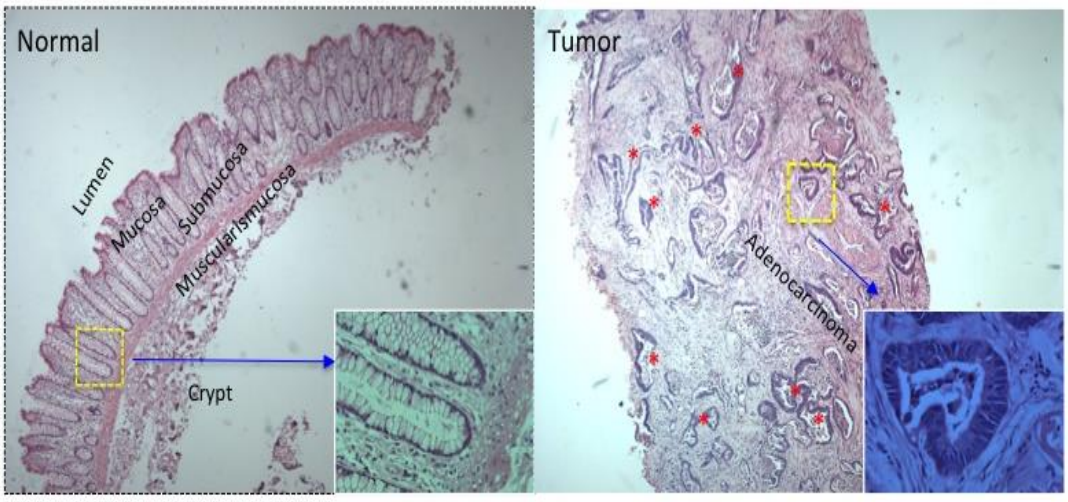

Figure 5-1. Histological confirmation of normal and cancerous colon and rectum tissues from patients with colorectal cancer

Haematoxylin and eosin staining was performed on paraffin-embedded sections of normal and tumor tissues. Enlarged insets show normal colonic crypts and crypts with adenocarcinoma. Asterisks in tumor section display the loci of adenocarcinoma. Mag. 10x.

5.3.2 Development of semi-quantitative analysis of DAB stained immunohistochemical images

We developed a semi-quantitative analysis method to quantify the staining intensity of DAB-based immunohistochemistry (IHC) images based on a previous report [152]. Briefly, DAB- and haematoxylin-stained IHC images of hCTR1 were deconvoluted to display DAB staining only (Fig. 5-2). The percentage of pixel counts were used to define the staining intensity as negative, medium positive or high positive of hCTR1 immunoreactivity (Fig. 5-2A). The full range of pixel intensity was defined as ranging from 0 to 255, where 0 represents the darkest shade and 255 the lightest shade. A pixel-by-pixel analysis was conducted to produce a histogram, where the X-axis represents the pixel intensity (0-255), and the Y-axis indicates the pixel count. The pixel intensity values were stratified into four categories, namely, 0-60, 61-120, 121-170 and 171-229, to represent high positive, positive, low positive or negative staining. Pixel intensities of >230 were excluded from the calculation because they represent largely background baseline values. The percentage of each category was then calculated based on the total pixel counts.

The summary of the software program-generated percentages of high positive, positive and low positive was used to represent the category of high positive (>70%), medium positive (6-69%) and negative (<5%) staining of hCTR1 for each image. Three representative fields were

randomly selected from each tissue section and subjected to the semi-quantitative analysis as above described (Fig. 5-2B). The software-generated percentages for the different categories were used to calculate the final percentage of hCTR1 positivity for the tissue section, which was 76 ± 3.9% in the example sample and deemed as high positive (Tab 5-2). We then applied the semi-quantitative analysis method to quantifying the expression of the Cu transporters hCTR1, ATP7A and ATP7B in normal and tumor tissues of colorectal cancer patients.

A

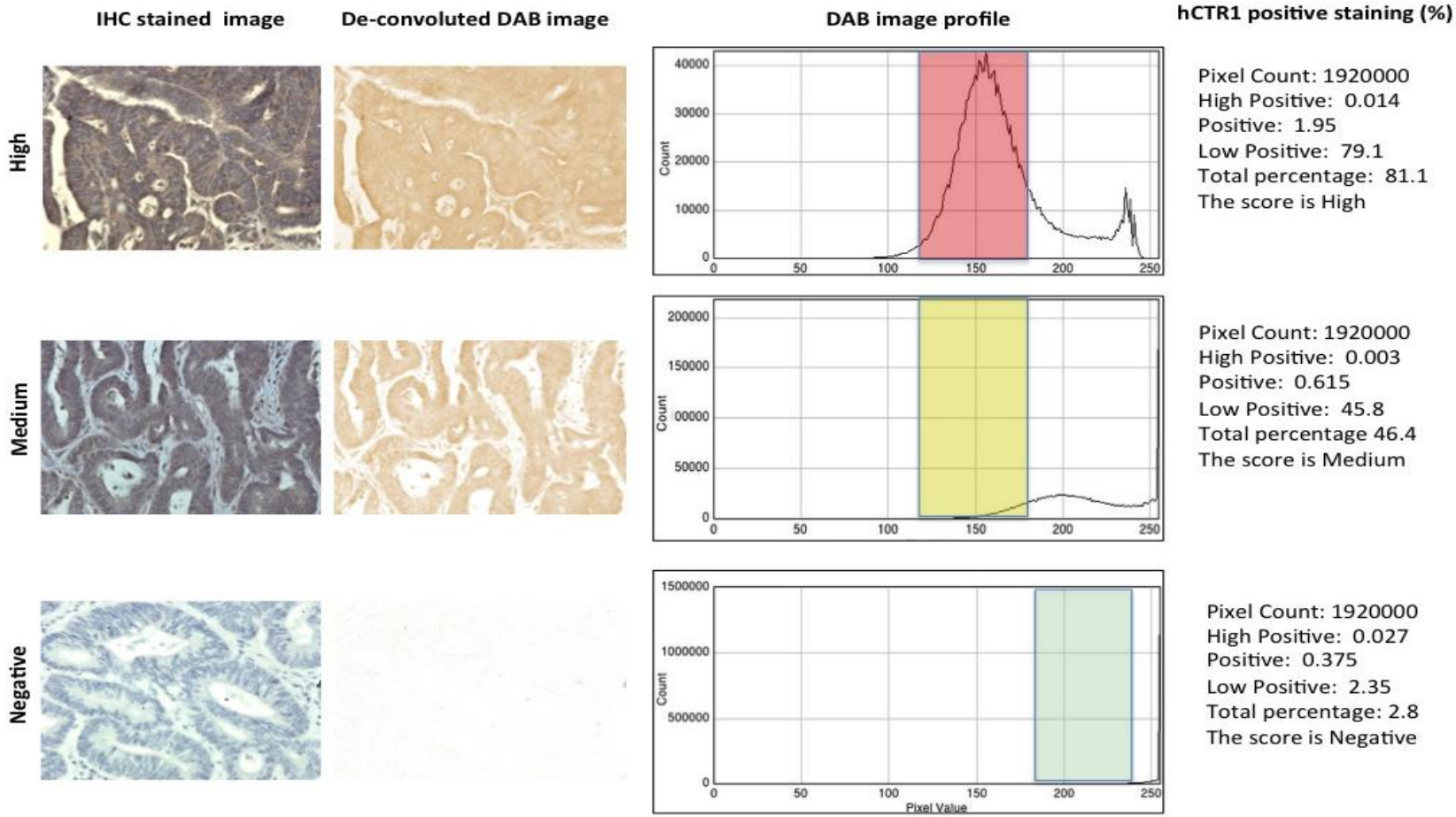
IHC stained image
De-convoluted DAB image
DAB image profile
hCTR1 positive staining (%)
High
Medium
Negative
Count
Pixel Value
Pixel Count: 1920000
High Positive: 0.014
Positive: 1.95
Low Positive: 79.1
Total percentage: 81.1
The score is High
Pixel Count: 1920000
High Positive: 0.003
Positive: 0.615
Low Positive: 45.8
Total percentage 46.4
The score is Medium
Pixel Count: 1920000
High Positive: 0.027
Positive: 0.375
Low Positive: 2.35
Total percentage: 2.8
The score is Negative

B

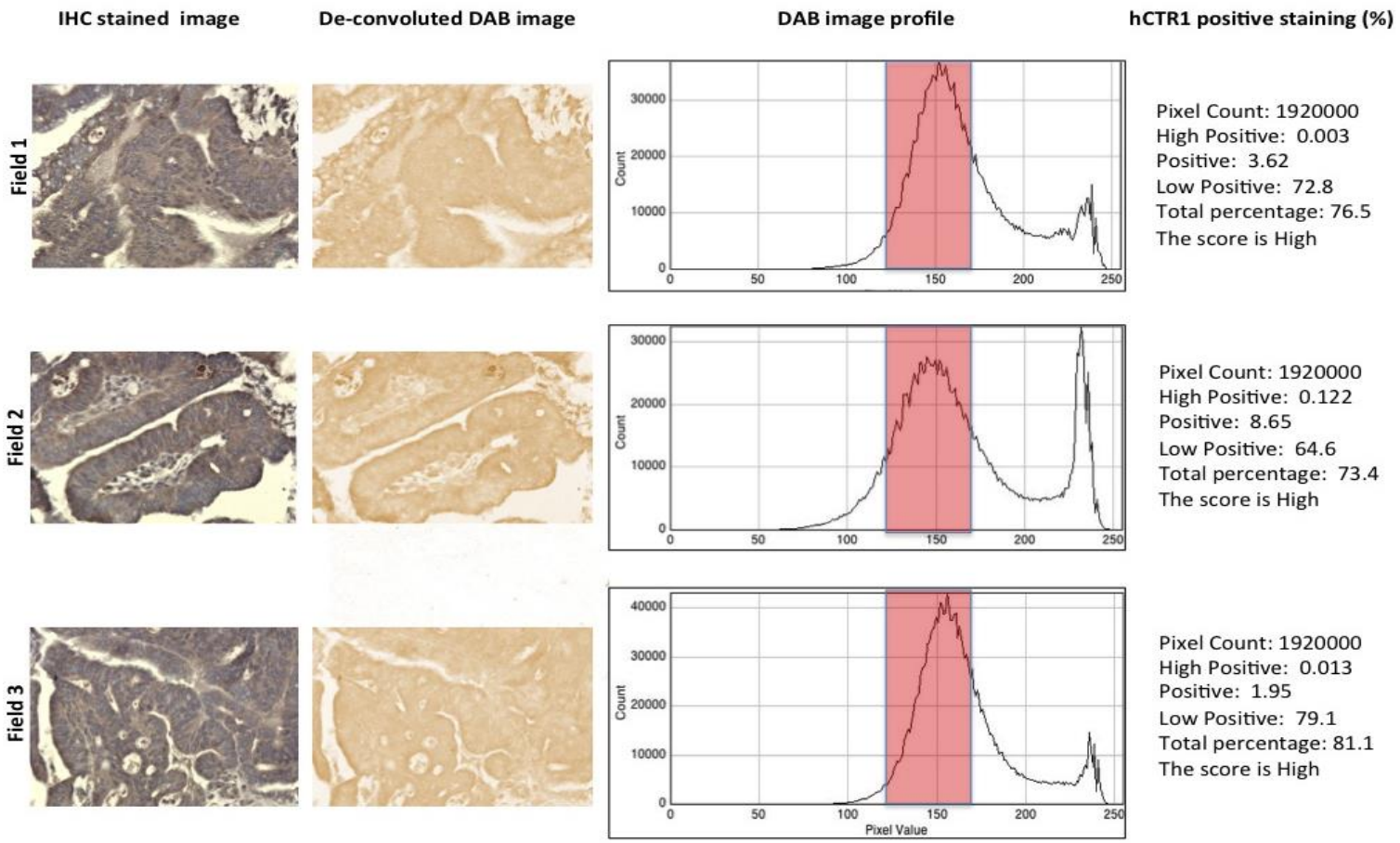
IHC stained image
De-convoluted DAB image
DAB image profile
hCTR1 positive staining (%)
Field 1
Field 2
Field 3
Count
Pixel Value
Pixel Count: 1920000
High Positive: 0.003
Positive: 3.62
Low Positive: 72.8
Total percentage: 76.5
The score is High
Pixel Count: 1920000
High Positive: 0.122
Positive: 8.65
Low Positive: 64.6
Total percentage: 73.4
The score is High
Pixel Count: 1920000
High Positive: 0.013
Positive: 1.95
Low Positive: 79.1
Total percentage: 81.1
The score is High

Figure 5-2. Semi-quantitative analysis of DAB stained immunohistochemical images of hCTR1 in tumor tissues of colorectal cancer patient

A. Digitally scoring of deconvoluted DAB-stained IHC images of hCTR1 illustrating the negative, medium and high positive staining intensity defined by the percentage of pixel counts. B. Three randomly selected fields of each tissue section were used to represent a single tissue sample for semi-quantitative analysis. Standard immunohistochemistry was performed on paraffin-embedded tumor tissues using a rabbit anti-hCTR1 primary antibody and a goat anti-rabbit secondary antibody, stained with DAB and haematoxylin. Colored columns in the DAB image profile represent the percentage of pixel counts scored as high (red), medium (yellow) and negative (green) levels. Mag. 40x.

Table 5-2. Semi-quantitative analysis of DAB-stained immunohistochemistry images for hCTR1 positivity in tumor tissues of human colorectal cancer

Field	Program-generated percentage (%)			Total percentage (%)	Mean ± SD (%)
	High positive	Positive	Low positive		
Field 1	0.003	3.6	72	76	
Field 2	0.12	8.6	64	73	76 ± 4
Field 3	0.01	1.9	79	81	

5.3.3 Immunochemical findings

Standard DAB immunohistochemistry was performed on paraffin-embedded sections of tumor tissues and matched normal tissues collected from six colorectal cancer patients. DAB-stained images were deconvoluted and analyzed using the semi-quantitative method as described above. Representative IHC image and the deconvoluted DAB stained images were shown for tumor and normal tissues of 6 individual patients (Fig 5-3 and S-1, 2, 3). The average of percentages of hCTR1, ATP7A and ATP7B staining of three randomly selected fields was

summarized in Tab 5-3. The staining of three transporters was limited to the areas of adenocarcinoma in tumor tissue and associated with crypts in normal tissue (Fig. 5-10). The combined average percentage staining for all 3 three transporters in the tumor tissues was significantly higher than that observed in the normal tissues (57.2 ± 11.4% vs 49.3 ± 9.6%, P = 0.03, paired t test). However, there was no significant variation in transporter expression when tumor and normal tissues were grouped together (P = 0.1083, ANOVA).

The percentage of hCTR1 positive immunostaining in tumor tissues was determined as 35 ± 4.9%, 41 ± 2.9%, 45 ± 1.8%, 74 ± 4.5, 53 ± 2.9%, 56 ± 3.7% for six colorectal cancer patients respectively. This indicates an approximately 2-fold difference between the lowest and highest hCTR1 expression in these samples. Likewise, the percentage of positive hCTR1 immunostaining in normal tissues was determined as 34 ± 4.3%, 46 ± 2.7%, 65 ± 3.1%, 64 ± 2.5, 41 ± 1.5%, 54 ± 2.6% for six patients respectively, which indicates about 2-fold difference. Comparison between matched tumor and normal tissues for hCTR1 showed no significant differences across six patients (50.7 ± 13.8% vs 51 ± 12.6%, P = 0.99, paired t test).

The percentage of positive ATP7A immunostaining in tumor tissues was determined as 53 ± 1.9%, 40 ± 7.9%, 57 ± 3.5%, 55 ± 6.1, 62 ± 3%, 64 ± 5.4% respectively for six colorectal cancer patients, indicating a slight difference between the lowest and highest ATP7A expression. Likewise, the percentage of positive ATP7A immunostaining in normal tissues was determined as 49 ± 2.1%, 45 ± 3.7%, 50 ± 2.6%, 51 ± 2, 44 ± 2.5%, 32 ± 2.3% respectively for six patients, indicating a ~1.7-fold difference between lowest and highest expression levels. Tumors also showed higher expression of ATP7A, although this was not statistically significant (55.3 ± 8.5% vs 45.3 ± 7%, P = 0.123, paired t-test).

The percentage of positive ATP7B immunostaining in tumor tissues was determined as 69 ± 2.5%, 65 ± 1.4%, 55 ± 4.1%, 73 ± 4.3, 63 ± 4.5%, 69 ± 2.1% respectively for six colorectal

cancer patients, indicating a slight difference between the lowest and highest ATP7B expression. Likewise, the percentage of positive hCTR1 immunostaining in normal tissues was determined as 35 ± 2.9%, 53 ± 3.3%, 50 ± 3%, 59 ± 1.4, 57 ± 1.7%, 57 ± 3.8% respectively for six patients, indicating a ~1.7-fold difference between lowest and highest expression. Tumor tissues had significantly higher ATP7B percentage staining than those in the matched normal tissues (65.7 ± 6.3% vs 51.8 ± 8.9%, $P = 0.0234$, paired *t* test).

A

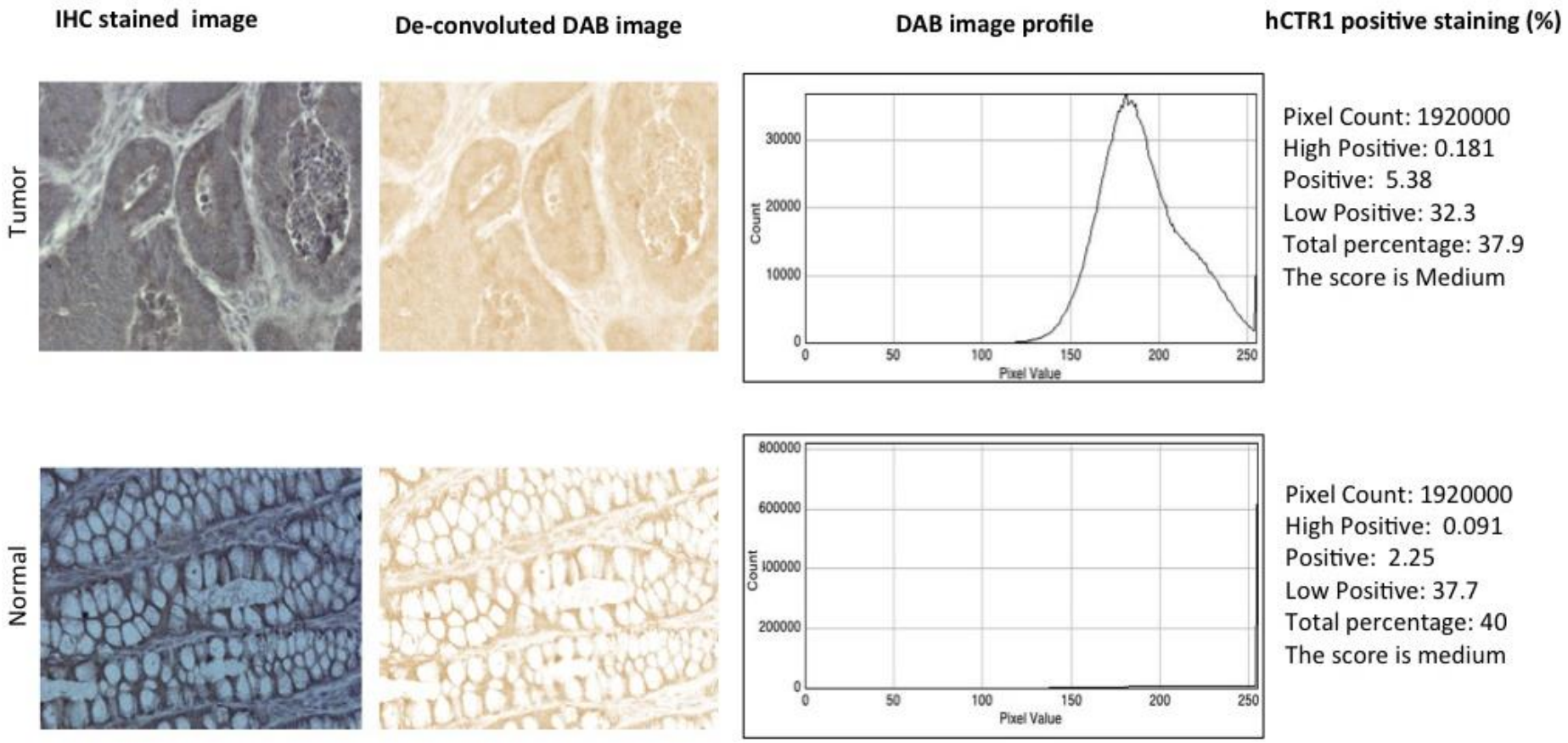
IHC stained image
De-convoluted DAB image
DAB image profile
hCTR1 positive staining (%)
Tumor
Count
Pixel Value
Pixel Count: 1920000
High Positive: 0.181
Positive: 5.38
Low Positive: 32.3
Total percentage: 37.9
The score is Medium
Normal
Count
Pixel Value
Pixel Count: 1920000
High Positive: 0.091
Positive: 2.25
Low Positive: 37.7
Total percentage: 40
The score is medium

B

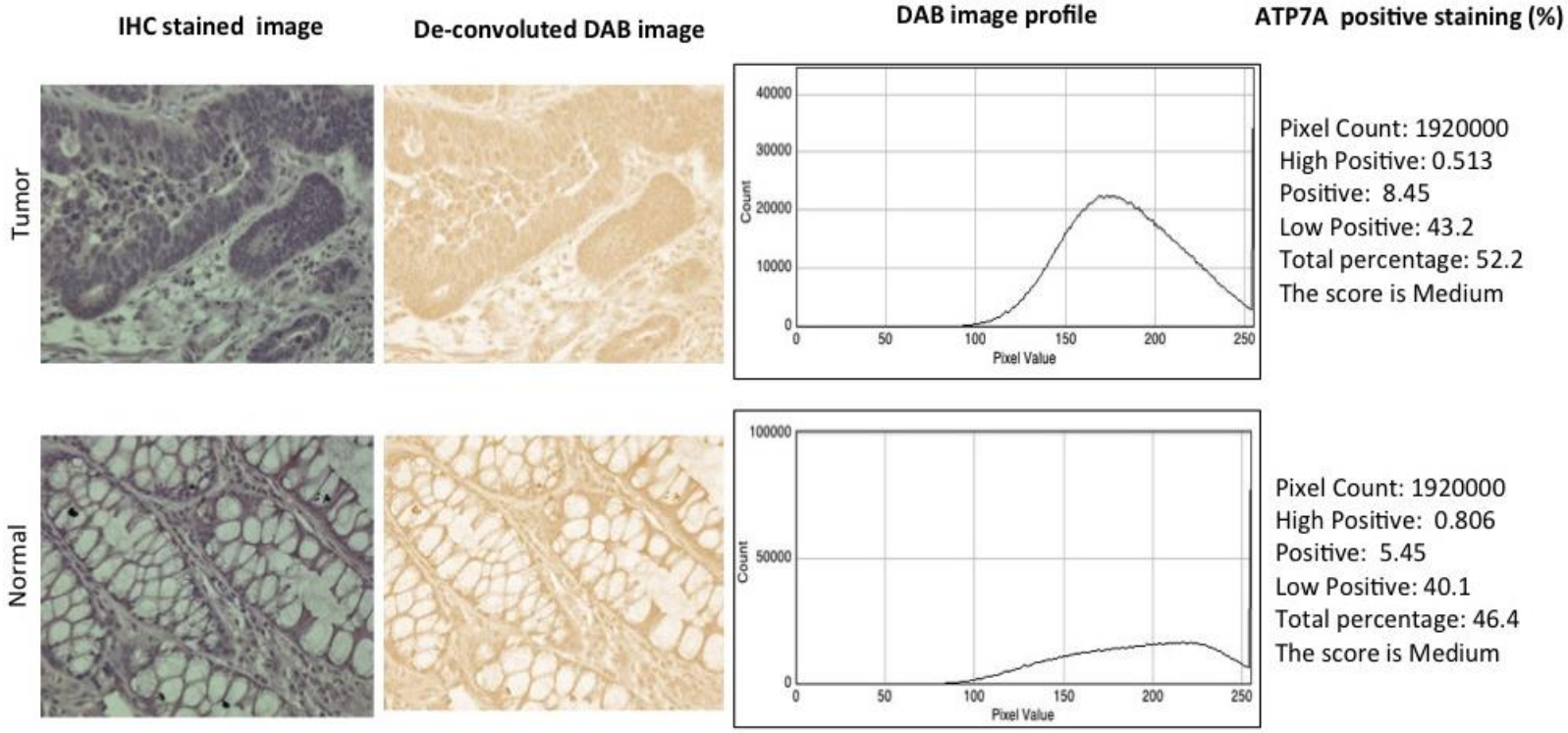
IHC stained image
De-convoluted DAB image
DAB image profile
ATP7A positive staining (%)
Tumor
Normal
Count
Pixel Value
Pixel Count: 1920000
High Positive: 0.513
Positive: 8.45
Low Positive: 43.2
Total percentage: 52.2
The score is Medium
Pixel Count: 1920000
High Positive: 0.806
Positive: 5.45
Low Positive: 40.1
Total percentage: 46.4
The score is Medium

C

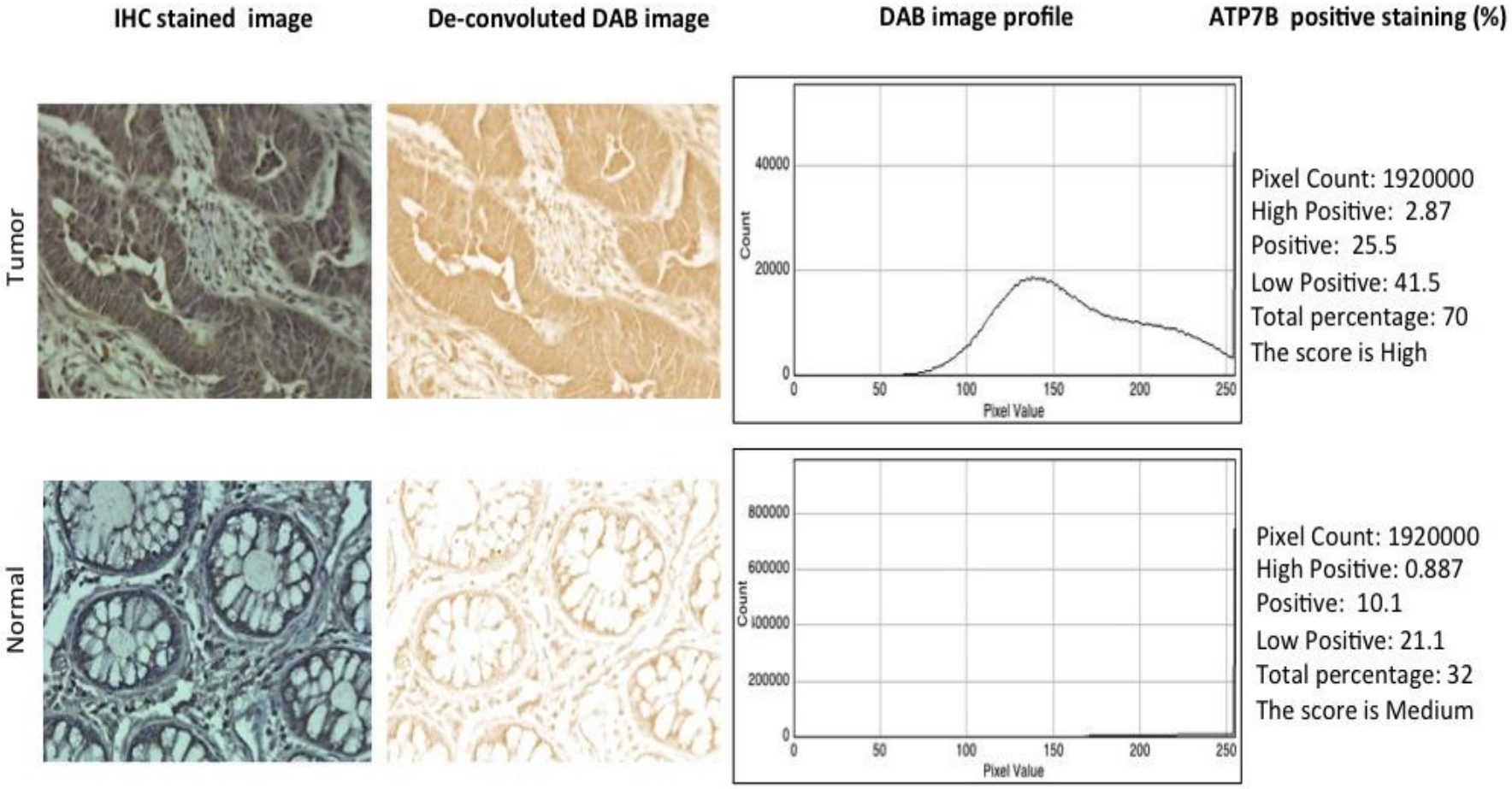
IHC stained image
De-convoluted DAB image
DAB image profile
ATP7B positive staining (%)
Tumor
Normal
Count
Pixel Value
0
20000
40000
50
100
150
200
250
200000
400000
600000
800000
Pixel Count: 1920000
High Positive: 2.87
Positive: 25.5
Low Positive: 41.5
Total percentage: 70
The score is High
Pixel Count: 1920000
High Positive: 0.887
Positive: 10.1
Low Positive: 21.1
Total percentage: 32
The score is Medium

Figure 5-3. Representative immunohistochemical images of hCTR1, ATP7A and ATP7B in tumor and the matched normal tissues

A. The expression of hCTR1 in tumor and normal tissue. B. The expression of ATP7A in tumor and normal tissue. C. The expression of ATP7B in tumor and normal tissue. Tumor and matched adjacent normal tissues were collected from six colorectal cancer patients, processed using standard DAB-based immunohistochemistry and counterstained with haematoxylin. DAB-IHC images were deconvoluted and analyzed using a semi-quantitative method to acquire the percentage of pixel intensity and counts of immunoreactivity. Mag. 40x.

Table 5-3. The expression of copper transporters in human colon samples

Patient No.	hCTR1		ATP7A		ATP7B	
	Tumor	Normal	Tumor	Normal	Tumor	Normal
1	35 ± 4.9	34 ± 4.3	53.3 ± 1.9	49.3 ± 2.1	69 ± 2.5	35 ± 2.9
2	41 ± 2.9	46 ± 2.7	40.2 ± 7.9	45.2 ± 3.7	65 ± 1.4	53 ± 3.3
3	45 ± 1.8	65 ± 3.1	57.1 ± 3.5	50.3 ± 2.6	55 ± 4.1	50 ± 3
4	74 ± 4.5	64 ± 2.5	54.9 ± 6.1	51.1 ± 2	73 ± 4.3	50 ± 1.4
5	53 ± 2.9	41 ± 1.5	62.2 ± 3	43.7 ± 2.5	63 ± 4.5	57 ± 1.7
6	56 ± 3.7	54 ± 2.6	63.9 ± 5.4	32.3 ± 2.3	69 ± 2.1	57 ± 3.8
Mean ± S.D	50.7 ± 13.8	51 ± 12.6	55.3 ± 8.5	45.3 ± 7	65.7 ± 6.3*	51.8 ± 8.9

*, $P < 0.05$ compared to value of normal for ATP7B

5.4 Discussion

In this chapter, we have systematically studied the expression of Cu transporters hCTR1, ATP7A and ATP7B in tumor tissues of colorectal cancer patients. All of these three transporters were expressed in tumor tissues with significant differences between matched tumor and normal tissues for some colorectal cancer patients.

We investigated the expression of Cu transporters in tumor tissues of colorectal cancer patients, in comparison to matched adjacent normal colonic tissues using a semi-quantitative DAB-based immunohistochemistry method. Interestingly, the expression in colorectal cancer tumor tissues was largely in consistent with that in colorectal cancer cells. hCTR1 is widely expressed in tumor tissues of all six patients. This finding is consistent with previous reports that hCTR1 is expressed in tumor samples of all 75 patients with colorectal cancer [101], [51]. The function of hCTR1 in colorectal cancer is unclear at present but may be related to the higher demand of copper during development and metastasis of this cancer type [195].

In the meantime, we detected a similar level of hCTR1 expression in normal colonic tissues in all six patients. hCTR1 immunoreactivity was strongly associated with epithelia of the enterocytes in the crypts. In a previous study, hCTR1 is expressed in human colon mucosa in about 16 of 42 cases using immunohistochemistry [100]. The higher positive rate of hCTR1 expression detected in our samples may result from the different sensitivity of methods used to quantity hCTR1. mRNA transcripts of hCTR1 were also found in colon tissues of human [208] and zebrafish [209]. hCTR1 may function to absorb Cu and other nutrients across the colonic mucosa, which is complementary to the absorptive function of the small intestine [210]. Moreover, the variation of hCTR1 expression levels in normal colon tissues may indicate that hCTR1 expression is influenced by patient's age, gender or other factors [54].

We compared the expression levels of hCTR1 between normal colon tissue and CRC due to the importance of copper for the development of CRC. This study is the first where hCTR1 expression in normal tissue was compared to matched CRC tissue with a quantitative and objective IHC profiling software. While Holzer *et al* reports that the frequency positive hCTR1 expression increases with the clinical staging of CRC [100], we found that hCTR1 was not elevated in CRC cancers. The observation that hCTR1 was down regulated in some CRC cancer samples compared to the normal counterpart provides an opportunity to use Cu chelators to enhance the cytotoxicity of OXL by up regulating hCTR1.

The expression of copper efflux transporters was confirmed in both malignant and normal colon tissues. ATP7A and ATP7B are copper-transporting P-type ATPases closely related to each other with respect to both structure and function. They are involved in both biosynthetic pathways and copper efflux in mammalian cells [54]. In addition to cancer tissues, ATP7B was widely detected in normal colon tissue, which is consistent with reports that ATP7B is also widely distributed in human liver, brain, heart and lung [211]. However, the function of ATP7B in normal colon samples is uncertain. Our results show ATP7B seems to be up regulated in colorectal cancer tissues, which is in line with reports from human gastric cancer [212], liver cancer [213] and ovarian cancer [214]. Here, again, the increased expression of ATP7B in colorectal tumor samples relative to that of normal colon samples could highlight its importance in colon carcinogenesis of colon tissues.

In our study, we detected ATP7A in all colorectal cancer and normal colon tissue samples. These results are consistent with a report that ATP7A is ubiquitously expressed in the majority of tissues except for the liver [54], although a detailed understanding of the function of ATP7A in these tissues was beyond the aims of this study. ATP7A is reportedly up regulated in several cancers compared to their corresponding normal tissues [102-104] and is expressed in 8 of 34 cases (23.5%) of clinical colon cancer specimens [102]. Therefore, detection of ATP7A in the

tumor tissues in our study did not come as a surprise. Perhaps colorectal cancer cells need more ATP7A to deliver copper to enzyme-synthetizing compartments or perhaps it involves in other important pathophysiological roles such as angiogenesis that is important for the progression of CRC [215].

Lastly, it has to be pointed out that simultaneous expression of both ATP7A and ATP7B in colon tissues is not an uncommon phenomenon since this dual expression has also been described in other normal tissues, such as placenta, mammary gland, eye and lung [54]. At present however, it is not clear if they play complementary or synergistic roles in the translocation of copper across the membrane or if this process is essential to prevent cytoplasmic Cu-dependent toxicity.

Chapter 6 Expression of Copper Transporters in Colon Tissues of Winnie Mice with Chronic Colitis or Colonic Dysplasia

6.1 Introduction

The results of the previous chapter have demonstrated that ATP7B protein was up-regulated significantly in some colorectal tumor samples compared to normal tissue samples. Although the tumors also showed higher expression of ATP7A, this effect did not reach statistical significance. Nevertheless, these observations seem to support the hypothesis that copper or copper transporters may be involved in the development of colorectal cancer (Section 1.4.3), despite this assumption has not been tested in appropriate animal models to date.

Chronic inflammation, in particular, ulcerative colitis (UC) is one of the important risk factors that can accelerate the transformation of colorectal mucosa to adenocarcinomas [151]. Dysplasia, as a precancerous condition is intertwined with both UC and colorectal cancer and is increasingly recognized as a diagnostic marker for colorectal cancer. In the context of intestinal inflammation, the development of colorectal cancer seems to follow a step-wise transition from normal mucosa to colitis, dysplasia and adenocarcinomas [216]. There is growing evidence that copper or copper-containing enzymes are correlated with inflammation and the development of malignancy of normal tissues. However, the role of copper transporters in these serial events has not been elucidated yet.

The *Winnie* mouse model of colitis has been developed by chemically inducing a point mutation rather than a deletion of the *Muc2* gene [151]. These mice display spontaneous inflammation in the distant colon at 6 weeks after birth and full colitis by the age of 16 weeks

[151]. In addition, *Winnie* mice show increased local production of IL-1b, TNF-a, and IFN-c as well as increased intestinal permeability in the distal colon, which are common pathological changes observed in human UC [217]. When exposed to DSS, most of *Winnie* mice will develop dysplasia, which is a precursor for colorectal cancer, suggesting of the suitability of this model as model of colorectal cancer development.

Therefore, the overall goal of this chapter is to determine the roles of copper transporters in the development of colorectal cancer by studying their expression in colorectal tissues of wild-type C57BL/6 mice, Winnie mice and dextran sulphate sodium (DSS)-treated Winnie mice that can reflect the normal, inflammatory, and precancerous condition of colon tissue as mentioned above.

6.2 Experimental design

6.2.1 Establishment of the colitis and dysplasia models

We obtained colonic tissues from 10 *Winnie* mice with chronic colitis (n = 10), colonic tissues with histologically confirmed dysplasia from DSS-treated *Winnie* mice (n = 10) and colonic tissues from wild-type C57BL/6 mice (n = 10) as a normal tissue control (from Dr Raj Eri, School of Health Sciences, University of Tasmania). *Winnie* mice show spontaneous and inheritable intestinal colitis at the age of 6 weeks and full colitis by the age of 16 weeks because of a point mutation of the *Muc2* gene [154]. When treated with the luminal agent DSS, most of these mice develop dysplasia, which is a precursor to colorectal cancer. Detailed information about these two animal models and how they were produced were described in Section 1.4.4. The Animal Ethics Committee of the University of Tasmania has approved this project (Ethics approval No: A0013576).

6.2.2 Histological confirmation of chronic colitis and dysplasia in colon of mice

Histologically, chronic colitis is characterized with thickening of mucosa layer, irregularity or branching of crypts, presence and infiltration of inflammatory cells into submucosa [25]. Colonic dysplasia displays typical pathological changes such as focal presentation, loss of polarity of crypts and increased nucleus-to-cytoplasm ratio [27]. Therefore, H&E staining was performed on paraffin-embedded sections of colon tissues of *Winnie*, DSS-treated *Winnie* and wild-type C57BL/6 mice (See section of 2.9) to identify the nature of samples before undertaking following experiments.

6.2.3 Characterization of the expression of mCTR1, ATP7A and ATP7B

Standard DAB-based immunohistochemistry (IHC) was performed on paraffin-embedded sections of colon tissue using anti-mouse CTR1, ATP7A and ATP7BA primary antibodies and species-specific biotin-labeled secondary antibodies. The expression of the transporters was further quantified by analyzing the DAB-stained images using a semi-quantitative method as described previously (see Section 5.2.3). Briefly, IHC images of mCtr1 were deconvoluted to display DAB staining only. Pixel-by-pixel digital analysis of DAB-only images was conducted to produce corresponding histograms showing the percentages of immunostained areas based on the staining intensity. The percentage of drug transporter immunostaining was calculated as the sum of percentages of high positive, positive and low positive staining that were generated using Image J software. Positive staining was defined based on the percentages as high (>65%), medium positive (30-64%), low positive (6-29%) and negative (<5%), respectively. Three fields were randomly selected for analysis and represented the final percent of positive staining for a specific tissue sample. Comparison of expression levels was either made between tissue types or across transporter proteins. To properly illustrate these processes, a semi quantitative analysis was performed on DAB-stained IHC images of colon tissue for the Cu transporter mCTR1 (See Section 6.3.2).

6.3 Results

6.3.1 Histological confirmation of chronic colitis in Winnie mice and colonic dysplasia in DSS-treated *Winnie* mice

Standard H&E staining was performed on paraffin-embedded sections of colon tissues of *Winnie*, DSS-treated *Winnie* and wild-type C57BL/6 mice (Fig. 6-1A). Representative microphotographs illustrate abnormal pathological changes of chronic colitis in the colon of *Winnie* mice. These included a thickened mucosa, irregular, elongated or branching structure of crypts, loss of epithelium on the luminal side, infiltration of inflammatory cells into the lamina propia and submucosa, and crypt abscesses (Fig. 6-1A, b-f), when compared with normal colon tissue from C57BL/6 mice (Fig. 6-1A, a)

A

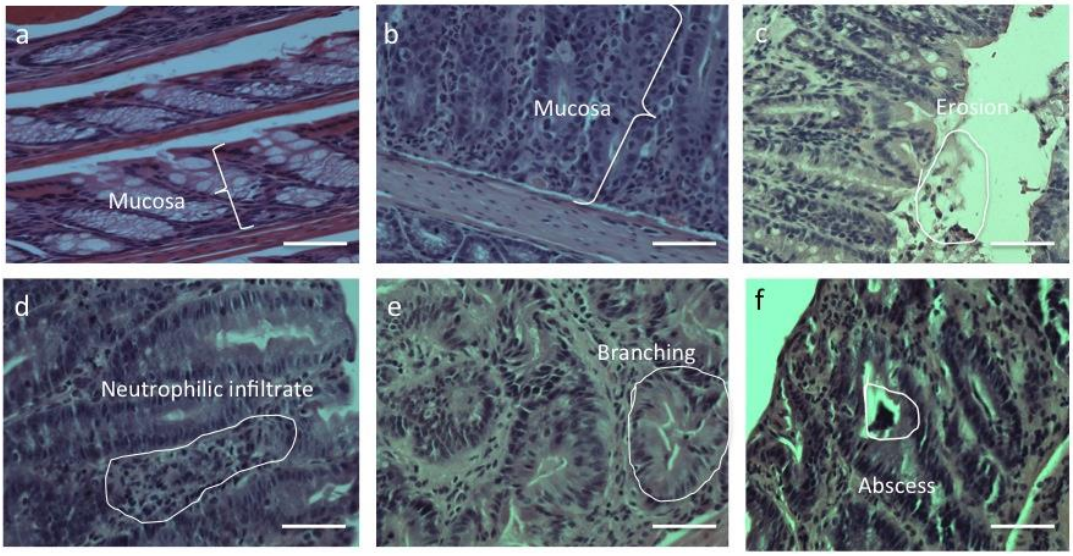

B

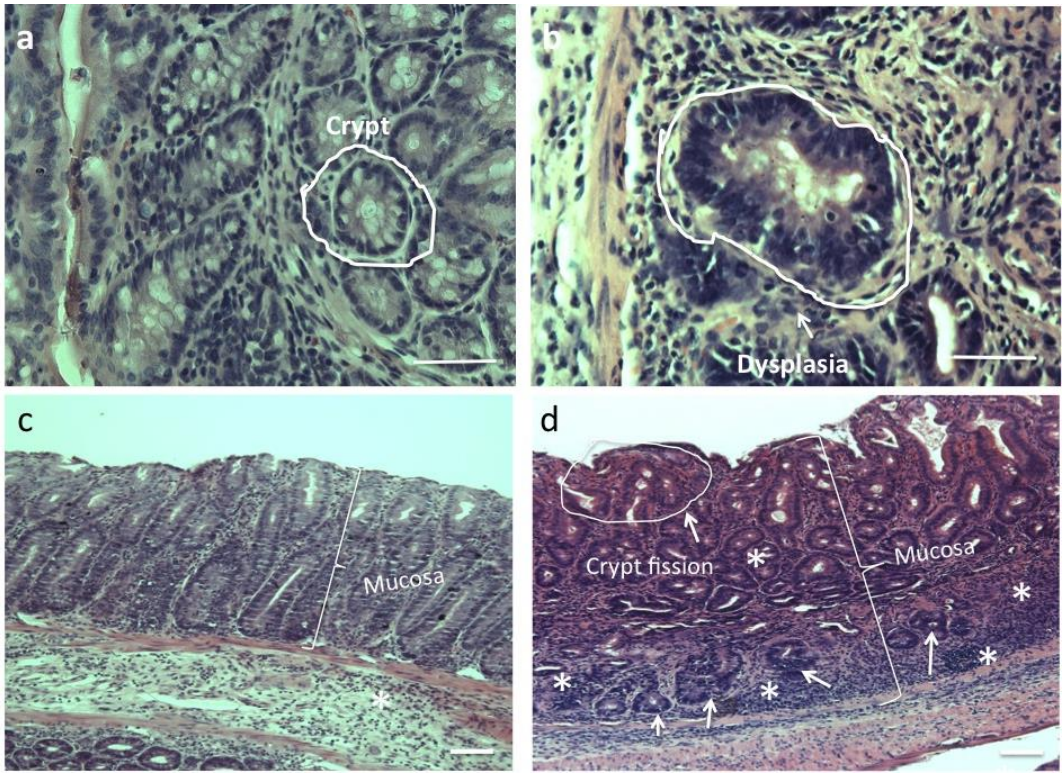

Figure 6-1. Representative colon microphotographs of histology of colitis of Winnie mice and colonic dysplasia in DSS-treated *Winnie* mice

A. Histology of colitis in *Winnie* mice. (a) Normal distal colon tissue of wild-type C57BL/6 mouse. (b-f) Distal colon tissue of *Winnie* mice with colitis displaying mucosal thickening (b), mucosal erosion (c), neutrophilic infiltration (d), branching crypts (e) and crypt abscesses (f), which were labeled or demarcated accordingly. B. Histology of colonic dysplasia in DSS-treated *Winnie* mice. (a) Normal colon tissue. (b) Colon tissue of DSS-treated *Winnie* mouse with dysplasia displaying loss of polarity of crypt and increased nucleus-to-cytoplasm ratio. (c) Colon tissue of *Winnie* mouse with colitis showing elongated crypts and leukocyte infiltration into the mucosa and submucosa (asterisk). (d) Colon tissue of DSS-treated *Winnie* mouse displaying high extent of proliferation, focal dysplasia (arrows) and active chronic inflammation in mucosa featured by crypt fission, mucosal thickening and leukocyte infiltration (asterisks). Scale bars represent 50 μm.

In the DSS-treated *Winnie* mice, the representative microphotographs of H&E stained distal colon tissues displayed typical pathological changes of colonic dysplasia, such as focal presentation, loss of polarity of crypts and increased nucleus-to-cytoplasm ratio (Fig. 6-1B). Abnormal crypt structure was evident with enlarged or fission appearance, proliferation of epithelial nuclei and increased nucleus-to-cytoplasm ratio compared to normal colon tissue (Fig. 6-1B, c). In addition, inflammation was exacerbated in colon tissues of DSS-treated *Winnie* mice with thickening of crypts, increased infiltration of leukocytes into the mucosa and submucosa layers, large areas of erosion, fission or loss of crypts.

6.3.2 Example of semi-quantitative analysis of DAB-stained images of immunohistochemistry

An example is shown in Fig. 6-2 to illustrate the semi-qualitative analysis method for DAB-stained IHC images of colon tissue for the Cu transporter mCTR1. Deconvoluted DAB-only images were processed to generate histograms of frequency of positively stained areas of colon tissues. The total percentages were calculated as 84%, 60%, 25.2% and 2.1%, which represent high, medium, low and negative staining of Cu transporter mCTR1 (Fig. 6-2A). As shown in Fig. 6-2B, three randomly selected fields in a tissue section produced reproducible percentages of mCTR1 positive staining as 56.7%, 56.4% and 57.5% (mean ± SD (57 ± 0.5%), therefore, this mCTR1 staining was categorized as medium for this particular tissue sample.

A

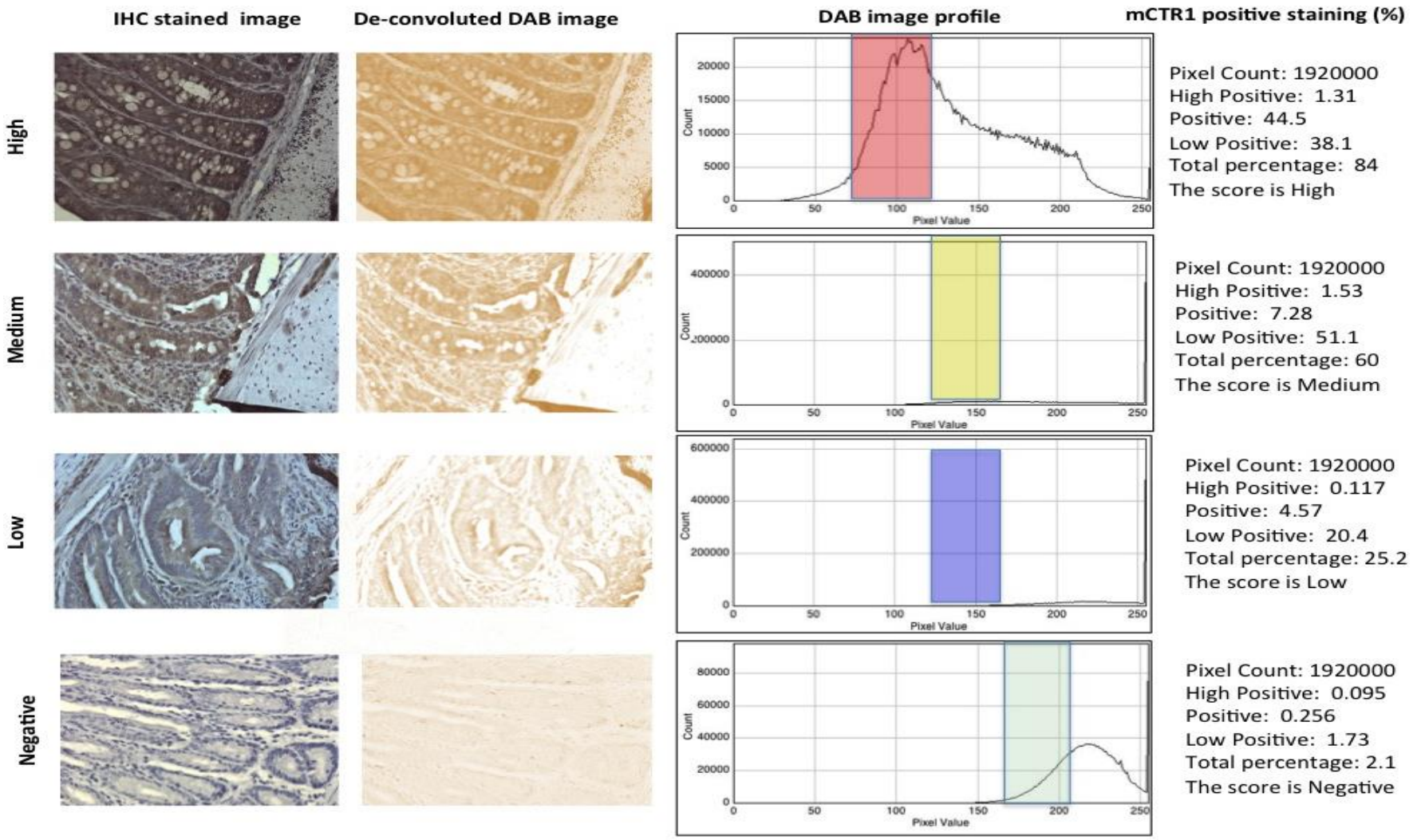
IHC stained image
De-convoluted DAB image
DAB image profile
mCTR1 positive staining (%)
High
Medium
Low
Negative
Count
Pixel Value
Pixel Count: 1920000
High Positive: 1.31
Positive: 44.5
Low Positive: 38.1
Total percentage: 84
The score is High
Pixel Count: 1920000
High Positive: 1.53
Positive: 7.28
Low Positive: 51.1
Total percentage: 60
The score is Medium
Pixel Count: 1920000
High Positive: 0.117
Positive: 4.57
Low Positive: 20.4
Total percentage: 25.2
The score is Low
Pixel Count: 1920000
High Positive: 0.095
Positive: 0.256
Low Positive: 1.73
Total percentage: 2.1
The score is Negative

B

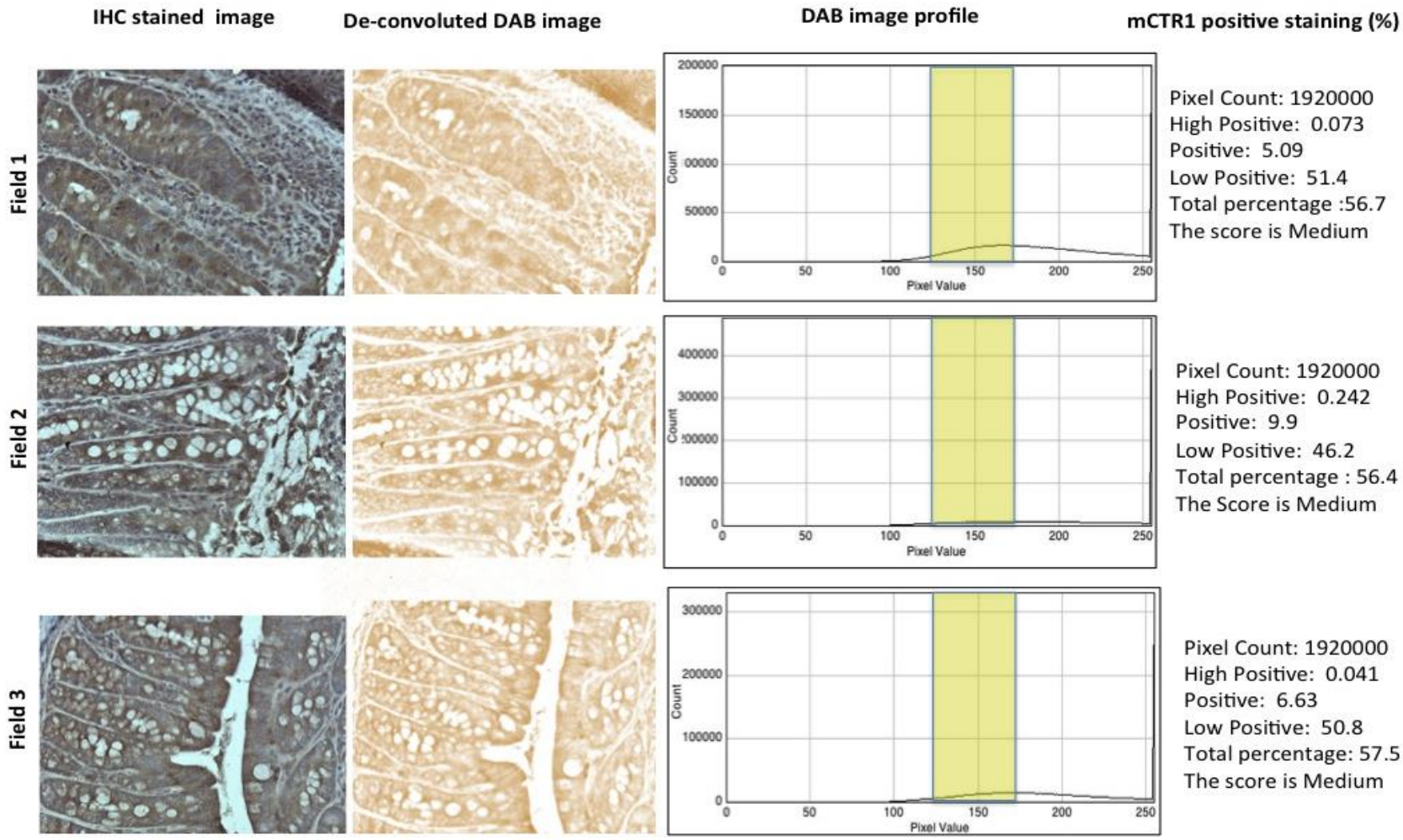
IHC stained image
De-convoluted DAB image
DAB image profile
mCTR1 positive staining (%)
Field 1
Field 2
Field 3
Count
Pixel Value
Pixel Count: 1920000
High Positive: 0.073
Positive: 5.09
Low Positive: 51.4
Total percentage :56.7
The score is Medium
Pixel Count: 1920000
High Positive: 0.242
Positive: 9.9
Low Positive: 46.2
Total percentage : 56.4
The Score is Medium
Pixel Count: 1920000
High Positive: 0.041
Positive: 6.63
Low Positive: 50.8
Total percentage: 57.5
The score is Medium

Figure 6-2. Semi-quantitative analysis of DAB stained immunohistochemical images of mCTR1 in colonic tissues of *Winnie* mice

Standard DAB immunohistochemistry (IHC) was performed on paraffin-embedded colonic tissue sections using an anti-mCTR1 primary antibody and an anti-rabbit secondary antibody. Sections were counterstained with haematoxylin. A. Digitally scoring of deconvoluted DAB-stained IHC images of mCTR1 illustrating negative, low, medium and high positive staining defined by the percentage of pixel counts. Colored columns in DAB image profiles represent the percentage of staining intensity as high (red), medium (yellow), low (blue) or negative (green) levels. B. Three randomly selected fields of a section represent a specific tissue sample for semi-quantitative analysis. Mag. 40x.

We subsequently applied this semi-quantitative analysis to quantify the expression level of Cu transporter mCTR1, ATP7A and ATP7B in colonic tissues from *Winnie* mice of colitis, DSS-treated *Winnie mice* and wild-type normal mice.

6.3.3 Expression of copper transporters in mouse tissues

mCTR1 immunoreactivity was detected in all colonic tissues of these mice but this staining was limited to the colonic crypts of *Winnie* mice and C56BL/6 mice. The overall percentage of positive mCTR1 immunostaining for all these samples was measured as 66 ± 13%, which was significantly higher than that of normal tissues (66 ± 13% vs 50 ± 7.9, $P < 0.05$). In *Winnie* mice exposed to DSS, mCTR1 staining was detected in all these colon samples (Fig. 6-3C). Strikingly, the overall staining level for mCTR1 was significantly reduced by 3 folds in DSS-treated *Winnie* mice compared to that of untreated *Winnie* mice (23 ± 12% vs 66 ± 13, $P < 0.05$) (Fig. 6-3A and Tab 6-1).

Next, we analyzed the expression of ATP7A in colonic tissues collected from *Winnie* mice of colitis, DSS-treated *Winnie* mice and wild-type C57BL/6 mice using the same method used to quantify mCTR1 expression. Overall, ATP7A immunoreactivity was detected in all colonic tissues analyzed. The overall percentage of positive ATP7A immunostaining of all ten samples from DSS-treated mice was measured as 51 ± 9.7%, which was similar to that of normal colon samples (50 ± 15%). In *Winnie* mice, ATP7A staining was detectable in all these colon samples despite overall weaker expression intensity. The overall level of ATP7A expression was significantly reduced compared to that of untreated *Winnie* mice (20 ± 5.3% vs 51 ± 9.7%, $P < 0.05$) (Fig. 6-3B and Tab 6-1).

Subsequently, we analyzed the expression of ATP7B in colonic tissues collected from *Winnie* mice of colitis, DSS-treated *Winnie* mice and wild-type C57BL/6 mice with the same methods used to quantify mCTR1 and ATP7A. Overall, ATP7B immunoreactivity was detected in all colonic tissues of mice. The overall percentage of positive ATP7B immunostaining of all ten samples was measured as 64 ± 9.5%, which was similar to that of normal colon samples (66 ± 4.9%). Immunohistochemistry was also performed on paraffin-embedded sections of dysplastic colon samples from ten *Winnie* mice exposed to DSS. ATP7B staining was detectable in all these colon samples despite weak expression. The overall level for ATP7B staining significantly reduced compared to untreated *Winnie* mice (11 ± 3% vs 64 ± 9.5%, $P < 0.05$) (Fig. 6-3C and Tab 6-1)

A

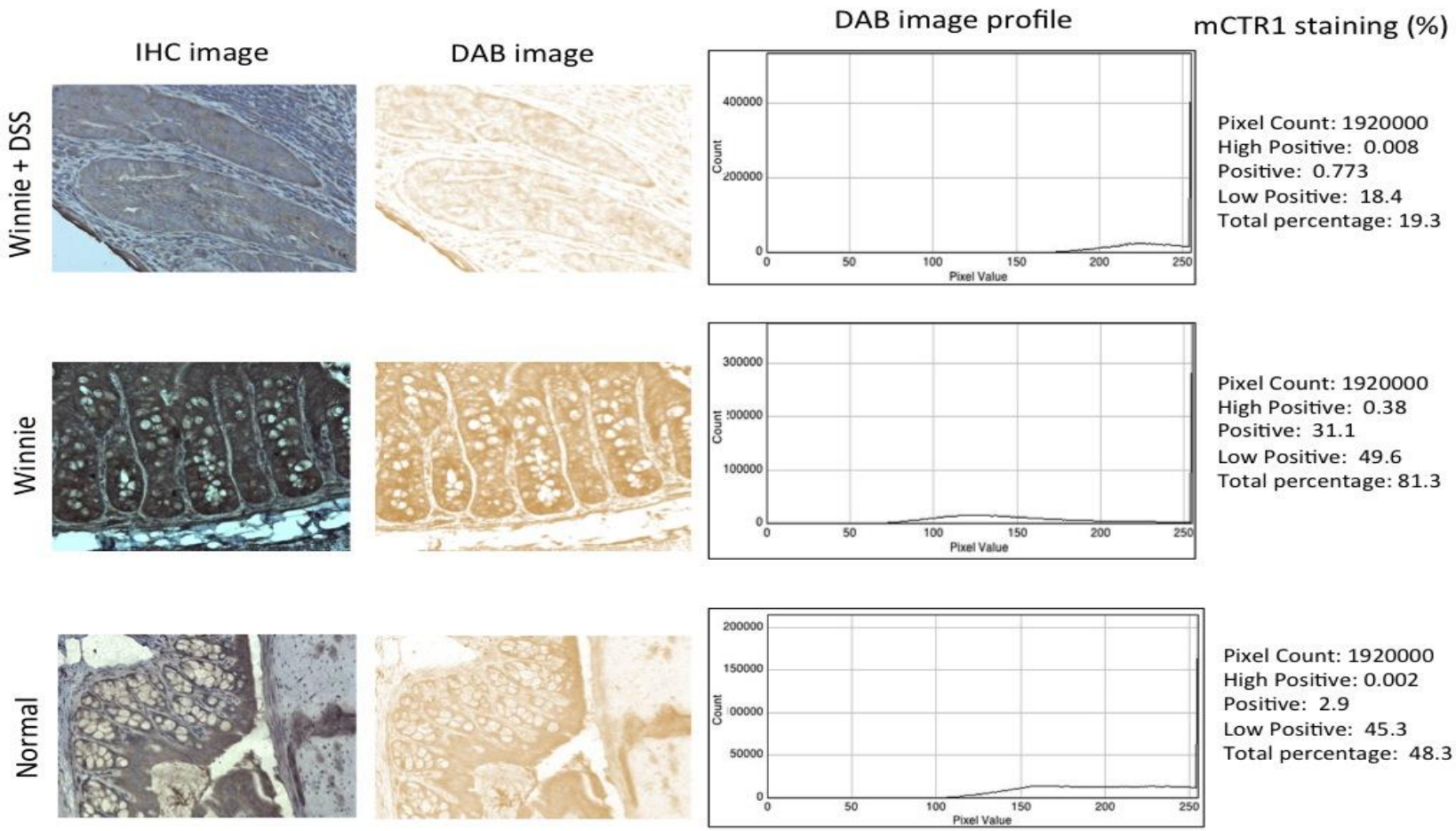
IHC image
DAB image
DAB image profile
mCTR1 staining (%)
Winnie + DSS
Pixel Count: 1920000
High Positive: 0.008
Positive: 0.773
Low Positive: 18.4
Total percentage: 19.3
Winnie
Pixel Count: 1920000
High Positive: 0.38
Positive: 31.1
Low Positive: 49.6
Total percentage: 81.3
Normal
Pixel Count: 1920000
High Positive: 0.002
Positive: 2.9
Low Positive: 45.3
Total percentage: 48.3
Count
Pixel Value

B

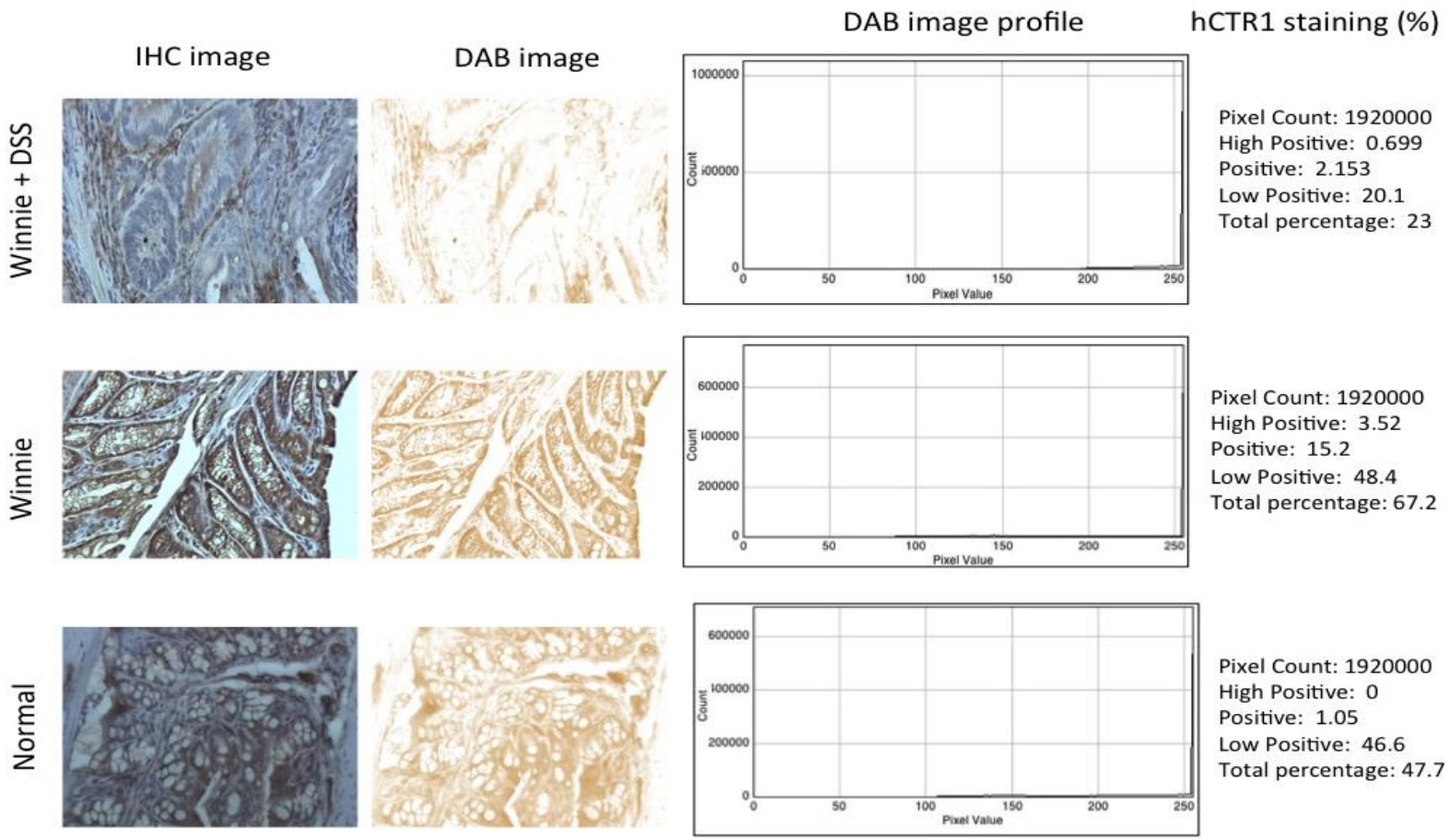
IHC image
DAB image
DAB image profile
hCTR1 staining (%)
Winnie + DSS
Winnie
Normal
Count
Pixel Value
Pixel Count: 1920000
High Positive: 0.699
Positive: 2.153
Low Positive: 20.1
Total percentage: 23
Pixel Count: 1920000
High Positive: 3.52
Positive: 15.2
Low Positive: 48.4
Total percentage: 67.2
Pixel Count: 1920000
High Positive: 0
Positive: 1.05
Low Positive: 46.6
Total percentage: 47.7

C

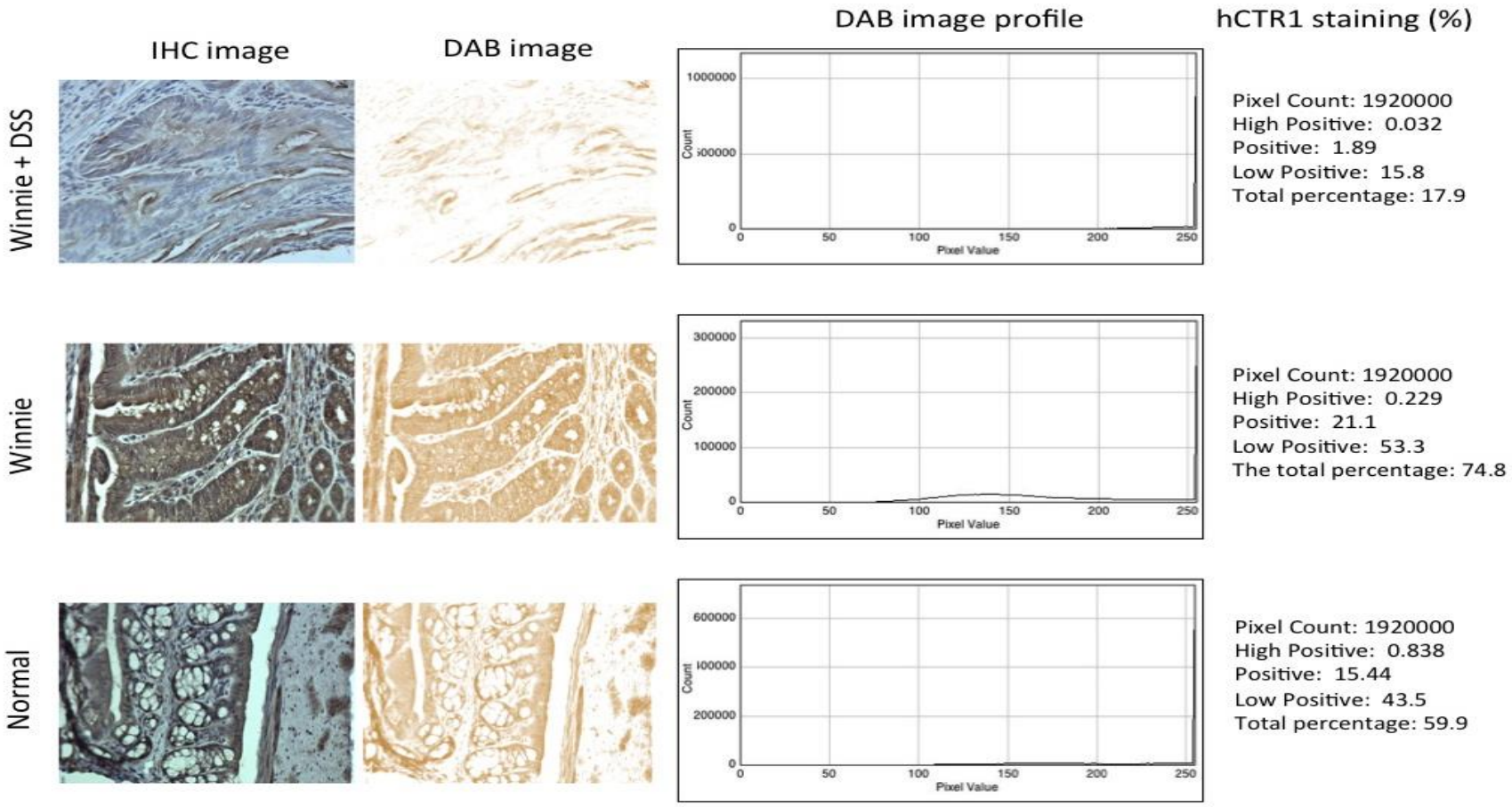
IHC image
DAB image
DAB image profile
hCTR1 staining (%)
Winnie + DSS
Winnie
Normal
Count
Pixel Value
Pixel Count: 1920000
High Positive: 0.032
Positive: 1.89
Low Positive: 15.8
Total percentage: 17.9
Pixel Count: 1920000
High Positive: 0.229
Positive: 21.1
Low Positive: 53.3
The total percentage: 74.8
Pixel Count: 1920000
High Positive: 0.838
Positive: 15.44
Low Positive: 43.5
Total percentage: 59.9

Figure 6-3. Semi-quantitative analysis of representative DAB-stained images showing immunostaining of mCTR1, ATP7A and ATP7B in colonic tissues

A. Immunostaining of mCTR1 in colonic tissues of normal mice, *Winnie* mice with chronic colitis and DSS-treated *Winnie* mice with colonic dysplasia. B. Immunostaining of ATP7A in colonic tissues of normal mice, *Winnie* mice with chronic colitis and DSS-treated *Winnie* mice with colonic dysplasia. C. Immunostaining of ATP7B in colonic tissues of normal mice, *Winnie* mice with chronic colitis and DSS-treated *Winnie* mice with colonic dysplasia. Standard DAB immunohistochemistry was performed on paraffin-embedded colonic tissue sections using specific antibodies as mentioned in Section 2.1. Sections were counterstained with haematoxylin. DAB-IHC images were deconvoluted and analyzed using a semi-quantitative method to acquire the percentage of pixel intensity and counts of immunoreactivity. Mag. 40x.

Table 6-1. The expression percentage of copper transporters in colonic tissues of mice

*, $P < 0.05$ compared to values of normal mice; +, $P < 0.05$ compared to values of mCTR1.

Group	Percentage expression of copper transporters (Mean ±S.D, n=10)		
	mCTR1	ATP7A	ATP7B
Winnie + DSS	23 ± 12 *	20 ± 5.3 *	11 ± 3*, +
Winnie	66 ± 13 *	51 ± 9.7 +	64 ± 9.5
Normal	50 ± 8	50 ± 15	66 ± 4.9 +

6.4 Discussion

Colitis-associated colorectal cancer is a chronic disease that normally takes 15-20 years to develop from inflammatory bowel disease over colonic dysplasia to adenocarcinoma [218]. The *Winnie* mouse model provides an opportunity to study the expression of copper transporters in colon tissues within a shorter time period. For the first time, this study observed that mCTR1 expression is elevated in colon tissues of *Winnie* mice compared to normal C57BL/6 mice, which supports our hypothesis that copper transporters play a role in the development of inflammatory bowel disease.

Histological examination evaluated the severity of inflammation and the presence of neoplasia in the colon of *Winnie* and DSS-treated *Winnie* mice. Typical inflammation associated histological or structural changes were detected in all colon samples of *Winnie* mice, suggesting that this chronic colitis model recapitulates the main pathological features of the human disease [151]. Upon challenging with DSS, all examined samples showed low to medium-level dysplasia as well as signs of exacerbated inflammation of the colon wall. These results are consistent with another report that characterizes histological inflammation and dysplasia-related pathology in these two models [148].

Following confirmation of inflammation and dysplasia in colon samples, the expression of copper transporters was examined. mCTR1 expression was up regulated in colon tissues of *Winnie* mice but reduced in the precancerous colon tissues compared to the normal tissue samples. Our first result is in line with previous reports that CTR1 expression is elevated in the eyes of patients with Eales disease, an idiopathic inflammatory disease [219] or chemical induced inflammation in rat liver [220]. A complete understanding of the mechanisms behind this phenomenon is beyond the

scope of this study, however, due to their wide involvement in several inflammation processes, copper or copper containing enzymes may be the key to explain this result.

The second finding that mCTR1 was down regulated in dysplastic colon tissue is contradictory to the expected role of hCTR1 in the carcinogenesis of colorectal cancer as discussed in Chapter 5. Considering that copper can be pro-inflammatory, mCTR1 down-regulation may be the result of the mucosa's response to acute DSS-induced inflammation. On the other hand, there is evidence that DSS can suppress the transcription of a multitude of genes by directly inhibiting DNA polymerase activity [221]. Consequently, this down regulation could be a consequence of DSS itself and might have nothing to do with the carcinogenic process *per se*. Therefore, one should be cautious to extrapolate this finding to the human condition.

Next, we compared the expression of the copper efflux transporters, ATP7A and ATP7B in colonic samples of *Winnie* mice with that of normal C57BL/6 mice. However, the overall expression of ATP7A or ATP7B was similar in colitis compared to normal tissue. The roles of copper efflux transporters in colon tissues under inflammatory conditions have not been studied yet. However, there is some evidence suggesting that copper efflux transporters might be altered under inflammatory conditions. Increased expression of ATP7A and trafficking of these proteins into cytoplasmic vesicles is observed in cultured BV-2 microglial cells in the presence of the pro-inflammatory agent interferon-gamma [222]. Mutation of ATP7B in Wilson disease is a well-known cause of severe inflammation in liver [127]. Perhaps copper efflux transporters are different from mCTR1 in the roles they play in the inflammation of colon.

Given the numerous reports that ATP7A and ATP7B are up regulated in many human cancers [103], [63], we expected to see increased expression. However, we observed a

consistent reduction of AP7A or ATP7B in colonic samples of colonic dysplasia, similar to the response of mCTR1 in the same tissues. Consequently, the same limitations of DSS treatment postulated for mCTR1 expression could also apply for the expression levels Cu-efflux transporters. Therefore, these results should be interpreted with caution, especially when comparing them to the human condition.

Chapter 7 General Discussion

The results described in this thesis demonstrate that hCTR1 regulates the transport and cytotoxicity of OXL in colorectal cancer cells, and that pharmacologically modulating hCTR1 protein level with some commonly used copper chelators could be used to enhance OXL cytotoxicity. We gained some preliminary understanding about the expression of copper transporters in colorectal cancer and in the precancerous stages including inflammation and dysplasia. In this thesis, recombinant and wild-type colorectal cancer cells were used as cellular models. Human colorectal tissues from colorectal cancer patients provided the clinically relevant biological samples. *Winnie* mice and DSS-treated *Winnie* mice were employed as animal models of chronic intestinal colitis and colonic dysplasia, respectively.

Stable, recombinant expression of hCTR1 mRNA in colon cancer cells was directly correlated with enhanced uptake of OXL and increased cytotoxicity compared to empty vector transfected control cells (Chapter 3). Clinically used copper chelators enhanced hCTR1 protein expression in CRC cell lines in a time-dependent manner. Pre-incubation of resistant colorectal cancer cells with these copper chelators under the same experimental conditions sensitized these cells to OXL cytotoxicity. Our results also suggest that this effect is mainly transmitted by hCTR1-dependent mechanisms, as the utilized Cu chelators had little effect on the expression or localization of the copper efflux transporter ATP7A and ATP7B (Chapter 4). Abundant expression of hCTR1 was detected in human colorectal cancer tissues. In contrast to hCTR1, we observed that ATP7B protein was up regulated in some of tumor samples compared to the normal tissues (Chapter 5). The percentage of mCTR1 staining increased in colonic tissues of *Winnie* mice, but decreased in tissues of dysplasia model compared to that of the normal

colon tissues. ATP7A and ATP7B expression were unaltered in tissues of colitis but decreased significantly in colonic tissues of dysplasia (Chapter 6).

Taken together, these findings suggest that copper transporters are widely expressed in colorectal cancers and they are not only responsible for uptake and cytotoxicity of OXL but may also be involved in the development of colorectal cancer itself.

In this chapter, the results are divided into four categories: copper uptake transporter hCTR1 and the uptake of OXL, the synergistic effect of copper chelators with OXL in the treatment of colorectal cancer, the differential expression of copper transporters in colorectal cancer tissues, and the expression of copper transporters in colon tissues of *Winnie* mice with chronic colitis or colonic dysplasia. Potential implications of each result and their possible applications are also discussed, which is based on the results of this thesis and previously published reports. Finally, future research directions that have arisen based on the results of this thesis are described at the end of this chapter.

7.1 Human Cu uptake transporter 1 contributes to the uptake and cytotoxicity of oxaliplatin

The precise mechanisms of OXL resistance are still not well characterized yet, despite decades of intensive studies. A common view is that tumor cells may become resistant to OXL via multiple approaches including alterations in cellular transport and accumulation, detoxification, cell death, DNA damage response and repair, and epigenetic mechanisms [29,30]. Of all these complex factors that may affect the pharmacology of OXL, the pathways that control the cellular accumulation of OXL are increasingly accepted as the main factor to affect the anticancer efficacy of OXL [47,49]. OXL is a polarized molecule and this chemical property determines it enters cancer cells mainly through a transporter-mediated routes rather than passive diffusion

as some have proposed [42]. Over the years, many membrane transporters such as copper transporters, solute carrier transporters, and the ABC family of drug efflux transporters have been implicated in the accumulation of OXL in cancer cells or tumor tissues. These transporters have been demonstrated to either control the influx of OXL as uptake transporters, or regulate the efflux of OXL as efflux transporters [34] (see section 1.2.4 on page 26). Since the first report implicating hCTR1 in the transport of platinum drugs in yeast [146], there have been multiple lines of evidence supporting that hCTR1 regulates the cytotoxicity of cisplatin by affecting drug uptake [148]. Reports have been published about the roles of the copper exporters ATP7A and ATP7B in cisplatin resistance by enhancing its efflux [150]. Similarly, it seems that copper transporters may also regulate cellular accumulation and cytotoxicity of other platinum drug such as carboplatin [64].

Herein, it can be speculated that copper transporters may also be implicated in the transport of OXL, as these drugs are structural analogues of cisplatin. Results from early studies have revealed the positive role of CTR1 in OXL uptake in some non-cancerous cellular models such as yeast cells, mouse embryonic cells and HEK293 cells (Page 27-28, section 1.3.1.1). However, direct evidence linking copper transporters and OXL transport in colorectal cancer is still missing.

The first finding in this thesis is the link between hCTR1 expression and OXL uptake in recombinant colorectal cancer cells. Transfection of hCTR1 into colorectal cancer cells resulted in increased sensitivity of cells to copper and OXL (see section 3.3.2 on page 68, and section 3.3.3 on page 70). The study using special fluorescence probe FDCPt1 demonstrated the direct contribution of hCTR1 to the cellular uptake of OXL in these cells (see section 3.3.4 on page 73). These result support previous reports that also describe a positive role of recombinant hCTR1 in OXL uptake in other cell models

[47,49]. The extent to which overexpression of hCTR1 can enhance OXL uptake is variable between different studies. This difference is likely a consequence of different transfection regimens, different plasmid backbones, stable clone selection and cell types in general that likely alter achievable overexpression levels. In addition, the efficiency of hCTR1 to transport OXL may be also different among different forms of recombinant hCTR1. However, it is likely that in addition to hCTR1, other mechanisms and transporters are involved in the uptake of OXL, since mouse hCTR1 knockout fibroblasts still show some OXL accumulation [42].

Although we have proved the hypothesis that hCTR1 mediates the transport of and OXL in colorectal cancer cells, the exact mechanisms by which hCTR1 mobilize OXL into cells have not been fully understood yet. In fact, it is still not clear about the precise mechanisms by which cisplatin is transported across the plasma membrane by hCTR1. Although, it has been suggested that cisplatin, similar to copper, is translocated into cellular compartments through the methionine residues in the putative hCTR1 pore [160], direct evidence at molecular level is still lacking. In addition, some studies show these two anti-cancer platinum analogues differ a lot in the ways they interact with hCTR1 [72]. Given the bulky size of OXL molecule and the bi-dente structure, the pore of hCTR1 trimer is not larger enough to translocate OXL towards cells, even though OXL has a strong tendency to bind with sulfa-containing motifs in the hCTR1 molecule [70].

Lastly, it should be pointed out that the translational value of this study using recombinant cells is limited. While the transfection technique used in our experiments is able to assess the role of hCTR1 *in vitro*, it is clearly associated with some drawbacks such as low transfection efficiency *in vivo*, risk of viral infections to the host, and lack of tumor specificity [224]. Moreover, the high endogenous levels of hCTR1 protein in

DLD-1 cells determine that there is a limitation to how much the hCTR1 gene can be overexpressed in this cell line via transfection. In contrast, hCTR1 is overexpressed by 80 folds in the small cell lung cancer cells which have modest endogenous hCTR1 expression after transfection [64].

7.2 Cu chelators enhance the cytotoxicity of oxaliplatin

Cu chelators have been used widely in the treatment of many human diseases including cancers, copper disorders such as Wilson and Alzheimer's diseases. The anti-cancer effect of Cu chelators as demonstrated in ovarian cancer, breast cancer, liver cancer, leukemia, and prostate cancer is mainly through the inhibition of angiogenesis [228, 229].

Reports about the application of copper chelators in colorectal cancer are rare yet still show promising therapeutic potential. ATTM in combination with irinotecan and florouracil improve the overall response rate after treatment by 25% and the median time to progression by 6 months than irinotecan or florouracil alone [230]. This synergism with these chemotherapies is in part attributable to the inhibitory effect of ATTM on angiogenesis of the tumour. TPEN, another copper chelator, selectively induces cell death in HCT116 colon cancer cells without affecting the viability of non-cancerous colon or intestinal cells. Consistently, TPEN exhibits robust anti-tumour activity in mouse model of colorectal cancer [231].

In addition, copper chelators have the potential to increase the expression of hCTR1 and this property has been utilized to enhance the efficacy of platinum anti-cancer drugs in many chemo-resistant cancers. For example, the literature has reported the potentiation of uptake and cytotoxicity of platinum anticancer drugs in ovarian cancer cells following preincubation with copper chelators, ammonium tetrathiomolybdate

(ATTM), D-penicillamine (D-P), and an experimental Cu-chelating compound called bathocuprione disulfonate (BCS) [73], the enhancement of anti-tumour activity of cisplatin in mouse xenograft model of small cell lung cancer cells, following exposure to D-P [225,226] and the synergistic effect of ATTM on antitumor activity of cisplatin in the HPV16/E2 mouse model of cervical cancer model [225]. Furthermore, trientine was reported to resensitize terminal ovarian cancer patients to carboplatin with clinical responses in 4/5 patients [227].

However, the effect of copper chelators on the expression of hCTR1 and the possibility of using it enhance the uptake of oxaliplatin have not been studied in colorectal cancer cells. Given the role of hCTR1 in OXL uptake and the abundant baseline expression of hCTR1 as demonstrated in both colorectal cancer cells and tissues, we therefore adopted pharmacological approach to target hCTR1 with copper chelators to increase the sensitivity of colon cancer cells to OXL-containing chemotherapies.

In the work presented in this thesis, three different copper chelators were used, that included the experimentally used BCS and the clinically used ATTM, and D-P. BCS does not enter the plasma membrane but it prevents copper entry into cells by forming stabilized extracellular copper complexes. D-P binds to intracellular copper and facilitates its excretion out of cells. ATTM forms a ternary complex with copper ions and proteins, making copper unavailable to cells [225, 226]. Despite the different mechanisms of action, these chemicals consistently up regulated the expression of hCTR1 protein in colorectal cancer cells in a time-dependent way, which implies a common copper-dependent regulatory mechanism to control hCTR1 levels in colorectal cancer cells (see Fig. 4-10 and Fig. 4-11 from page 97 to page 102). Our results in this regard seem to correlate well with the reports showing that these copper chelators can be used to enhance the expression of hCTR1 in ovarian cancer and small

cell lung cancer cells [73]. However, we noticed a difference in the magnitude by which hCTR1 was upregulated by copper chelators. For example, hCTR1expression was increased by around 9-15 folds in ovarian cancer cells (OVACAR3 and SKOV3), which was in contrast to the approximately 40% increase in hCTR1 expression in what cells in our study. Similar to our results, a lower increase of about 50% was observed in ovarian cancer cells (59M and GROV1) [71]. Since the former cell lines have higher baseline levels of hCTR1 than the latter counterparts [71]. This discrepancy could be attributed to the difference in basal expression of endogenous hCTR1. All these results seem to suggest that the strategy of using copper chelators to enhance OXL uptake works better in colorectal cancer cells with lower basal hCTR1 expression.

Despite the observation that both DLD-1 and SW620 cell achieved around 30% increase in hCTR1 expression with copper chelators, subsequent studies showed that pre-incubation of these cells with chelators significantly potentiated cellular sensitivity DLD-1 cells to OXL but not for SW620 cells (see Fig. 4-12 on page 104), suggesting other mechanisms other than hCTR1 may exist to determine the cellular sensitivity to OXL.

Strikingly, these chelators did not alter the expression patterns or density of the Cu efflux transporters ATP7A and ATP7B (see Fig. 4-13 on page 105 and 106, and Fig. 4-14 on page 107), which suggests that the synergistic effect of Cu chelators with OXL is mainly mediated via modulating hCTR1 expression.

Taken together, our finding in conjunction with previous reports suggest that copper chelators may be advantageous via multiple mechanisms that also include hCTR1-mediated transport, as combination treatment with OXL in colorectal cancers.

7.3 The differential expression of Cu transporters in colorectal cancer cells and tissues

Our data provided support to the idea that hCTR1 directly affects cellular sensitivity to OXL. These results warrant a systemic and integrated investigation of hCTR1 expression in human colorectal cancers. In addition, copper or copper-containing enzymes seem to be elevated in colorectal cancer tissues compared to that of the normal tissues [132], [139]. This phenomenon supports the role of copper as micronutrient that is essential to the development and progression of many cancers including colorectal cancers [135]. The diagnostic and prognostic value of copper transporters has been shown in ovarian cancer and small cell lung cancer but has not been systematically studied in native colorectal cancers [62], [232]. In our study, the expression profiles of copper transporters were determined in four colorectal cancer cell lines that were selected to represent the genotypic and phenotypic diversity of colorectal cancer *in vivo*. Moreover, these cell lines derived from human primary tumours provide several advantages, such as sufficient supply of live cells, a high reproducibility of experimental results and low cost. In addition, this allowed us to directly compare the expression of copper transporters *in vitro* with their expression in human colorectal cancer tissues *ex vivo*. Cell based studies provided for the first time the comprehensive information about transporter expression, including the cellular localization, the expression intensity, and the transcriptional levels. The abundant and consistent expression of hCTR1 in all tested cell lines may be one of reasons that can explain the vulnerability of CRC cancer to oxaliplatin treatment (see section 4.3.1.1 on page 84). However, since the observed expression levels represented baseline levels, there is an option to pharmacologically manipulate their expression with copper chelators. The co-

expression of ATP7A and ATP7B with hCTR1 in these cells demonstrated again that these transporters work together to maintain copper homeostasis. The down regulation of hCTR1 in some tumour samples may suggest there is a need to apply copper chelator to target hCTR1 to achieve effect of OXL (see Table 5-3 on page 139). The relative up regulation of the immmuostaining of ATP7B in some of tumour tissues to normal tissues may imply its contribution to growth of cancer cells (see Table 5-3 on page 139).

7.4 The expression of Cu transporters in colon tissues of *Winnie* mice with chronic colitis or colonic dysplasia

Colitis-associated colorectal cancer seems to follow a step-wise transition from normal mucosa to colitis, dysplasia and adenocarcinomas [216]. Copper homeostasis may be altered in the transition from inflammation to adenocarcinomas [151]. The *Winnie* mouse model of colitis and colonic dysplasia offered us a unique opportunity to determine the expression of Cu transporters and their relationship with the precancerous conditions of colonic tissues.

In our study, we firstly observed that copper mCTR1 seems to be up regulated in the inflammation of colon mucosa from *Winnie* mice model of chronic colitis. While we did not observe altered levels of copper efflux transporters during colitis in the colon of *Winnie* mice (see Table 6-1 on page 156), there is still the possibility that their localization may be altered. This finding is in accordance with the previous reports that suggest either copper levels or copper-containing enzymes are increased in human colon tissues with inflammation [121], [126]. Although the causality of this observation is unknown yet, our results suggest that there is a possibility to treat intestinal colitis by pharmacologically targeting the different components responsible for copper homeostasis such as copper transporters, copper or even copper-containing enzymes.

We noticed that copper transporter expression was consistently reduced in colon tissues of DSS-treated Winnie mice with dysplasia (see Table 6-1 on page 156), This finding is contradictory to the reported phenomena that copper or copper-containing enzymes rise in different types of cancers including colorectal cancer. At present it is unclear why copper transporter expression was consistently reduced in the dysplastic colon tissues but suspect is that this could be a non-specific effect of the DSS treatment and unrelated to tumorigenesis.

7.5 Future directions

In the future it will be essential to understanding how hCTR1 interacts with OXL at the molecular level to transport OXL into cancer cells. This project will be challenging and may require coordinated effort of research teams across many disciplines including crystallography, biochemistry, genetics and even analytical chemistry. Perhaps a more practical approach would be to validate our main result in an *in vivo* colorectal cancer model that has been genetically altered to provide a range of defined levels of hCTR1 expression. This tumor model would be also useful to test the translational value of our second finding with regards to the effect of copper chelators on hCTR1 expression *in vivo*.

However, systemic exposure with copper chelators may cause adverse effects in human cancer patients [74], therefore, direct targeting hCTR1 in tumor tissues with tissue-specific transfection technique (*in situ gene* transfection technique) may be a strategy to avoid this drawback (233).

The negative response of these two transporters towards OXL or copper treatment seemed to suggest that they are irrelevant for OXL resistance as previously reported [64]. However, considering the inconclusive roles of ATP7A or ATP7B as

demonstrated in platinum drug resistance (section 1.3.1.2), their contribution to OXL transport need to be explored in colorectal cancer cells with recombinant expression of ATP7A and ATP7B alone or in combination. If, in the future, they are tested to be the efflux transporters of OXL in colorectal cancer cells, perhaps they can be also targeted with pharmacological agents to enhance the effect of OXL.

Alterations of colonic copper transporter expression under condition of colitis suggest that copper homeostasis is disturbed in the process of intestinal inflammation. However, the exact roles of copper or copper enzymes in this process are not well understood and need further research. One possibility would be to perform intervention studies with anti-inflammatory agents or by directly examining the interplays between copper and the pro-inflammation cytokines in the same colitis model. Once confirmed to play active roles in the intestinal inflammation, copper transporters can be targeted to prevent or even treat this disease.

Finally, the unexpected finding that oxaliplatin can up regulate hCTR1 expression deserves further attention as similar observation has been made by other researchers investigating the effect of cisplatin on the expression of hCTR1 in ovarian cancer [70]. Understanding the mechanisms behind may inform about a possible role of hCTR1 in the development of OXL resistance of colon cancer.

7.6 Conclusion

In conclusion, this thesis demonstrated for the first time that the hCTR1 might be one of many factors that influence the pharmacology of OXL, probably through mediating its transport in colorectal cancer cells. The finding that some commonly used Cu chelators are able to enhance the endogenous expression of hCTR1 in CRC cells, and their synergistic use with OXL against some resistant CRC cell lines can be utilized to

improve the anti-tumor activity of OXL-based chemotherapy. The abundant expression of hCTR1 in human colorectal cancer cells and tumor tissues highlighted the importance of copper in the development of colorectal adenocarcinoma, while the altered expression of Cu transporters in the precancerous colonic tissues of *Winnie* mice suggests that Cu homeostasis may be disturbed during the progression of chronic colonic inflammation towards colorectal carcinogenesis.

References

1. World Health Organization. World cancer report 2014. 2014.
2. Australian Institute of Health and Welfare (AIHW). Cancer incidence projections (2011-2020).Cancer Series. Number 66. 2012.
3. Australian Institute of Health and Welfare (AIHW). Health system expenditures on cancer and other neoplasms in Australia, 2000-01.; 2005.
4. Sameer AS. Colorectal cancer: molecular mutations and polymorphisms. Frontiers in Oncology 2013;3:114.
5. Gatalica Z, Torlakovic E. Pathology of the hereditary colorectal carcinoma. Familial Cancer 2008;7(1):15-26.
6. Kajitani T, Yamada S. [TNM classification--cancer of the colon and rectum]. Gan no rinsho. Japan Journal of Cancer Clinics 1967;13(5):336-7.
7. Weiss JM, Pfau PR, O'Connor ES, *et al*. Mortality by stage for right- vs left-sided colon cancer: analysis of surveillance, epidemiology, and end results--Medicare data. Journal of clinical oncology : official journal of the American Society of Clinical Oncology 2011;29(33):4401-9.
8. Diez-Fernandez R, Salinas Hernandez P, Giron-Duch C. A review of chemotherapy for metastatic colon cancer. Farmacia Hospitalaria : organo oficial de expresion cientifica de la Sociedad Espanola de Farmacia Hospitalaria 2006;30(6):359-69.
9. Simpson D, Dunn C, Curran M, *et al*. Oxaliplatin: a review of its use in combination therapy for advanced metastatic colorectal cancer. Drugs 2003;63(19):2127-56.

10. Burz C, Berindan-Neagoe IB, Balacescu O, *et al*. Clinical and pharmacokinetics study of oxaliplatin in colon cancer patients. Journal of Gastrointestinal and Liver Diseases : JGLD 2009;18(1):39-43.

11. Jerremalm E, Wallin I, Ehrsson H. New insights into the biotransformation and pharmacokinetics of oxaliplatin. Journal of Pharmaceutical Sciences 2009;98(11):3879-85.

12. Johnstone TC, Park GY, Lippard SJ. Understanding and improving platinum anticancer drugs--phenanthriplatin. Anticancer Research 2014;34(1):471-6.

13. Luo FR, Wyrick SD, Chaney SG. Cytotoxicity, cellular uptake, and cellular biotransformations of oxaliplatin in human colon carcinoma cells. Oncology Research 1998;10(11-12):595-603.

14. Shackleton GL, and Allen, J,. The in vitro metabolism of [3H]-oxaliplatin in human microsomes.Sanofi Research Report No.MIV0250, 1997.

15. Graham MA, Lockwood GF, Greenslade D, *et al*. Clinical pharmacokinetics of oxaliplatin: a critical review. Clinical Cancer Research : an official journal of the American Association for Cancer Research 2000;6(4):1205-18.

16. Seetharam R, Sood A, Goel S. Oxaliplatin: pre-clinical perspectives on the mechanisms of action, response and resistance. Ecancer Medical Science 2009;3:153.

17. Eastman A. The formation, isolation and characterization of DNA adducts produced by anticancer platinum complexes. Pharmacology and Therapeutics 1987;34(2):155-66.

18. Zwelling LA, Anderson T, Kohn KW. DNA-protein and DNA interstrand cross-linking by cis- and trans-platinum(II) diamminedichloride in L1210 mouse leukemia cells and relation to cytotoxicity. Cancer Research 1979;39(2 Pt 1):365-9.

19. Marchetti P, Galla DA, Russo FP, *et al*. Apoptosis induced by oxaliplatin in human colon cancer HCT15 cell line. Anticancer Research 2004;24(1):219-26.

20. Raymond E, Chaney SG, Taamma A, *et al*. Oxaliplatin: a review of preclinical and clinical studies. Annals of Oncology : official journal of the European Society for Medical Oncology 1998;9(10):1053-71.

21. Becker JP, Weiss J, Theile D. Cisplatin, oxaliplatin, and carboplatin unequally inhibit in vitro mRNA translation. Toxicology Letters 2014;225(1):43-7.

22. Siegel R, Desantis C, Jemal A. Colorectal cancer statistics, 2014. CA Cancer Journal Clinics 2014;64(2):104-17.

23. Longley DB, Johnston PG. Molecular mechanisms of drug resistance. Journal of Pathology 2005;205(2):275-92.

24. Martinez-Balibrea E, Martinez-Cardus A, Gines A, *et al*. Tumor-Related Molecular Mechanisms of Oxaliplatin Resistance. Molecular Cancer Therapeutics 2015;14(8):1767-76.

25. Ekblad L, Kjellstrom J, Johnsson A. Reduced drug accumulation is more important in acquired resistance against oxaliplatin than against cisplatin in isogenic colon cancer cells. Anti-cancer Drugs 2010;21(5):523-31.

26. Rixe O, Ortuzar W, Alvarez M, *et al*. Oxaliplatin, tetraplatin, cisplatin, and carboplatin: spectrum of activity in drug-resistant cell lines and in the cell lines of the National Cancer Institute's Anticancer Drug Screen panel. Biochemical Pharmacology 1996;52(12):1855-65.

27. Mishima M, Samimi G, Kondo A, *et al*. The cellular pharmacology of oxaliplatin resistance. Europeean Journal of Cancer 2002;38(10):1405-12.

28. Hall MD, Okabe M, Shen DW, *et al*. The role of cellular accumulation in determining sensitivity to platinum-based chemotherapy. Annual Review of Pharmacology and Toxicology 2008;48:495-535.

29. Liu JJ, Lu J, McKeage MJ. Membrane transporters as determinants of the pharmacology of platinum anticancer drugs. Curr Cancer Drug Targets 2012;12(8):962-86.

30. Harrach S, Ciarimboli G. Role of transporters in the distribution of platinum-based drugs. Frontiers in Pharmacology 2015;6:85.

31. Zhang S, Lovejoy KS, Shima JE, *et al*. Organic cation transporters are determinants of oxaliplatin cytotoxicity. Cancer Research 2006;66(17):8847-57.

32. Yokoo S, Masuda S, Yonezawa A, *et al*. Significance of organic cation transporter 3 (SLC22A3) expression for the cytotoxic effect of oxaliplatin in colorectal cancer. Drug Metabolism and Disposition: the biological fate of chemicals 2008;36(11):2299-306.

33. Ceckova M, Vackova Z, Radilova H, *et al*. Effect of ABCG2 on cytotoxicity of platinum drugs: interference of EGFP. Toxicology *In Vitro* : an international journal published in association with BIBRA 2008;22(8):1846-52.

34. Hasan NM, Lutsenko S. Regulation of copper transporters in human cells. Current Topics Membranes 2012;69:137-61.

35. Holzer AK, Varki NM, Le QT, *et al*. Expression of the human copper influx transporter 1 in normal and malignant human tissues. J Histochemistry and Cytochemistry 2006;54(9):1041-9.

36. Klomp AE, Tops BB, Van Denberg IE, *et al*. Biochemical characterization and subcellular localization of human copper transporter 1 (hCTR1). The Biochemical Journal 2002;364(Pt 2):497-505.

37. van den Berghe PVE, Klomp LWJ. Posttranslational regulation of copper transporters. Journal of Bio and inorganic Chemstry 2010;15(1):37-46.

38. Puig S, Lee J, Lau M, *et al*. J Biol Chem. The Journal of Biological Chemistry 2002;277(29):26021-30.

39. Nose Y, Rees EM, Thiele DJ. Structure of the Ctr1 copper trans'PORE'ter reveals novel architecture. Trends Biochemistry Science 2006;31(11):604-7.

40. Howell SB, Safaei R, Larson CA, *et al*. Copper transporters and the cellular pharmacology of the platinum-containing cancer drugs. Molecular Pharmacology 2010;77(6):887-94.

41. Lin X, Okuda T, Holzer A, *et al*. The copper transporter CTR1 regulates cisplatin uptake in Saccharomyces cerevisiae. Molecular Pharmacology 2002;62(5):1154-9.

42. Holzer AK, Manorek GH, Howell SB. Contribution of the major copper influx transporter CTR1 to the cellular accumulation of cisplatin, carboplatin, and oxaliplatin. Molecular Pharmacology 2006;70(4):1390-4.

43. Larson CA, Blair BG, Safaei R, *et al*. The role of the mammalian copper transporter 1 in the cellular accumulation of platinum-based drugs. Molecular Pharmacology 2009;75(2):324-30.

44. Liu JJ, Kim Y, Yan F, *et al*. Contributions of rat Ctr1 to the uptake and toxicity of copper and platinum anticancer drugs in dorsal root ganglion neurons. Biochemical Pharmacology 2013;85(2):207-15.

45. Chen CC, Chen LT, Tsou TC, *et al*. Combined modalities of resistance in an oxaliplatin-resistant human gastric cancer cell line with enhanced sensitivity to 5-fluorouracil. British Journal of Cancer 2007;97(3):334-44.

46. Song I-S, Savaraj N, Siddik ZH, *et al*. Role of human copper transporter Ctr1 in the transport of platinum-based antitumor agents in cisplatin-sensitive and cisplatin-resistant cells. Molecular Cancer Therapeutics 2004;3(12):1543-9.

47. Plasencia C, Martinez-Balibrea E, Martinez-Cardus A, *et al*. Expression analysis of genes involved in oxaliplatin response and development of oxaliplatin-resistant HT29 colon cancer cells. International Journal of Oncology 2006;29(1):225-35.

48. Kitada N, Takara K, Minegaki T, *et al*. Factors affecting sensitivity to antitumor platinum derivatives of human colorectal tumor cell lines. Cancer Chemotherapy and Pharmacology 2008;62(4):577-84.

49. Noordhuis P, Laan AC, van de Born K, *et al*. Oxaliplatin activity in selected and unselected human ovarian and colorectal cancer cell lines. Biochemical Pharmacology 2008;76(1):53-61.

50. Ivy KD, Kaplan JH. A re-evaluation of the role of hCTR1, the human high-affinity copper transporter, in platinum-drug entry into human cells. Molecular Pharmacology 2013;83(6):1237-46.

51. Le Roy B, Tixier L, Pereira B, *et al*. Assessment of the Relation between the Expression of Oxaliplatin Transporters in Colorectal Cancer and Response to FOLFOX-4 Adjuvant Chemotherapy: A Case Control Study. PloSone 2016;11(2):e0148739.

52. Lutsenko S, Petris MJ. Function and regulation of the mammalian copper-transporting ATPases: insights from biochemical and cell biological approaches. Journal of Membrane Biology 2003;191(1):1-12.

53. Dierick HA, Ambrosini L, Spencer J, *et al*. Molecular structure of the Menkes disease gene (ATP7A). Genomics 1995;28(3):462-9.

54. Lutsenko S, Barnes NL, Bartee MY, *et al*. Function and regulation of human copper-transporting ATPases. Physiology Review 2007;87(3):1011-46.

55. La Fontaine S, Mercer JF. Trafficking of the copper-ATPases, ATP7A and ATP7B: role in copper homeostasis. Archive of Biochemistry and Biophysics 2007;463(2):149-67.

56. Langner C, Denk H. Wilson disease. Virchows Arch 2004;445(2):111-8.

57. Samimi G, Safaei R, Katano K, *et al*. Increased expression of the copper efflux transporter ATP7A mediates resistance to cisplatin, carboplatin, and oxaliplatin in ovarian cancer cells. Clinical Cancer Research 2004;10(14):4661-9.

58. Kitada N, Takara K, Minegaki T, *et al*. Factors affecting sensitivity to antitumor platinum derivatives of human colorectal tumor cell lines. Cancer Chemotherapy Pharmacology 2008;62(4):577-84.

59. Plasencia C, Martinez-Balibrea E, Martinez-Cardus A, *et al*. Expression analysis of genes involved in oxaliplatin response and development of oxaliplatin-resistant HT29 colon cancer cells. International Journal of Oncology 2006;29(1):225-35.

60. Theile D, Grebhardt S, Haefeli WE, *et al*. Involvement of drug transporters in the synergistic action of FOLFOX combination chemotherapy. Biochemical Pharmacology 2009;78(11):1366-73.

61. Aida T, Takebayashi Y, Shimizu T, *et al*. Expression of copper-transporting P-type adenosine triphosphatase (ATP7B) as a prognostic factor in human endometrial carcinoma. Gynecologic Oncology 2005;97(1):41-5.

62. Martinez-Balibrea E, Martinez-Cardus A, Musulen E, *et al*. Increased levels of copper efflux transporter ATP7B are associated with poor outcome in colorectal cancer patients receiving oxaliplatin-based chemotherapy. International journal of cancer. Journal International Du Cancer 2009;124(12):2905-10.

63. Miyashita H, Nitta Y, Mori S, *et al*. Expression of copper-transporting P-type adenosine triphosphatase (ATP7B) as a chemoresistance marker in human oral squamous cell carcinoma treated with cisplatin. Oral Oncology 2003;39(2):157-62.

64. Song IS, Savaraj N, Siddik ZH, *et al*. Role of human copper transporter Ctr1 in the transport of platinum-based antitumor agents in cisplatin-sensitive and cisplatin-resistant cells. Molecular Cancer therapeutics 2004;3(12):1543-9.

65. Samimi G, Katano K, Holzer AK, *et al*. Modulation of the cellular pharmacology of cisplatin and its analogs by the copper exporters ATP7A and ATP7B. Molecular Pharmacology 2004;66(1):25-32.

66. Samimi G, Safaei R, Katano K, *et al*. Increased expression of the copper efflux transporter ATP7A mediates resistance to cisplatin, carboplatin, and oxaliplatin in ovarian cancer cells. Clinical Cancer Research : an official journal of the American Association for Cancer Research 2004;10(14):4661-9.

67. Samimi G, Safaei R, Katano K, *et al*. Increased expression of the copper efflux transporter ATP7A mediates resistance to cisplatin, carboplatin, and oxaliplatin in ovarian cancer cells. Clin. Cancer Research. 2004;10(14):4661-9.

68. Liang ZD, Long Y, Tsai WB, *et al*. Mechanistic basis for overcoming platinum resistance using copper chelating agents. Molecular Cancer Therapy 2012;11(11):2483-94.

69. Chen HH, Song IS, Hossain A, *et al*. Elevated glutathione levels confer cellular sensitization to cisplatin toxicity by up regulation of copper transporter hCtr1. Molecular Pharmacology 2008;74(3):697-704.

70. Ishida S, McCormick F, Smith-McCune K, *et al*. Enhancing tumor-specific uptake of the anticancer drug cisplatin with a copper chelator. Cancer Cell 2010;17(6):574-83.

71. Liang ZD, Stockton D, Savaraj N, *et al*. Mechanistic comparison of human high-affinity copper transporter 1-mediated transport between copper ion and cisplatin. Molecular Pharmacology 2009;76(4):843-53.

72. Liang ZD, Tsai WB, Lee MY, *et al*. Specificity protein 1 (sp1) oscillation is involved in copper homeostasis maintenance by regulating human high-affinity copper transporter 1 expression. Molecular Pharmacology 2012;81(3):455-64.

73. Fu S, Naing A, Fu C, *et al*. Overcoming platinum resistance through the use of a copper-lowering agent. Molecular Cancer Therapy 2012;11(6):1221-5.

74. Chisholm CL, Wang H, Wong AH, *et al*. Ammonium tetrathiomolybdate treatment targets the copper transporter ATP7A and enhances sensitivity of breast cancer to cisplatin. Oncotarget 2016;7(51):84439-52.

75. Liang ZD, Long Y, Chen HH, *et al*. Regulation of the high-affinity copper transporter (hCtr1) expression by cisplatin and heavy metals. J Biol Inorganic Chemstry 2014;19(1):17-27.

76. Petris MJ, Smith K, Lee J, *et al*. Copper-stimulated endocytosis and degradation of the human copper transporter, hCtr1. The Journal of Biological Chemistry 2003;278(11):9639-46.

77. Molloy SA, Kaplan JH. Copper-dependent recycling of hCTR1, the human high affinity copper transporter. Journal of Biology and Chemistry 2009;284(43):29704-13.

78. Guo Y, Smith K, Lee J, *et al*. Identification of methionine-rich clusters that regulate copper-stimulated endocytosis of the human Ctr1 copper transporter. The Journal of Biological Chemistry 2004;279(17):17428-33.

79. Clifford RJ, Maryon EB, Kaplan JH. Dynamic internalization and recycling of a metal ion transporter: Cu homeostasis and CTR1, the human Cu(+) uptake system. Journal of Cell Science 2016;129(8):1711-21.

80. Gao C, Zhu L, Zhu F, *et al*. Effects of different sources of copper on Ctr1, ATP7A, ATP7B, MT and DMT1 protein and gene expression in Caco-2 cells. Journal

of Trace Elements in Medicine and Biology : organ of the Society for Minerals and Trace Elements 2014;28(3):344-50.

81. Al-Eisawi Z, Beale P, Chan C, *et al*. Carboplatin and oxaliplatin in sequenced combination with bortezomib in ovarian tumour models. Journal of Ovarian Research 2013;6(1):78.

82. Zhang Y, Zhang Q, Fan Z, *et al*. A Chinese herbal Formula, Chang-Wei-Qin, Synergistically Enhances Antitumor Effect of Oxaliplatin. Pathology Oncology Research : POR 2015;21(2):389-97.

83. Li X, Lin Z, Zhang B, *et al*. beta-elemene sensitizes hepatocellular carcinoma cells to oxaliplatin by preventing oxaliplatin-induced degradation of copper transporter 1. Scientific Reports 2016;6:21010.

84. Lutsenko S. Human copper homeostasis: a network of interconnected pathways. Current Opinion on Chemistry Biology 2010;14(2):211-7.

85. Matsui MS, Petris MJ, Niki Y, *et al*. Omeprazole, a gastric proton pump inhibitor, inhibits melanogenesis by blocking ATP7A trafficking. The Journal of Investigative Dermatology 2015;135(3):834-41.

86. Holloway ZG, Velayos-Baeza A, Howell GJ, *et al*. Trafficking of the Menkes copper transporter ATP7A is regulated by clathrin-, AP-2-, AP-1-, and Rab22-dependent steps. Molecular Biology Cell 2013;24(11):1735-48, S1-8.

87. Monty JF, Llanos RM, Mercer JF, *et al*. Copper exposure induces trafficking of the menkes protein in intestinal epithelium of ATP7A transgenic mice. Journal of Nutrition 2005;135(12):2762-6.

88. Barnes N, Bartee MY, Braiterman L, *et al*. Cell-specific trafficking suggests a new role for renal ATP7B in the intracellular copper storage. Traffic 2009;10(6):767-79.

89. Minghetti M, Leaver MJ, Taggart JB, *et al*. Copper induces Cu-ATPase ATP7A mRNA in a fish cell line, SAF1. Comparative Biochemistry and Physiology. Toxicology & Pharmacology : CBP 2011;154(2):93-9.

90. Xie L, Collins JF. Transcriptional regulation of the Menkes copper ATPase (Atp7a) gene by hypoxia-inducible factor in intestinal epithelial cells. American journal of physiology. Cell Physiology 2011;300(6):C1298-305.

91. Kalayda GV, Wagner CH, Buss I, *et al*. Altered localisation of the copper efflux transporters ATP7A and ATP7B associated with cisplatin resistance in human ovarian carcinoma cells. BMC Cancer 2008;8:175.

92. Katano K, Safaei R, Samimi G, *et al*. Confocal microscopic analysis of the interaction between cisplatin and the copper transporter ATP7B in human ovarian carcinoma cells. Clinical Cancer Research 2004;10(13):4578-88.
93. Nagaya H, Satoh H. [Possible mechanisms for (H+ + K+)-ATPase inhibition by proton pump inhibitors, omeprazole, lansoprazole and SCH 28080]. Nihon rinsho. Japanese Journal of Clinical Medicine 1992;50(1):26-32.
94. Mary Matsui DY, inventor. Small molecule inhibitors of p-type atpases. USA. 2013.
95. Lowndes SA, Harris AL. The role of copper in tumour angiogenesis. Journal of Mammary Gland Biology and Neoplasia 2005;10(4):299-310.
96. Nasulewicz A, Mazur A, Opolski A. Role of copper in tumour angiogenesis--clinical implications. Journal of Trace Elements in Medicine and Biology : organ of the Society for Minerals and Trace Elements 2004;18(1):1-8.
97. Ishida S, Andreux P, Poitry-Yamate C, *et al*. Bioavailable copper modulates oxidative phosphorylation and growth of tumors. Proceedings of the National Academy of Sciences of the United States of America 2013;110(48):19507-12.
98. De Wit M, Jimenez CR, Carvalho B, *et al*. Cell surface proteomics identifies glucose transporter type 1 and prion protein as candidate biomarkers for colorectal adenoma-to-carcinoma progression. Gut 2012;61(6):855-64.
99. Barresi V, Trovato-Salinaro A, Spampinato G, *et al*. Transcriptome analysis of copper homeostasis genes reveals coordinated upregulation of SLC31A1,SCO1, and COX11 in colorectal cancer. FEBS open biology 2016;6(8):794-806.
100. Holzer AK, Varki NM, Le QT, *et al*. Expression of the human copper influx transporter 1 in normal and malignant human tissues. Journal of Histochemistry and Cytochemistry 2006;54(9):1041-9.
101. Zhang Y, Sun XW, Xu JH, *et al*. [Effects of medicated serum prepared with Chinese herbal medicine Changweiqing on pharmacokinetics of oxaliplatin in colon cancer cells]. Zhong Xi Yi Jie He Xue Bao 2012;10(8):901-10.
102. Owatari S, Akune S, Komatsu M, *et al*. Copper-transporting P-type ATPase, ATP7A, confers multidrug resistance and its expression is related to resistance to SN-38 in clinical colon cancer. Cancer Research 2007;67(10):4860-8.
103. Samimi G, Varki NM, Wilczynski S, *et al*. Increase in expression of the copper transporter ATP7A during platinum drug-based treatment is associated with poor survival in ovarian cancer patients. Clinical Cancer Research 2003;9(16 Pt 1):5853-9.

104. Li ZH, Qiu MZ, Zeng ZL, *et al*. Copper-transporting P-type adenosine triphosphatase (ATP7A) is associated with platinum-resistance in non-small cell lung cancer (NSCLC). Journal of Translational Medicine 2012;10:21.

105. Martinez-Balibrea E, Martinez-Cardus A, Musulen E, *et al*. Increased levels of copper efflux transporter ATP7B are associated with poor outcome in colorectal cancer patients receiving oxaliplatin-based chemotherapy. International Journal of Cancer 2009;124(12):2905-10.

106. Nakayama K, Kanzaki A, Ogawa K, *et al*. Copper-transporting P-type adenosine triphosphatase (ATP7B) as a cisplatin based chemoresistance marker in ovarian carcinoma: comparative analysis with expression of MDR1, MRP1, MRP2, LRP and BCRP. International Journal of Cancer 2002;101(5):488-95.

107. Wu DL, Yi HX, Sui FY, *et al*. Expression of ATP7B in human gastric cardiac carcinomas in comparison with distal gastric carcinomas. World Journal of Gastroenterology 2006;12(47):7695-8.

108. Kanzaki A, Toi M, Neamati N, *et al*. Copper-transporting P-type adenosine triphosphatase (ATP7B) is expressed in human breast carcinoma. Japanese Journal of Cancer Research : Gann 2002;93(1):70-7.

109. Sugeno H, Takebayashi Y, Higashimoto M, *et al*. Expression of copper-transporting P-type adenosine triphosphatase (ATP7B) in human hepatocellular carcinoma. Anticancer Research 2004;24(2C):1045-8.

110. Jackman RJ, Mayo CW. The adenoma-carcinoma sequence in cancer of the colon. Surgery, Gynecology & Obstetrics 1951;93(3):327-30.

111. Bazensky I, Shoobridge-Moran C, Yoder LH. Colorectal cancer: an overview of the epidemiology, risk factors, symptoms, and screening guidelines. Medsurg nursing : official journal of the Academy of Medical-Surgical Nurses 2007;16(1):46-51; quiz 2.

112. Riddell RH, Goldman H, Ransohoff DF, *et al*. Dysplasia in inflammatory bowel disease: standardized classification with provisional clinical applications. Human Pathology 1983;14(11):931-68.

113. Lu H, Ouyang W, Huang C. Inflammation, a key event in cancer development. Molecular Cancer Research : MCR 2006;4(4):221-33.

114. Fox JG, Wang TC. Inflammation, atrophy, and gastric cancer. The Journal of Clinical Investigation 2007;117(1):60-9.

115. Weber A, Boege Y, Reisinger F, *et al*. Chronic liver inflammation and hepatocellular carcinoma: persistence matters. Swiss Medical Weekly 2011;141:w13197.

116. Whitehouse MW, Walker WR. Copper and inflammation. Agents and Actions 1978;8(1-2):85-90.

117. Uriu-Adams JY, Keen CL. Copper, oxidative stress, and human health. Molecular Aspects of Medicine 2005;26(4-5):268-98.

118. Ringstad J, Kildebo S, Thomassen Y. Serum selenium, copper, and zinc concentrations in Crohn's disease and ulcerative colitis. Scandinavian Journal of Gastroenterology 1993;28(7):605-8.

119. M.Shokrzadeh TT, P.Haghighi-Hasanalideh, M.H. Shahidi. The relationship between copper and zinc levels in the serum and urine and the risk of ulcerative colitis. Mazandaran University of Medical Sciences 2013;23(106):77-84.

120. Ojuawo A, Keith L. The serum concentrations of zinc, copper and selenium in children with inflammatory bowel disease. The Central African Journal of Medicine 2002;48(9-10):116-9.

121. Fox JG, Wang TC. Inflammation, atrophy, and gastric cancer. The Journal of Clinical Investigation 2007;117(1):60-9.

122. Nielsen OH, Ahnfelt-Ronne I. Involvement of oxygen-derived free radicals in the pathogenesis of chronic inflammatory bowel disease. Klinische Wochenschrift 1991;69(21-23):995-1000.

123. Onoda M, Yoshimura K, Aoki H*, et al*. Lysyl oxidase resolves inflammation by reducing monocyte chemoattractant protein-1 in abdominal aortic aneurysm. Atherosclerosis 2010;208(2):366-9.

124. Rivera E, Flores I, Appleyard CB. Molecular profiling of a rat model of colitis: validation of known inflammatory genes and identification of novel disease-associated targets. Inflammatory Bowel Diseases 2006;12(10):950-66.

125. O'Sullivan J, Unzeta M, Healy J*, et al*. Semicarbazide-sensitive amine oxidases: enzymes with quite a lot to do. Neurotoxicology 2004;25(1-2):303-15.

Salter-Cid LM, Wang E, O'Rourke AM, *et al*. Anti-inflammatory effects of inhibiting the amine oxidase activity of semicarbazide-sensitive amine oxidase. The Journal of Pharmacology and Experimental Therapeutics 2005;315(2):553-62.

126. Kruidenier L, Kuiper I, van Duijn W, *et al*. Differential mucosal expression of three superoxide dismutase isoforms in inflammatory bowel disease. The Journal of pathology 2003;201(1):7-16.
127. Lutsenko S. Human copper homeostasis: a network of interconnected pathways. Current Opinion in Chemical Biology 2010;14(2):211-7.
128. Margalioth EJ, Schenker JG, Chevion M. Copper and zinc levels in normal and malignant tissues. Cancer 1983;52(5):868-72.
129. Klimczak M, Dziki A, Kilanowicz A, *et al*. Concentrations of cadmium and selected essential elements in malignant large intestine tissue. Przeglad Gastroenterologiczny 2016;11(1):24-9.
130. Gupta SK, Shukla VK, Vaidya MP, *et al*. Serum and tissue trace elements in colorectal cancer. Journal of Surgical Oncology 1993;52(3):172-5.
131. Rizk SL, Sky-Peck HH. Comparison between concentrations of trace elements in normal and neoplastic human breast tissue. Cancer Research 1984;44(11):5390-4.
132. Edyta Reszka WW, Jolanta Gromadzinska, Wieslaw Szymczak,. Evaluation of selenium, zinc and copper levels related to GST genetic polymorphism in lung cancer patients. Trace Elements in Medicine 2005;22(1):23-32.
133. Denoyer D, Masaldan S, La Fontaine S, *et al*. Targeting copper in cancer therapy: 'Copper That Cancer'. Metallomics : Integrated Biometal Science 2015;7(11):1459-76.
134. Theophanides T, Anastassopoulou J. Copper and carcinogenesis. Critical Reviews in Oncology/Hematology 2002;42(1):57-64.
135. Ward RJ, Scarino ML, Leone A, *et al*. Copper and iron homeostasis in mammalian cells and cell lines. Biochemical Society Transactions 1998;26(2):S191.
136. Cox TR, Erler JT. Lysyl oxidase in colorectal cancer. American journal of physiology. Gastrointestinal and Liver Physiology 2013;305(10):G659-66.
137. Govatati S, Malempati S, Saradamma B, *et al*. Manganese-superoxide dismutase (Mn-SOD) overexpression is a common event in colorectal cancers with mitochondrial microsatellite instability. Tumour Biology : the journal of the International Society for Oncodevelopmental Biology and Medicine 2016;37(8):10357-64.
138. Oberley TD, Sempf JM, Oberley MJ, *et al*. Immunogold analysis of antioxidant enzymes in human renal cell carcinoma. Virchows Archive : an international journal of pathology 1994;424(2):155-64.

139. Izutani R, Katoh M, Asano S, *et al*. Enhanced expression of manganese superoxide dismutase mRNA and increased TNFalpha mRNA expression by gastric mucosa in gastric cancer. World Journal of Surgery 1996;20(2):228-33.

140. Hart PC, Mao M, de Abreu AL, *et al*. MnSOD upregulation sustains the Warburg effect via mitochondrial ROS and AMPK-dependent signalling in cancer. Nature Communications 2015;6:6053.

141. Herrmann PC, Gillespie JW, Charboneau L, *et al*. Mitochondrial proteome: altered cytochrome c oxidase subunit levels in prostate cancer. Proteomics 2003;3(9):1801-10.

142. Zhang K, Chen Y, Huang X, *et al*. Expression and clinical significance of cytochrome c oxidase subunit IV in colorectal cancer patients. Archives of Medical Science : AMS 2016;12(1):68-77.

143. Ussakli CH, Ebaee A, Binkley J, *et al*. Mitochondria and tumor progression in ulcerative colitis. Journal of the National Cancer Institute 2013;105(16):1239-48.

144. Payne CM, Holubec H, Bernstein C, *et al*. Crypt-restricted loss and decreased protein expression of cytochrome C oxidase subunit I as potential hypothesis-driven biomarkers of colon cancer risk. Cancer epidemiology, biomarkers & prevention : a publication of the American Association for Cancer Research, cosponsored by the American Society of Preventive Oncology 2005;14(9):2066-75.

145. Goyal N, Rana A, Ahlawat A, *et al*. Animal models of inflammatory bowel disease: a review. Inflammopharmacology 2014;22(4):219-33.

146. Heazlewood CK, Cook MC, Eri R, *et al*. Aberrant mucin assembly in mice causes endoplasmic reticulum stress and spontaneous inflammation resembling ulcerative colitis. PLoS Medicine 2008;5(3):e54.

147. Van der Sluis M, De Koning BA, De Bruijn AC, *et al*. Muc2-deficient mice spontaneously develop colitis, indicating that MUC2 is critical for colonic protection. Gastroenterology 2006;131(1):117-29.

147. Randall-Demllo S, Fernando R, Brain T, *et al*. Characterisation of colonic dysplasia-like epithelial atypia in murine colitis. World Journal of Gastroenterology 2016;22(37):8334-48.

148. Origene. pCMV6-Entry, mammalian vector with C-terminal Myc- DDK Tag, 10ug; Available from: http://www.origene.com/destination_vector/PS100001.aspx.

149. Ip V, Liu JJ, Mercer JF, *et al*. Differential expression of ATP7A, ATP7B and CTR1 in adult rat dorsal root ganglion tissue. Molecular Pain 2010;6:53.

150. Robinson AM, Rahman AA, Carbone SE, *et al*. Alterations of colonic function in the Winnie mouse model of spontaneous chronic colitis. American journal of physiology. Gastrointestinal and Liver Physiology 2017;312(1):G85-G102.

151. Varghese F, Bukhari AB, Malhotra R, *et al*. IHC Profiler: an open source plugin for the quantitative evaluation and automated scoring of immunohistochemistry images of human tissue samples. PloS one 2014;9(5):e96801.

152. https://http://www.atcc.org/Products/All/CCL-221.aspx. DLD-1 (ATCC® CCL-221™).

153. Ahmed D, Eide PW, Eilertsen IA, *et al*. Epigenetic and genetic features of 24 colon cancer cell lines. Oncogenesis 2013;2:e71.

154. Pendyala L, Creaven PJ. In vitro cytotoxicity, protein binding, red blood cell partitioning, and biotransformation of oxaliplatin. Cancer Research 1993;53(24):5970-6.

155. Zhu G, Myint M, Ang WH, *et al*. Monofunctional platinum-DNA adducts are strong inhibitors of transcription and substrates for nucleotide excision repair in live mammalian cells. Cancer Research 2012;72(3):790-800.

156. Shen C, Harris BD, Dawson LJ, *et al*. Fluorescent sensing of monofunctional platinum species. Chemical Communications 2015;51(29):6312-4.

157. Riss TL, Moravec RA, Niles AL, *et al*. Cell Viability Assays. In: Sittampalam GS, Coussens NP, Brimacombe K, Grossman A, Arkin M, Auld D, et al, editors. Assay Guidance Manual. Bethesda (MD); 2004.

158. Franken NA, Rodermond HM, Stap J, *et al*. Clonogenic assay of cells in vitro. Nature Protocols 2006;1(5):2315-9.

159. Ip V, McKeage MJ, Thompson P, *et al*. Platinum-specific detection and quantification of oxaliplatin and Pt(R,R-diaminocyclohexane)Cl_2 in the blood plasma of colorectal cancer patients. Journal of Spectrometry. 2008;23:881-4.

160. Holzer AK, Samimi G, Katano K, *et al*. The copper influx transporter human copper transport protein 1 regulates the uptake of cisplatin in human ovarian carcinoma cells. Molecular Pharmacology 2004;66(4):817-23.

161. Song IS, Savaraj N, Siddik ZH, *et al*. Role of human copper transporter Ctr1 in the transport of platinum-based antitumor agents in cisplatin-sensitive and cisplatin-resistant cells. Molecular Cancer Therapy. 2004;3(12):1543-9.

162. More SS, Akil O, Ianculescu AG, *et al*. Role of the copper transporter, CTR1, in platinum-induced ototoxicity. The Journal of Neuroscience : the official journal of the Society for Neuroscience 2010;30(28):9500-9.
163. Larson CA, Blair BG, Safaei R, *et al*. The role of the mammalian copper transporter 1 in the cellular accumulation of platinum-based drugs. Molecular Pharmacology. 2009;75(2):324-30.
164. Holzer AK, Manorek GH, Howell SB. Contribution of the major copper influx transporter CTR1 to the cellular accumulation of cisplatin, carboplatin, and oxaliplatin. Molecular Pharmacology. 2006;70(4):1390-4.
165. Liu JJ, Kim Y, Yan F, *et al*. Contributions of rat Ctr1 to the uptake and toxicity of copper and platinum anticancer drugs in dorsal root ganglion neurons. Biochem. Pharmacology. 2013;85(2):207-15.
166. Haigang C, AJZ, Mark J. M, Louise M, N, Dominic Geraghty, Nuri G, Johnson J L. Copper transporter 1 in human colorectal cancer cell lines: Effects of endogenous and modified expression on oxaliplatin cytotoxicity. Journal of Inorganic Chemistry 2017.
167. Sinani D, Adle DJ, Kim H, *et al*. Distinct mechanisms for Ctr1-mediated copper and cisplatin transport. Journal of Biology and Chemistry. 2007;282(37):26775-85.
168. Du X, Wang X, Li H, *et al*. Comparison between copper and cisplatin transport mediated by human copper transporter 1 (hCTR1). Metallomics 2012;4(7):679-85.
169. Martelli L, Di Mario F, Botti P, *et al*. Accumulation, platinum-DNA adduct formation and cytotoxicity of cisplatin, oxaliplatin and satraplatin in sensitive and resistant human osteosarcoma cell lines, characterized by p53 wild-type status. Biochemical Pharmacology 2007;74(1):20-7.
170. Song IS, Chen HH, Aiba I, *et al*. Transcription factor Sp1 plays an important role in the regulation of copper homeostasis in mammalian cells. Molecular Pharmacology 2008;74(3):705-13.
171. Chen TR, Dorotinsky CS, McGuire LJ, *et al*. DLD-1 and HCT-15 cell lines derived separately from colorectal carcinomas have totally different chromosome changes but the same genetic origin. Cancer Genetics and Cytogenetics 1995;81(2):103-8.

172. Semple TU, Quinn LA, Woods LK, *et al*. Tumor and lymphoid cell lines from a patient with carcinoma of the colon for a cytotoxicity model. Cancer Research 1978;38(5):1345-55.

173. Kaplan JH, Lutsenko S. Copper transport in mammalian cells: special care for a metal with special needs. The Journal of Biological Chemistry 2009;284(38):25461-5.

174. Holloway ZG, Velayos-Baeza A, Howell GJ, *et al*. Trafficking of the Menkes copper transporter ATP7A is regulated by clathrin-, AP-2-, AP-1-, and Rab22-dependent steps. Molecular Biology of the Cell 2013;24(11):1735-48, S1-8.

175. Mangala LS, Zuzel V, Schmandt R, *et al*. Therapeutic Targeting of ATP7B in Ovarian Carcinoma. Clinical Cancer Research : an official journal of the American Association for Cancer Research 2009;15(11):3770-80.

176. Delangle P, Mintz E. Chelation therapy in Wilson's disease: from D-penicillamine to the design of selective bioinspired intracellular Cu(I) chelators. Dalton Translational. 2012;41(21):6359-70.

177. Fu S, Naing A, Fu C, *et al*. Overcoming platinum resistance through the use of a copper-lowering agent. Molecular Cancer Therapy. 2012;11(6):1221-5.

178. Ravia JJ, Stephen RM, Ghishan FK, *et al*. Menkes Copper ATPase (Atp7a) is a novel metal-responsive gene in rat duodenum, and immunoreactive protein is present on brush-border and basolateral membrane domains. Journal of Biology and Chemistry. 2005;280(43):36221-7.

179. Hernandez S, Tsuchiya Y, Garcia-Ruiz JP, *et al*. ATP7B copper-regulated traffic and association with the tight junctions: copper excretion into the bile. Gastroenterology 2008;134(4):1215-23.

180. Holloway ZG, Velayos-Baeza A, Howell GJ, *et al*. Trafficking of the Menkes copper transporter ATP7A is regulated by clathrin-, AP-2-, AP-1-, and Rab22-dependent steps. Molecular Biology. Cell 2013;24(11):1735-48, S1-8.

181. Monty JF, Llanos RM, Mercer JF, *et al*. Copper exposure induces trafficking of the menkes protein in intestinal epithelium of ATP7A transgenic mice. Journal of Nutrition. 2005;135(12):2762-6.

182. Leonhardt K, Gebhardt R, Mossner J, *et al*. Functional interactions of Cu-ATPase ATP7B with cisplatin and the role of ATP7B in the resistance of cells to the drug. J. Biology and Chemistry. 2009;284(12):7793-802.

183. Mangala LS, Zuzel V, Schmandt R, *et al*. Therapeutic targeting of ATP7B in ovarian carcinoma. Clinical Cancer Research. 2009;15(11):3770-80.

184. Ishida S, Lee J, Thiele DJ, *et al*. Uptake of the anticancer drug cisplatin mediated by the copper transporter Ctr1 in yeast and mammals. Proceedings of the National Academy of Sciences of the United States of America 2002;99(22):14298-302.

185. Holzer AK, Howell SB. The internalization and degradation of human copper transporter 1 following cisplatin exposure. Cancer Research 2006;66(22):10944-52.

186. Jandial DD, Farshchi-Heydari S, Larson CA, *et al*. Enhanced delivery of cisplatin to intraperitoneal ovarian carcinomas mediated by the effects of bortezomib on the human copper transporter 1. Clinical Cancer Research : an official journal of the American Association for Cancer Research 2009;15(2):553-60.

187. Polishchuk EV, Concilli M, Iacobacci S, *et al*. Wilson disease protein ATP7B utilizes lysosomal exocytosis to maintain copper homeostasis. Developmental Cell 2014;29(6):686-700.

188. Liang ZD, Long Y, Chen HH, *et al*. Regulation of the high-affinity copper transporter (hCtr1) expression by cisplatin and heavy metals. Journal of Biological Inorganic Chemistry : JBIC : a publication of the Society of Biological Inorganic Chemistry 2014;19(1):17-27.

189. Su AI, Wiltshire T, Batalov S, *et al*. A gene atlas of the mouse and human protein-encoding transcriptomes. Proceedings of National Academy of Science U. S. A. 2004;101(16):6062-7.

190. Wu C, Jin X, Tsueng G, *et al*. BioGPS: building your own mash-up of gene annotations and expression profiles. Nucleic Acids Research. 2016;44(D1):D313-6.

191. Ip V, Liu JJ, Mercer JF, *et al*. Differential expression of ATP7A, ATP7B and CTR1 in adult rat dorsal root ganglion tissue. Mollecular Pain 2010;6:53.

192. Kalayda GV, Wagner CH, Jaehde U. Relevance of copper transporter 1 for cisplatin resistance in human ovarian carcinoma cells. Journal of Inorganic Biochemistry. 2012;116:1-10.

193. Klomp AE, Tops BB, Van Denberg IE, *et al*. Biochemical characterization and subcellular localization of human copper transporter 1 (hCTR1). Biochemistry Journal. 2002;364(Pt 2):497-505.

194. Gupta SK, Shukla VK, Vaidya MP, *et al*. Serum and tissue trace elements in colorectal cancer. Journal of Surgical Oncology 1993;52(3):172-5.

195. Skrzycki M, Majewska M, Podsiad M, *et al*. Expression and activity of superoxide dismutase isoenzymes in colorectal cancer. Acta Biochemimistry of Polland 2009;56(4):663-70.

196. Ellis LM, Takahashi Y, Liu W, *et al*. Vascular endothelial growth factor in human colon cancer: Biology and Therapeutic Implications. Oncologist 2000;5 Suppl 1:11-5.

197. Galzie Z, Fernig DG, Smith JA, *et al*. Invasion of human colorectal carcinoma cells is promoted by endogenous basic fibroblast growth factor. International Journal of Cancer 1997;71(3):390-5.

198. Ning Y, Manegold PC, Hong YK, *et al*. Interleukin-8 is associated with proliferation, migration, angiogenesis and chemosensitivity in vitro and in vivo in colon cancer cell line models. International Journal of Cancer 2011;128(9):2038-49.

199. Prohaska JR. Role of copper transporters in copper homeostasis. American Journal of Clinical Nutrition. 2008;88(3):826S-9S.

200. Kitada N, Takara K, Minegaki T, *et al*. Factors affecting sensitivity to antitumor platinum derivatives of human colorectal tumor cell lines. Cancer Chemotherapy and Pharmacology. 2008;62(4):577-84.

201. Samimi G, Varki NM, Wilczynski S, *et al*. Increase in expression of the copper transporter ATP7A during platinum drug-based treatment is associated with poor survival in ovarian cancer patients. Clinical Cancer Research. 2003;9(16 Pt 1):5853-9.

202. Plasencia C, Martinez-Balibrea E, Martinez-Cardus A, *et al*. Expression analysis of genes involved in oxaliplatin response and development of oxaliplatin-resistant HT29 colon cancer cells. International Journal of Oncology. 2006;29(1):225-35.

203. Owatari S, Akune S, Komatsu M, *et al*. Copper-transporting P-type ATPase, ATP7A, confers multidrug resistance and its expression is related to resistance to SN-38 in clinical colon cancer. Cancer Research 2007;67(10):4860-8.

204. Lutsenko S, Barnes NL, Bartee MY, *et al*. Function and regulation of human copper-transporting ATPases. Physiology Review. 2007;87(3):1011-46.

205. Yamaguchi Y, Heiny ME, Suzuki M, *et al*. Biochemical characterization and intracellular localization of the Menkes disease protein. Proceeding of National Academy of Science. U. S. A. 1996;93(24):14030-5.

206. Petris MJ, Mercer JF. The Menkes protein (ATP7A; MNK) cycles via the plasma membrane both in basal and elevated extracellular copper using a C-terminal di-leucine endocytic signal. Human Molecular Genetics. 1999;8(11):2107-15.

207. Zhou B, Gitschier J. hCTR1: a human gene for copper uptake identified by complementation in yeast. Proceedings of the National Academy of Sciences of the United States of America 1997;94(14):7481-6.

208. Mackenzie NC, Brito M, Reyes AE, *et al*. Cloning, expression pattern and essentiality of the high-affinity copper transporter 1 (ctr1) gene in zebrafish. Gene 2004;328:113-20.

209. Turner JC, Shanks V, Osborn PJ, *et al*. Copper absorption in sheep. Comparative biochemistry and physiology. C, Comparative Pharmacology and Toxicology 1987;86(1):147-50.

210. Kuo YM, Gitschier J, Packman S. Developmental expression of the mouse mottled and toxic milk genes suggests distinct functions for the Menkes and Wilson disease copper transporters. Human Molecular Genetics 1997;6(7):1043-9.

211. Ohbu M, Ogawa K, Konno S, *et al*. Copper-transporting P-type adenosine triphosphatase (ATP7B) is expressed in human gastric carcinoma. Cancer Letters 2003;189(1):33-8.

212. Sugeno H, Takebayashi Y, Higashimoto M, *et al*. Anticancer Research. Anticancer Res 2004;24(2C):1045-8.

213. Mangala LS, Zuzel V, Schmandt R, *et al*. Therapeutic Targeting of ATP7B in Ovarian Carcinoma. Clinical Cancer Research 2009;15(11):3770-80.

214. La Fontaine S, Ackland ML, Mercer JF. Mammalian copper-transporting P-type ATPases, ATP7A and ATP7B: emerging roles. International Journal of Biochemistry and Cell Biology 2010;42(2):206-9.

215. Harpaz N, Polydorides AD. Colorectal dysplasia in chronic inflammatory bowel disease: pathology, clinical implications, and pathogenesis. Archives of Pathology & Laboratory Medicine 2010;134(6):876-95.

216. Rosenberg DW, Giardina C, Tanaka T. Mouse models for the study of colon carcinogenesis. Carcinogenesis 2009;30(2):183-96.

217. Treanor D, Quirke P. Pathology of colorectal cancer. Clinical Oncology 2007;19(10):769-76.

218. Gomathy Narayanan I, Saravanan R, Bharathselvi M, *et al*. Localization of Human Copper Transporter 1 in the Eye and its Role in Eales Disease. Ocular Immunology and Inflammation 2016;24(6):678-83.
219. Han M, Lin Z, Zhang Y. The alteration of copper homeostasis in inflammation induced by lipopolysaccharides. Biological Trace Element Research 2013;154(2):268-74.
220. Viennois E, Chen F, Laroui H, *et al*. Dextran sodium sulfate inhibits the activities of both polymerase and reverse transcriptase: lithium chloride purification, a rapid and efficient technique to purify RNA. BMC Research Notes 2013;6:360.
221. Zheng Z, White C, Lee J, *et al*. Altered microglial copper homeostasis in a mouse model of Alzheimer's disease. Journal of Neurochemistry 2010;114(6):1630-8.
222. Spreckelmeyer S, Orvig C, Casini A. Cellular transport mechanisms of cytotoxic metallodrugs: an overview beyond cisplatin. Molecules 2014;19(10):15584-610.
223. Sinani D, Adle DJ, Kim H, *et al*. Distinct mechanisms for Ctr1-mediated copper and cisplatin transport. The Journal of Biological Chemistry 2007;282(37):26775-85.
224. Misra S. Human gene therapy: a brief overview of the genetic revolution. The Journal of the Association of Physicians of India 2013;61(2):127-33.
225. Ding X, Xie H, Kang YJ. The significance of copper chelators in clinical and experimental application. The Journal of Nutritional Biochemistry 2011;22(4):301-10.
226. Tegoni M, Valensin D, Toso L, *et al*. Copper chelators: chemical properties and bio-medical applications. Current Medicinal Chemistry 2014;21(33):3785-818.
227. Brewer GJ, Dick RD, Grover DK, *et al*. Treatment of metastatic cancer with tetrathiomolybdate, an anticopper, antiangiogenic agent: Phase I study. Clinical Cancer Research : an official journal of the American Association for Cancer Research 2000;6(1):1-10.
228. Kim ES, Tang X, Peterson DR, *et al*. Copper transporter CTR1 expression and tissue platinum concentration in non-small cell lung cancer. Lung Cancer 2014;85(1):88-93.
229. Samimi G, Varki NM, Wilczynski S, *et al*. Increase in expression of the copper transporter ATP7A during platinum drug-based treatment is associated with poor survival in ovarian cancer patients. Clinical Cancer Research : an official journal of the American Association for Cancer Research 2003;9(16 Pt 1):5853-9.

230. Gartner EM, Griffith KA, Pan Q*, et al*. A pilot trial of the anti-angiogenic copper lowering agent tetrathiomolybdate in combination with irinotecan, 5-flurouracil, and leucovorin for metastatic colorectal cancer. Investigational New Drugs 2009;27(2):159-65.

231. Fatfat M, Merhi RA, Rahal O*, et al*. Copper chelation selectively kills colon cancer cells through redox cycling and generation of reactive oxygen species. BMC Cancer 2014;14:527.

232. Inoue Y, Matsumoto H, Yamada S*, et al*. ATP7B expression is associated with in vitro sensitivity to cisplatin in non-small cell lung cancer. Oncology Letters 2010;1(2):279-82.

233. Edward J, Felipe N, David L *, et al*. In situ gene transfection and neuronal programming on electroconductive nanocomposite to reduce inflammatory response. Journal of Materials Chemistry 2011;21(4):1109-1114.

Supplementary Figures

Figure S-1:

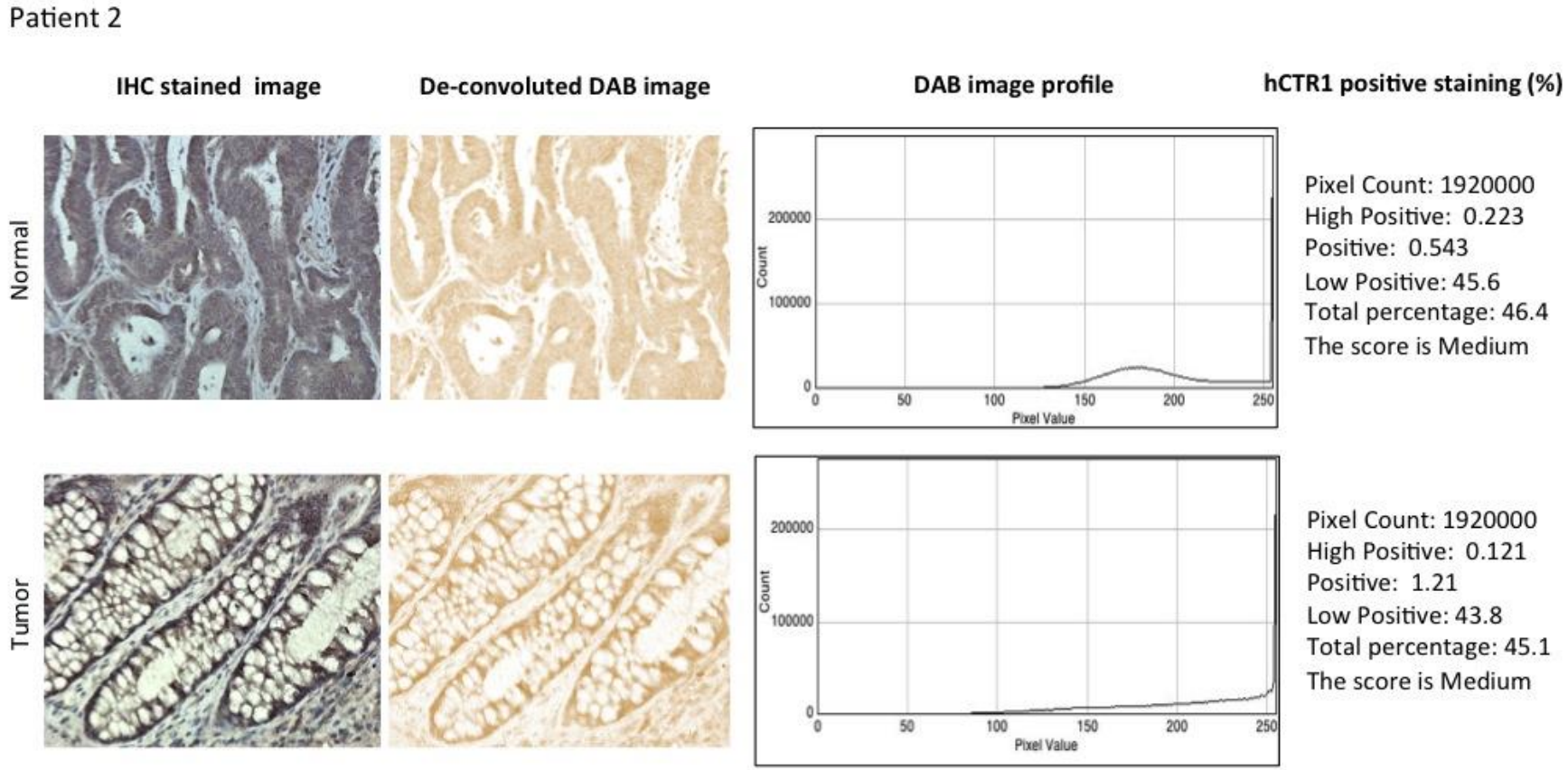

Patient 3

	IHC stained image	De-convoluted DAB image	DAB image profile	hCTR1 positive staining (%)
Tumor	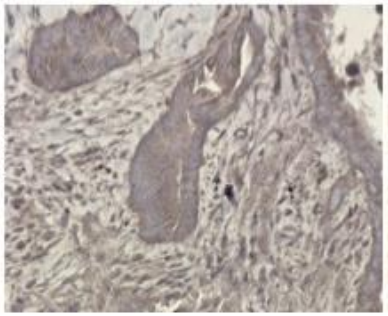	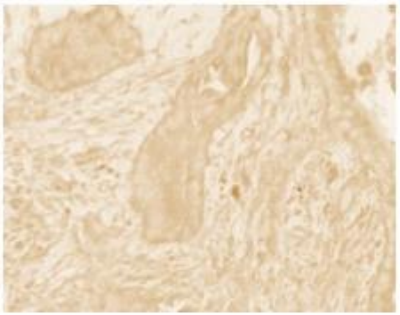	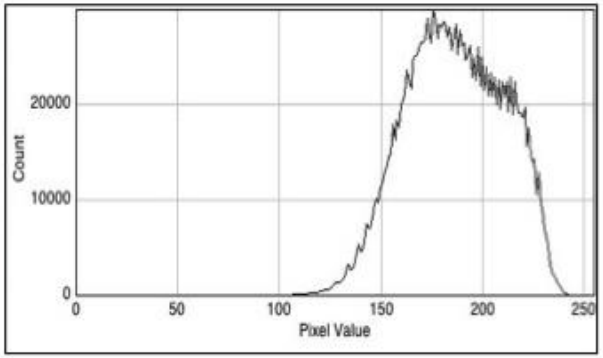	Pixel Count: 1920000 High Positive: 0.179 Positive: 0.255 Low Positive: 41.8 Total percentage: 42.2 The score is Medium
Normal	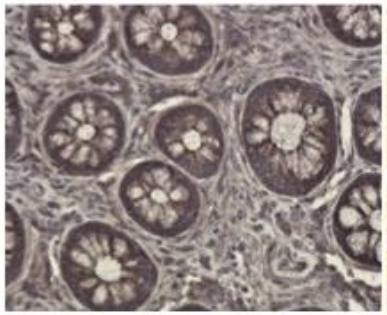	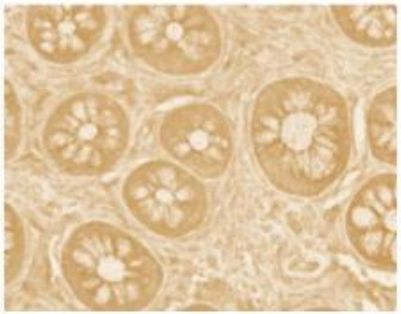	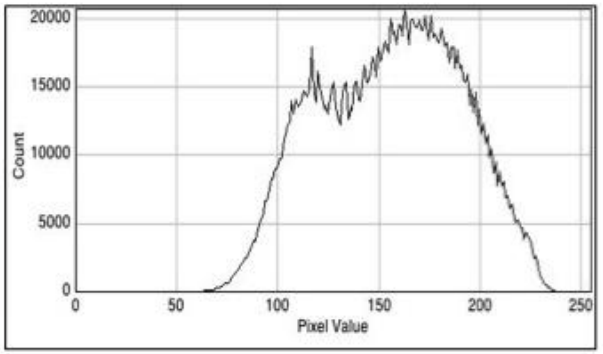	Pixel Count: 1920000 High Positive: 0.681 Positive: 1.25 Low Positive: 70.7 Total percentage: 72.7 The score is High

Patient 4

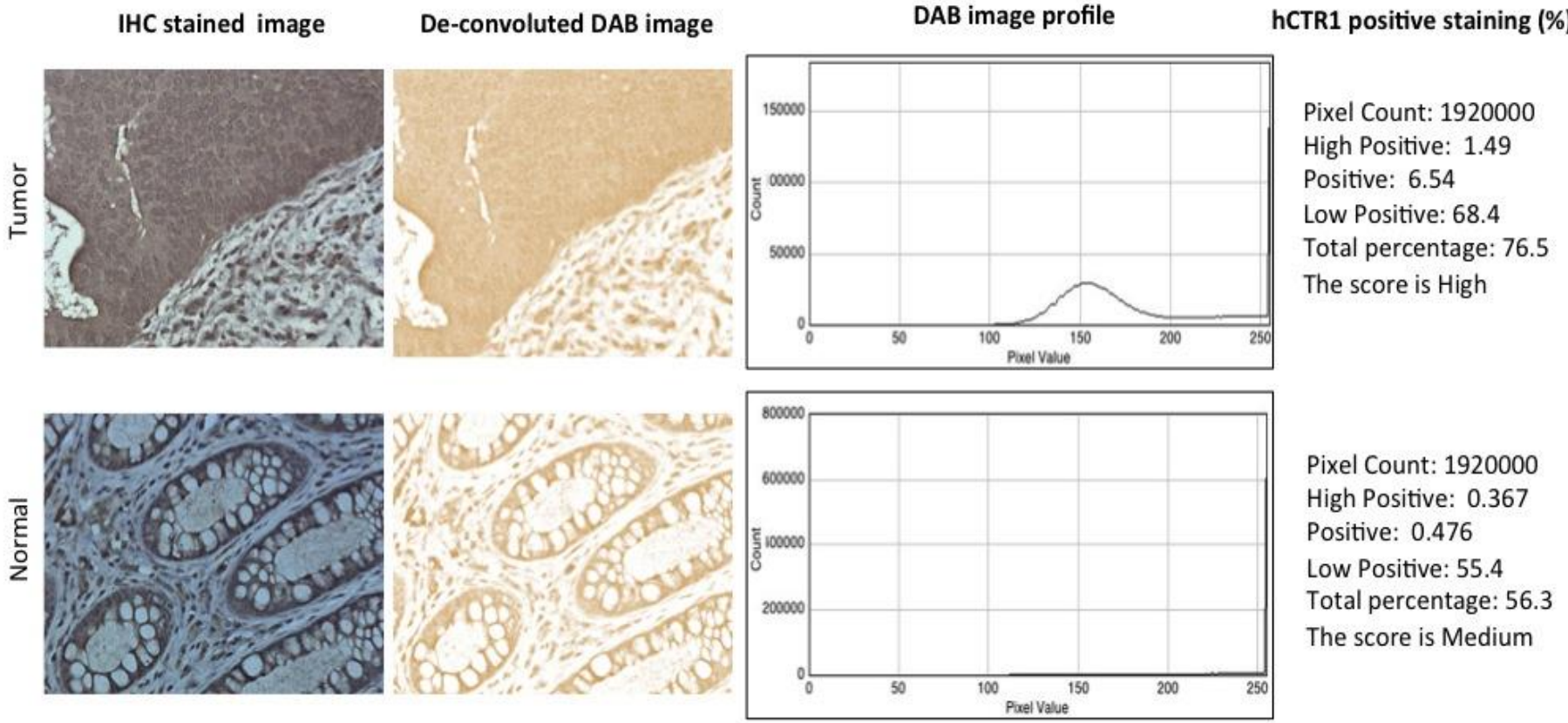
IHC stained image
De-convoluted DAB image
DAB image profile
hCTR1 positive staining (%)
Tumor
Normal
Count
Pixel Value
150000
00000
50000
0
800000
600000
100000
200000
0
50
100
150
200
250
Pixel Count: 1920000
High Positive: 1.49
Positive: 6.54
Low Positive: 68.4
Total percentage: 76.5
The score is High
Pixel Count: 1920000
High Positive: 0.367
Positive: 0.476
Low Positive: 55.4
Total percentage: 56.3
The score is Medium

Patient 5

	IHC stained image	De-convoluted DAB image	DAB image profile	hCTR1 positive staining (%)
Tumor	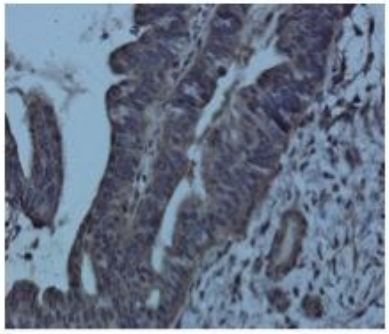	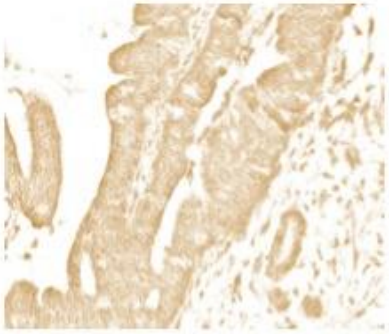	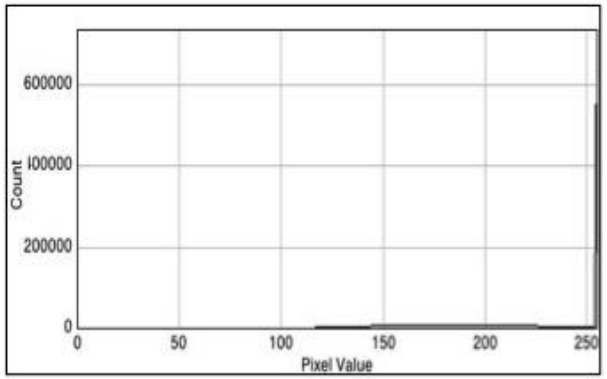	Pixel Count: 1920000 High Positive: 0.421 Positive: 2.12 Low Positive: 52.1 Total percentage: 54.6 The score is Medium
Normal	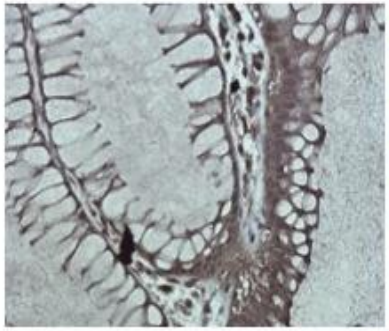	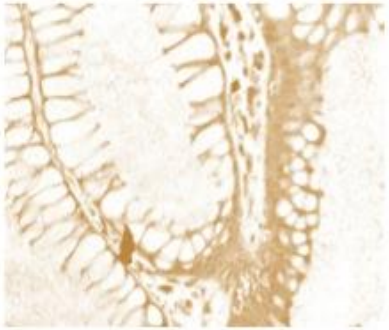	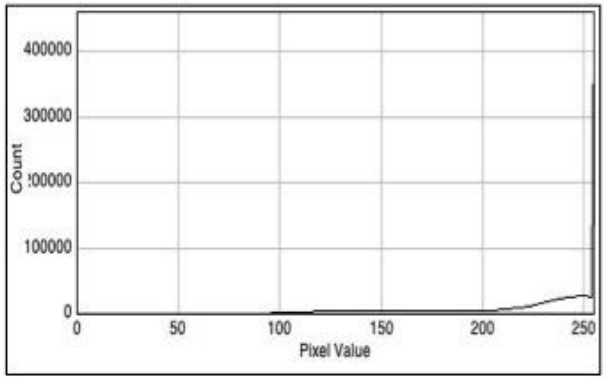	Pixel Count: 1920000 High Positive: 0.06 Positive: 1.21 Low Positive: 45.1 Total percentage: 46.4 The score is medium

Patient 6

IHC stained image | **De-convoluted DAB image** | **DAB image profile** | **hCTR1 positive staining (%)**

Tumor

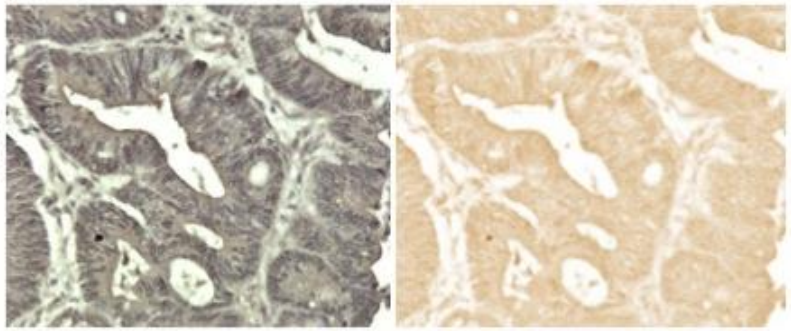

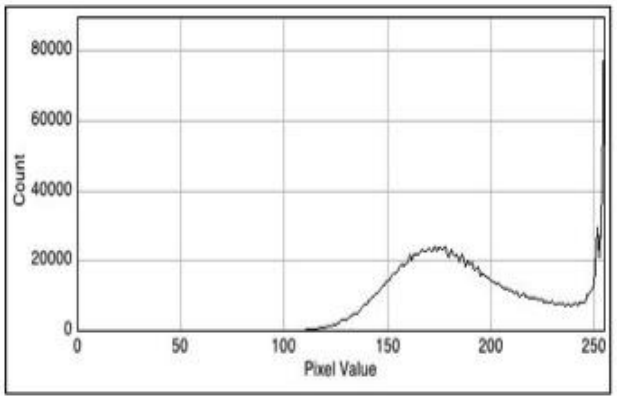

Pixel Count: 1920000
High Positive: 0.513
Positive: 1.45
Low Positive: 51.2
Total percentage: 53.2
The score is Medium

Normal

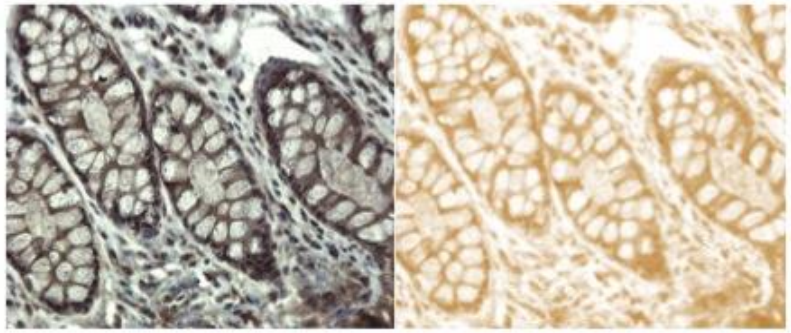

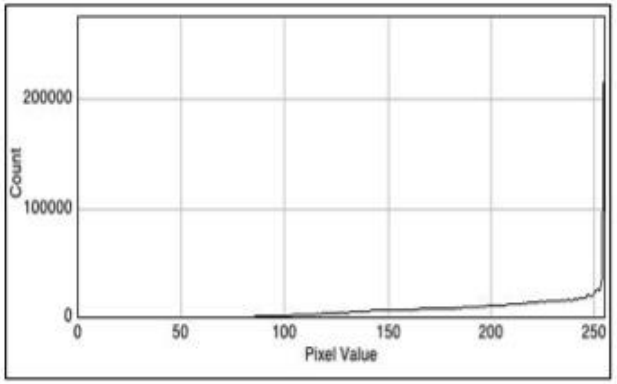

Pixel Count: 1920000
High Positive: 0.192
Positive: 2.02
Low Positive: 50.7
Total percentage: 53
The score is Medium

Figure S-1. Semi-quantitative analysis of representative DAB stained immunohistochemical images of hCTR1 in tumor and the matched normal tissues of four colorectal cancer patients

Standard immunohistochemistry was performed on paraffin-embedded tumor and normal tissues using a rabbit anti-hCTR1 primary antibody and a goat anti-rabbit secondary antibody, stained with DAB and hematoxylin. The DAB-stained IHC images were then deconvoluted and digitally scored of hCTR1 to illustrate the negative, medium and high positive staining intensity defined by the percentage of pixel counts. Mag. 40x.

Figure S-2:

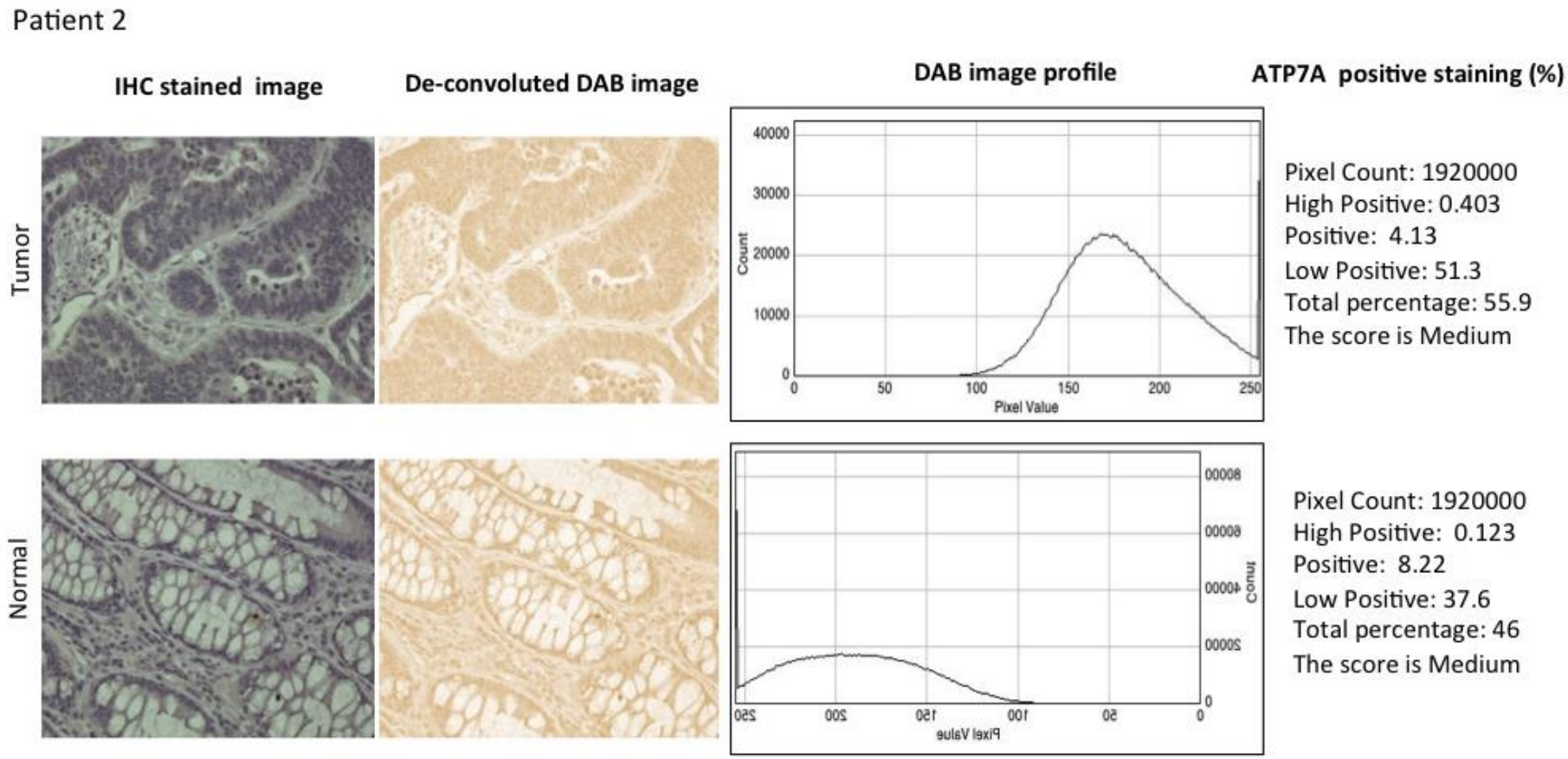
Patient 2
IHC stained image
De-convoluted DAB image
DAB image profile
ATP7A positive staining (%)
Tumor
Normal
Count
Pixel Value
Pixel Count: 1920000
High Positive: 0.403
Positive: 4.13
Low Positive: 51.3
Total percentage: 55.9
The score is Medium
Pixel Count: 1920000
High Positive: 0.123
Positive: 8.22
Low Positive: 37.6
Total percentage: 46
The score is Medium

Patient 3

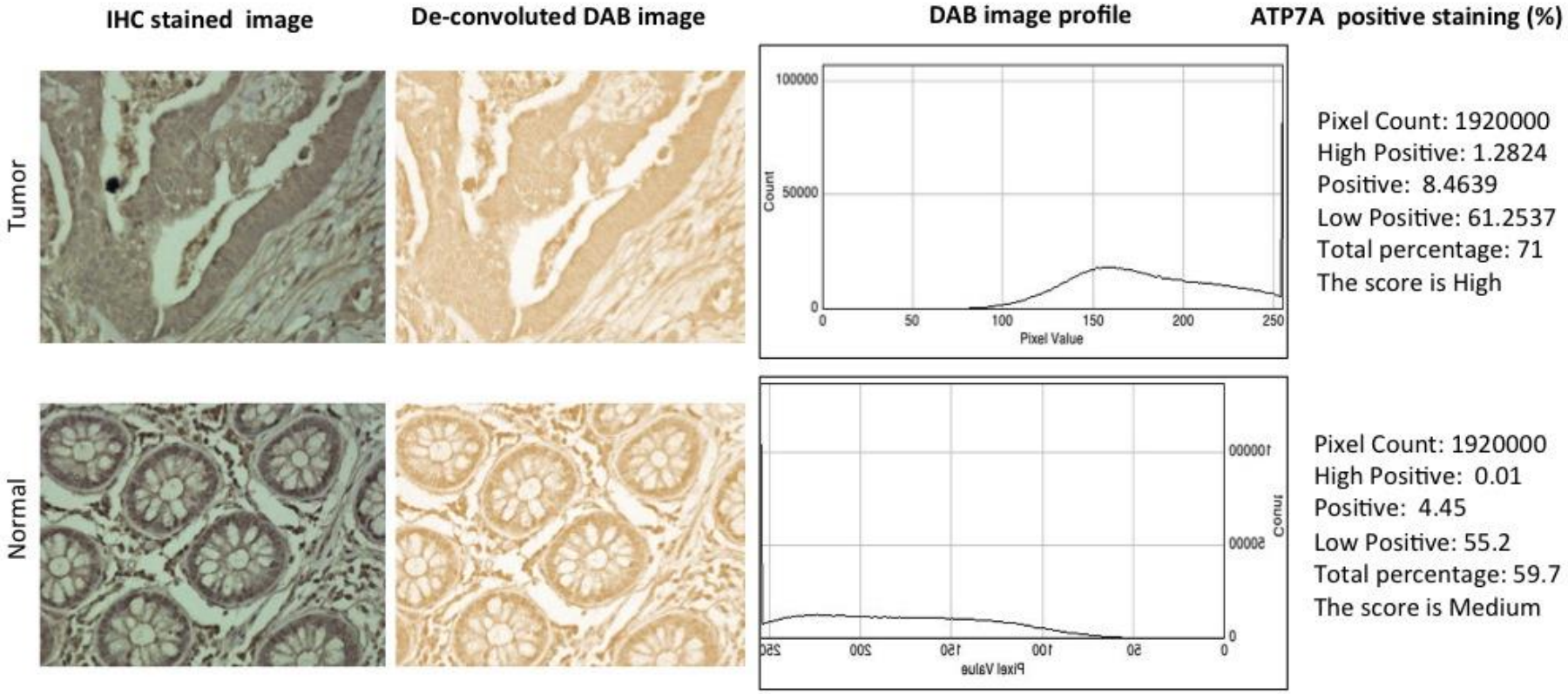
IHC stained image
De-convoluted DAB image
DAB image profile
ATP7A positive staining (%)
Tumor
Normal
100000
50000
0
Count
0
50
100
150
200
250
Pixel Value
Pixel Count: 1920000
High Positive: 1.2824
Positive: 8.4639
Low Positive: 61.2537
Total percentage: 71
The score is High
Pixel Count: 1920000
High Positive: 0.01
Positive: 4.45
Low Positive: 55.2
Total percentage: 59.7
The score is Medium

Patient 4

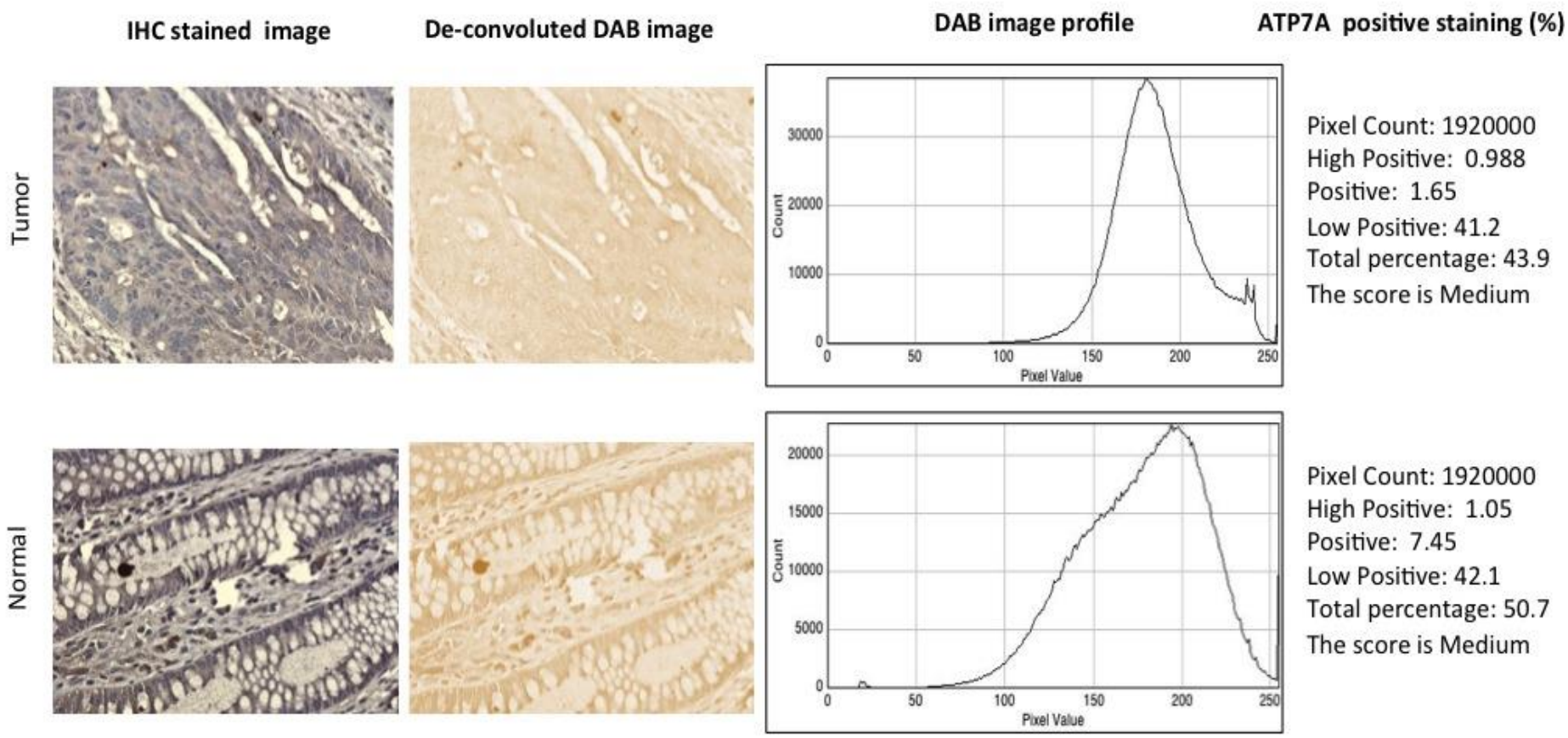
IHC stained image
De-convoluted DAB image
DAB image profile
ATP7A positive staining (%)
Tumor
Normal
Count
Pixel Value
0
50
100
150
200
250
10000
20000
30000
5000
15000
Pixel Count: 1920000
High Positive: 0.988
Positive: 1.65
Low Positive: 41.2
Total percentage: 43.9
The score is Medium
Pixel Count: 1920000
High Positive: 1.05
Positive: 7.45
Low Positive: 42.1
Total percentage: 50.7
The score is Medium

Patient 5

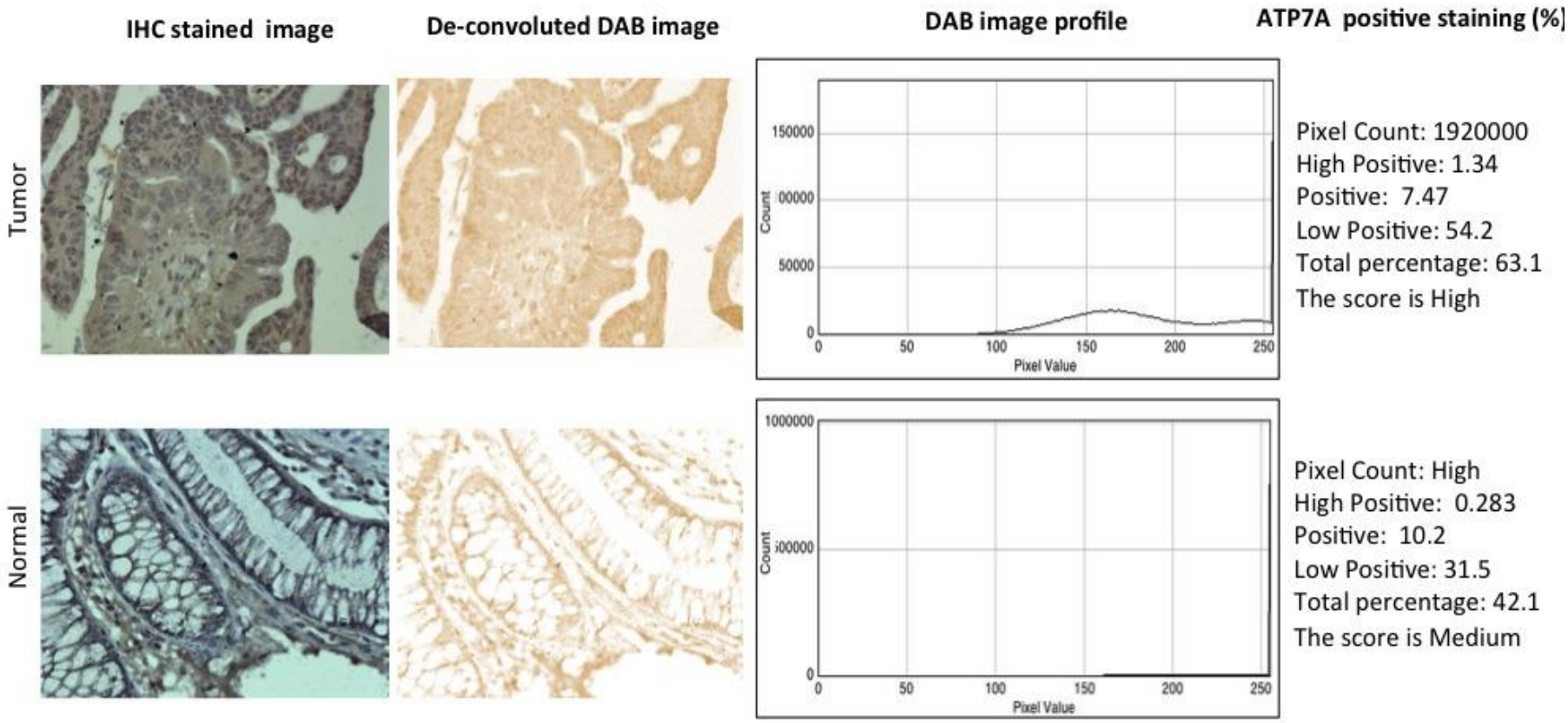
IHC stained image
De-convoluted DAB image
DAB image profile
ATP7A positive staining (%)
Tumor
Normal
Count
Pixel Value
0
50
100
150
200
250
150000
50000
1000000
Pixel Count: 1920000
High Positive: 1.34
Positive: 7.47
Low Positive: 54.2
Total percentage: 63.1
The score is High
Pixel Count: High
High Positive: 0.283
Positive: 10.2
Low Positive: 31.5
Total percentage: 42.1
The score is Medium

Patient 6

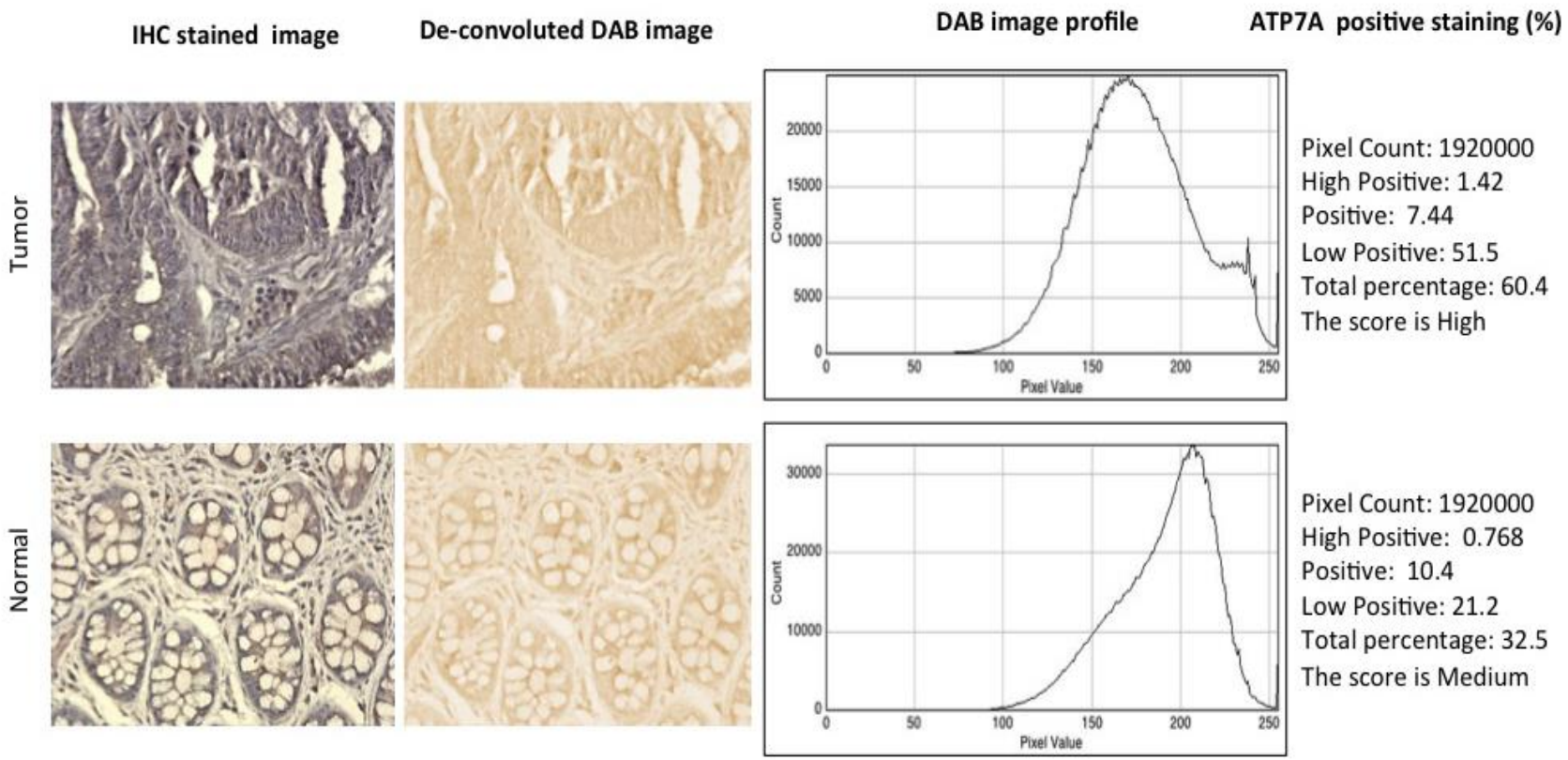
IHC stained image
De-convoluted DAB image
DAB image profile
ATP7A positive staining (%)
Tumor
Normal
Count
Pixel Value
0
5000
10000
15000
20000
30000
50
100
150
200
250
Pixel Count: 1920000
High Positive: 1.42
Positive: 7.44
Low Positive: 51.5
Total percentage: 60.4
The score is High
Pixel Count: 1920000
High Positive: 0.768
Positive: 10.4
Low Positive: 21.2
Total percentage: 32.5
The score is Medium

Figure S-2. Semi-quantitative analysis of representative DAB stained immunohistochemical images of ATP7A in tumor and the matched normal tissues of four colorectal cancer patients

Standard immunohistochemistry was performed on paraffin-embedded tumor and normal tissues using a rabbit anti-ATP7A primary antibody and a goat anti-rabbit secondary antibody, stained with DAB and hematoxylin. The DAB-stained IHC images were then deconvoluted and digitally scored of ATP7A to illustrate the negative, medium and high positive staining intensity defined by the percentage of pixel counts. Mag. 40x.

Figure S-3:

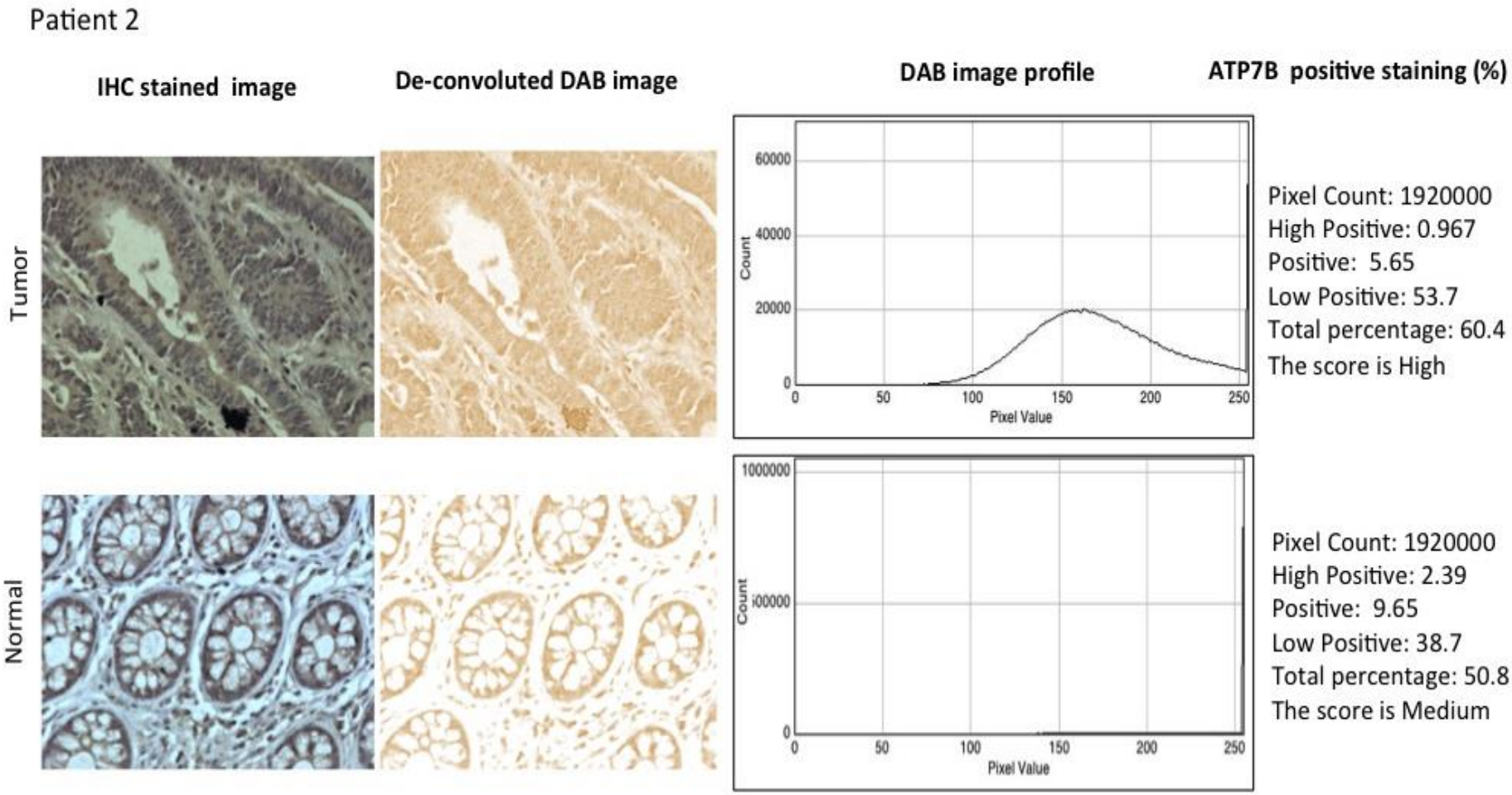
Patient 2
IHC stained image
De-convoluted DAB image
DAB image profile
ATP7B positive staining (%)
Tumor
Normal
Count
Pixel Value
60000
40000
20000
0
50
100
150
200
250
1000000
Pixel Count: 1920000
High Positive: 0.967
Positive: 5.65
Low Positive: 53.7
Total percentage: 60.4
The score is High
Pixel Count: 1920000
High Positive: 2.39
Positive: 9.65
Low Positive: 38.7
Total percentage: 50.8
The score is Medium

Patient 3

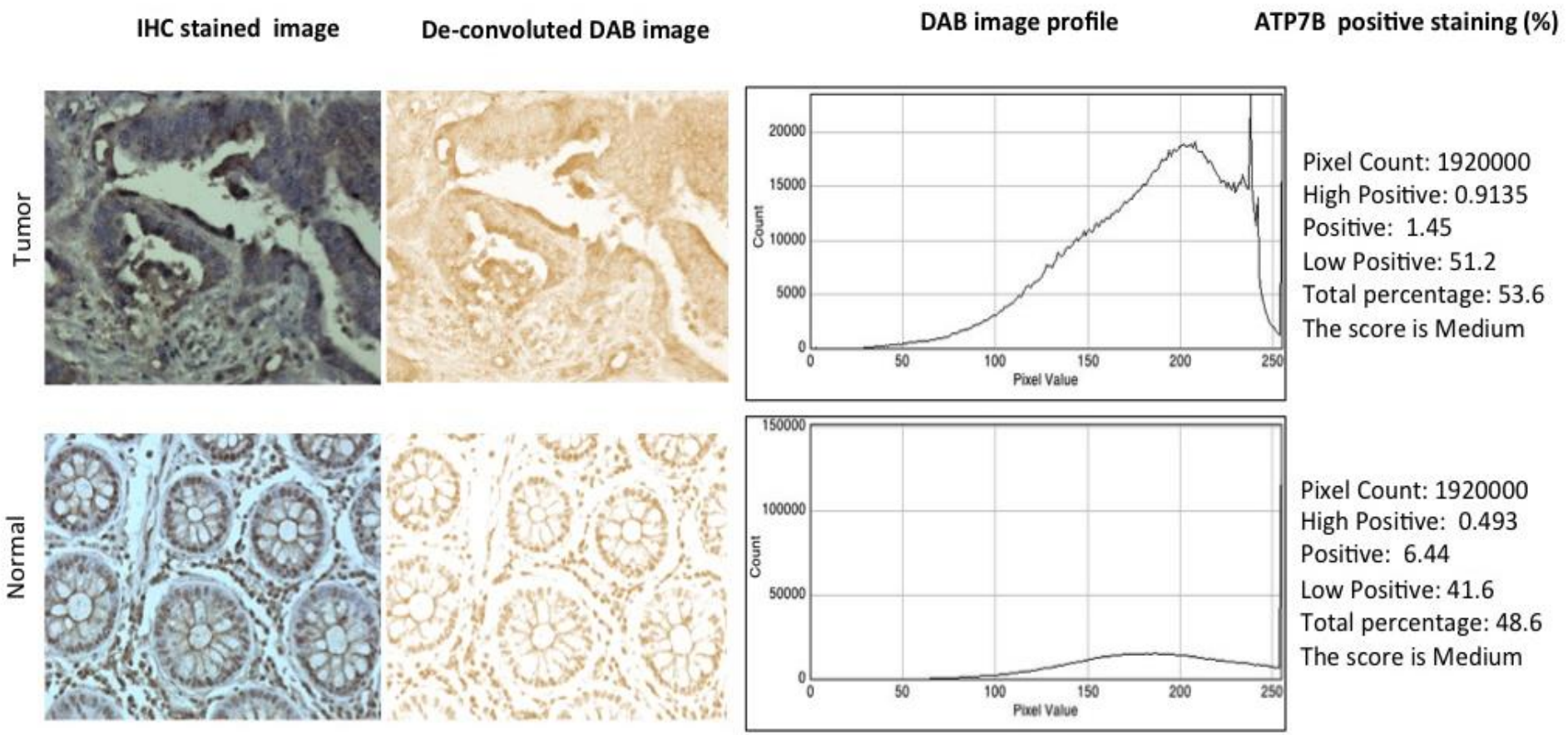
IHC stained image
De-convoluted DAB image
DAB image profile
ATP7B positive staining (%)
Tumor
Normal
Count
Pixel Value
20000
15000
10000
5000
0
50
100
150
200
250
150000
100000
50000
Pixel Count: 1920000
High Positive: 0.9135
Positive: 1.45
Low Positive: 51.2
Total percentage: 53.6
The score is Medium
Pixel Count: 1920000
High Positive: 0.493
Positive: 6.44
Low Positive: 41.6
Total percentage: 48.6
The score is Medium

Patient 4

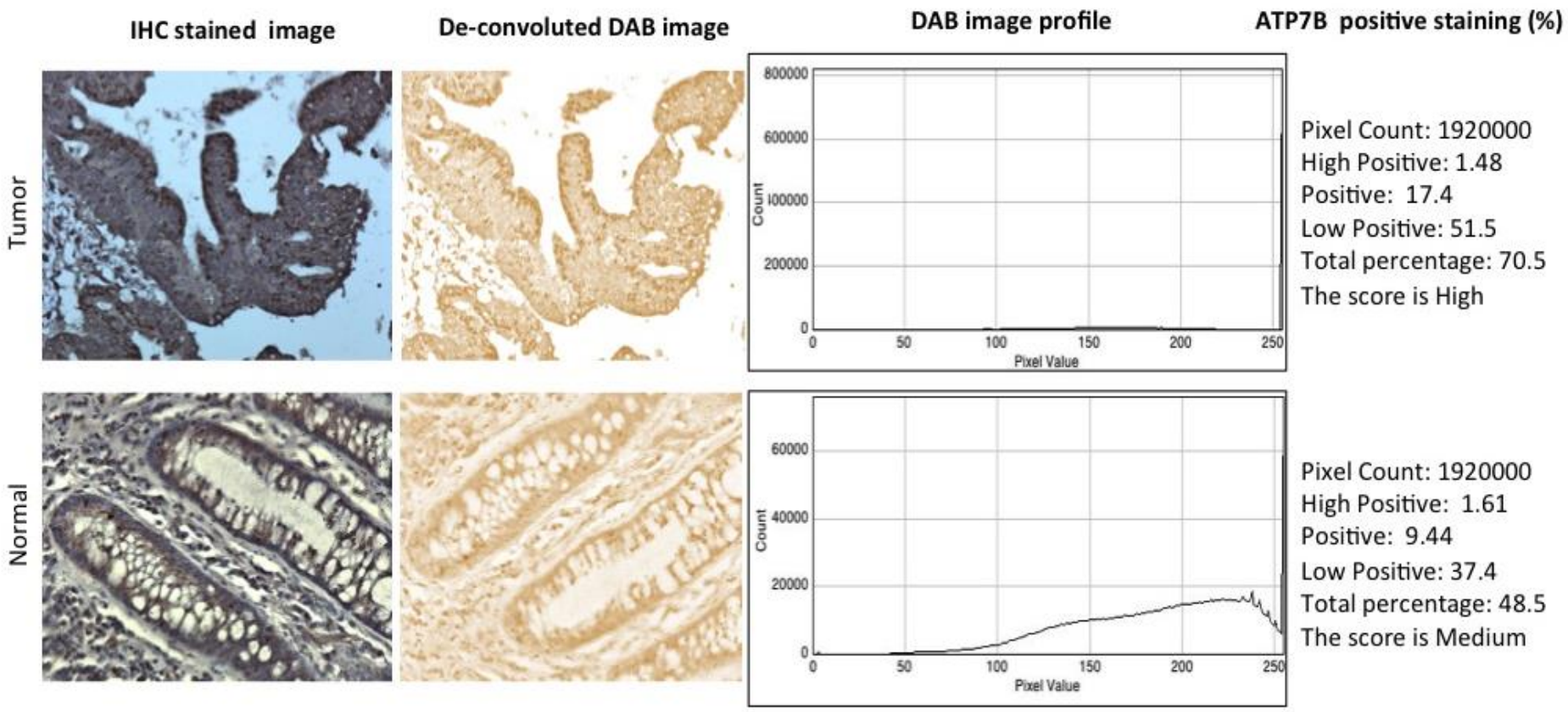
IHC stained image
De-convoluted DAB image
DAB image profile
ATP7B positive staining (%)
Tumor
Normal
800000
600000
400000
200000
0
Count
0
50
100
150
200
250
Pixel Value
Pixel Count: 1920000
High Positive: 1.48
Positive: 17.4
Low Positive: 51.5
Total percentage: 70.5
The score is High
60000
40000
20000
0
Count
0
50
100
150
200
250
Pixel Value
Pixel Count: 1920000
High Positive: 1.61
Positive: 9.44
Low Positive: 37.4
Total percentage: 48.5
The score is Medium

Patient 5

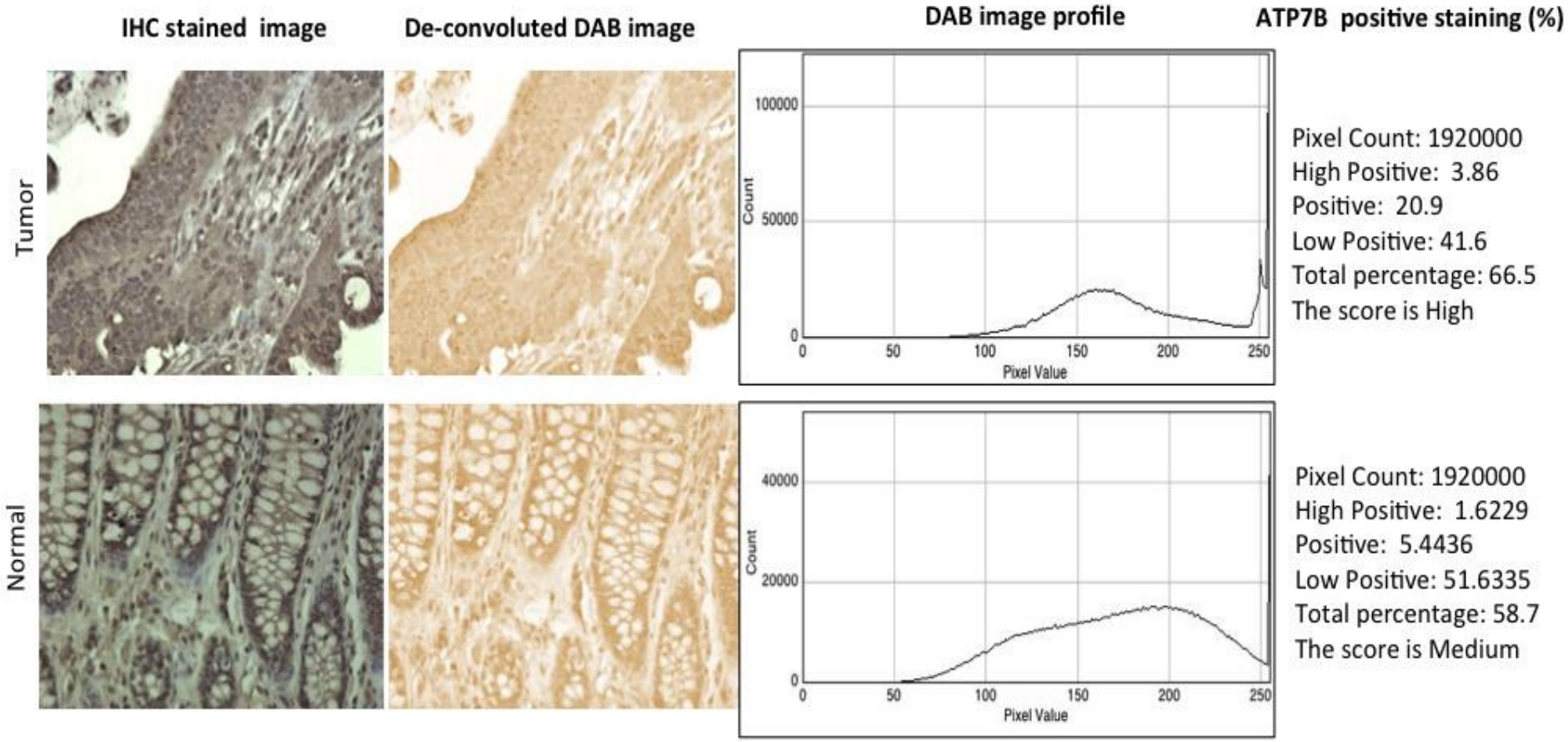
IHC stained image
De-convoluted DAB image
DAB image profile
ATP7B positive staining (%)
Tumor
Normal
Count
Pixel Value
100000
50000
0
40000
20000
0
50
100
150
200
250
Pixel Count: 1920000
High Positive: 3.86
Positive: 20.9
Low Positive: 41.6
Total percentage: 66.5
The score is High
Pixel Count: 1920000
High Positive: 1.6229
Positive: 5.4436
Low Positive: 51.6335
Total percentage: 58.7
The score is Medium

Patient 6

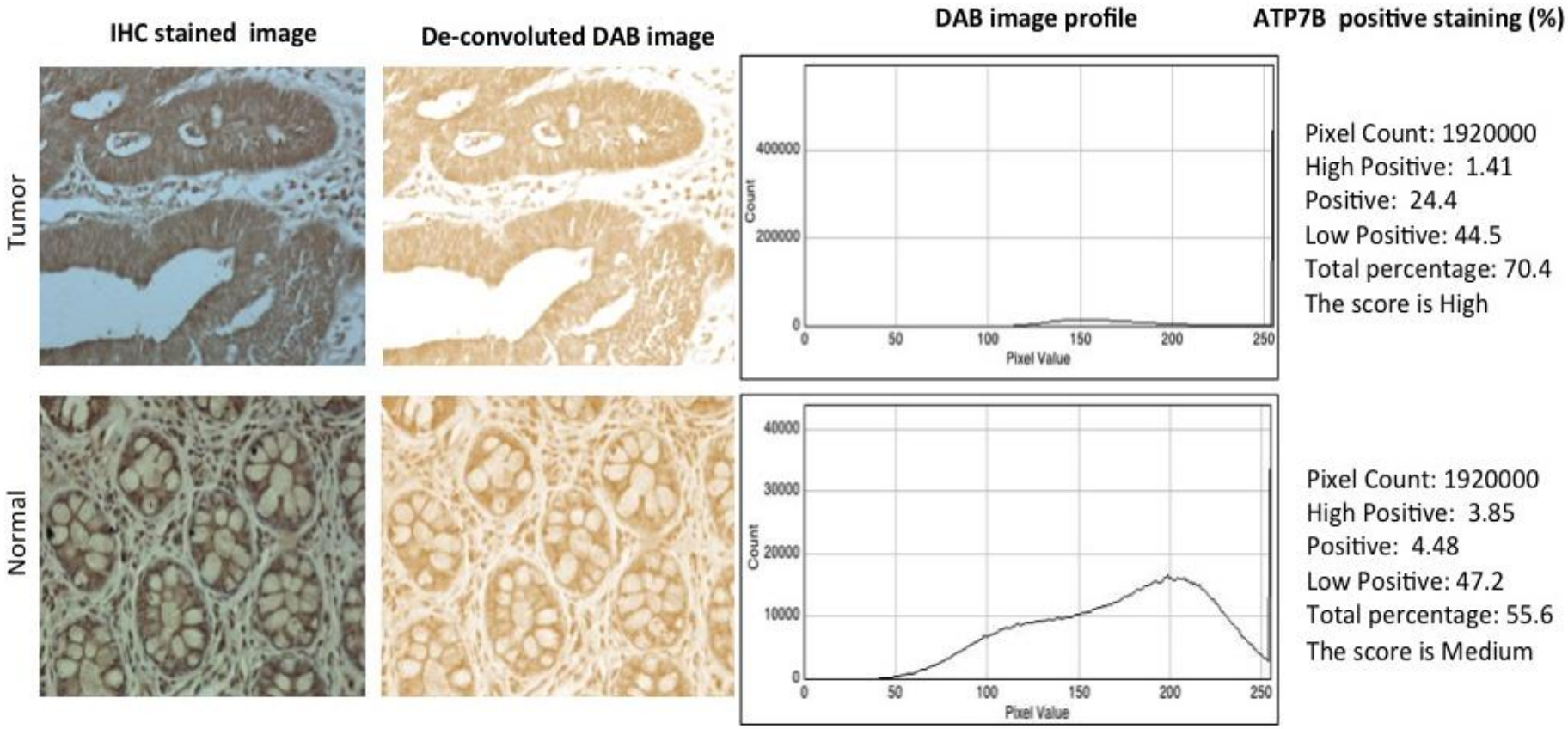
IHC stained image
De-convoluted DAB image
DAB image profile
ATP7B positive staining (%)
Tumor
Normal
Count
Pixel Value
0
50
100
150
200
250
400000
200000
40000
30000
20000
10000
Pixel Count: 1920000
High Positive: 1.41
Positive: 24.4
Low Positive: 44.5
Total percentage: 70.4
The score is High
Pixel Count: 1920000
High Positive: 3.85
Positive: 4.48
Low Positive: 47.2
Total percentage: 55.6
The score is Medium

Figure S-3. Semi-quantitative analysis of representative DAB stained immunohistochemical images of ATP7B in tumor and the matched normal tissues of four colorectal cancer patients

Standard immunohistochemistry was performed on paraffin-embedded tumor and normal tissues using a mouse anti-ATP7B primary antibody and a goat anti-mouse secondary antibody, stained with DAB and hematoxylin. The DAB-stained IHC images were then deconvoluted and digitally scored of ATP7B to illustrate the negative, medium and high positive staining intensity defined by the percentage of pixel counts. Mag. 40x.

Appendix 1 has been removed for copyright or proprietary reasons.

It is the following published article: Cui, H., Zhang, A. J., McKeage, M. J., Nott, L. M., Geraghty, D., Guven, N., Liu, J. J. 2017. Copper transporter 1 in human colorectal cancer cell lines: Effects of endogenous and modified expression on oxaliplatin cytotoxicity, Journal of inorganic biochemistry, 177, 249-258 doi: 10.1016/j.jinorgbio.2017.04.022

Appendix 2: Cover page of Publication 2 by Cui H *et al.*

FINAL

Send Orders for Reprints to reprints@benthamscience.ae

Current Drug Targets, 2015, *16*, 000-000 1

ABC Transporter Inhibitors in Reversing Multidrug Resistance to Chemotherapy

Haigang Cui[1], Anna J.Zhang[1], Mingwei Chen[2] and Johnson J. Liu[1,*]

[1]*School of Medicine, Faculty of Health, University of Tasmania, Hobart, Tasmania 7001, Australia;*
[2]*The First Affiliated Hospital, College of Medicine, Xi'an Jiaotong University, PR China*

Please provide corresponding author(s) photograph
size should be 4" x 4" inches

Abstract: The superfamily of human ATP-binding cassette (ABC) transporters comprises seven subfamilies (ABCA to G) with 48 members. In addition to their profound physiologic and pharmacological functions, ABC transporters play important roles in mediating multidrug resistance (MDR) in cancer by mediating the efflux of many anticancer drugs, particularly, ABCB1, ABCG2 and ABCC subfamily members. Previous development of ABCB1 transporter inhibitors has provided insights into seeking novel strategies in developing new classes of compound that inhibit ABCB1 and other MDR-related ABC transporters. We herein review and evaluate current evidence in this area, with an emphasis on experimental and investigational agents that are under preclinical and clinical tests, including tyrosine kinase inhibitors, natural products, microRNAs and novel chemical entities. New strategies targeting ABC transporters in cancer stem cells and future perspectives in this field are also discussed.

Keywords: ABC transporter inhibitor, cancer stem cell, chemotherapy, microRNA, multidrug resistance, tyrosine kinase inhibitor.

INTRODUCTION

The remainder of this page has been redacted for copyright reasons

1389-4501/15 $58.00+.00

Appendix 3: Human ethics approval letter:

Office of Research Services
University of Tasmania
Private Bag 1
Hobart Tasmania 7001
Telephone + 61 3 6226 7479
Facsimile + 61 3 6226 7148
Email Human.Ethics@utas.edu.au
www.research.utas.edu.au/human_ethics/

HUMAN RESEARCH ETHICS COMMITTEE (TASMANIA) NETWORK

UTAS

20 May 2015

Dr Louise Nott
Department of Haematology and Oncology
Royal Hobart Hospital

Sent via email

Dear Dr Nott

REF NO: H0014706
TITLE: Profiling and functional studies of drug transporters in colorectal cancer: a pilot study in Tasmanian patients

Document	***Version***	***Date***
NEAF	-	February 2015
Patient Information and Consent Form RHH	Version 4	15 May 2015
TSRAC Study Protocol	-	-

The Tasmanian Health and Medical Human Research Ethics Committee considered and approved the above documentation on **15 May 2015** to be conducted at the following site(s):

Royal Hobart Hospital
University of Tasmania

Please ensure that all investigators involved with this project have cited the approved versions of the documents listed within this letter and use only these versions in conducting this research project.

This approval constitutes ethical clearance by the Health and Medical HREC. The decision and authority to commence the associated research may be dependent on factors beyond the remit of the ethics review process. For example, your research may need ethics clearance from other organisations or review by your research governance coordinator or Head of Department. It is your responsibility to find out if the approvals of other bodies or authorities are required. It is recommended that the proposed research should not commence until you have satisfied these requirements.

All committees operating under the Human Research Ethics Committee (Tasmania) Network are registered and required to comply with the *National Statement on the Ethical Conduct in Human Research* (NHMRC 2007 updated 2014).

Therefore, the Chief Investigator's responsibility is to ensure that:

(1) The individual researcher's protocol complies with the HREC approved

protocol.

(2) Modifications to the protocol do not proceed until **approval** is obtained in writing from the HREC. Please note that all requests for changes to approved documents must include a version number and date when submitted for review by the HREC.

(3) Section 5.5.3 of the National Statement states:

Researchers have a significant responsibility in monitoring approved research as they are in the best position to observe any adverse events or unexpected outcomes. They should report such events or outcomes promptly to the relevant institution/s and ethical review body/ies and take prompt steps to deal with any unexpected risks.

The appropriate forms for reporting such events in relation to clinical and non-clinical trials and innovations can be located at the website below. All adverse events must be reported regardless of whether or not the event, in your opinion, is a direct effect of the therapeutic goods being tested. http://www.research.utas.edu.au/human_ethics/medical_forms.htm

(4) All research participants must be provided with the current Patient Information Sheet and Consent Form, unless otherwise approved by the Committee.

(5) The Committee is notified if any investigators are added to, or cease involvement with, the project.

(6) This study has approval for four years contingent upon annual review. A *Progress Report* is to be provided on the anniversary date of your approval. Your first report is due **15 May 2016.** You will be sent a courtesy reminder closer to this due date.

(7) A *Final Report* and a copy of the published material, either in full or abstract, must be provided at the end of the project.

Should you have any queries please do not hesitate to contact me on (03) 6226 6254.

Yours sincerely

Lynda Hobman
Administration Officer (Integrity and Ethics)
Research Integrity and Ethics Unit
Office of Research Services
University of Tasmania